frontiers | Research Topics

Deciphering the regulatory role of transcription factors in cancer immune infiltration

Edited by
Qian Yang, Yujia Lan and Jin-Fen Xiao

Published in
Frontiers in Oncology
Frontiers in Immunology

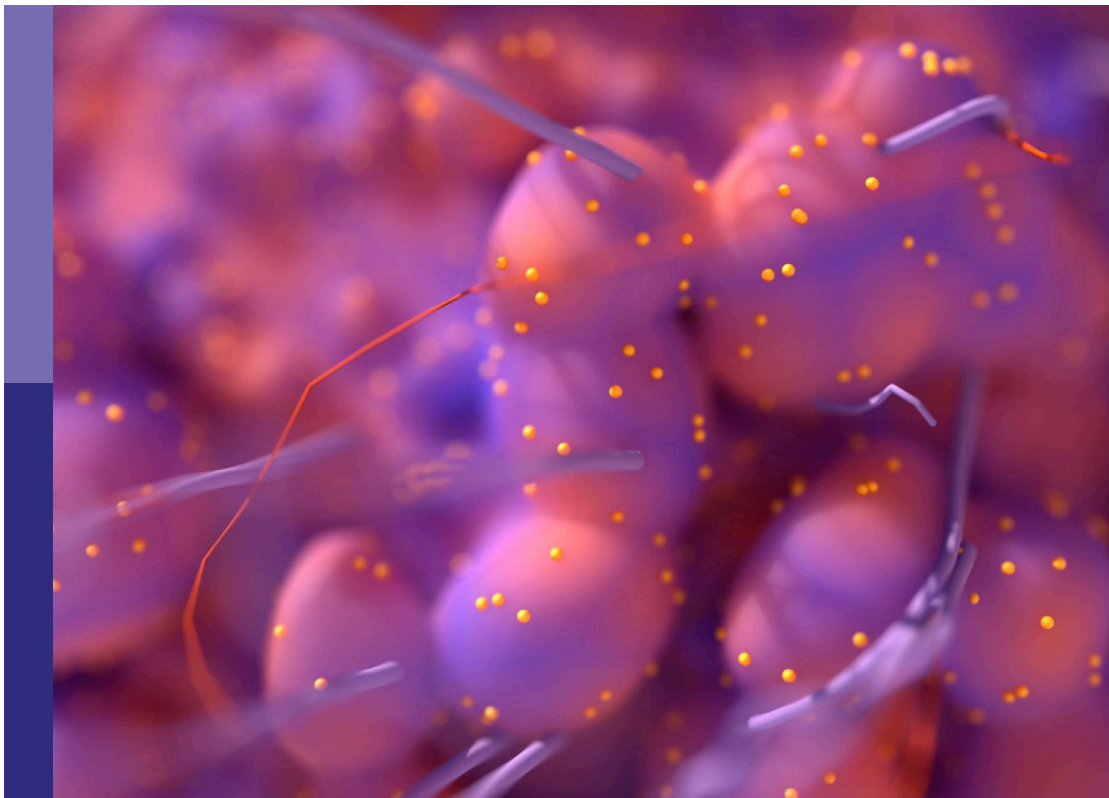

ISSN 1664-8714
ISBN 978-2-8325-6022-8
DOI 10.3389/978-2-8325-6022-8

About Frontiers

Frontiers is more than just an open access publisher of scholarly articles: it is a pioneering approach to the world of academia, radically improving the way scholarly research is managed. The grand vision of Frontiers is a world where all people have an equal opportunity to seek, share and generate knowledge. Frontiers provides immediate and permanent online open access to all its publications, but this alone is not enough to realize our grand goals.

Frontiers journal series

The Frontiers journal series is a multi-tier and interdisciplinary set of open-access, online journals, promising a paradigm shift from the current review, selection and dissemination processes in academic publishing. All Frontiers journals are driven by researchers for researchers; therefore, they constitute a service to the scholarly community. At the same time, the *Frontiers journal series* operates on a revolutionary invention, the tiered publishing system, initially addressing specific communities of scholars, and gradually climbing up to broader public understanding, thus serving the interests of the lay society, too.

Dedication to quality

Each Frontiers article is a landmark of the highest quality, thanks to genuinely collaborative interactions between authors and review editors, who include some of the world's best academicians. Research must be certified by peers before entering a stream of knowledge that may eventually reach the public - and shape society; therefore, Frontiers only applies the most rigorous and unbiased reviews. Frontiers revolutionizes research publishing by freely delivering the most outstanding research, evaluated with no bias from both the academic and social point of view. By applying the most advanced information technologies, Frontiers is catapulting scholarly publishing into a new generation.

What are Frontiers Research Topics?

Frontiers Research Topics are very popular trademarks of the *Frontiers journals series*: they are collections of at least ten articles, all centered on a particular subject. With their unique mix of varied contributions from Original Research to Review Articles, Frontiers Research Topics unify the most influential researchers, the latest key findings and historical advances in a hot research area.

Find out more on how to host your own Frontiers Research Topic or contribute to one as an author by contacting the Frontiers editorial office: frontiersin.org/about/contact

Deciphering the regulatory role of transcription factors in cancer immune infiltration

Topic editors

Qian Yang — Cedars Sinai Medical Center, United States

Yujia Lan — Harbin Medical University, China

Jin-Fen Xiao — University of Texas MD Anderson Cancer Center, United States

Citation

Yang, Q., Lan, Y., Xiao, J.-F., eds. (2025). *Deciphering the regulatory role of transcription factors in cancer immune infiltration*. Lausanne: Frontiers Media SA. doi: 10.3389/978-2-8325-6022-8

Table of contents

frontiers | Frontiers in Oncology

TYPE Editorial
PUBLISHED 07 February 2025
DOI 10.3389/fonc.2025.1563949

OPEN ACCESS

EDITED AND REVIEWED BY
Peter Brossart,
University of Bonn, Germany

*CORRESPONDENCE
Qian Yang
qian.yang@cshs.org

RECEIVED 20 January 2025
ACCEPTED 27 January 2025
PUBLISHED 07 February 2025

CITATION
Yang Q, Xiao J and Lan Y (2025) Editorial: Deciphering the regulatory role of transcription factors in cancer immune infiltration.
Front. Oncol. 15:1563949.
doi: 10.3389/fonc.2025.1563949

Editorial: Deciphering the regulatory role of transcription factors in cancer immune infiltration

Qian Yang[1,2]*, Jinfen Xiao[3] and Yujia Lan[4]

[1]Department of Urology, Samuel Oschin Comprehensive Cancer Institute, Cedars-Sinai Medical Center, Los Angeles, CA, United States, [2]Department of Computational Biomedicine, Samuel Oschin Comprehensive Cancer Institute, Cedars-Sinai Medical Center, Los Angeles, CA, United States, [3]University of Texas MD Anderson Cancer Center, Houston, TX, United States, [4]College of Bioinformatics Science and Technology, Harbin Medical University, Harbin, China

KEYWORDS

transcription factors, cancer, immune infiltration, tumor micro environment (TME), immunotherapy

Editorial on the Research Topic
Deciphering the regulatory role of transcription factors in cancer immune infiltration

Introduction

Transcription factors (TF) are proteins that bind to specific DNA sequences and regulate gene transcription, playing essential roles in various cellular processes, such as cell proliferation, differentiation, and immune responses (1). Tumor immune infiltration, the process by which immune cells infiltrate tumor tissues is a critical component of the tumor microenvironment (TME) significantly influencing cancer progression and therapeutic outcomes (2). Dysregulated TF activities can contribute to cancer malignancies by modulating the expression of immune-related genes, impacting immune cell recruitment, activation, and function (3) and thus reshape the anti-tumor immune response (3). Understanding the regulatory role of TFs in cancer immune infiltration offers promising avenues for the development of novel therapeutic strategies and biomarkers for cancer treatment.

Tumors can be classified as "hot" and "cold" based on the degree and type of immune cell infiltration, immune cell activity, and the heterogeneity of the tumor microenvironment (4). Some cancer types are frequently identified as "hot" tumors, such as bladder, head and neck, kidney, liver, melanoma, and non-small cell lung cancers. In contrast, ovarian, prostate, and pancreatic cancers are often classified as "cold" tumors due to low immune infiltration and immune response (4). Immunotherapy shows clinical benefits in some cancer types. However, challenges such as low response rate, high recurrence, and metastasis risk remain significant hurdles, particularly in treating "cold" tumors (4). TFs, especially master transcript factors, play a crucial role in driving lineage plasticity in cancers and modulating the tumor microenvironment. Targeting TFs could be explored as a potential therapeutic strategy for combinational therapy in cancer treatment.

Identifying immune-related TFs could also help transform "cold" tumors into "hot" tumors by reconstructing the TME.

For this Research Topic, we aimed to unravel the intricate interplay between TFs and immune cells in the context of cancer immune infiltration. We investigated the potential functionalities of TFs in cancer through various mechanisms, including direct transcriptional regulation of immune-related genes, crosstalk with signaling pathways involved in immune cell activation, and interactions with other cellular components of the tumor microenvironment. In summary, deciphering the regulatory role of TFs in cancer immune infiltration is a crucial step toward understanding the complexities of the tumor microenvironment. This knowledge holds significant potential for advancing the development of more effective immunotherapy strategies.

NF-κB transcription factors in the TME

The tumor microenvironment is a multifaceted and dynamic ecosystem comprising not only tumor cells but also various non-cancerous cells, secreted ligands, and the extracellular matrix (5, 6). This intricate environment plays a pivotal role in tumor progression, metastasis, and therapeutic response. NF-κB transcription factors were known for their central roles in inflammation and innate immunity, garnering attention for their critical involvement in cancer development and progression, as well as the configuration of the TME (7). A systematic review by Cao et al. emphasizes the multifaceted role of the NF-κB signaling pathway in regulating various aspects of the TME, including immune modulation, stromal cell function, angiogenesis, invasion, and the link between inflammation and tumorigenesis. They also discussed how NF-κB transcription factors recruit immune cells and their complex roles in immune cell types, such as T, B, NK, and DC cells. Last but not least, the links among tumor progression, metabolism, and immune infiltration have been summarized in this review. A review by Kumar and Gupta also discussed the connection between epigenetic regulation of one NF-kB downstream gene, NKG2D, and NK cell-based immunotherapy in cancer.

These findings suggest the crucial functions of transcription factors in the TME, and targeting these kinds of TFs could be a novel method to increase immune infiltration and enhance the efficiency of immunotherapy.

NRF-1 function in the melanoma TME

Previous studies have identified the integrin-associated protein, CD47, to be a critical myeloid lineage checkpoint, which is overexpressed in various types of cancer cells, especially in melanoma, and can inhibit innate immunity-mediated anti-tumor responses (8–11). In Makwana et al.'s original study, they demonstrate that upregulation of CD47 occurs at the mRNA level and chromatin accessibility at the CD47 promoter region also changed in melanoma. Real-time PCR confirmed elevated CD47 mRNA production across multiple transcript variants. Analysis using the MotifMap algorithm identified binding consensus sequences for Nuclear Respiratory Factor-1 (NRF-1) within the CD47 proximal promoter region. Chromatin Immunoprecipitation (ChIP) assays further showed NRF-1 binding at predicted sites, with differential affinities observed between malignant and normal cell types, contributing to increased CD47 mRNA and protein levels in cancer cells. Bioluminescence reporter assays defined the minimal CD47 promoter region and identified the number of NRF-1 binding sites essential for the efficient activation of CD47. These findings highlight the regulatory role of NRF-1 to CD47 expression in melanoma. NRF-1 transcription factor serves as a critical regulatory hub, uniquely capable of controlling genes involved in both mitochondrial biogenesis and the evasion of innate immunity in the TME.

PGC1α reshapes the TME in diverse cancers

The peroxisome proliferator-activated receptor gamma coactivator 1-alpha (PGC1α) importantly acts as a tissue-specific transcription coactivator by interacting with a multitude of transcription factors and regulates metabolic processes in cancer cells (12). PGC1α can also reshape the TME and modulate the immune response by coordinating metabolic networks between cancer cells and immune cells. Inhibition of PGC1α facilitates overcome of immune-evasive and therapeutic resistance. Therefore, a comprehensive elucidation of PGC1α in the TME is necessary. In this Research Topic, Wang et al. systematically reviewed the role of PGC1α in cancer and discussed specific functions of PGC1α in several cancer types. The magnitude of PGC1α at the transcriptional regulation level suggests that many crucial transcription factors contribute to the reshaping of the TME in cancer, such as FOXO1 and MYC. They summarized the significance of PGC1α in the cancer TME, especially in immune cells. Targeting PGC1 modulates immune cell metabolism and in turn alters the immune landscape of tumors by reducing immune suppression and enhancing the efficacy of immunotherapies. These studies indicate that transcriptional regulation sculptures TME and transcription coactivators such as PGC1α, could reshape immune cells in the microenvironment of diverse cancers.

Author contributions

QY: Writing – original draft, Writing – review & editing. JX: Writing – review & editing. YL: Writing – review & editing.

Conflict of interest

The authors declare that the research was conducted in the absence of any commercial or financial relationships that could be construed as a potential conflict of interest.

The author(s) declared that they were an editorial board member of Frontiers, at the time of submission. This had no impact on the peer review process and the final decision.

Publisher's note

References

1. Latchman DS. Transcription factors: an overview. *Int J Biochem Cell Biol*. (1997) 29:1305–12. doi: 10.1016/S1357-2725(97)00085-X

2. Anderson NM, Simon MC. The tumor microenvironment. *Curr Biol*. (2020) 30: R921–5. doi: 10.1016/j.cub.2020.06.081

3. Melssen MM, Sheybani ND, Leick KM, Slingluff CL Jr. Barriers to immune cell infiltration in tumors. *J Immunother Cancer*. (2023) 11. doi: 10.1136/jitc-2022-006401

4. Wang L, Geng H, Liu Y, Liu L, Chen Y, Wu F, et al. Hot and cold tumors: Immunological features and the therapeutic strategies. *MedComm (2020)*. (2023) 4: e343. doi: 10.1002/mco2.v4.5

5. de Visser KE, Joyce JA. The evolving tumor microenvironment: From cancer initiation to metastatic outgrowth. *Cancer Cell*. (2023) 41:374–403. doi: 10.1016/j.ccell.2023.02.016

6. Lan Y, Zhao E, Zhang X, Zhu X, Wan L, S. A, et al. Prognostic impact of a lymphocyte activation-associated gene signature in GBM based on transcriptome analysis. *PeerJ*. (2021) 9:e12070. doi: 10.7717/peerj.12070

7. Hayden MS, Ghosh S. NF-kappaB in immunobiology. *Cell Res*. (2011) 21:223–44. doi: 10.1038/cr.2011.13

8. Willingham SB, Volkmer JP, Gentles AJ, Sahoo D, Dalerba P, Mitra SS, et al. The CD47-signal regulatory protein alpha (SIRPa) interaction is a therapeutic target for human solid tumors. *Proc Natl Acad Sci U.S.A*. (2012) 109:6662–7.

9. Ngo M, Han A, Lakatos A, Sahoo D, Hachey SJ, Weiskopf K, et al. Antibody therapy targeting CD47 and CD271 effectively suppresses melanoma metastasis in patient-derived xenografts. *Cell Rep*. (2016) 16:1701–16. doi: 10.1016/j.celrep.2016.07.004

10. Jaiswal S, Jamieson CH, Pang WW, Park CY, Chao MP, Majeti R, et al. CD47 is upregulated on circulating hematopoietic stem cells and leukemia cells to avoid phagocytosis. *Cell*. (2009) 138:271–85. doi: 10.1016/j.cell.2009.05.046

11. Majeti R, Chao MP, Alizadeh AA, Pang WW, Jaiswal S, Gibbs KD Jr., et al. CD47 is an adverse prognostic factor and therapeutic antibody target on human acute myeloid leukemia stem cells. *Cell*. (2009) 138:286–99. doi: 10.1016/j.cell.2009.05.045

12. Tan Z, Luo X, Xiao L, Tang M, Bode AM, Dong Z, et al. The role of PGC1alpha in cancer metabolism and its therapeutic implications. *Mol Cancer Ther*. (2016) 15:774–82. doi: 10.1158/1535-7163.MCT-15-0621

frontiers | Frontiers in Oncology

TYPE Review
PUBLISHED 07 May 2024
DOI 10.3389/fonc.2024.1383809

OPEN ACCESS

EDITED BY
Maria Elena Pisanu,
National Institute of Health (ISS), Italy

REVIEWED BY
Elena Rapizzi,
University of Florence, Italy
Maria Letizia Taddei,
University of Florence, Italy

*CORRESPONDENCE
Lei Su
suleinjglyy@fastmail.com
Bing Ouyang
boy20041188@sina.com

†These authors have contributed equally to this work

RECEIVED 08 February 2024
ACCEPTED 16 April 2024
PUBLISHED 07 May 2024

CITATION
Wang Y, Peng J, Yang D, Xing Z, Jiang B, Ding X, Jiang C, Ouyang B and Su L (2024) From metabolism to malignancy: the multifaceted role of PGC1α in cancer. *Front. Oncol.* 14:1383809. doi: 10.3389/fonc.2024.1383809

From metabolism to malignancy: the multifaceted role of PGC1α in cancer

Yue Wang[1†], Jianing Peng[2†], Dengyuan Yang[1†], Zhongjie Xing[1], Bo Jiang[3], Xu Ding[1], Chaoyu Jiang[3], Bing Ouyang[1*] and Lei Su[3,4*]

[1]Department of Surgery, Nanjing Central Hospital, Nanjing, China, [2]Division of Biosciences, University College London, London, United Kingdom, [3]Department of General Surgery, Nanjing Drum Tower Hospital, Clinical College of Nanjing Medical University, Nanjing, China, [4]Department of General Surgery, Affiliated Drum Tower Hospital, Medical School of Nanjing University, Nanjing, China

PGC1α, a central player in mitochondrial biology, holds a complex role in the metabolic shifts seen in cancer cells. While its dysregulation is common across major cancers, its impact varies. In some cases, downregulation promotes aerobic glycolysis and progression, whereas in others, overexpression escalates respiration and aggression. PGC1α's interactions with distinct signaling pathways and transcription factors further diversify its roles, often in a tissue-specific manner. Understanding these multifaceted functions could unlock innovative therapeutic strategies. However, challenges exist in managing the metabolic adaptability of cancer cells and refining PGC1α-targeted approaches. This review aims to collate and present the current knowledge on the expression patterns, regulators, binding partners, and roles of PGC1α in diverse cancers. We examined PGC1α's tissue-specific functions and elucidated its dual nature as both a potential tumor suppressor and an oncogenic collaborator. In cancers where PGC1α is tumor-suppressive, reinstating its levels could halt cell proliferation and invasion, and make the cells more receptive to chemotherapy. In cancers where the opposite is true, halting PGC1α's upregulation can be beneficial as it promotes oxidative phosphorylation, allows cancer cells to adapt to stress, and promotes a more aggressive cancer phenotype. Thus, to target PGC1α effectively, understanding its nuanced role in each cancer subtype is indispensable. This can pave the way for significant strides in the field of oncology.

KEYWORDS

PGC1α, tumor progression, cancer metabolism, signaling pathways, therapeutic target, metabolic heterogeneity

Introduction

The peroxisome proliferator-activated receptor gamma coactivator 1-alpha (PGC1α) is a pivotal transcriptional coactivator with multifaceted roles in regulating cellular energy metabolism and mitochondrial biogenesis (1). Since its first identification as a binding partner of the nuclear receptor peroxisome proliferator-activated receptor gamma (PPARα) in 1998, the significance of PGC1α in orchestrating diverse metabolic pathways has become increasingly evident (2, 3). Its functions include mitochondrial biogenesis, fatty acid oxidation, gluconeogenesis, and oxidative phosphorylation (4).

The versatility of PGC1α is emphasized by its ability to interact with a multitude of transcription factors and coactivators (5, 6). This enables PGC1α to exert intricate control over the expression of genes relevant to these pathways. As the cornerstone of mitochondrial biogenesis (7), PGC1α can augment the number and activity of mitochondria. This amplification enhances cellular energy production and adaptability, ensuring a balance between energy homeostasis and the response to shifts in energy demands. Beyond its metabolic functions, PGC1α is pivotal in processes such as cell growth, differentiation, and survival (8), underscoring its role in preserving cellular integrity and function. The prominence of PGC1α in physiological processes implies its potential involvement in pathologies. Indeed, perturbations in PGC1α expression or activity have been linked to a spectrum of diseases, ranging from neurodegenerative disorders (9) and metabolic syndromes to cardiovascular diseases (10). Notably, emerging evidence suggests a role for PGC1α in cancer pathogenesis (11). Its dysregulation has been implicated in metabolic reprogramming and disease progression across a variety of malignancies, both solid and hematological (1).

Unfortunately, challenges exist in managing the metabolic adaptability of cancer cells and refining PGC1α-targeted approaches. There is a need to decode the intricate molecular ties of PGC1α's interactions with cancer cells. This is a critical step in comprehending both PGC1α's multifaceted involvement in cancer and the ability to use this knowledge for cancer prevention and treatment. Therefore, this review aims to collate and present the current knowledge on the expression patterns, regulators, binding partners, and roles of PGC1α in diverse cancers. We examined PGC1α's tissue-specific functions and elucidated its dual nature as both a potential tumor suppressor and an oncogenic collaborator. A comprehensive understanding of PGC1α's intricate relationship with cancer metabolism could pave the way for novel biomarker identification and therapeutic interventions against this pervasive global health challenge. We hope that this review will serve as a foundational guide for researchers interested in the further exploration of this domain.

Structure and functions of PGC1α

The PGC1α gene, located on chromosome 4 at the 4p15.1 position, features several functional domains crucial for its activity (3). These domains include the N-terminal transcriptional coactivatory domains, which facilitate interactions with various transcription factors; a central inhibitory domain that moderates its coactivatory functions; and an RNA recognition motif (RRM) located at the C-terminus. The N-terminal region is particularly significant for its role in engaging with nuclear receptors such as peroxisome proliferator-activated receptor gamma (PPARγ), nuclear respiratory factor 1 (NRF1), and estrogen-related receptor alpha (ERRα) (1, 12). These interactions are essential for the transcriptional regulation of genes that play a role in mitochondrial functionality and oxidative metabolism. Upon activation, PGC1α primarily functions by coactivating nuclear receptors and other transcription factors, thereby promoting the expression of genes related to energy metabolism (13). This gene is fundamental to the adaptation to changing metabolic demands during shifts in nutrient availability or energy requirements. Specifically, PGC1α enhances mitochondrial replication, respiratory capacity, and oxidative phosphorylation, which collectively increase cellular energy production (14). The regulation of its activity involves various post-translational modifications and protein interactions, allowing for a responsive adjustment to cellular energy conditions (15, 16). Through these multifaceted roles and complex regulatory mechanisms, PGC1α acts as a central regulator of metabolic processes, highlighting its importance in both normal physiology and various pathological conditions, including cancer.

Roles of PGC1α in cancer cells

PGC1α is an important gene that regulates metabolism in cancer cells, controlling pathways like glycolysis, tricarboxylic acid (TCA) cycle and fatty acid synthesis etc. But the interesting thing is its actual role differs a lot between different cancer types – sometimes it suppresses tumors, but other times it promotes cancer growth instead! This depends on the complex interplay between various intracellular signaling pathways. PGC1α closely interacts with molecules like β-catenin, AMP-activated protein kinase (AMPK), and can modulate downstream gene expression based on these upstream signals. So, it acts like a central integrator of signals that reprogram metabolism. Its expression and functions are super tissue-specific. For example, from the latest studies, PGC1α expression is upregulated in ovarian cancer (OC), colorectal cancer (CRC), gastric cancer (GC), nasopharyngeal (NPC) and cholangiocarcinoma (CCA), while downregulated in thyroid cancer (TC), liver cancer and renal cancer. However, in some types of cancers, like melanoma, prostate and breast cancer, low and high expressions of PGC1α are coexisted (Figure 1). PGC1α also reshapes the tumor microenvironment by coordinating metabolic crosstalk between cancer cells and immune cells. Targeting PGC1α could potentially help overcome therapeutic resistance, but overcoming metabolic plasticity of cancer cells remains a big challenge! Here, we elucidate the mechanisms of PGC1α from the perspective of different tumor cells in detail.

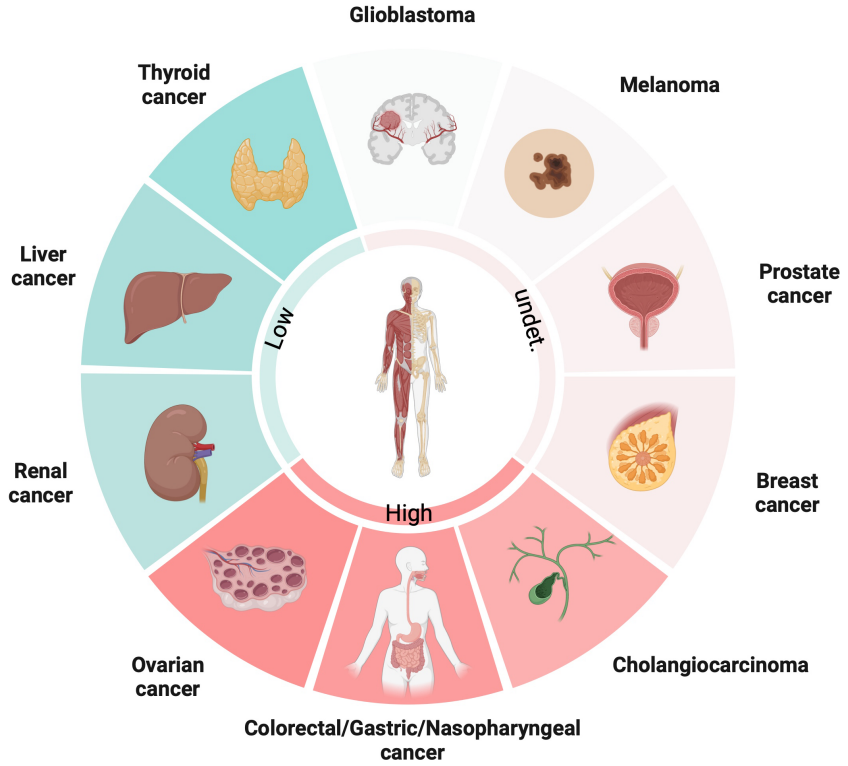

FIGURE 1
The expression patterns of PGC1α in diverse cancers.

PGC1α in thyroid cancer

The conventional perspective on metabolic changes observed in thyroid carcinomas is that they arise as a consequence of disease progression rather than as instigators themselves (17, 18). However, growing evidence suggests that these metabolic alterations also play regulatory roles in driving cancer progression. Studies have revealed the downregulation of PGC1α expression, particularly in the advanced stages of thyroid cancer (19) and notably in tumors harboring the BRAF V600E mutation (17), which is the most prevalent somatic oncogenic mutation in papillary thyroid carcinoma (20, 21). A comprehensive analysis on The Cancer Genome Atlas (TCGA) data from hundreds of patients with papillary thyroid carcinoma underscored the significance of PGC1α downregulation, as it correlated with a higher disease stage and an increased risk of recurrence (17). Multiple mechanisms appear to be involved in suppressing PGC1α expression in TC. The intricate AMPK signaling pathway is implicated in this regulatory process, whereby the activation of protein kinase B (AKT) leads to the suppression of PGC1α expression (17). Further, oxidative metabolism appears to inflict damage upon PGC1α mRNA, consequently dampening its expression (17). This forms a vicious feedforward loop as PGC1α loss exacerbates oxidative stress by curtailing mitochondria and antioxidant responses. Given multifaceted aspects of negative regulation, PGC1α is capable of playing important roles in TC development. Indeed, PGC1α deficiency damages mitochondrial function, elevates oxidative stress, and enhances glycolytic phenotype and disease progression (17).

PGC1α in colorectal cancer

PGC1α is frequently found to be overexpressed in CRC tissues and cell lines. It serves as a key energy mediator, and is induced by aerobic glycolysis (22) and hypoxia (23) in CRC cells. Interestingly, lactate metabolites generated from these processes contribute to the elevation of PGC1α mRNA levels in cancer cells (24, 25). Sirtuin3 (SIRT3), a principal mitochondrial deacetylase, has been implicated in modulating PGC1α levels. In metastatic CRC cell lines, the inhibition of SIRT3 using shRNAs has been found to lead to a decrease in both PGC1α mRNA and protein levels (26). Additionally, oncogenic phosphatase PRL3, a regulator of reactive oxygen species (ROS), has been found to exert its influence on upregulated PGC1α expression through the mediation of Ras-proximate-1(RAP1) (27). However, in specific scenarios where CRC cells are quiescent, the level of PGC1α has been found to be reduced. For example, linoleic acid was found to induce dormancy in CRC cells by increasing the expression of miR-494, which suppressed energy metabolism genes and maintained cell quiescence through reducing PGC1α levels (28). Interestingly, miR-494 was present at low levels in non-metastatic cases (28). In addition, in normoxic CRC cancer stem cells (CSCs), the expression of hypoxia-inducible factor 1-alpha (HIF-1α) was significantly

reduced, leading to the restoration of PGC1α expression in these areas (29). This suggests that HIF1α can act as a negative regulator of PGC1α. Additionally, substances secreted from the tumor microenvironment (TME) may also impact PGC1α expression. For instance, neutrophil elastase (NE), which is released from the neutrophil extracellular traps (NETs) activated toll-like receptor 4 (TLR4) on cancer cells, has been shown to trigger the TLR4/p38/PGC1α axis, resulting in PGC1α upregulation (30). Notably, PGC1α levels have been found to not only be upregulated in cancer cells but also be heightened in adipose tissues (20), particularly in the context of obesity-related CRC (31) and in cases of cancer cachexia (32). This cachexia-related elevation of PGC1α has been shown to be achieved through the secretion of interleukin-8 (IL-8) in extracellular vesicles (EVs) from CRC cells (32). Cachexia, a late-stage complication of various cancers, is promoted by tumor growth and chemotherapy administration (33). In muscle tissues affected by wasting, abnormal PGC1α expression contributes to mitochondrial dysfunction, which in turn causes cachexia-related symptoms (34). Retrospective studies analyzing clinical tumor samples from patients with CRC have underscored the clinical relevance of PGC1α in CRC (35). Notably, PGC1α expression is positively correlated with nodal metastasis (36), and high tumor PGC1α expression is correlated with reduced overall survival (OS) (36). Hence, PGC1α might serve as a biomarker for assessing CRC invasion and progression.

Functionally, PGC1α plays a crucial role in enhancing mitochondrial biogenesis and oxidative phosphorylation, thereby reprogramming the metabolism to support cell proliferation, growth, and survival (23, 30, 37). Particularly under hypoxic conditions, PGC1α exerts an antioxidant effect to shield cancer cells from accumulation of ROS (23). Moreover, PGC1α enhances lipid biosynthesis by increasing fatty acid synthase (FASN) levels indirectly through the upregulation of Sp1 and SREBP-1c. This process provides essential building blocks for cell membranes in rapidly proliferating cells (38). Further, PGC1α activates multiple pro-tumorigenic signaling pathways in CRC. It promotes the activation of the AKT/GSK-3β pathway through physical interactions with AKT, although the exact mechanisms remain undefined (39). Additionally, PGC1α boosts leucyl-tRNA synthetase 1 (LARS1) expression, further stimulating AKT/GSK-3β signaling (37).WNT/β-catenin pathway can also be activated by PGC1α, which promotes CRC cell proliferation and inhibits apoptosis (37, 39). PGC1α activates the epithelial-mesenchymal transition (EMT) pathway by upregulating transcription factors like Snail, Slug, and Twist (37, 39), thereby facilitating cancer cell migration and invasion. Recent findings have also indicated that PGC1α can orchestrate lactate oxidation, further promoting the migration and invasion of normoxic CSCs in CRC (29). Additionally, PGC1α can upregulate oxidative phosphorylation and antioxidant genes in chemo resistant cells to adapt to metabolic stress and evade damage from chemotherapeutic agents (23, 40). In 5FU-resistant CRC cells, elevated PGC1α expression has been found to be associated with enhanced mitochondrial biogenesis (40), increased expression of BCL2 while simultaneous decreases BAX, cleaved caspase-3, and cleaved PARP-1 (23). Although SIRT1 is not found to regulate PGC1α transcriptionally, it controls deacetylation and activation of PGC1α, thus protecting CRC cells against chemotherapy (41). Suppression of PGC1α restores chemosensitivity in CRC cells (41). Consequently, monitoring changes in PGC1α expression in patient samples during and after treatment can provide insights into tumor response and the progression towards chemoresistance, enabling timely adjustments to alternative treatment regimens before the disease advances.

Above all, PGC1α integrates various oncogenic pathways in CRC, including metabolism, EMT, inflammation, and survival. Targeting PGC1α holds promise as an approach to counter metastasis and improve patient outcomes. Importantly, dietary interventions offer a potential strategy. For instance, linoleic acid (LA) has been shown to induce quiescence in CRC by suppressing PGC1α expression in mice models (28). *In vitro* studies have demonstrated that manuka honey (MH) reduces colon cancer cell growth in a dose-dependent manner by deactivating PGC1α (42). Clinical trials for CRC are also exploring metabolic drugs such as metformin, which indirectly inhibit PGC1α activity and reprogram metabolism (11, 43). Given their favorable safety profiles and ability to target cancer metabolism, these PGC1α-related drugs could offer new treatment avenues for patients with advanced or chemotherapy-refractory CRC.

PGC1α in gastric cancer

Mirroring its expression pattern in CRC, PGC1α has been found to be highly expressed in GC and gastric epithelial cells (44). This elevated expression appears to be influenced by oxidative stress induced by exogenous molecules. Indeed, research has demonstrated that quercetin, a potential prooxidant, increases PGC1α expression under oxidative stress conditions, thereby safeguarding gastric cells from damage (45). Notably, this effect is particularly pronounced after prolonged exposure to H_2O_2, whereas quercetin lacks this effect under normal circumstances (45).

Upregulated PGC1α has been found to promote GC progression through the inhibition of cell apoptosis and promotion of EMT (44). A more precise mechanism has now been revealed, wherein PGC1α orchestrates the transcription of SNAI1, subsequently affecting the levels of miR-128b (44). This regulatory cascade, which has been observed both *in vitro* and *in vivo*, enhances cell growth and metastasis in GC (44). The influence of posttranscriptional modifications on PGC1α's function is also notable. In GC, PGC1α has been found to undergo phosphorylation by CAB39L-induced p-AMPK, culminating in the regulation of genes associated with mitochondrial respiration complexes (46). Furthermore, PGC1α possesses a pivotal role in the chemoresistance of GC, characterized by disrupted metabolism (47, 48). The HCP5/miR-3619-5p axis controls PGC1α expression, subsequently enabling its interaction with CCAAT/enhancer binding protein beta (CEBPB), thereby triggering transcription of carnitine palmitoyltransferase I (CPT1). This in turn enhances fatty acid oxidation (FAO) in GC, ultimately conferring chemoresistance to cancer cells (49). Remarkably, PGC1α suppression could sensitize GC cells to chemotherapeutic agents by inducing metabolic deficiencies and increasing oxidative stress (49).

PGC1α in liver cancer

Liver cancer, also known as hepatocellular carcinoma (HCC), is a major cause of cancer-related mortality worldwide (50). The main risk factors for HCC include chronic hepatitis B and C viral infections, alcohol abuse, nonalcoholic steatohepatitis (NASH), and aflatoxin exposure (51, 52).

Emerging evidence suggest that PGC1α is downregulated in HCC tissues and cell lines (2, 53). However, the cause of the abnormal expression remains unclear. One proposed mechanism is the accumulation of Parkin-interacting substrate (PARIS) in response to oxidative stress (54), which inhibits PGC1α expression transcriptionally. Additionally, sestrin2 (SESN2), a stress-inducible protein in HCC, has been found to mediate glutamine-dependent activation of PGC1α. SESN2 forms a complex with JNK and FOXO1, enhancing PGC1α transcription. Thus, the reduced SESN2 leads to a decreased PGC1α expression under glucose deprivation (55). The Yes-associated protein 1 (YAP1), a key effector of the Hippo signaling pathway, suppresses PGC1α expression in HCC (56). Moreover, mitochondrial transcription factor B2 (TFB2M), acts as a pivotal oncogene in HCC (57), decreases PGC1α expression at both mRNA and protein level through SIRT3/HIF-1α signaling (58). Interestingly, although hypoxia generally induces PGC1α expression in many diseases (59–61), HIF-1α has been reported to negatively regulate PGC1α expression (58, 62). However, the precise mechanism underlying this regulation remains unclear, due to a lack of Chip-Seq data and in-depth investigations.

Functional studies have demonstrated that PGC1α inhibits HCC cell proliferation and metastasis. Low PGC1α expression is associated with poor prognosis and aggressive tumor features in HCC patients (2). Mechanistically, PGC1α has been found to counter the Warburg effect, a well-known process promoting cancer progression in HCC cells (63, 64). PGC1α achieves this by promoting oxidative phosphorylation (OXPHOS) and inhibiting aerobic glycolysis, partially through PDK1 in a PPARγ-dependent manner (2). PGC1α activates PPARγ, leading to reduced β-catenin protein levels and inhibition of the WNT/β-catenin pathway and PDK1 expression (2). This results in a decrease in the Warburg effect and tumor suppression. Conversely, impaired PGC1α reverses these effects (2). Moreover, PGC1α regulates gluconeogenic genes with several coactivators, such as hepatic nuclear factor 4 alpha (HNF4α), which has been found to repress pathogenesis of HCC (65). Important targets like G6PC and PCK1, affecting the glycogen accumulation and driving HCC progression (66), are mediated by PGC1α and HNF4α. YAP reduces the ability of PGC1α to coactivate HNF4α at its promoter (56). Post-translational modifications of PGC1α also plays roles in HCC progression. Mitochondrial fission, important in promoting tumor progression in HCC (67, 68), reduces NAD^+ levels and SIRT1 activity, leading to increased acetylation of PGC1α protein. Reduced PGC1α activity has been found to be associated with downregulation of CPT1A and acyl-CoA oxidase 1 (ACOX1) and inhibition of FAO in HCC cells (53), both contributing to HCC growth and metastasis (69, 70). Interestingly, general control non-depressible 5 (GCN5) has been found to inhibit PGC1α activity via acetylation (16), but the knockout of GCN5 in mouse liver has not been found to have a significant effect on cancer development (71).

PGC1α also has implications in precancerous or tumorigenic stages. High mobility group AT-hook 1 (HMGA1), a non-histone nuclear protein (72), has been found to recruit protein PGC1α to enhance HBV replication and antigen production through HBV EII/Cp promoter activation, which is associated with liver cirrhosis and HCC oncogenesis (73–75). PGC1α's relationship with viral expression of HBV has also been observed in other studies (76, 77). Liver cirrhosis, stemming from non-alcoholic fatty liver disease (NAFLD), occasionally precedes HCC and involves Bcl-3 (78), while Bcl-3 reduces PGC1α activity, suggesting that higher PGC1α activity might protect against NAFLD-related liver cirrhosis (78, 79). Indeed, pharmacologically activating PGC1α has shown promise for NAFLD treatment (78, 80).

However, several studies have proposed an oncogenic function for PGC1α downregulation validations in HCC. For instance, SET8 inhibits Keap1 expression through PGC1α, activating the Nrf2/ARE pathway and supporting HCC progression (81, 82). Interestingly, gankyrin elevates TIGAR level, a well-known regulator of glucose metabolism, via the Nrf2/ARE pathway. This elevation promotesPGC1α nuclear importation, and drives increased glucose metabolism in HCC (83). Therefore, the synergy between Nrf2/ARE activation and nuclear localization of PGC1α could serve as a critical loop in the metabolic changes that support HCC progression. In addition, the phosphoserine aminotransferase 1 (PSAT1)'s interaction with $p53^{72P}$ variant in HCC cells dissociates PGC1α binding, promotes PGC1α's nuclear translocation (84), mitochondrial transcription factor A (TFAM)-mediated OXPHOS and TCA cycle activation (15). Converse effects have been observed for wild-type p53. In HCC, CD147 promotes p53 degradation via the PI3K/AKT pathway (85). Intriguingly, when p53 is exogenously expressed, there is an upregulation of PGC1α levels (86). This suggests that CD147 might impede mitochondrial biogenesis and functionality by suppressing PGC1α/TFAM levels. In this context, PGC1α appears to play a tumor-suppressive role. Thus, targeting PGC1α upstream or downstream pathways is a promising therapeutic strategy for HCC. PPARα agonists that mimic PGC1α re-expression have shown efficacy in HCC models. For example, GW7647 diminishes hepatocarcinogenesis in-humanized mice models (87, 88).

PGC1α in renal cancer

Research has indicated a decline in PGC1α expression in clear cell renal cell carcinoma (ccRCC) tumors compared to normal tissues. This reduction in PGC1α levels aligns with higher tumor grades (89), advanced disease stage (90), worse disease progression, and worse OS (91). One possible reason for this suppression could be the activation of transforming growth factor beta (TGF-β) signaling, which is commonly observed in ccRCC. In fact, when TGF-β signaling is inhibited, PGC1α levels see an increase (92). Moreover, histone deacetylase 1 (HDAC1) and histone deacetylase 7 (HDAC7) have been identified as corepressors,

playing a role in suppressing PGC1α via the TGF-β signaling pathway (92). In a related observation, retinoic acid 13 (Stra13 or Dec1) is found to transcriptionally inhibit PGC1α expression. This suggests that Stra13 could be a mediator of HIF-mediated PGC1α suppression during von Hippel-Lindau (VHL) deficiency and hypoxia in ccRCC (90). The actions of Stra13 appear to be closely related to HDAC activity (93). On another front, the epigenetic changes also seem to play a part, particularly through m6A modifications that impacts the stability of PGC1α. A decrease in FTO expression in ccRCC has been linked to a rise in methylated PGC1α mRNA, leading to reduced stability (91).

Functional experiments have uncovered PGC1α's potential as a tumor suppressor in ccRCC. Evidence suggests that reintroducing PGC1α restores the levels of TCA cycle enzymes and mitochondrial functions, reversing the metabolic effects of TGF-β signaling in mice models (92). In addition to inducing oxidative stress, PGC1α sensitizes ccRCC cells to cytotoxic therapies (90). Moreover, PGC1α inhibits cell metastasis *in vitro* and *in vivo* by reducing collagen gene expression via miR-29a induction, including collagen type I alpha 1 chain (COL1A1) and collagen type VI alpha 2 chain (COL6A2) (94). Loss of PGC1α in metastatic RCC promotes collagen expression, discoidin domain receptor tyrosine kinase 1 (DDR1) activation, and subsequent snail family transcriptional repressor 1 (SNAIL) stabilization (89). Another tumor suppressor, mitochondrial pyruvate carrier 1 (MPC1), is also regulated by PGC1α (95, 96). PGC1α stimulates the transcription of MPC1 in conjunction with ERR-α and reduced MPC1 negates PGC1α's effects on mitochondrial respiration and biogenesis (95).

However, PGC1α's role seems subtype-dependent. Divergent conclusions have been drawn for the other subtypes. One instance involves the loss of MYBBP1A in 9% of renal tumors (97). MYBBP1A represses PGC1α levels, so the decline of MYBBP1A activates PGC1α directly and indirectly through c-MYB, shifting cellular metabolism from glycolysis to OXPHOS (98). This occurs primarily in the absence of c-MYB or pVHL (97, 98). Another scenario involves inactivation of SETD2 in approximately 12% of ccRCC cases (99). SETD2, a histone H3 lysine trimethyltransferase, acts as a ccRCC tumor suppressor (100, 101). Loss of SETD2 boosts PGC1α expression and mitochondrial mass in ccRCC (102), prompting a metabolic shift towards oxidative phosphorylation and lipogenesis. In both these contexts, PGC1α takes on a tumor-promoting role in ccRCC.

PGC1α in cholangiocarcinoma

The metabolic reprogramming observed in CCA plays a crucial role in driving its progression (103, 104). CCA cells exhibit increased aerobic glycolysis and glutamine anaplerosis, which allows them to produce essential biosynthetic intermediates vital for their rapid growth and survival (103). Recently, the significance of PGC1α in CCA has been emphasized. Patients with elevated levels of PGC1α expression tend to experience reduced OS and progression-free survival (PFS) and are associated with increased angioinvasion and accelerated recurrence (105). Furthermore, the upregulation of PGC1α drives CCA metastasis by elevating the expression of two critical factors: pyruvate dehydrogenase-alpha 1 (PDHA1) and mitochondrial pyruvate carrier 1 (MPC1) (96). This molecular mechanism reverses the Warburg effect, a hallmark metabolic characteristic often observes in cancer cells. Notably, PGC1α also exerts a significant influence on mitochondrial metabolism regulation and the maintenance of stem-like characteristics in CCA stem cells (105). Therefore, pharmacological interventions involving substances like metformin or SR-18292 have shown promise in inhibiting the effects associated with PGC1α upregulation, mitigating its impact on CCA progression and metastasis (105).

PGC1α in glioblastoma

Emerging evidence underscores the pivotal role of PGC1α in GBM oncogenesis, progression, and treatment resistance. Notably, data from the GBM TCGA and GBM PDX Mayo Clinic databases indicates that GBM exhibits decreased PGC1α mRNA expression compared to normal brain tissue (106). Intriguingly, protein levels of PGC1α have also been reported to be highly expressed in GBM patients, which are located not only in the perinuclear or cytoplasmic regions but also prominently within mitochondria, as proven by publicly available TMAs from US Biomax (107). However, compared to WHO grade IV gliomas, lower-grade gliomas (WHO grade II and III) show increased expression of PGC1α (108). Further survival analysis have indicated that higher PGC1α expression in patients with GBM corresponds to shorter survival times (108), implying that PGC1α loss contributes to gliomagenesis and the transition to glioblastoma. Once a GBM develops, the upregulation of PGC1α within a subset of tumors can promote aggressiveness by driving mitochondrial metabolism. Interestingly, the expression of PGC1α varies in distinct PTEN status; therefore, the protein levels of PGC1α are highest in the SF767 cells (PTEN wildtype) and lowest in the A172 cells (PTEN-deleted) (109).

Functional studies demonstrate that PGC1α seems to act as a tumor suppressor in GBM. Aurora kinase A (AURKA) has been implicated in GBM progression and is a potential therapeutic target for this aggressive brain cancer (106, 110). Research has shown that the inhibition of AURKA leads to c-Myc suppression, subsequently resulting in the upregulation of PGC1α, which in turn promotes oxidative metabolism. Furthermore, H3K27ac ChIP-seq and ATAC-seq show that chromatin accessibility at the potential c-Myc-binding region in the PGC1α promoter is increased, whereas following AURKA inhibition, the binding of c-Myc to the PGC1α promoter is reduced. Concurrently, an enhanced acetylation of the same region in PGC1α promoter has been observed following exposure to AURKA inhibition, indicating that c-Myc may act as a suppressor of PGC1α (106). Moreover, FDA-approved HDAC inhibitors, such as panobinostat, vorinostat, and romidepsin, have been shown to replicate these effects by blocking the Warburg effect in GBM cells. This interference with HDAC1/-2 reduces c-Myc levels while increasing PGC1α expression (111). Another inhibitor, crizotinib, which targets MET kinase (112, 113), induces the metabolic reprogramming of GBM cells. This reprogramming, characterized by heightened oxidative phosphorylation and fatty acid oxidation, is

also mediated by upregulated PGC1α expression and facilitated by increased CREB phosphorylation after Crizotinib exposure (14, 114). The mTORC1 pathway, crucial for cell growth and proliferation in GBM (115), is often activated by epidermal growth factor receptor (EGFR). However, mTORC1 inhibition, accompanied by reduced PGC1α expression, protects GBM cells from hypoxia-induced cell death under the conditions of the TME (116, 117). Thus, preclinical experiments have shown that, rapamycin, an mTORC1 inhibitor, triggers adverse effects by promoting cell survival in GBM under hypoxic conditions (116). Concurrently, mTORC1 activation, followed by increased PGC1α expression, sensitizes GBM cells to hypoxia-induced cell death (116).

Similar to other tumors, PGC1α exhibits dual effects in GBM, displaying both anticancer and pro-cancer roles in distinct subtypes. In particular, the fusion of the FGFR3 and TACC3 genes (F3-T3), which act as potent oncogenes, has been identified in approximately 3% of GBM cases (118, 119). PGC1α has been shown to be notably overexpressed in F3-T3-positive GBM cells in the presence of PIN4. Elevated PGC1α contributes to mitochondrial biogenesis and respiration through ERRγ. Conversely, dampening PGC1α activity hinders the tumor-promoting effects of F3-T3, as demonstrated in both cellular and animal models in GBM (120).

PGC1α in melanoma

Melanoma cells exhibit two distinct transcriptional signatures, proliferative and invasive, which correspond to different cellular phenotypes (121). The metastatic spread of melanoma is thought to involve a transition in cell behavior, shifting from a proliferative program to acquiring migratory and invasive characteristics (122). The expression of PGC1α generally defines these two subsets of melanoma cells (123). In the first subset, PGC1α has been found to be expressed at high levels and plays an important role in melanoma progression and survival. Its upregulation may be triggered by the microphthalmia-associated transcription factor (MITF) via its binding to the upstream regulatory promoter (5, 123, 124), an event regulated by the Wnt/β-Catenin pathway (125) or an important lipogenic enzyme-ATP-citrate lyase (ACLY) (126). Elevated levels of PGC1α are correlated with poor survival (13, 123). In this subset, PGC1α supports melanoma through various mechanisms, with programmed cell death being key. Apoptosis, a process that triggers cell death, is regulated by PGC1α through the regulation of reactive oxygen species (ROS) levels. Thus, suppression of PGC1α leads to a decrease in the expression of genes involved in ROS detoxification, resulting in elevated ROS levels and subsequent induction of apoptosis (123). Ferroptosis, another form of cell death, is involved in melanoma progression and chemoresistance (127). Small molecules that induce ferroptosis, such as RSL3 and ML162, suppress the expression of PGC1α through the Wnt/β-Catenin-MITF pathway. Loss of PGC1α impairs mitochondrial function and antioxidant capacity, leading to excess accumulation of mitochondrial ROS and sensitizing cells to ferroptosis (125). As the activation of the Wnt/β-Catenin pathway in melanoma guides resistance to anti-PD-L1/anti-CTLA-4 treatment (128, 129), targeting the Wnt/β-Catenin signaling pathway or PGC1α may improve the effectiveness of immunotherapy by inducing ferroptosis (129). Furthermore, PGC1α tightly interacts with ERRα in melanomas, promoting mitochondrial oxidative metabolism by regulating the expression of genes involved in oxidative phosphorylation and the TCA cycle (13). Depletion or pharmacological inhibition of ERRα selectively inhibits the growth of PGC1α-positive melanomas, but not PGC1α-negative melanomas (13). BAY 1238097, a potent inhibitor of BET binding to histones, strongly represses the expression of PGC1α in melanoma cells, impairing mitochondrial function and inhibiting melanoma cell proliferation (130). These findings support the concept that PGC1α-positive melanomas depend on mitochondrial metabolism for growth.

Conversely, another subpopulation of melanoma cells exhibits lower PGC1α expression, possesses a limited number of mitochondria, and relies heavily on glycolysis to produce energy. This phenotype is often observed in invasive and metastatic melanomas (131, 132). In this subset of melanoma cells, PGC1α may be epigenetically silenced through chromatin modifications involving H3K27 trimethylation at its promoter. Pharmacological inhibition of EZH2, an enzyme involved in chromatin modifications, diminishes H3K27me3 markers (133, 134), leading to increased PGC1α level and suppression of invasion in PGC1α-silenced cells (122). Additionally, BRAF mutation (V600E) suppresses MITF and PGC1α expression in melanoma cells (135). Knocking down PGC1α in these cells promotes a pro-metastatic gene program and enhances metastasis in mice models (131). PGC1α upregulates the expression of inhibitor of DNA binding protein (ID2), which binds and inhibits a diverse array of bHLH transcription factors (136). The binding of ID2 suppresses the transcription factor TCF4, resulting in the suppression of metastasis-related genes including integrins, which are known to affect metastasis (131, 137). Moreover, ID2 suppresses the activity of TCF12, which increases the expression of WNT5A (122). As WNT5A can stabilize YAP protein levels (138, 139), inhibition of TCF12, WNT5A, or YAP blocks melanoma migration and metastasis (122). BRAF inhibitors, such as PLX4032, which have been reported to upregulate PGC1α expression in melanomas (140, 141), inhibit metastasis partly by suppressing the Wnt/β-Catenin-MITF pathway and promoting the expression of PGC1α (125). This effect is independent of their cytotoxic or growth-inhibitory properties (131). Kisspeptin-1 (KISS1) functions as a metastasis suppressor by inhibiting metastasis without affecting primary tumor growth (142). In melanoma cells, the transcriptional coactivator PGC1α plays a crucial role in mediating the effects of KISS1 on cell metabolism and metastasis suppression (143). PGC1α helps KISS1 upregulate genes that promote fatty acid oxidation, activates AMPK signaling to inhibit acetyl-CoA carboxylase (ACC), and ultimately shifts cells towards mitochondrial oxidative phosphorylation instead of glycolysis (144). The loss of PGC1α blunts these metabolic changes and abolishes KISS1's anti-metastatic effects. The major implication of these bi-signatures is that effective melanoma therapies should target both proliferative and invasive cell types, as they coexist within tumors and can interconvert. Targeting only one phenotype may lead to the selection and outgrowth of alternative phenotypes. Indeed,

suppressing of PGC1α-dependent oxidative metabolism activates glycolysis via HIF1α as a compensatory survival mechanism in melanomas. Dual inhibition of PGC1α and HIF1α causes energetic deficits, but partial rescue of melanoma cells have been observed through glutamine utilization (145). Hence, a triple targeting approach involving PGC1α, HIF1α, and glutamine metabolism is necessary to completely block melanoma growth by shutting down oxidative metabolism, glycolysis, and glutaminolysis (145), suggesting that a combination therapy targeting multiple nodes of tumor metabolism is necessary to effectively disrupt energy production and viability, However, overcoming the challenges posed by metabolic heterogeneity and redundancy remains a significant obstacle.

PGC1α in prostate cancer

The expression of PGC1α has generally been found to be reduced in PC, with a further decrease observed in metastatic tissues (146). This downregulation of PGC1α is associated with decreased disease-free survival (DFS) (147–149). The exact reasons for the downregulation of PGC1α in PC are not fully understood; however, they are believed to be a result of selective pressure during disease progression and metabolic changes. Reports suggest that miRNAs, such as miR-34a-5p, can downregulate PGC1α (150).

It has been reported that PGC1α plays a tumor-suppressor role in the development of PC, inhibiting cancer progression and metastasis (146). Interestingly, some studies have found that the protein level of PGC1α is undetectable in PC cell lines, despite comparable transcript levels to metastatic PC specimens (146, 151). The re-expression of PGC1α *in vitro* and *in vivo* has been shown to inhibit cell proliferation and cell cycle progression, supporting its antiproliferative activity (146). Moreover, PGC1α suppresses the metastatic properties of PC cells by decreasing integrin signaling, causing cytoskeletal changes (152), and downregulating MYC levels and activity (153). This effect is mediated by its interaction with the transcriptional partner estrogen-related receptor alpha (ERRα). Knockout of ERRα prevents PGC1α from inhibiting invasion, suggesting that the PGC1α/ERRα axis acts as an antagonist to the progression of PC metastasis (146, 152). Furthermore, AMPK, a metabolic regulator in PC, safeguards against cancer progression in mice models (154–156). Activation of AMPK leads to increased expression of PGC1α and its downstream targets, promoting a switch to a more oxidative and catabolic metabolism and opposing the pro-tumorigenic program of increased lipogenesis (154). However, it has been found that androgens-activated AMPK can increase the expression of PGC1α, promoting mitochondrial content and PC cell growth in cell line models (151). Intriguingly, in a mouse model of benign prostatic hyperplasia, androgen/testosterone increased prostate size but did not affect PGC1α levels (151). These findings elucidate the complex roles of the AMPK/PGC1α axis in PC development.

In a subpopulation of clinical PC samples, PGC1α level is found to be overexpressed, and PGC1α may therefore exert a tumor supporting role (151, 157). In addition to the aforementioned AMPK signaling pathway, another mechanism contributing to the abnormal expression of PGC1α is the loss or mutation of p53 (158). In PC cells with mutated or deleted p53, PGC1α has been found to be expressed at high levels. Overexpression of wild-type p53 in these cells decreases the expression of PGC1α and causes mitochondrial dysfunction (157). However, this regulation axis is highly metabolic-pattern dependence, as p53 suppresses PGC1α level and nuclear localization through redox modification (159). In these settings, the tumor-supporting role of PGC1α is found to depend on the transcription factors (TFs) it partnered with. For example, PPARG activation results in the upregulation of AKT3, which subsequently promotes the nuclear localization of PGC1α. The genes induced by PGC1α promotes mitochondrial biogenesis and energy metabolism, fueling PC progression (160).

In addition, the ETS-related gene (ERG) functions as an oncogenic transcription factor in PC (161). In such cases, PGC1α has been shown to act as a coactivator for ERG, specifically under metabolic stress conditions like glucose deprivation and serum starvation (8). This interaction and coactivation of ERG by PGC1α leads to increased expression of antioxidant genes, such as SOD1 and TXN, which can help clear ROS and benefit PC growth (8).This suggests that PGC1α allows ERG fusion-positive PC cells to adapt and survive under metabolic stress by coactivating the antioxidant transcriptional program of ERG.

PGC1α in ovarian cancer

While PGC1α activity is typically low in normal tissues, several studies have reported frequent overexpression of PGC1α in ovarian tumors compared to that in normal ovaries (162, 163). However, it is important to note that the results of the high tumor expression of PGC1α only correlates with tumor differentiation and did not exhibit significant correlations with other clinical features (164). When combined with ERRα, the overexpression of PGC1α reveals a tendency towards increased risk of metastasis and reduced OS (163). Additionally, the expression of both PGC1α and PGC1β has allowed for the classification of ovarian cancer (OC) patients into distinct subgroups. Approximately 25% of studies tumors exhibits high expression of both genes (164), indicating the presence of an overactive mitochondrial gene program. These tumors demonstrates increased mitochondrial content, oxidative metabolism, and OXPHOS (164). Mechanistic studies have shed light on how the aberrant activation of PGC1α contributes to OC progression and therapeutic resistance. Recent studies have identified PGC1α as a critical driver of OC progression, particularly in high-grade serous OC (HGSOC), which exhibits metabolic heterogeneity (165–167). In OC, the high-OXPHOS state has been linked to chronic oxidative stress (165). This stress leads to the increased aggregation of PML nuclear bodies, which subsequently activates PGC1α through deacetylation. As a result, PGC1α induces the expression of electron transport chain (ETC) components, enhancing mitochondrial respiration in high-OXPHOS cancer cells. Knockdown of PGC1α reduces both ETC gene expression and oxygen consumption rate in these cells (165). Furthermore, PGC1α plays a pivotal role in mediating the response to conventional chemotherapies. PGC1α has been found to be a key regulator of

reactive ROS production (165), which are crucial determinants of the apoptotic response to cisplatin in OC cells (168). Elevated expression or activity of PGC1α is correlated with enhanced chemosensitivity by promoting mitochondrial oxidative metabolism and respiration (165). Conversely, reducing PGC1α activity and levels decreases sensitivity to chemotherapy in OC.

PGC1α in nasopharyngeal carcinoma

There is increasing evidence that metabolic reprogramming driven by PGC1α promotes NPC progression and resistance to treatment. PGC1α has been found to be upregulated in NPC and its high expression has been associated with shorter OS after radiation therapy (169). PGC1α contributes to NPC cell survival by activating FAO pathways, which provide cells with ATP and the antioxidant NADPH. These metabolic alterations allow NPC cells to adapt and thrive under challenging conditions. PGC1α works in conjunction with the transcription factor CEBPB to enhance the expression of CPT1A, a gene involved in FAO, thereby sustaining this metabolic reprogramming (169). Consequently, these changes confer radioresistance to NPC cells (169). Furthermore, TGFβ1, a signaling molecule, can upregulate PGC1α and activate FAO to facilitate EMT and invasion of NPC cells. Specifically, TGFβ1 stimulates phosphorylation and expression of AMPKα1 (170), which, in turn, phosphorylates and activates PGC1α in NPC. This activation leads to transcriptional upregulation of FAO-related genes (170). Inhibiting PGC1α expression and components of the FAO pathway have been shown to reduce EMT, invasion, and metastasis of NPC both *in vitro* and *in vivo*.

PGC1α in breast cancer

Overall, PGC1α expression has been found to be reduced in breast tumor tissues compared to that in the normal breast epithelium (171, 172). This downregulation of PGC1α potentially facilitates the Warburg effect, in which cells increase their dependence on glycolysis and glucose uptake, while decreasing mitochondrial oxidative phosphorylation, even when oxygen is available (173). Such metabolic shifts enhance the proliferation and survival of cancer cells. A key mechanism that drives this shift is the regulation of mitochondrial deacetylase SIRT3 (171, 174). Although the exact cause of PGC1α's downregulation in BC cells is yet to be fully elucidated, certain epigenetic modifications such as negative regulation by miR-485 and miR-217 have been proposed (175, 176). Interestingly, despite its general downregulation in breast tumors, the expression of PGC1α varies according to tumor subtypes and their metastatic tendencies. Specifically, $HER2^+$ and triple-negative breast tumors (TNBT) express high levels of PGC1α (177, 178). Moreover, elevated expression of PGC1α has been detected in BC cells that predominantly metastasize to the lungs or bone, as opposed to the liver and brain (179). Similarly, circulating tumor cells (CTCs) released from BC in mice models and patients exhibit elevated PGC1α expression (180). Indeed, PGC1α knockdown in a metastatic cell line has been found to result in reduced CTC numbers and metastasis, whereas overexpression of PGC1α has been found to increase lung metastasis *in vivo* (179, 180). Interestingly, BC cells with low PGC1α levels possess increased metastatic ability when overexpressing PGC1α levels (180). It is worth noting that inhibiting mitochondrial respiration with biguanides in such cells is not found to mitigate PGC1α-induced metastasis (179), suggesting that the augmented metastatic phenotype is not simply attributed to the PGC1α-induced escalation in oxidative phosphorylation. Instead, PGC1α increases overall bioenergetic capacity and flexibility to facilitate metastasis, allowing cancer cells to cope with energy disruptors (179). In these conditions, the induced PGC1α ensures the metabolic demands of aggressive breast tumors.

Early research has also highlighted PGC1α's involvement in the initiation of BC (181). In particular, its interaction with EglN2, an enzyme involved in the regulation of the hypoxia-inducible factor (HIF) pathway, appears to be central to the modulation of mitochondrial function and has been implicated in BC tumorigenesis (182, 183). In both normoxic and hypoxia conditions, EglN2 forms a complex with both PGC1α and NRF1, leading to the induction of FDXR. This maintains mitochondrial function and contributes to breast tumorigenesis in an HIF-independent manner (182). Importantly, in the absence of PGC1α, the effects of EglN2 overexpression on BC cells are blocked.

Furthermore, PGC1α's metabolic regulatory functions in BC often operate in collaboration with other transcription factors like ERRα or p53. For instance, the interplay between PGC1α and ERRα governs a spectrum of metabolic genes (172), driving increased mitochondrial respiration, ATP production, and other processes that culminate in heightened tumor aggression and drug resistance in BC (177, 184, 185). In $ERBB2^+$ cancer cells, PGC1α positively regulates glutamine metabolism in conjunction with ERRα (177). This regulation contributes to increased glutamine uptake, increased flux through the citric acid cycle (CAC), and enhanced lipogenesis from glutamine, particularly under hypoxic conditions (177). The AMPK orchestrates this energy-sensor axis of PGC1α/ERRα (186). When AMPK is activated, PGC1α/ERRα represses folate cycle and one-carbon metabolism, which are vital for sustaining cell growth in cancer cells. Consequently, repression increases the sensitivity to anti-folate therapy (186). It is well established that mutant p53 confers pro-tumorigenic functions in BCs. Notably, as a key downstream of p53, its function is differentially controlled by the codon 72 variant, highlighting the importance of PGC1α as a "gain-of-function" partner of mutant p53 (187).

From a therapeutic point of view, early studies have hinted at the potential benefits of targeting PGC1α in BC treatment. For instance, interventions with vascular endothelial growth factor receptor 2 (VEGFR2) blockade or the AMPK signaling activator, 5-aminoimidazole-4-carboxamide riboside (AICAR), have shown promising shifts in mitochondrial biogenesis and cancer cell behaviors by modulating PGC1α. One study shows that VEGFR2 blockade by Ki8751 leads to increased activity of PGC1α and thereby stimulates the expression of TFAM, which is essential for mitochondrial DNA transcription and replication (188).

Subsequent metabolic reprogramming contributes to increased ROS production and apoptosis in BC cells treated with Ki8751 (188). Moreover, AICAR increases PGC1α expression in triple-negative BC (TNBC) cells (189), mediating mitochondrial biogenesis and contributing to a reduced pro-tumor phenotype and increased chemosensitivity (189). Compound 11, a novel inverse agonist targeting ERRα (190), disrupts ERRα binding to its coactivator PGC1α, with promising anti-tumor activity against triple-negative BC cells and tumors (190). The use of polyethylene glycol-modified graphene oxide (PEG-GO) also results in the selective suppression of PGC1α in cancer cells (191). The reduced ATP production impairs the assembly of the F-actin cytoskeleton and formation of lamellipodia, consequently inhibiting the migration and invasion of metastatic BC cells (191). Importantly, the induction of PGC1α guides drug resistance in the course of chemotherapy of BC (5). Endocrine-resistant BC cells have shown higher PGC1α expression than the parental sensitive lines. PGC1α sensitizes BC cells to low estrogen levels during estrogen deprivation therapy (192–194). This may be an early adaptive response to endocrine therapy that potentially contributes to the development of chemoresistance over time by allowing estrogen hypersensitivity (192). Therefore, inhibiting PGC1α with SR-18292 prevents the growth of therapy resistant cell lines in a dose-dependent manner, while re-expression of PGC1α increases the viability of resistant cells when treating with certain endocrine therapies, such as tamoxifen, fulvestrant, palbociclib, or aromatase inhibitors (193).

Implications of PGC1α in the tumor microenvironment

The tumor microenvironment (TME) is a complex and dynamic landscape where cancer cells interact with, including immune cells, fibroblasts, and the extracellular matrix. The role of PGC1α in the TME is pivotal yet underexplored. Its involvement goes beyond mere energy metabolism, extending to modulating immune responses and influencing tumor progression and therapy resistance.

Significant insights have been gathered from studies on T cells. Naive T cells normally have high levels of PGC1α, which support their metabolic demands for proliferation and effector functions through mitochondrial biogenesis and oxidative metabolism. However, during T-cell activation, PGC1α expression is progressively repressed (195, 196). Notably, one study observes that, although the mRNA expression of PGC1α in memory $CD8^+$ T cells decreases upon activation, its protein expression increases (197). This suggests that specific post-translational mechanisms may regulate the stability of PGC1α in $CD8^+$ T cells. In melanomas, tumor-infiltrating T cells have shown a loss of PGC1α level due to the chronic AKT signal activation (195). Additionally, exhausted T cells, experiencing continuous stimulation and hypoxia increase expression of Blimp-1, which further suppress PGC1α expression (196). This impairs their adaptive metabolic responses to hypoxia via mitochondrial biogenesis. Of note, overexpressing PGC1α in these cells enhances their persistence and recall responses, particularly improving the central memory T cell formation and sustained metabolic fitness upon re-exposure to infections (197). Interestingly, the co-stimulatory molecule 4-1BB, which is abundantly expressed in exhausted T cells, promotes mitochondrial biogenesis, fusion, and respiratory capacity (198–200). Costimulation with 4-1BB elevates PGC1α levels, mediating the metabolic effects of 4-1BB signaling (199). Without PGC1α, 4-1BB agonists are less effective at enhancing mitochondrial function and improving anti-tumor responses, or enhance adoptive T cell therapy (199). Thus, restoring the PGC1α expression in functional T cells could offer a strategy to reprogram metabolism in tumor-infiltrating T cells and boost their anti-tumor activity.

Research also shows that PPARγ is essential for maturation of alternatively activated macrophages, enabling monocytes to differentiate into M2 macrophages (201, 202). Indeed, the expression of PGC1α is elevated in these macrophages (203). In breast cancer, a reduced level of miR-382 maintains PGC1α expression in tumor-associated macrophages (203), facilitating the induction of the M2 type through the PPARγ signaling pathway. Fibroblasts also respond to regulation by PGC1α. A recent study found that knocking down PGC1α in normal human lung fibroblasts reduces mitochondrial mass and function (204). This alteration increases activation of matrix synthetic fibroblasts along with secretion of soluble profibrotic factors (204). In mouse models, the loss of PGC1α in induced mouse embryonic fibroblasts (iMEFs) leads to a more aggressive and metastatic melanoma phenotype (205). Similarly, lower PGC1α expression in cancer-associated fibroblasts (CAFs) of oral squamous cell carcinoma (OSCC) enhances the proangiogenic phenotype of CAFs through the PGC1α/PFKFB3 axis (206). Moreover, PGC1α impacts mesenchymal stromal cells (MSCs) (207). In melanoma, cancer cells attract MSCs to the tumor site and induce mitochondrial biogenesis by upregulating PGC1α (207). Furthermore, PGC1α controls mitochondrial transfer from MSCs to melanoma cells, thereby supporting melanoma growth (207).

Discussion

PGC1α is rapidly establishing itself as an indispensable regulator of cancer cell metabolism across numerous malignancies. In cancers, multiple mechanisms are involved in the abnormal expression of PGC1α, particularly in the transcriptional regulation. Therefore, based on the current research progress, we have summarized the relevant findings (Figure 2).

Although the expression and functions of PGC1α are context-dependent, it primarily serves as a pivotal orchestrator of mitochondrial biogenesis, oxidative metabolism, antioxidant defenses, and other cellular processes. When PGC1α expression is downregulated, the Warburg effect is facilitated, leading to disease advancement. Subsequent metabolic aberrations can be rectified by reinstating PGC1α levels. This may halt cell proliferation and invasion, and make cells more receptive to chemotherapy. In contrast, PGC1α upregulation promotes oxidative phosphorylation, allows cancer cells to adapt to stress, and promotes a more aggressive cancer phenotype. This duality in biological behavior shows PGC1α's adaptability in aligning with various co-regulators and executing

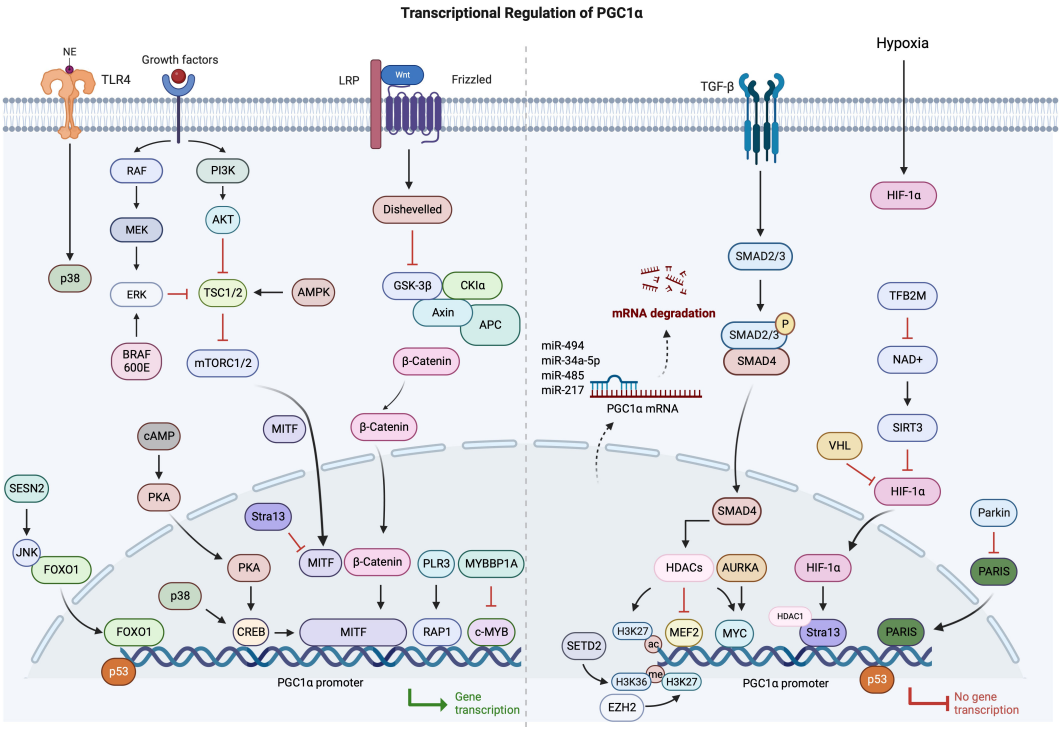

FIGURE 2
Schematic overview of transcriptional regulation of PGC1a in cancers.

functions tailored to its environment. Thus, to target PGC1α effectively, understanding its nuanced role in each cancer subtype is indispensable.

Central to PGC1α's operations is its position at the crossroads of several pivotal signaling pathways involved in cancer. It processes signals from the Wnt/β-catenin, TGF-β, AMPK, AKT, and p53 pathways to regulate downstream metabolic activities. By partnering with transcription factors like ERRα, NRF1, and YAP, PGC1α can drive specific changes in gene expression. Moreover, post-translational modifications such as phosphorylation and acetylation offer another layer of control over its activity. Decoding these intricate molecular ties is a critical step in comprehending PGC1α's multifaceted functions and how they may go awry in cancer. An intriguing development is the increasing evidence of PGC1α's profound effect on the tumor microenvironment, particularly its interaction with immune cells.

Strategic targeting of PGC1α in cancer therapy, therefore, requires a nuanced approach that considers its dual functionality. In cases where PGC1α functions as a tumor suppressor, its upregulation or enhanced activity can shift cancer cell metabolism away from the Warburg effect. This metabolic shift involves reducing glycolysis and increasing oxidative phosphorylation, which typically slows cancer progression and may make cancer cells more amenable to interventions that induce metabolic stress. Enhancing PGC1α's expression could be achieved through gene therapy techniques, and small molecule activators. Conversely, in cancers where PGC1α contributes to a more aggressive phenotype, its function is linked to enhanced oxidative phosphorylation, supporting cancer cell adaptation to metabolic and oxidative stress. In such cases, inhibiting PGC1α might reduce the cancer cells' ability to sustain high energy demands and resist hostile environments, such as those imposed by chemotherapy. This can be approached through the use of small molecule inhibitors that disrupt PGC1α's interaction with its coactivators or transcription factors it regulates. Additionally, RNA interference technologies could selectively knock down PGC1α mRNA, diminishing its protein levels and thus its functionality in cancer cells. Both strategies—enhancing or inhibiting PGC1α—must consider the cancer type, the specific metabolic profile of the tumor, and the systemic implications of altering metabolic pathways. For instance, enhancing oxidative metabolism in non-tumor cells might also affect normal cells, leading to unintended consequences like increased reactive oxygen species. Similarly, inhibiting PGC1α in aggressive tumors must be carefully managed to avoid crippling normal cells' ability to manage oxidative stress. Effective therapeutic strategies should aim to disrupt this metabolic adaptability by targeting PGC1α along with its regulatory network to block compensatory pathways that facilitate resistance to therapy. Furthermore, PGC1α's impact on the tumor microenvironment, particularly through its influence on the metabolic states of T cells and macrophages, is gaining attention. By modulating immune cell metabolism, PGC1α could potentially alter the immunological landscape of tumors, reducing immune suppression and enhancing the efficacy of immunotherapies. This understanding suggests that strategies which leverage PGC1α's role in the tumor microenvironment could complement direct targeting approaches, creating a multifaceted attack on tumor growth.

In summary, PGC1α's multifaceted roles in cancer metabolism indicate that it is a promising therapeutic target for cancer. Developing drugs that can specifically modulate PGC1α's activity, tailored to the unique metabolic profiles of different cancer types,

represents a promising approach in oncology. By doing these, we are now on the brink of translating our understanding of this metabolic mediator into its clinical benefits against cancer.

Author contributions

YW: Writing – review & editing, Writing – original draft, Investigation. JP: Resources, Methodology, Writing – review & editing, Writing – original draft. DY: Software, Writing – review & editing, Writing – original draft. ZX: Validation, Writing – review & editing, Writing – original draft. BJ: Resources, Writing – review & editing, Writing – original draft. XD: Methodology, Writing – review & editing, Writing – original draft. CJ: Investigation, Conceptualization, Writing – review & editing, Writing – original draft. BO: Visualization, Validation, Methodology, Data curation, Writing – review & editing, Writing – original draft, Funding acquisition. LS: Supervision, Software, Resources, Project administration, Investigation, Funding acquisition, Formal analysis, Conceptualization, Writing – review & editing, Writing – original draft, Visualization, Validation, Methodology, Data curation.

Funding

The author(s) declare financial support was received for the research, authorship, and/or publication of this article. This work was supported by Nanjing Medical Science and technique Development Foundation (Grant No. QRX17105).

Acknowledgments

We would like to thank Editage (www.editage.cn) for English language editing. We also thank the bioRender website (BioRender.com) for providing us with great convenience in creating graphics.

Conflict of interest

The authors declare that the research was conducted in the absence of any commercial or financial relationships that could be construed as a potential conflict of interest.

Publisher's note

All claims expressed in this article are solely those of the authors and do not necessarily represent those of their affiliated organizations, or those of the publisher, the editors and the reviewers. Any product that may be evaluated in this article, or claim that may be made by its manufacturer, is not guaranteed or endorsed by the publisher.

References

1. Tan Z, Luo X, Xiao L, Tang M, Bode AM, Dong Z, et al. The role of PGC1α in cancer metabolism and its therapeutic implications. *Mol Cancer Ther*. (2016) 15:774–82. doi: 10.1158/1535-7163.MCT-15-0621

2. Zuo Q, He J, Zhang S, Wang H, Jin G, Jin H, et al. PPARγ Coactivator-1α Suppresses metastasis of hepatocellular carcinoma by inhibiting warburg effect by PPARγ-dependent WNT/β-catenin/pyruvate dehydrogenase kinase isozyme 1 axis. *Hepatology*. (2021) 73:644–60. doi: 10.1002/hep.31280

3. Mastropasqua F, Girolimetti G, Shoshan M. PGC1α: friend or foe in cancer? *Genes (Basel)*. (2018) 9(1):48. doi: 10.3390/genes9010048

4. Bost F, Kaminski L. The metabolic modulator PGC-1α in cancer. *Am J Cancer Res*. (2019) 9:198–211.

5. Luo C, Widlund HR, Puigserver P. PGC-1 coactivators: shepherding the mitochondrial biogenesis of tumors. *Trends Cancer*. (2016) 2:619–31. doi: 10.1016/j.trecan.2016.09.006

6. Finck BN, Kelly DP. PGC-1 coactivators: inducible regulators of energy metabolism in health and disease. *J Clin Invest*. (2006) 116:615–22. doi: 10.1172/JCI27794

7. Lin J, Handschin C, Spiegelman BM. Metabolic control through the PGC-1 family of transcription coactivators. *Cell Metab*. (2005) 1:361–70. doi: 10.1016/j.cmet.2005.05.004

8. Dhara A, Aier I, Paladhi A, Varadwaj PK, Hira SK, Sen N. PGC1 alpha coactivates ERG fusion to drive antioxidant target genes under metabolic stress. *Commun Biol*. (2022) 5:416. doi: 10.1038/s42003-022-03385-x

9. Jamwal S, Blackburn JK, Elsworth JD. PPARγ/PGC1α signaling as a potential therapeutic target for mitochondrial biogenesis in neurodegenerative disorders. *Pharmacol Ther*. (2021) 219:107705. doi: 10.1016/j.pharmthera.2020.107705

10. Zhu X, Shen W, Yao K, Wang H, Liu B, Li T, et al. Fine-tuning of PGC1α Expression regulates cardiac function and longevity. *Circ Res*. (2019) 125:707–19. doi: 10.1161/CIRCRESAHA.119.315529

11. Sainero-Alcolado L, Liaño-Pons J, Ruiz-Pérez MV, Arsenian-Henriksson M. Targeting mitochondrial metabolism for precision medicine in cancer. *Cell Death Differ*. (2022) 29:1304–17. doi: 10.1038/s41418-022-01022-y

12. Qian L, Zhu Y, Deng C, Liang Z, Chen J, Chen Y, et al. Peroxisome proliferator-activated receptor gamma coactivator-1 (PGC-1) family in physiological and pathophysiological process and diseases. *Signal Transduct Target Ther*. (2024) 9:50. doi: 10.1038/s41392-024-01756-w

13. Luo C, Balsa E, Thomas A, Hatting M, Jedrychowski M, Gygi SP, et al. ERRα Maintains mitochondrial oxidative metabolism and constitutes an actionable target in PGC1α-elevated melanomas. *Mol Cancer Res*. (2017) 15:1366–75. doi: 10.1158/1541-7786.MCR-17-0143

14. Xing F, Luan Y, Cai J, Wu S, Mai J, Gu J, et al. The Anti-Warburg Effect Elicited by the cAMP-PGC1α Pathway Drives Differentiation of Glioblastoma Cells into Astrocytes. *Cell Rep*. (2017) 18:468–81. doi: 10.1016/j.celrep.2016.12.037

15. Qian X, Li X, Shi Z, Bai X, Xia Y, Zheng Y, et al. KDM3A senses oxygen availability to regulate PGC-1α-mediated mitochondrial biogenesis. *Mol Cell*. (2019) 76:885–95.e7. doi: 10.1016/j.molcel.2019.09.019

16. Dominy JEJr., Lee Y, Jedrychowski MP, Chim H, Jurczak MJ, Camporez JP, et al. The deacetylase Sirt6 activates the acetyltransferase GCN5 and suppresses hepatic gluconeogenesis. *Mol Cell*. (2012) 48:900–13. doi: 10.1016/j.molcel.2012.09.030

17. Liu CL, Yang PS, Wang TY, Huang SY, Kuo YH, Cheng SP. PGC1α downregulation and glycolytic phenotype in thyroid cancer. *J Cancer*. (2019) 10:3819–29. doi: 10.7150/jca.30018

18. Li Y, Hei H, Zhang S, Gong W, Liu Y, Qin J. PGC-1α participates in tumor chemoresistance by regulating glucose metabolism and mitochondrial function. *Mol Cell Biochem*. (2023) 478:47–57. doi: 10.1007/s11010-022-04477-2

19. Cheng SP, Chen MJ, Chien MN, Lin CH, Lee JJ, Liu CL. Overexpression of teneurin transmembrane protein 1 is a potential marker of disease progression in papillary thyroid carcinoma. *Clin Exp Med*. (2017) 17:555–64. doi: 10.1007/s10238-016-0445-y

20. Veschi V, Turdo A, Modica C, Verona F, Di Franco S, Gaggianesi M, et al. Recapitulating thyroid cancer histotypes through engineering embryonic stem cells. *Nat Commun*. (2023) 14:1351. doi: 10.1038/s41467-023-36922-1

21. Chen D, Su X, Zhu L, Jia H, Han B, Chen H, et al. Papillary thyroid cancer organoids harboring BRAF(V600E) mutation reveal potentially beneficial effects of

BRAF inhibitor-based combination therapies. *J Transl Med*. (2023) 21:9. doi: 10.1186/s12967-022-03848-z

22. Witherspoon M, Sandu D, Lu C, Wang K, Edwards R, Yeung A, et al. ETHE1 overexpression promotes SIRT1 and PGC1α mediated aerobic glycolysis, oxidative phosphorylation, mitochondrial biogenesis and colorectal cancer. *Oncotarget*. (2019) 10:4004–17. doi: 10.18632/oncotarget.v10i40

23. Yun CW, Lee JH, Lee SH. Hypoxia-induced PGC-1α Regulates mitochondrial function and tumorigenesis of colorectal cancer cells. *Anticancer Res*. (2019) 39:4865–76. doi: 10.21873/anticanres.13672

24. Lai HT, Chiang CT, Tseng WK, Chao TC, Su Y. GATA6 enhances the stemness of human colon cancer cells by creating a metabolic symbiosis through upregulating LRH-1 expression. *Mol Oncol*. (2020) 14:1327–47. doi: 10.1002/1878-0261.12647

25. Kitaoka Y, Takeda K, Tamura Y, Hatta H. Lactate administration increases mRNA expression of PGC-1α and UCP3 in mouse skeletal muscle. *Appl Physiol Nutr Metab*. (2016) 41:695–8. doi: 10.1139/apnm-2016-0016

26. Torrens-Mas M, Hernández-López R, Pons DG, Roca P, Oliver J, Sastre-Serra J. Sirtuin 3 silencing impairs mitochondrial biogenesis and metabolism in colon cancer cells. *Am J Physiol Cell Physiol*. (2019) 317:C398–c404. doi: 10.1152/ajpcell.00112.2019

27. Yang Y, Lian S, Meng L, Tian Z, Feng Q, Wang Y, et al. Knockdown of PRL-3 increases mitochondrial superoxide anion production through transcriptional regulation of RAP1. *Cancer Manag Res*. (2018) 10:5071–81. doi: 10.2147/CMAR

28. Ogata R, Mori S, Kishi S, Sasaki R, Iwata N, Ohmori H, et al. Linoleic acid upregulates microrna-494 to induce quiescence in colorectal cancer. *Int J Mol Sci*. (2021) 23(1):225. doi: 10.3390/ijms23010225

29. Liu S, Zhao H, Hu Y, Yan C, Mi Y, Li X, et al. Lactate promotes metastasis of normoxic colorectal cancer stem cells through PGC-1α-mediated oxidative phosphorylation. *Cell Death Dis*. (2022) 13:651. doi: 10.1038/s41419-022-05111-1

30. Yazdani HO, Roy E, Comerci AJ, van der Windt DJ, Zhang H, Huang H, et al. Neutrophil extracellular traps drive mitochondrial homeostasis in tumors to augment growth. *Cancer Res*. (2019) 79:5626–39. doi: 10.1158/0008-5472.CAN-19-0800

31. Boughanem H, Cabrera-Mulero A, Hernández-Alonso P, Bandera-Merchán B, Tinahones A, Tinahones FJ, et al. The expression/methylation profile of adipogenic and inflammatory transcription factors in adipose tissue are linked to obesity-related colorectal cancer. *Cancers (Basel)*. (2019) 11(11):1629. doi: 10.3390/cancers11111629

32. Xiong H, Ye J, Xie K, Hu W, Xu N, Yang H. Exosomal IL-8 derived from Lung Cancer and Colon Cancer cells induced adipocyte atrophy via NF-κB signaling pathway. *Lipids Health Dis*. (2022) 21:147. doi: 10.1186/s12944-022-01755-2

33. Huot JR, Novinger LJ, Pin F, Bonetto A. HCT116 colorectal liver metastases exacerbate muscle wasting in a mouse model for the study of colorectal cancer cachexia. *Dis Model Mech*. (2020) 13(1):dmm043166. doi: 10.1242/dmm.043166

34. Barreto R, Mandili G, Witzmann FA, Novelli F, Zimmers TA, Bonetto A. Cancer and chemotherapy contribute to muscle loss by activating common signaling pathways. *Front Physiol*. (2016) 7:472. doi: 10.3389/fphys.2016.00472

35. Alonso-Molero J, González-Donquiles C, Fernández-Villa T, de Souza-Teixeira F, Vilorio-Marqués L, Molina AJ, et al. Alterations in PGC1α expression levels are involved in colorectal cancer risk: a qualitative systematic review. *BMC Cancer*. (2017) 17:731. doi: 10.1186/s12885-017-3725-3

36. Yun SH, Roh MS, Jeong JS, Park JI. Peroxisome proliferator-activated receptor γ coactivator-1α is a predictor of lymph node metastasis and poor prognosis in human colorectal cancer. *Ann Diagn Pathol*. (2018) 33:11–6. doi: 10.1016/j.anndiagpath.2017.11.007

37. Cho JG, Park SJ, Han SH, Park JI. PGC-1α Regulates cell proliferation, migration, and invasion by modulating leucyl-tRNA synthetase 1 expression in human colorectal cancer cells. *Cancers (Basel)*. (2022) 15(1):159. doi: 10.3390/cancers15010159

38. Yun SH, Shin SW, Park JI. Expression of fatty acid synthase is regulated by PGC −1α and contributes to increased cell proliferation. *Oncol Rep*. (2017) 38:3497–506. doi: 10.3892/or

39. Yun SH, Park JI. PGC-1α Regulates cell proliferation and invasion via AKT/GSK-3β/β-catenin pathway in human colorectal cancer SW620 and SW480 cells. *Anticancer Res*. (2020) 40:653–64. doi: 10.21873/anticanres.13995

40. Yun CW, Han YS, Lee SH. PGC-1α Controls mitochondrial biogenesis in drug-resistant colorectal cancer cells by regulating endoplasmic reticulum stress. *Int J Mol Sci*. (2019) 20(7):1707. doi: 10.3390/ijms20071707

41. Vellinga TT, Borovski T, de Boer VC, van Schelven S, Trumpi K, Verheem A, et al. SIRT1/PGC1α-dependent increase in oxidative phosphorylation supports chemotherapy resistance of colon cancer. *Clin Cancer Res*. (2015) 21:2870–9. doi: 10.1158/1078-0432.CCR-14-2290

42. Afrin S, Giampieri F, Gasparrini M, Forbes-Hernández TY, Cianciosi D, Reboredo-Rodriguez P, et al. The inhibitory effect of Manuka honey on human colon cancer HCT-116 and LoVo cell growth. Part 2: Induction of oxidative stress, alteration of mitochondrial respiration and glycolysis, and suppression of metastatic ability. *Food Funct*. (2018) 9:2158–70. doi: 10.1039/C8FO00165K

43. Kamarudin MNA, Sarker MMR, Zhou JR, Parhar I. Metformin in colorectal cancer: molecular mechanism, preclinical and clinical aspects. *J Exp Clin Cancer Res*. (2019) 38:491. doi: 10.1186/s13046-019-1495-2

44. Wang P, Guo X, Zong W, Li Y, Liu G, Lv Y, et al. PGC-1α/SNAI1 axis regulates tumor growth and metastasis by targeting miR-128b in gastric cancer. *J Cell Physiol*. (2019) 234:17232–41. doi: 10.1002/jcp.28193

45. Hu XT, Ding C, Zhou N, Xu C. Quercetin protects gastric epithelial cell from oxidative damage in *vitro* and in vivo. *Eur J Pharmacol*. (2015) 754:115–24. doi: 10.1016/j.ejphar.2015.02.007

46. Li W, Wong CC, Zhang X, Kang W, Nakatsu G, Zhao Q, et al. CAB39L elicited an anti-Warburg effect via a LKB1-AMPK-PGC1α axis to inhibit gastric tumorigenesis. *Oncogene*. (2018) 37:6383–98. doi: 10.1038/s41388-018-0402-1

47. Pavlova NN, Thompson CB. The emerging hallmarks of cancer metabolism. *Cell Metab*. (2016) 23:27–47. doi: 10.1016/j.cmet.2015.12.006

48. Hanahan D, Weinberg RA. Hallmarks of cancer: the next generation. *Cell*. (2011) 144:646–74. doi: 10.1016/j.cell.2011.02.013

49. Wu H, Liu B, Chen Z, Li G, Zhang Z. MSC-induced lncRNA HCP5 drove fatty acid oxidation through miR-3619-5p/AMPK/PGC1α/CEBPB axis to promote stemness and chemo-resistance of gastric cancer. *Cell Death Dis*. (2020) 11:233. doi: 10.1038/s41419-020-2426-z

50. Foda ZH, Annapragada AV, Boyapati K, Bruhm DC, Vulpescu NA, Medina JE, et al. Detecting liver cancer using cell-free DNA fragmentomes. *Cancer Discovery*. (2023) 13:616–31. doi: 10.1158/2159-8290.CD-22-0659

51. Toh MR, Wong EYT, Wong SH, Ng AWT, Loo LH, Chow PK, et al. Global epidemiology and genetics of hepatocellular carcinoma. *Gastroenterology*. (2023) 164:766–82. doi: 10.1053/j.gastro.2023.01.033

52. Åberg F, Byrne CD, Pirola CJ, Männistö V, Sookoian S. Alcohol consumption and metabolic syndrome: Clinical and epidemiological impact on liver disease. *J Hepatol*. (2023) 78:191–206. doi: 10.1016/j.jhep.2022.08.030

53. Wu D, Yang Y, Hou Y, Zhao Z, Liang N, Yuan P, et al. Increased mitochondrial fission drives the reprogramming of fatty acid metabolism in hepatocellular carcinoma cells through suppression of Sirtuin 1. *Cancer Commun (Lond)*. (2022) 42:37–55. doi: 10.1002/cac2.12247

54. Kim H, Lee JY, Park SJ, Kwag E, Koo O, Shin JH. ZNF746/PARIS promotes the occurrence of hepatocellular carcinoma. *Biochem Biophys Res Commun*. (2021) 563:98–104. doi: 10.1016/j.bbrc.2021.05.051

55. Kumar A, Giri S, Shaha C. Sestrin2 facilitates glutamine-dependent transcription of PGC-1α and survival of liver cancer cells under glucose limitation. *FEBS J*. (2018) 285:1326–45. doi: 10.1111/febs.14406

56. Hu Y, Shin DJ, Pan H, Lin Z, Dreyfuss JM, Camargo FD, et al. YAP suppresses gluconeogenic gene expression through PGC1α. *Hepatology*. (2017) 66:2029–41. doi: 10.1002/hep.29373

57. Geng X, Geng Z, Li H, Zhang Y, Li J, Chang H. Over-expression of TFB2M facilitates cell growth and metastasis via activating ROS-Akt-NF-κB signalling in hepatocellular carcinoma. *Liver Int*. (2020) 40:1756–69. doi: 10.1111/liv.14440

58. Chang H, Li J, Luo Y, Wu B, Yuan C, Geng X. TFB2M activates aerobic glycolysis in hepatocellular carcinoma cells through the NAD(+) /SIRT3/HIF-1α signaling. *J Gastroenterol Hepatol*. (2021) 36:2978–88. doi: 10.1111/jgh.15548

59. Zhu L, Wang Q, Zhang L, Fang Z, Zhao F, Lv Z, et al. Hypoxia induces PGC-1α expression and mitochondrial biogenesis in the myocardium of TOF patients. *Cell Res*. (2010) 20:676–87. doi: 10.1038/cr.2010.46

60. Arany Z, Foo SY, Ma Y, Ruas JL, Bommi-Reddy A, Girnun G, et al. HIF-independent regulation of VEGF and angiogenesis by the transcriptional coactivator PGC-1alpha. *Nature*. (2008) 451:1008–12. doi: 10.1038/nature06613

61. Tohme S, Yazdani HO, Liu Y, Loughran P, van der Windt DJ, Huang H, et al. Hypoxia mediates mitochondrial biogenesis in hepatocellular carcinoma to promote tumor growth through HMGB1 and TLR9 interaction. *Hepatology*. (2017) 66:182–97. doi: 10.1002/hep.29184

62. Yao G, Yin J, Wang Q, Dong R, Lu J. Glypican-3 enhances reprogramming of glucose metabolism in liver cancer cells. *BioMed Res Int*. (2019) 2019:2560650. doi: 10.1155/2019/2560650

63. Iansante V, Choy PM, Fung SW, Liu Y, Chai JG, Dyson J, et al. PARP14 promotes the Warburg effect in hepatocellular carcinoma by inhibiting JNK1-dependent PKM2 phosphorylation and activation. *Nat Commun*. (2015) 6:7882. doi: 10.1038/ncomms8882

64. Icard P, Simula L, Wu Z, Berzan D, Sogni P, Dohan A, et al. Why may citrate sodium significantly increase the effectiveness of transarterial chemoembolization in hepatocellular carcinoma? *Drug Resist Update*. (2021) 59:100790. doi: 10.1016/j.drup.2021.100790

65. Gunewardena S, Huck I, Walesky C, Robarts D, Weinman S, Apte U. Progressive loss of hepatocyte nuclear factor 4 alpha activity in chronic liver diseases in humans. *Hepatology*. (2022) 76:372–86. doi: 10.1002/hep.32326

66. Liu Q, Li J, Zhang W, Xiao C, Zhang S, Nian C, et al. Glycogen accumulation and phase separation drives liver tumor initiation. *Cell*. (2021) 184:5559–76.e19. doi: 10.1016/j.cell.2021.10.001

67. Yu Y, Peng XD, Qian XJ, Zhang KM, Huang X, Chen YH, et al. Fis1 phosphorylation by Met promotes mitochondrial fission and hepatocellular carcinoma metastasis. *Signal Transduct Target Ther*. (2021) 6:401. doi: 10.1038/s41392-021-00790-2

68. Li S, Han S, Zhang Q, Zhu Y, Zhang H, Wang J, et al. FUNDC2 promotes liver tumorigenesis by inhibiting MFN1-mediated mitochondrial fusion. *Nat Commun*. (2022) 13:3486. doi: 10.1038/s41467-022-31187-6

69. Huang D, Li T, Li X, Zhang L, Sun L, He X, et al. HIF-1-mediated suppression of acyl-CoA dehydrogenases and fatty acid oxidation is critical for cancer progression. *Cell Rep*. (2014) 8:1930–42. doi: 10.1016/j.celrep.2014.08.028

70. Wu JM, Skill NJ, Maluccio MA. Evidence of aberrant lipid metabolism in hepatitis C and hepatocellular carcinoma. *HPB (Oxford)*. (2010) 12:625–36. doi: 10.1111/j.1477-2574.2010.00207.x

71. Mutlu B, Puigserver P. GCN5 acetyltransferase in cellular energetic and metabolic processes. *Biochim Biophys Acta Gene Regul Mech*. (2021) 1864:194626. doi: 10.1016/j.bbagrm.2020.194626

72. Resar LM. The high mobility group A1 gene: transforming inflammatory signals into cancer? *Cancer Res*. (2010) 70:436–9. doi: 10.1158/0008-5472.CAN-09-1212

73. Shen Z, Wu J, Gao Z, Zhang S, Chen J, He J, et al. High mobility group AT-hook 1 (HMGA1) is an important positive regulator of hepatitis B virus (HBV) that is reciprocally upregulated by HBV X protein. *Nucleic Acids Res*. (2022) 50:2157–71. doi: 10.1093/nar/gkac070

74. Kar A, Samanta A, Mukherjee S, Barik S, Biswas A. The HBV web: An insight into molecular interactomes between the hepatitis B virus and its host en route to hepatocellular carcinoma. *J Med Virol*. (2023) 95:e28436. doi: 10.1002/jmv.28436

75. Papatheodoridis GV, Lekakis V, Voulgaris T, Lampertico P, Berg T, Chan HLY, et al. Hepatitis B virus reactivation associated with new classes of immunosuppressants and immunomodulators: A systematic review, meta-analysis, and expert opinion. *J Hepatol*. (2022) 77:1670–89. doi: 10.1016/j.jhep.2022.07.003

76. Melis M, Diaz G, Kleiner DE, Zamboni F, Kabat J, Lai J, et al. Viral expression and molecular profiling in liver tissue versus microdissected hepatocytes in hepatitis B virus-associated hepatocellular carcinoma. *J Transl Med*. (2014) 12:230. doi: 10.1186/s12967-014-0230-1

77. Deng JJ, Kong KE, Gao WW, Tang HV, Chaudhary V, Cheng Y, et al. Interplay between SIRT1 and hepatitis B virus X protein in the activation of viral transcription. *Biochim Biophys Acta Gene Regul Mech*. (2017) 1860:491–501. doi: 10.1016/j.bbagrm.2017.02.007

78. Gehrke N, Wörns MA, Huber Y, Hess M, Straub BK, Hövelmeyer N, et al. Hepatic B cell leukemia-3 promotes hepatic steatosis and inflammation through insulin-sensitive metabolic transcription factors. *J Hepatol*. (2016) 65:1188–97. doi: 10.1016/j.jhep.2016.06.026

79. Wan X, Zhu X, Wang H, Feng Y, Zhou W, Liu P, et al. PGC1α protects against hepatic steatosis and insulin resistance via enhancing IL10-mediated anti-inflammatory response. *FASEB J*. (2020) 34:10751–61. doi: 10.1096/fj.201902476R

80. Xu L, Huang Z, Lo TH, Lee JTH, Yang R, Yan X, et al. Hepatic PRMT1 ameliorates diet-induced hepatic steatosis via induction of PGC1α. *Theranostics*. (2022) 12:2502–18. doi: 10.7150/thno.63824

81. Qi J, Chen X, Wu Q, Wang J, Zhang H, Mao A, et al. Fasting induces hepatocellular carcinoma cell apoptosis by inhibiting SET8 expression. *Oxid Med Cell Longev*. (2020) 2020:3985089. doi: 10.1155/2020/3985089

82. Kudo Y, Sugimoto M, Arias E, Kasashima H, Cordes T, Linares JF, et al. PKCλ/ι Loss induces autophagy, oxidative phosphorylation, and NRF2 to promote liver cancer progression. *Cancer Cell*. (2020) 38:247–62.e11. doi: 10.1016/j.ccell.2020.05.018

83. Yang C, Cui XW, Ding ZW, Jiang TY, Feng XF, Pan YF, et al. Gankyrin and TIGAR cooperatively accelerate glucose metabolism toward the PPP and TCA cycle in hepatocellular carcinoma. *Cancer Sci*. (2022) 113:4151–64. doi: 10.1111/cas.15593

84. Jiang J, Chen HN, Jin P, Zhou L, Peng L, Huang Z, et al. Targeting PSAT1 to mitigate metastasis in tumors with p53-72Pro variant. *Signal Transduct Target Ther*. (2023) 8:65. doi: 10.1038/s41392-022-01266-7

85. Li Y, Wu J, Song F, Tang J, Wang SJ, Yu XL, et al. Extracellular membrane-proximal domain of HAb18G/CD147 binds to metal ion-dependent adhesion site (MIDAS) motif of integrin β1 to modulate Malignant properties of hepatoma cells. *J Biol Chem*. (2012) 287:4759–72. doi: 10.1074/jbc.M111.277699

86. Huang Q, Li J, Xing J, Li W, Li H, Ke X, et al. CD147 promotes reprogramming of glucose metabolism and cell proliferation in HCC cells by inhibiting the p53-dependent signaling pathway. *J Hepatol*. (2014) 61:859–66. doi: 10.1016/j.jhep.2014.04.035

87. Foreman JE, Koga T, Kosyk O, Kang BH, Zhu X, Cohen SM, et al. Diminished hepatocarcinogenesis by a potent, high-affinity human PPARα Agonist in PPARA-humanized mice. *Toxicol Sci*. (2021) 183:70–80. doi: 10.1093/toxsci/kfab067

88. Foreman JE, Koga T, Kosyk O, Kang BH, Zhu X, Cohen SM, et al. Species differences between mouse and human PPARα in modulating the hepatocarcinogenic effects of perinatal exposure to a high-affinity human PPARα Agonist in mice. *Toxicol Sci*. (2021) 183:81–92. doi: 10.1093/toxsci/kfab068

89. Nam H, Kundu A, Brinkley GJ, Chandrashekar DS, Kirkman RL, Chakravarthi B, et al. PGC1α suppresses kidney cancer progression by inhibiting collagen-induced SNAIL expression. *Matrix Biol*. (2020) 89:43–58. doi: 10.1016/j.matbio.2020.01.001

90. LaGory EL, Wu C, Taniguchi CM, Ding CC, Chi JT, von Eyben R, et al. Suppression of PGC-1α Is critical for reprogramming oxidative metabolism in renal cell carcinoma. *Cell Rep*. (2015) 12:116–27. doi: 10.1016/j.celrep.2015.06.006

91. Zhuang C, Zhuang C, Luo X, Huang X, Yao L, Li J, et al. N6-methyladenosine demethylase FTO suppresses clear cell renal cell carcinoma through a novel FTO-PGC-1α signalling axis. *J Cell Mol Med*. (2019) 23:2163–73. doi: 10.1111/jcmm.14128

92. Nam H, Kundu A, Karki S, Brinkley GJ, Chandrashekar DS, Kirkman RL, et al. The TGF-β/HDAC7 axis suppresses TCA cycle metabolism in renal cancer. *JCI Insight*. (2021) 6(22):e148438. doi: 10.1172/jci.insight.148438

93. Ivanov SV, Salnikow K, Ivanova AV, Bai L, Lerman MI. Hypoxic repression of STAT1 and its downstream genes by a pVHL/HIF-1 target DEC1/STRA13. *Oncogene*. (2007) 26:802–12. doi: 10.1038/sj.onc.1209842

94. Yamada Y, Sugawara S, Arai T, Kojima S, Kato M, Okato A, et al. Molecular pathogenesis of renal cell carcinoma: Impact of the anti-tumor miR-29 family on gene regulation. *Int J Urol*. (2018) 25:953–65. doi: 10.1111/iju.13783

95. Koh E, Kim YK, Shin D, Kim KS. MPC1 is essential for PGC-1α-induced mitochondrial respiration and biogenesis. *Biochem J*. (2018) 475:1687–99. doi: 10.1042/BCJ20170967

96. Dan L, Wang C, Ma P, Yu Q, Gu M, Dong L, et al. PGC1α promotes cholangiocarcinoma metastasis by upregulating PDHA1 and MPC1 expression to reverse the Warburg effect. *Cell Death Dis*. (2018) 9:466. doi: 10.1038/s41419-018-0494-0

97. Felipe-Abrio B, Carnero A. The tumor suppressor roles of MYBBP1A, a major contributor to metabolism plasticity and stemness. *Cancers (Basel)*. (2020) 12(1):254. doi: 10.3390/cancers12010254

98. Felipe-Abrio B, Verdugo-Sivianes EM, Carnero A. c-MYB- and PGC1a-dependent metabolic switch induced by MYBBP1A loss in renal cancer. *Mol Oncol*. (2019) 13:1519–33. doi: 10.3390/cancers12010254

99. Cancer Genome Atlas Research Network. Comprehensive molecular characterization of clear cell renal cell carcinoma. *Nature*. (2013) 499:43–9. doi: 10.1038/nature12222

100. Xie Y, Sahin M, Sinha S, Wang Y, Nargund AM, Lyu Y, et al. SETD2 loss perturbs the kidney cancer epigenetic landscape to promote metastasis and engenders actionable dependencies on histone chaperone complexes. *Nat Cancer*. (2022) 3:188–202. doi: 10.1038/s43018-021-00316-3

101. Kanu N, Grönroos E, Martinez P, Burrell RA, Yi Goh X, Bartkova J, et al. SETD2 loss-of-function promotes renal cancer branched evolution through replication stress and impaired DNA repair. *Oncogene*. (2015) 34:5699–708. doi: 10.1038/onc.2015.24

102. Liu J, Hanavan PD, Kras K, Ruiz YW, Castle EP, Lake DF, et al. Loss of SETD2 induces a metabolic switch in renal cell carcinoma cell lines toward enhanced oxidative phosphorylation. *J Proteome Res*. (2019) 18:331–40. doi: 10.1021/acs.jproteome.8b00628

103. Raggi C, Taddei ML, Rae C, Braconi C, Marra F. Metabolic reprogramming in cholangiocarcinoma. *J Hepatol*. (2022) 77:849–64. doi: 10.1016/j.jhep.2022.04.038

104. Colyn L, Alvarez-Sola G, Latasa MU, Uriarte I, Herranz JM, Arechederra M, et al. New molecular mechanisms in cholangiocarcinoma: signals triggering interleukin-6 production in tumor cells and KRAS co-opted epigenetic mediators driving metabolic reprogramming. *J Exp Clin Cancer Res*. (2022) 41:183. doi: 10.1186/s13046-022-02386-2

105. Raggi C, Taddei ML, Sacco E, Navari N, Correnti M, Piombanti B, et al. Mitochondrial oxidative metabolism contributes to a cancer stem cell phenotype in cholangiocarcinoma. *J Hepatol*. (2021) 74:1373–85. doi: 10.1016/j.jhep.2020.12.031

106. Nguyen TTT, Shang E, Shu C, Kim S, Mela A, Humala N, et al. Aurora kinase A inhibition reverses the Warburg effect and elicits unique metabolic vulnerabilities in glioblastoma. *Nat Commun*. (2021) 12:5203. doi: 10.1038/s41467-021-25501-x

107. Cho SY, Kim SH, Yi MH, Zhang E, Kim E, Park J, et al. Expression of PGC1α in glioblastoma multiforme patients. *Oncol Lett*. (2017) 13:4055–76. doi: 10.3892/ol.2017.5972

108. Bruns I, Sauer B, Burger MC, Eriksson J, Hofmann U, Braun Y, et al. Disruption of peroxisome proliferator-activated receptor γ coactivator (PGC)-1α reverts key features of the neoplastic phenotype of glioma cells. *J Biol Chem*. (2019) 294:3037–50. doi: 10.1074/jbc.RA118.006993

109. Comelli M, Pretis I, Buso A, Mavelli I. Mitochondrial energy metabolism and signalling in human glioblastoma cell lines with different PTEN gene status. *J Bioenerg Biomembr*. (2018) 50:33–52. doi: 10.1007/s10863-017-9737-5

110. Čančer M, Drews LF, Bengtsson J, Bolin S, Rosén G, Westermark B, et al. BET and Aurora Kinase A inhibitors synergize against MYCN-positive human glioblastoma cells. *Cell Death Dis*. (2019) 10:881. doi: 10.1038/s41419-019-2120-1

111. Nguyen TTT, Zhang Y, Shang E, Shu C, Torrini C, Zhao J, et al. HDAC inhibitors elicit metabolic reprogramming by targeting super-enhancers in glioblastoma models. *J Clin Invest*. (2020) 130:3699–716. doi: 10.1172/JCI129049

112. Meng X, Zhao Y, Han B, Zha C, Zhang Y, Li Z, et al. Dual functionalized brain-targeting nanoinhibitors restrain temozolomide-resistant glioma via attenuating EGFR and MET signaling pathways. *Nat Commun*. (2020) 11:594. doi: 10.1038/s41467-019-14036-x

113. Lu KV, Chang JP, Parachoniak CA, Pandika MM, Aghi MK, Meyronet D, et al. VEGF inhibits tumor cell invasion and mesenchymal transition through a MET/VEGFR2 complex. *Cancer Cell*. (2012) 22:21–35. doi: 10.1016/j.ccr.2012.05.037

114. Zhang Y, Nguyen TTT, Shang E, Mela A, Humala N, Mahajan A, et al. MET inhibition elicits PGC1α-dependent metabolic reprogramming in glioblastoma. *Cancer Res*. (2020) 80:30–43. doi: 10.1158/0008-5472.CAN-19-1389

115. Fan QW, Nicolaides TP, Weiss WA. Inhibiting 4EBP1 in glioblastoma. *Clin Cancer Res*. (2018) 24:14–21. doi: 10.1158/1078-0432.CCR-17-0042

116. Thiepold AL, Lorenz NI, Foltyn M, Engel AL, Divé I, Urban H, et al. Mammalian target of rapamycin complex 1 activation sensitizes human glioma cells to hypoxia-induced cell death. *Brain*. (2017) 140:2623–38. doi: 10.1093/brain/awx196

117. Ronellenfitsch MW, Brucker DP, Burger MC, Wolking S, Tritschler F, Rieger J, et al. Antagonism of the mammalian target of rapamycin selectively mediates metabolic effects of epidermal growth factor receptor inhibition and protects human Malignant glioma cells from hypoxia-induced cell death. *Brain*. (2009) 132:1509–22. doi: 10.1093/brain/awp093

118. Singh D, Chan JM, Zoppoli P, Niola F, Sullivan R, Castano A, et al. Transforming fusions of FGFR and TACC genes in human glioblastoma. *Science*. (2012) 337:1231–5. doi: 10.1126/science.1220834

119. Lasorella A, Sanson M, Iavarone A. FGFR-TACC gene fusions in human glioma. *Neuro Oncol*. (2017) 19:475–83. doi: 10.1093/neuonc/now240

120. Frattini V, Pagnotta SM, Tala, Fan JJ, Russo MV, Lee SB, et al. A metabolic function of FGFR3-TACC3 gene fusions in cancer. *Nature*. (2018) 553:222–7. doi: 10.1038/nature25171

121. Hoek KS, Eichhoff OM, Schlegel NC, Döbbeling U, Kobert N, Schaerer L, et al. *In vivo* switching of human melanoma cells between proliferative and invasive states. *Cancer Res*. (2008) 68:650–6. doi: 10.1158/0008-5472.CAN-07-2491

122. Luo C, Balsa E, Perry EA, Liang J, Tavares CD, Vazquez F, et al. H3K27me3-mediated PGC1α gene silencing promotes melanoma invasion through WNT5A and YAP. *J Clin Invest*. (2020) 130:853–62. doi: 10.1172/jci130038

123. Vazquez F, Lim JH, Chim H, Bhalla K, Girnun G, Pierce K, et al. PGC1α expression defines a subset of human melanoma tumors with increased mitochondrial capacity and resistance to oxidative stress. *Cancer Cell*. (2013) 23:287–301. doi: 10.1016/j.ccr.2012.11.020

124. Hartman ML, Czyz M. MITF in melanoma: mechanisms behind its expression and activity. *Cell Mol Life Sci*. (2015) 72:1249–60. doi: 10.1007/s00018-014-1791-0

125. Wang H, Zhang H, Chen Y, Wang H, Tian Y, Yi X, et al. Targeting wnt/β-catenin signaling exacerbates ferroptosis and increases the efficacy of melanoma immunotherapy via the regulation of MITF. *Cells*. (2022) 11(22):3580. doi: 10.3390/cells11223580

126. Guo W, Ma J, Yang Y, Guo S, Zhang W, Zhao T, et al. ATP-citrate lyase epigenetically potentiates oxidative phosphorylation to promote melanoma growth and adaptive resistance to MAPK inhibition. *Clin Cancer Res*. (2020) 26:2725–39. doi: 10.1158/1078-0432.CCR-19-1359

127. Talty R, Bosenberg M. The role of ferroptosis in melanoma. *Pigment Cell Melanoma Res*. (2022) 35:18–25. doi: 10.1111/pcmr.13009

128. DeVito NC, Sturdivant M, Thievanthiran B, Xiao C, Plebanek MP, Salama AKS, et al. Pharmacological Wnt ligand inhibition overcomes key tumor-mediated resistance pathways to anti-PD-1 immunotherapy. *Cell Rep*. (2021) 35:109071. doi: 10.1016/j.celrep.2021.109071

129. Spranger S, Bao R, Gajewski TF. Melanoma-intrinsic β-catenin signalling prevents anti-tumour immunity. *Nature*. (2015) 523:231–5. doi: 10.1038/nature14404

130. Gelato KA, Schöckel L, Klingbeil O, Rückert T, Lesche R, Toedling J, et al. Super-enhancers define a proliferative PGC-1α-expressing melanoma subgroup sensitive to BET inhibition. *Oncogene*. (2018) 37:512–21. doi: 10.1038/onc.2017.325

131. Luo C, Lim JH, Lee Y, Granter SR, Thomas A, Vazquez F, et al. A PGC1α-mediated transcriptional axis suppresses melanoma metastasis. *Nature*. (2016) 537:422–6. doi: 10.1038/nature19347

132. Piskounova E, Agathocleous M, Murphy MM, Hu Z, Huddlestun SE, Zhao Z, et al. Oxidative stress inhibits distant metastasis by human melanoma cells. *Nature*. (2015) 527:186–91. doi: 10.1038/nature15726

133. Hoffmann F, Niebel D, Aymans P, Ferring-Schmitt S, Dietrich D, Landsberg J. H3K27me3 and EZH2 expression in melanoma: relevance for melanoma progression and response to immune checkpoint blockade. *Clin Epigenetics*. (2020) 12:24. doi: 10.1186/s13148-020-0818-7

134. Cai Y, Zhang Y, Loh YP, Tng JQ, Lim MC, Cao Z, et al. H3K27me3-rich genomic regions can function as silencers to repress gene expression via chromatin interactions. *Nat Commun*. (2021) 12:719. doi: 10.1038/s41467-021-20940-y

135. Haq R, Fisher DE, Widlund HR. Molecular pathways: BRAF induces bioenergetic adaptation by attenuating oxidative phosphorylation. *Clin Cancer Res*. (2014) 20:2257–63. doi: 10.1158/1078-0432.CCR-13-0898

136. Lee SB, Garofano L, Ko A, D'Angelo F, Frangaj B, Sommer D, et al. Regulated interaction of ID2 with the anaphase-promoting complex links progression through mitosis with reactivation of cell-type-specific transcription. *Nat Commun*. (2022) 13:2089. doi: 10.1038/s41467-022-29502-2

137. Yu Y, Wu J, Wang Y, Zhao T, Ma B, Liu Y, et al. Kindlin 2 forms a transcriptional complex with β-catenin and TCF4 to enhance Wnt signalling. *EMBO Rep*. (2012) 13:750–8. doi: 10.1038/embor.2012.88

138. Park HW, Kim YC, Yu B, Moroishi T, Mo JS, Plouffe SW, et al. Alternative wnt signaling activates YAP/TAZ. *Cell*. (2015) 162:780–94. doi: 10.1016/j.cell.2015.07.013

139. Astudillo P. An emergent Wnt5a/YAP/TAZ regulatory circuit and its possible role in cancer. *Semin Cell Dev Biol*. (2022) 125:45–54. doi: 10.1016/j.semcdb.2021.10.001

140. Haq R, Shoag J, Andreu-Perez P, Yokoyama S, Edelman H, Rowe GC, et al. Oncogenic BRAF regulates oxidative metabolism via PGC1α and MITF. *Cancer Cell*. (2013) 23:302–15. doi: 10.1016/j.ccr.2013.02.003

141. Bollag G, Hirth P, Tsai J, Zhang J, Ibrahim PN, Cho H, et al. Clinical efficacy of a RAF inhibitor needs broad target blockade in BRAF-mutant melanoma. *Nature*. (2010) 467:596–9. doi: 10.1038/nature09454

142. Corno C, Perego P. KiSS1 in regulation of metastasis and response to antitumor drugs. *Drug Resist Updat*. (2019) 42:12–21. doi: 10.1016/j.drup.2019.02.001

143. Liu W, Beck BH, Vaidya KS, Nash KT, Feeley KP, Ballinger SW, et al. Metastasis suppressor KISS1 seems to reverse the Warburg effect by enhancing mitochondrial biogenesis. *Cancer Res*. (2014) 74:954–63. doi: 10.1158/0008-5472.CAN-13-1183

144. Manley SJ, Liu W, Welch DR. The KISS1 metastasis suppressor appears to reverse the Warburg effect by shifting from glycolysis to mitochondrial beta-oxidation. *J Mol Med (Berl)*. (2017) 95:951–63. doi: 10.1007/s00109-017-1552-2

145. Lim JH, Luo C, Vazquez F, Puigserver P. Targeting mitochondrial oxidative metabolism in melanoma causes metabolic compensation through glucose and glutamine utilization. *Cancer Res*. (2014) 74:3535–45. doi: 10.1158/0008-5472.CAN-13-2893-T

146. Torrano V, Valcarcel-Jimenez L, Cortazar AR, Liu X, Urosevic J, Castillo-Martin M, et al. The metabolic co-regulator PGC1α suppresses prostate cancer metastasis. *Nat Cell Biol*. (2016) 18:645–56. doi: 10.1038/ncb3357

147. Cerami E, Gao J, Dogrusoz U, Gross BE, Sumer SO, Aksoy BA, et al. The cBio cancer genomics portal: an open platform for exploring multidimensional cancer genomics data. *Cancer Discovery*. (2012) 2:401–4. doi: 10.1158/2159-8290.CD-12-0095

148. Gao J, Aksoy BA, Dogrusoz U, Dresdner G, Gross B, Sumer SO, et al. Integrative analysis of complex cancer genomics and clinical profiles using the cBioPortal. *Sci Signal*. (2013) 6:pl1. doi: 10.1126/scisignal.2004088

149. Siddappa M, Wani SA, Long MD, Leach DA, Mathé EA, Bevan CL, et al. Identification of transcription factor co-regulators that drive prostate cancer progression. *Sci Rep*. (2020) 10:20332. doi: 10.1038/s41598-020-77055-5

150. Wen Y, Huang H, Huang B, Liao X. HSA-miR-34a-5p regulates the SIRT1/TP53 axis in prostate cancer. *Am J Transl Res*. (2022) 14:4493–504.

151. Tennakoon JB, Shi Y, Han JJ, Tsouko E, White MA, Burns AR, et al. Androgens regulate prostate cancer cell growth via an AMPK-PGC-1α-mediated metabolic switch. *Oncogene*. (2014) 33:5251–61. doi: 10.1038/onc.2013.463

152. Valcarcel-Jimenez L, Macchia A, Crosas-Molist E, Schaub-Clerigué A, Camacho L, Martín-Martín N, et al. PGC1α Suppresses prostate cancer cell invasion through ERRα Transcriptional control. *Cancer Res*. (2019) 79:6153–65. doi: 10.1158/0008-5472.CAN-19-1231

153. Kaminski L, Torrino S, Dufies M, Djabari Z, Haider R, Roustan FR, et al. PGC1α Inhibits polyamine synthesis to suppress prostate cancer aggressiveness. *Cancer Res*. (2019) 79:3268–80. doi: 10.1158/0008-5472.CAN-18-2043

154. Penfold L, Woods A, Pollard AE, Arizanova J, Pascual-Navarro E, Muckett PJ, et al. AMPK activation protects against prostate cancer by inducing a catabolic cellular state. *Cell Rep*. (2023) 42:112396. doi: 10.1016/j.celrep.2023.112396

155. Penfold L, Woods A, Muckett P, Nikitin AY, Kent TR, Zhang S, et al. CAMKK2 promotes prostate cancer independently of AMPK via increased lipogenesis. *Cancer Res*. (2018) 78:6747–61. doi: 10.1158/0008-5472.CAN-18-0585

156. Yuan H, Han Y, Wang X, Li N, Liu Q, Yin Y, et al. SETD2 restricts prostate cancer metastasis by integrating EZH2 and AMPK signaling pathways. *Cancer Cell*. (2020) 38:350–65.e7. doi: 10.1016/j.ccell.2020.05.022

157. Li J, Li Y, Chen L, Yu B, Xue Y, Guo R, et al. p53/PGC–1α–mediated mitochondrial dysfunction promotes PC3 prostate cancer cell apoptosis. *Mol Med Rep*. (2020) 22:155–64. doi: 10.3892/mmr

158. McCann JJ, Vasilevskaya IA, McNair C, Gallagher P, Neupane NP, de Leeuw R, et al. Mutant p53 elicits context-dependent pro-tumorigenic phenotypes. *Oncogene*. (2022) 41:444–58. doi: 10.1038/s41388-021-01903-5

159. Aquilano K, Baldelli S, Pagliei B, Cannata SM, Rotilio G, Ciriolo MR. p53 orchestrates the PGC-1α-mediated antioxidant response upon mild redox and metabolic imbalance. *Antioxid Redox Signal*. (2013) 18:386–99. doi: 10.1089/ars.2012.4615

160. Galbraith LCA, Mui E, Nixon C, Hedley A, Strachan D, MacKay G, et al. PPAR-gamma induced AKT3 expression increases levels of mitochondrial biogenesis driving prostate cancer. *Oncogene*. (2021) 40:2355–66. doi: 10.1038/s41388-021-01707-7

161. Babu D, Fullwood MJ. Expanding the effects of ERG on chromatin landscapes and dysregulated transcription in prostate cancer. *Nat Genet*. (2017) 49:1294–5. doi: 10.1038/ng.3944

162. Signorile A, De Rasmo D, Cormio A, Musicco C, Rossi R, Fortarezza F, et al. Human ovarian cancer tissue exhibits increase of mitochondrial biogenesis and cristae remodeling. *Cancers (Basel)*. (2019) 11(9):1350. doi: 10.3390/cancers11091350

163. Huang X, Ruan G, Liu G, Gao Y, Sun P. Immunohistochemical analysis of PGC-1α and ERRα Expression reveals their clinical significance in human ovarian cancer. *Onco Targets Ther*. (2020) 13:13055–62. doi: 10.2147/OTT.S288332

164. Ghilardi C, Moreira-Barbosa C, Brunelli L, Ostano P, Panini N, Lupi M, et al. PGC1α/β Expression predicts therapeutic response to oxidative phosphorylation inhibition in ovarian cancer. *Cancer Res*. (2022) 82:1423–34. doi: 10.1158/0008-5472.CAN-21-1223

165. Gentric G, Kieffer Y, Mieulet V, Goundiam O, Bonneau C, Nemati F, et al. PML-regulated mitochondrial metabolism enhances chemosensitivity in human ovarian cancers. *Cell Metab*. (2019) 29:156–73.e10. doi: 10.1016/j.cmet.2018.09.002

166. Izar B, Tirosh I, Stover EH, Wakiro I, Cuoco MS, Alter I, et al. A single-cell landscape of high-grade serous ovarian cancer. *Nat Med*. (2020) 26:1271–9. doi: 10.1038/s41591-020-0926-0

167. Nath A, Cosgrove PA, Mirsafian H, Christie EL, Pflieger L, Copeland B, et al. Evolution of core archetypal phenotypes in progressive high grade serous ovarian cancer. *Nat Commun*. (2021) 12:3039. doi: 10.1038/s41467-021-23171-3

168. Kleih M, Böpple K, Dong M, Gaißler A, Heine S, Olayioye MA, et al. Direct impact of cisplatin on mitochondria induces ROS production that dictates cell fate of ovarian cancer cells. *Cell Death Dis*. (2019) 10:851. doi: 10.1038/s41419-019-2081-4

169. Du Q, Tan Z, Shi F, Tang M, Xie L, Zhao L, et al. PGC1α/CEBPB/CPT1A axis promotes radiation resistance of nasopharyngeal carcinoma through activating fatty acid oxidation. *Cancer Sci*. (2019) 110:2050–62. doi: 10.1111/cas.14011

170. Quan J, Li N, Tan Y, Liu H, Liao W, Cao Y, et al. PGC1α-mediated fatty acid oxidation promotes TGFβ1-induced epithelial-mesenchymal transition and metastasis of nasopharyngeal carcinoma. *Life Sci*. (2022) 300:120558. doi: 10.1016/j.lfs.2022.120558

171. Zu Y, Chen XF, Li Q, Zhang ST, Si LN. PGC-1α activates SIRT3 to modulate cell proliferation and glycolytic metabolism in breast cancer. *Neoplasma*. (2021) 68:352–61. doi: 10.4149/neo_2020_200530N584

172. Deblois G, St-Pierre J, Giguère V. The PGC-1/ERR signaling axis in cancer. *Oncogene*. (2013) 32:3483–90. doi: 10.1038/onc.2012.529

173. Vander Heiden MG, Cantley LC, Thompson CB. Understanding the Warburg effect: the metabolic requirements of cell proliferation. *Science*. (2009) 324:1029–33. doi: 10.1126/science.1160809

174. Torrens-Mas M, Pons DG, Sastre-Serra J, Oliver J, Roca P. SIRT3 silencing sensitizes breast cancer cells to cytotoxic treatments through an increment in ROS production. *J Cell Biochem*. (2017) 118:397–406. doi: 10.1002/jcb.v118.2

175. Lou C, Xiao M, Cheng S, Lu X, Jia S, Ren Y, et al. MiR-485-3p and miR-485-5p suppress breast cancer cell metastasis by inhibiting PGC-1α expression. *Cell Death Dis*. (2016) 7:e2159. doi: 10.1038/cddis.2016.27

176. Zhang S, Liu X, Liu J, Guo H, Xu H, Zhang G. PGC-1 alpha interacts with microRNA-217 to functionally regulate breast cancer cell proliferation. *BioMed Pharmacother*. (2017) 85:541–8. doi: 10.1016/j.biopha.2016.11.062

177. McGuirk S, Gravel SP, Deblois G, Papadopoli DJ, Faubert B, Wegner A, et al. PGC-1α supports glutamine metabolism in breast cancer. *Cancer Metab*. (2013) 1:22. doi: 10.1186/2049-3002-1-22

178. Deblois G, Hall JA, Perry MC, Laganière J, Ghahremani M, Park M, et al. Genome-wide identification of direct target genes implicates estrogen-related receptor alpha as a determinant of breast cancer heterogeneity. *Cancer Res*. (2009) 69:6149–57. doi: 10.1158/0008-5472.CAN-09-1251

179. Andrzejewski S, Klimcakova E, Johnson RM, Tabariès S, Annis MG, McGuirk S, et al. PGC-1α Promotes breast cancer metastasis and confers bioenergetic flexibility against metabolic drugs. *Cell Metab*. (2017) 26:778–87.e5. doi: 10.1016/j.cmet.2017.09.006

180. LeBleu VS, O'Connell JT, Gonzalez Herrera KN, Wikman H, Pantel K, Haigis MC, et al. PGC-1α mediates mitochondrial biogenesis and oxidative phosphorylation in cancer cells to promote metastasis. *Nat Cell Biol*. (2014) 16:992–1003, 1-15. doi: 10.1038/ncb3039

181. Im YK, Najyb O, Gravel SP, McGuirk S, Ahn R, Avizonis DZ, et al. Interplay between shcA signaling and PGC-1α Triggers targetable metabolic vulnerabilities in breast cancer. *Cancer Res*. (2018) 78:4826–38. doi: 10.1158/0008-5472.CAN-17-3696

182. Zhang J, Wang C, Chen X, Takada M, Fan C, Zheng X, et al. EglN2 associates with the NRF1-PGC1α complex and controls mitochondrial function in breast cancer. *EMBO J*. (2015) 34:2953–70. doi: 10.15252/embj.201591437

183. Zhang J, Zheng X, Zhang Q. EglN2 positively regulates mitochondrial function in breast cancer. *Mol Cell Oncol*. (2016) 3:e1120845. doi: 10.1080/23723556.2015.1120845

184. Brindisi M, Fiorillo M, Frattaruolo L, Sotgia F, Lisanti MP, Cappello AR. Cholesterol and mevalonate: two metabolites involved in breast cancer progression and drug resistance through the ERRα Pathway. *Cells*. (2020) 9(8):1819. doi: 10.3390/cells9081819

185. Tiraby C, Hazen BC, Gantner ML, Kralli A. Estrogen-related receptor gamma promotes mesenchymal-to-epithelial transition and suppresses breast tumor growth. *Cancer Res*. (2011) 71:2518–28. doi: 10.1158/0008-5472.CAN-10-1315

186. Jäger S, Handschin C, St-Pierre J, Spiegelman BM. AMP-activated protein kinase (AMPK) action in skeletal muscle via direct phosphorylation of PGC-1alpha. *Proc Natl Acad Sci USA*. (2007) 104:12017–22. doi: 10.1073/pnas.0705070104

187. Basu S, Gnanapradeepan K, Barnoud T, Kung CP, Tavecchio M, Scott J, et al. Mutant p53 controls tumor metabolism and metastasis by regulating PGC-1α. *Genes Dev*. (2018) 32:230–43. doi: 10.1101/gad.309062.117

188. Ni H, Guo M, Zhang X, Jiang L, Tan S, Yuan J, et al. VEGFR2 inhibition hampers breast cancer cell proliferation via enhanced mitochondrial biogenesis. *Cancer Biol Med*. (2021) 18:139–54. doi: 10.20892/j.issn.2095-3941.2020.0151

189. Tripathi V, Jaiswal P, Assaiya A, Kumar J, Parmar HS. Anti-cancer effects of 5-aminoimidazole-4-carboxamide-1-β-D-ribofuranoside (AICAR) on triple-negative breast cancer (TNBC) cells: mitochondrial modulation as an underlying mechanism. *Curr Cancer Drug Targets*. (2022) 22:245–56. doi: 10.2174/1568009622666220207101212

190. Du Y, Song L, Zhang L, Ling H, Zhang Y, Chen H, et al. The discovery of novel, potent ERR-alpha inverse agonists for the treatment of triple negative breast cancer. *Eur J Med Chem*. (2017) 136:457–67. doi: 10.1016/j.ejmech.2017.04.050

191. Zhou T, Zhang B, Wei P, Du Y, Zhou H, Yu M, et al. Energy metabolism analysis reveals the mechanism of inhibition of breast cancer cell metastasis by PEG-modified graphene oxide nanosheets. *Biomaterials*. (2014) 35:9833–43. doi: 10.1016/j.biomaterials.2014.08.033

192. Flågeng MH, Moi LL, Dixon JM, Geisler J, Lien EA, Miller WR, et al. Nuclear receptor co-activators and HER-2/neu are upregulated in breast cancer patients during neo-adjuvant treatment with aromatase inhibitors. *Br J Cancer*. (2009) 101:1253–60. doi: 10.1038/sj.bjc.6605324

193. Cotul EK, Zuo Q, Santaliz-Casiano A, Imir OB, Mogol AN, Tunc E, et al. Combined targeting of estrogen receptor alpha and exportin 1 in metastatic breast cancers. *Cancers (Basel)*. (2020) 12(9):2397. doi: 10.3390/cancers12092397

194. Skildum A, Dornfeld K, Wallace K. Mitochondrial amplification selectively increases doxorubicin sensitivity in breast cancer cells with acquired antiestrogen resistance. *Breast Cancer Res Treat*. (2011) 129:785–97. doi: 10.1007/s10549-010-1268-2

195. Scharping NE, Menk AV, Moreci RS, Whetstone RD, Dadey RE, Watkins SC, et al. The tumor microenvironment represses T cell mitochondrial biogenesis to drive intratumoral T cell metabolic insufficiency and dysfunction. *Immunity*. (2016) 45:374–88. doi: 10.1016/j.immuni.2016.07.009

196. Scharping NE, Rivadeneira DB, Menk AV, Vignali PDA, Ford BR, Rittenhouse NL, et al. Mitochondrial stress induced by continuous stimulation under hypoxia rapidly drives T cell exhaustion. *Nat Immunol*. (2021) 22:205–15. doi: 10.1038/s41590-020-00834-9

197. Dumauthioz N, Tschumi B, Wenes M, Marti B, Wang H, Franco F, et al. Enforced PGC-1α expression promotes CD8 T cell fitness, memory formation and antitumor immunity. *Cell Mol Immunol*. (2021) 18:1761–71. doi: 10.1038/s41423-020-0365-3

198. Pichler AC, Carrié N, Cuisinier M, Ghazali S, Voisin A, Axisa PP, et al. TCR-independent CD137 (4-1BB) signaling promotes CD8(+)-exhausted T cell proliferation and terminal differentiation. *Immunity*. (2023) 56(7):1631–48.e10. doi: 10.1016/j.immuni.2023.06.007

199. Menk AV, Scharping NE, Rivadeneira DB, Calderon MJ, Watson MJ, Dunstane D, et al. 4-1BB costimulation induces T cell mitochondrial function and biogenesis enabling cancer immunotherapeutic responses. *J Exp Med*. (2018) 215:1091–100. doi: 10.1084/jem.20171068

200. Kawalekar OU, O'Connor RS, Fraietta JA, Guo L, McGettigan SE, Posey AD Jr., et al. Distinct signaling of coreceptors regulates specific metabolism pathways and impacts memory development in CAR T cells. *Immunity*. (2016) 44:380–90. doi: 10.1016/j.immuni.2016.01.021

201. Abdalla HB, Napimoga MH, Lopes AH, de Macedo Maganin AG, Cunha TM, Van Dyke TE, et al. Activation of PPAR-γ induces macrophage polarization and reduces neutrophil migration mediated by heme oxygenase 1. *Int Immunopharmacol*. (2020) 84:106565. doi: 10.1016/j.intimp.2020.106565

202. Chawla A. Control of macrophage activation and function by PPARs. *Circ Res*. (2010) 106:1559–69. doi: 10.1161/CIRCRESAHA.110.216523

203. Zhou H, Gan M, Jin X, Dai M, Wang Y, Lei Y, et al. miR–382 inhibits breast cancer progression and metastasis by affecting the M2 polarization of tumor–associated macrophages by targeting PGC–1α. *Int J Oncol*. (2022) 61(4):126. doi: 10.3892/ijo

204. Caporarello N, Meridew JA, Jones DL, Tan Q, Haak AJ, Choi KM, et al. PGC1α repression in IPF fibroblasts drives a pathologic metabolic, secretory and fibrogenic state. *Thorax*. (2019) 74:749–60. doi: 10.1136/thoraxjnl-2019-213064

205. Prieto I, Alarcón CR, García-Gómez R, Berdún R, Urgel T, Portero M, et al. Metabolic adaptations in spontaneously immortalized PGC-1α knock-out mouse embryonic fibroblasts increase their oncogenic potential. *Redox Biol*. (2020) 29:101396. doi: 10.1016/j.redox.2019.101396

206. Li X, Jiang E, Zhao H, Chen Y, Xu Y, Feng C, et al. Glycometabolic reprogramming-mediated proangiogenic phenotype enhancement of cancer-associated fibroblasts in oral squamous cell carcinoma: role of PGC-1α/PFKFB3 axis. *Br J Cancer*. (2022) 127:449–61. doi: 10.1038/s41416-022-01818-2

207. Kumar PR, Saad M, Hellmich C, Mistry JJ, Moore JA, Conway S, et al. PGC-1α induced mitochondrial biogenesis in stromal cells underpins mitochondrial transfer to melanoma. *Br J Cancer*. (2022) 127:69–78. doi: 10.1038/s41416-022-01783-w

Glossary

PGC1α	Peroxisome proliferator-activated receptor gamma coactivator 1-alpha
PPARγ	Peroxisome proliferator-activated receptor gamma
TCGA	The Cancer Genome Atlas Program
AMPK	AMP-activated protein kinase
CRC	Colorectal cancer
SIRT3	NAD-dependent deacetylase sirtuin-3
shRNA	Short hairpin RNA
PRL3	Phosphatase of regenerating liver 3
CSCs	Cancer stem cells
TME	Tumor microenvironment
NET	Neutrophil extracellular trap
NE	Neutrophil elastase
TLR4	Toll-like receptor 4
EVs	Extracellular vesicles
ROS	Reactive oxygen species
FASN	Fatty acid synthase
Sp1	Specificity protein 1
SREBP-1c	Sterol regulatory element-binding protein 1
AKT	Protein kinase B
GSK-3β	Glycogen synthase kinase-3 beta
LARS1	Leucyl-tRNA synthetase 1
EMT	Epithelial–mesenchymal transition
BCL2	B-cell lymphoma 2
PARP-1	Poly [ADP-ribose] polymerase 1
SIRT1	NAD-dependent deacetylase sirtuin-1
LA	Linoleic Acid
MH	Manuka honey
GC	Gastric cancer
SNAI1	Snail family transcriptional repressor 1
CAB39L	Calcium binding protein 39 like
HCP5	HLA Complex P5
CEBPB	CCAAT/enhancer-binding protein beta
CPT1	Carnitine palmitoyltransferase 1
FAO	Fatty acid oxidation
HCC	Hepatocellular carcinoma
NASH	Non-alcoholic steatohepatitis
PARIS	Parkin-interacting substrate
SESN2	Sestrin2
FOXO1	Forkhead box protein O1
YAP	Yes-associated protein 1
TFB2M	Mitochondrial transcription factor B2
PDK1	Pyruvate Dehydrogenase Kinase 1
HNF4α	Hepatic nuclear factor 4 alpha
G6PC	Glucose 6-phosphatase alpha
PCK1	Phosphoenolpyruvate carboxykinase 1
GCN5	General control non-depressible 5
HMGA1	High mobility group AT-hook 1
NAFLD	Non-alcoholic fatty liver disease
Nrf2	Nuclear factor erythroid 2-related factor 2
ARE	Antioxidant response element
TIGAR	TP53 induced glycolysis regulatory phosphatase
PSAT1	Phosphoserine aminotransferase 1
TFAM	Mitochondrial transcription factor A
OXPHOS	Oxidative phosphorylation
TCA	Tricarboxylic acid cycle
RCC	Renal cell carcinoma
ccRCC	Clear cell renal cell carcinoma
TGF-β	Transforming growth factor beta
HDAC7	Histone deacetylase 7
Stra13	Retinoic acid 13
FTO	Fat mass and obesity associated
DDR1	Discoidin domain receptor family, member 1
MPC1	Mitochondrial pyruvate carrier 1
ERR-α	Estrogen-related receptor alpha
MYBBP1A	MYB binding protein 1A
pVHL	Von Hippel–Lindau tumor suppressor
SETD2	SET domain containing 2
CCA	Cholangiocarcinoma
PDHA1	Pyruvate dehydrogenase-alpha 1
GBM	Glioblastoma
PDX	Patient-derived xenograft
TMAs	Tissue microarrays
PTEN	Phosphatase and tensin homolog
AURKA	Aurora kinase A
CHIP	Chromatin immunoprecipitation
ATAC	Assay for transposase-accessible chromatin
CREB	cAMP response element-binding protein
EGFR	Epidermal growth factor receptor

Continued

mTORC1	Mammalian target of rapamycin complex 1
FGFR3	Fibroblast growth factor receptor 3
TACC3	Transforming acidic coiled-coil containing protein 3
MITF	Microphthalmia-associated transcription factor
ACLY	ATP-citrate lyase
RSL3	RAS-selective lethal 3
CTLA4	Cytotoxic T-lymphocyte associated protein 4
BET	Bromodomain and extra-terminal domain
EZH2	Enhancer of zeste homolog 2
ID2	Inhibitor of DNA binding 2
TCF4	Transcription factor 4
TCF12	Transcription factor 12
KISS1	Kisspeptin-1
ACC	Acetyl-CoA carboxylase
AMPK	AMP-activated protein kinase
MSCs	Mesenchymal stromal cells
iMEFs	induced mouse embryonic fibroblasts
PC	Prostate cancer
DFS	Disease-free survival
ERG	ETS-related gene
SOD1	Superoxide dismutase 1
CAFs	Cancer-associated fibroblasts
HGSOC	High-grade serous ovarian cancer
ETC	Electron transport chain
NPC	Nasopharyngeal carcinoma
BC	Breast cancer
TNBT	Triple-negative breast tumors
CTCs	Circulating tumor cells
EglN2	Egl nine homolog 2
HIF	Hypoxia-inducible factor
FDXR	Ferredoxin reductase
TAMs	Tumor-associated macrophages
AICAR	5-Aminoimidazole-4-carboxamide riboside
VEGFR2	Vascular endothelial growth factor receptor 2
PEG-GO	Polyethylene glycol-modified graphene oxide. CD147, Cluster of differentiation 147
TACC3	Transforming acidic coiled-coil containing protein 3
HBV	Hepatitis B virus
Blimp-1	B lymphocyte-induced maturation protein-1
ERRγ	Estrogen related receptor gamma.

frontiers | Frontiers in Oncology

TYPE Original Research
PUBLISHED 17 June 2024
DOI 10.3389/fonc.2024.1378087

OPEN ACCESS

EDITED BY
Hua Tan,
National Human Genome Research Institute (NIH), United States

REVIEWED BY
Florica Sandru,
Carol Davila University of Medicine and Pharmacy, Romania
Rajni Kant Shukla,
The Ohio State University, United States

*CORRESPONDENCE
Yiping Xiang
xiangyp94@163.com

†These authors share first authorship

RECEIVED 29 January 2024
ACCEPTED 30 May 2024
PUBLISHED 17 June 2024

CITATION
Cui Z, Liu C, Wang X and Xiang Y (2024) A pan-cancer analysis of EphA family gene expression and its association with prognosis, tumor microenvironment, and therapeutic targets.
Front. Oncol. 14:1378087.
doi: 10.3389/fonc.2024.1378087

A pan-cancer analysis of EphA family gene expression and its association with prognosis, tumor microenvironment, and therapeutic targets

Zhe Cui[1†], Chengwang Liu[2†], Xuechao Wang[2†] and Yiping Xiang[3*]

[1]Division of Hematology and Transfusion Medicine, Tianjin Baodi Hospital, Tianjin Baodi Affiliated Hospital of Tianjin Medical University, Tianjin, China, [2]Department of Laboratory Medicine, Tianjin Baodi Affiliated Hospital of Tianjin Medical University, Tianjin, China, [3]Department of Pathology, Tianjin Medical University Cancer Institute & Hospital, National Clinical Research Center for Cancer, Tianjin's Clinical Research Center for Cancer, Key Laboratory of Cancer Prevention and Therapy, Tianjin, China

Background: Erythropoietin-producing human hepatocellular (Eph) receptors stand out as the most expansive group of receptor tyrosine kinases (RTKs). Accumulating evidence suggests that within this expansive family, the EphA subset is implicated in driving cancer cell progression, proliferation, invasion, and metastasis, making it a promising target for anticancer treatment. Nonetheless, the extent of EphA family involvement across diverse cancers, along with its intricate interplay with immunity and the tumor microenvironment (TME), remains to be fully illuminated.

Methods: The relationships between EphA gene expression and patient survival, immunological subtypes, and TME characteristics were investigated based on The Cancer Genome Atlas (TCGA) database. The analyses employed various R packages.

Results: A significant difference in expression was identified for most EphA genes when comparing cancer tissues and non-cancer tissues. These genes independently functioned as prognostic factors spanning multiple cancer types. Moreover, a significant correlation surfaced between EphA gene expression and immune subtypes, except for EphA5, EphA6, and EphA8. EphA3 independently influenced the prognosis of papillary renal cell carcinoma (KIRP). This particular gene exhibited links with immune infiltration subtypes and clinicopathologic parameters, holding promise as a valuable biomarker for predicting prognosis and responsiveness to immunotherapy in patients with KIRP.

Conclusion: By meticulously scrutinizing the panorama of EphA genes in a spectrum of cancers, this study supplemented a complete map of the effect of EphA family in Pan-cancer and suggested that EphA family may be a potential target for cancer therapy.

KEYWORDS

Erythropoietin-producing human hepatocellular (Eph) receptors, pancancer, tumor microenvironment (TME), papillary renal cell carcinoma (KIRP), therapeutic targets, bioinformatics

Introduction

Globally, the incidence and mortality of cancer are steadily rising on an annual basis (1). With the development of radiotherapy, chemotherapy, targeted therapy and immunotherapy, continuous endeavors are made to improve our comprehension of the intricate pathogenesis of tumors and elevate the standard of treatment (2). Nevertheless, further research is required to substantiate the efficacy of immunotherapy in various types of cancer (3). Pan-cancer analysis might help us unearth valuable factors in diagnosis, prognosis, and immunotherapy by analyzing genes in a wide variety of cancers and evaluating the similarities and variances in gene expression (4).

Erythropoietin-producing hepatocellular receptors (Ephs) constitute a significant subset within the realm of receptor tyrosine kinases (RTKs). Ephs can be classified into two distinct subfamilies, namely EphA and EphB, a differentiation primarily grounded in their structural attributes and the strength of their binding affinity with specific ligands known as ephrins. The EphA subfamily is comprised of nine individual members, namely EphA1, EphA2, EphA3, EphA4, EphA5, EphA6, EphA7, EphA8, and EphA10. These receptors assume critical roles not only in the regular progression of cell development but also in the advancement of various cancer types (5, 6), such as colorectal cancer (7), lung cancer (8), gastric cancer (9), hepatocellular carcinoma (10), and breast cancer (11).

The EphA family has long been identified as tumor neoantigens, regulating tumor cell stemness, invasion, and angiogenesis, and garnered considerable attention due to its potential as a target for anticancer therapies (12–14). Emerging evidence now also indicates they likely impact the tumor immune microenvironment, an area in which Eph receptors remain understudied (15). Considering that immune-checkpoint inhibitors have shown clinical success, albeit in a small percentage of patients, further research into EphA's functions in controlling cancer immune-suppression is essential for comprehending and creating new targets against tumor immune evasion. So far there is no report on systematic analysis of EphA members from the perspective of pan-caner. Therefore, there is an evident need for performing pan-cancer analysis to achieve a comprehensive grasp of EphAs' functionality and their role in tumor immune microenvironment. Such an understanding is essential to maximize the effectiveness of anticancer treatments that are directed toward EphA receptors.

In light of this, we provide a study about the complete spectrum of EphA's activities and patterns of expression. The current study undertook a meticulous analysis of the expression profiles exhibited by all members of the EphA family across a diverse array of cancer types. This analysis leveraged data from TCGA databases to shed light on potential biological functions and shared characteristics of these receptors. Additionally, we delved into EphA's impact on immune infiltration across a pan-cancer context, accompanied by an examination of individual cancer types.

Materials and methods

Data source

The RNA sequencing (RNA-seq) data (HTSeq-FPKM), along with corresponding clinical data and immune subtypes, were acquired from UCSC Xena (https://xena.ucsc.edu/, originated from TCGA database) (16).

Expression analysis

The expression patterns of EphA genes in TCGA tumors were depicted through a boxplot graph. Subsequently, heatmaps were generated for 18 distinct tumor types, employing log2 (fold change) values to highlight discrepancies in EphA gene expression between primary tumors and adjacent normal tissues. Additionally, Spearman's correlation test was employed to compute gene expression correlations among EphA members across 33 cancer types. To scrutinize the differential expression of EphA family genes across diverse cancer types, the "Wil-cox. test" was applied. For graphical representation, we utilized the "ggpubr" and "pheatmap" R packages to craft a box plot and a heatmap, respectively. The exploration of correlations within the EphA family genes involved the utilization of the "corrplot" R package.

Survival analysis

We conducted univariate Cox regression and Kaplan-Meier (KM) analyses, facilitated by the "survminer" and "survival" R packages, to evaluate the influence of EphA on the survival outcomes associated with various cancers. Furthermore, the Cox proportional hazard model was applied to assess the connection between EphA gene expression and the prognosis of diverse cancer types. The "survival" and "forest plot" packages enabled the creation of a forest plot to visually present the results.

Association of EphA expression with immune cell infiltration

We gauged the extent of immune and stromal cell infiltration across diverse cancers using immune scores and stromal scores metrics from ESTIMATE (17). The relationship between these scores and EphA expression was assessed using the Spearman Correlation Coefficient. Additionally, six distinct immune subtypes were delineated to quantify immune infiltration in the tumor microenvironment (TME) (18). Employing Analysis of Variance (ANOVA), we examined the link between immune infiltration types and SEMA3 expression within the TME based on immune subtypes acquired from TCGA pan-cancer data.

The Tumor Immune Estimation Resource(TIMER, https://cistrome.shinyapps.io/timer/) was developed for quantifying immune cell infiltration across 10,897 cancer samples from TCGA (19, 20). Leveraging TIMER gene modules, we analyzed EphA expression across diverse cancer types and explored its relationship with immune cell infiltration levels. Furthermore, correlation modules were utilized to examine the connections between EphA expression and gene biomarkers linked to tumor-infiltrating immune cells, utilizing established gene biomarkers (21, 22).

Patients and tissues

KIRP tumor and adjacent normal kidney specimens were analyzed from a total of 157 patients with KIRP as part of a study approved by Tianjin Medical University Cancer Institute and Hospital. All patients were treated with radical or partial nephrectomy and rendered disease-free.

Immunohistochemistry

Immunohistochemical staining was performed on the sections from surgical specimens fixed in 10% formalin and embedded in paraffin according to a standard method (23). Briefly, tissue sections were incubated with anti-EphA3 antibody (ab126261, Abcam; 1: 50 dilution) overnight at 4°C, and then incubated with secondary antibody (ab207995, Abcam; 1:100 dilution) followed by avidin-biotin peroxidase complex (DAKO) at room temperature for 30min. Finally, color development was performed with 3, 3′-diaminobenzidine. The immunostained slides were evaluated separately by two pathologists. The intensity of antibody staining was used to semiquantitatively quantify the expression of EphA3 in cancer cells. Staining intensity was categorized as follows: absent staining as 0, weak as 1, moderate as 2, and strong as 3.

Statistical analysis

Statistical analyses were conducted using R 4.0.2 (https://www.r-project.org/). A linear mixed-effect model was employed to compare gene expression patterns between tumor and normal samples. Boxplots were utilized to illustrate gene expression variation across different cancer types. Univariate and multivariate Cox regression or Log-rank test were used to examine the relationship between gene expression and overall survival (OS) of patients. The correlation between gene expression and stemness scores, stromal scores, immune scores, and estimate scores was assessed using Spearman or Pearson correlation methods.

Results

Expression of EphA genes in pan-cancer

The levels of EphA mRNA were assessed across 33 cancer types using data sourced from UCSC Xena, aiming to uncover the diversity inherent within the EphA family. The results revealed prominent high expression levels for most EphA genes in multiple cancer types. However, this trend was not mirrored by three genes: EphA5, EphA6, and EphA8, which exhibited relatively diminished expression levels (Figure 1A). When examining individual EphA genes like EphA2 and EphA10, significant up-regulation was observed in cases of esophageal carcinoma (ESCA) and cholangiocarcinoma (CHOL). Conversely, EphA2 and EphA10 displayed a down-regulation in kidney chromophobe (KICH) and glioblastoma multiforme (GBM) (Figure 1B). Particularly noteworthy was the correlation analysis that pinpointed the strongest pairwise correlation between EphA1 and EphA2 among the nine genes (Correlation coefficient =0.47). This finding implied potential shared characteristics or functions between these two genes. In contrast, EphA1 and EphA5 demonstrated a distinct negative correlation (Correlation coefficient =−0.36, Figure 1C), suggesting intricate co-expression interactions involving numerous EphA genes across diverse cancer types.

On closer inspection, it became evident that nearly all EphA genes exhibited discernible disparities in expression between cancerous tissue samples and their normal counterparts (Figure 2). Moreover, significant differences in expression emerged across the spectrum of different cancer types.

Prognostic value of EphA genes in pan-cancer

To deeply delve into the prognostic implications of EphA family genes, we examined the impact of the expression level of each gene

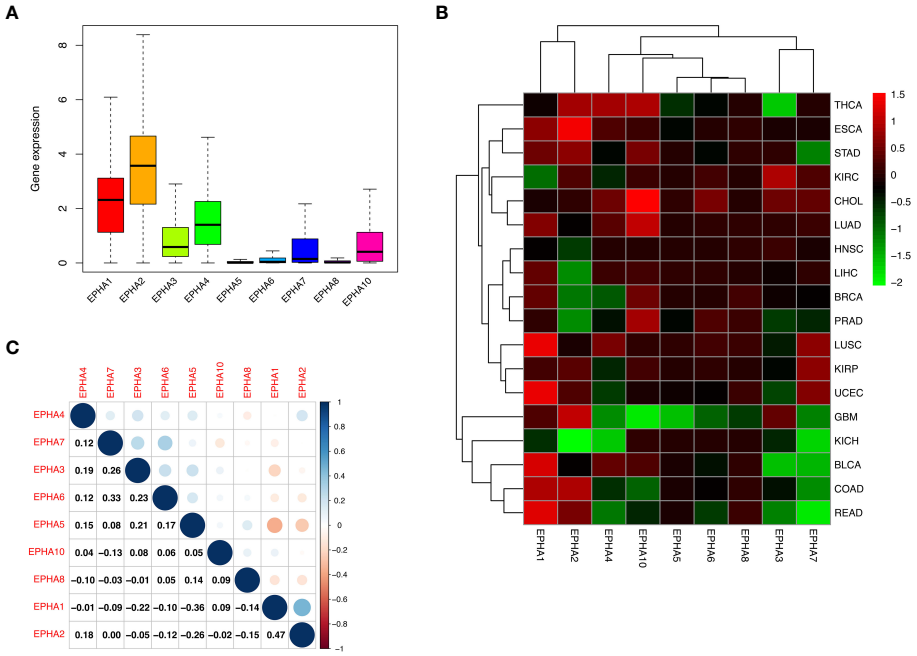

FIGURE 1
Our investigation delved into the expression of EphA genes across 33 cancer types utilizing the TCGA database. The outcomes unveiled a consistent up-regulation in the expression of EphA1, EphA2, EphA3, EphA4, EphA7, and EphA10 within cancerous tissues **(A)**. A deeper analysis highlighted intriguing dynamics, where specific EphA genes, namely EphA2 and EphA10 displayed overexpression in ESCA and CHOL, while EphA2 and EphA10 exhibited substantial down-regulation in KICH and GBM **(B)**. EphA1 and EphA2 emerged as the genes exhibiting the most robust positive correlation (Correlation coefficient =0.47). Conversely, EphA1 and EphA5 stood out as the two genes displaying the most prominent negative correlation (Correlation coefficient = -0.36, **C**).

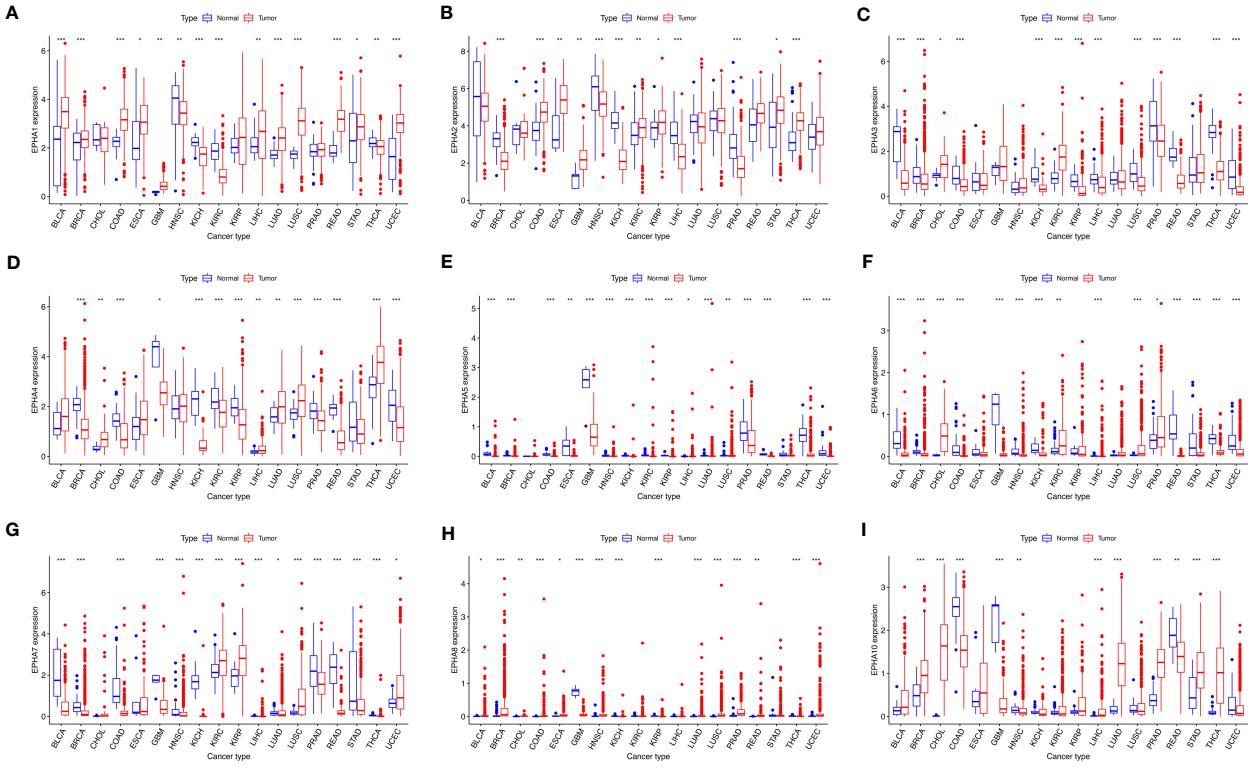

FIGURE 2
The visualizations derived from the TCGA database captured the expression patterns of EphA genes in diverse cancers. The EphA family genes include **(A)** EphA1; **(B)** EphA2; **(C)** EphA3; **(D)** EphA4; **(E)** EphA5; **(F)** EphA6; **(G)** EphA7; **(H)** EphA8; **(I)** EphA10. The outcomes consistently demonstrated distinct variations in the expression of EphA genes between cancerous tissues and their normal counterparts. *P < 0.05, **P < 0.01, ***P < 0.001.

on the prognosis of patients with specific cancers (Supplementary Figure 1). Through the application of the Cox proportional hazard model, the prognostic value of the nine EphA genes was evaluated across pan-cancer scenarios (Figure 3, Supplementary Table 1). The findings underscored a connection between EphA gene expression levels and the OS of patients, albeit with nuanced ramifications contingent on the specific cancer types. For example, heightened EphA5 expression correlated with an unfavorable prognosis of papillary renal cell carcinoma (KIRP) and uveal melanoma (UVM), whereas predicting improved survival in pancreatic adenocarcinoma (PAAD). Similarly, elevated EphA2 expression indicated a poor prognosis for patients with colon adenocarcinoma (COAD), diffuse large B-cell lymphoma (DLBC), low-grade glioma (LGG), and pancreatic adenocarcinoma (PAAD), yet correlated with higher survival rates in those with kidney chromophobe (KICH) and pheochromocytoma and paraganglioma (PCPG). Importantly, EphA genes emerged as independent prognostic markers for several distinct cancer types.

Association of EphA genes with immune response and tumor microenvironment

EphA genes occupy a critical position within the immune system due to their intricate involvement in the development, mobilization, and activation of both innate and adaptive immune cells (15, 24). Within the context of human malignancies, six distinct types of immune infiltration which were defined as the relative abundance of a set of immune cell populations, ranging from tumor promoting to tumor inhibiting, namely C1 (wound healing), C2 (INF-r dominant), C3 (inflammatory), C4 (lymphocyte depleted), C5 (immunologically quiet), and C6 (TGFβ dominant) (18). In the scope of our investigation, we conducted a thorough examination of immune infiltration patterns across the TCGA pan-cancer dataset, aligning them with the expression profiles of EphA genes (Figure 4A). Remarkably, the data illuminated connections between the expression levels of EphA genes and diverse categories of immune infiltration, except for EphA5, EphA6, and EphA8. Notably, EphA1 and EphA2 exhibited heightened expression in the C1 and C2 subtypes, indicating a plausible involvement in tumor promotion. This assumption found support in the observation of poorer survival rates among patients exhibiting these types of immune infiltration (C1 and C2). In contrast, EphA6 and EphA10 displayed elevated expression in the C3 and C5 subtypes, suggesting a potential tumor-suppressive effect. Nevertheless, it's important to highlight that these correlations contradicted the roles of certain EphA members as promoters of cancer, which in some cases translated to diminished survival rates. A case in point was the poor prognosis linked to heightened EphA6 expression in UCEC (Supplementary Figure 1). These conflicting outcomes can

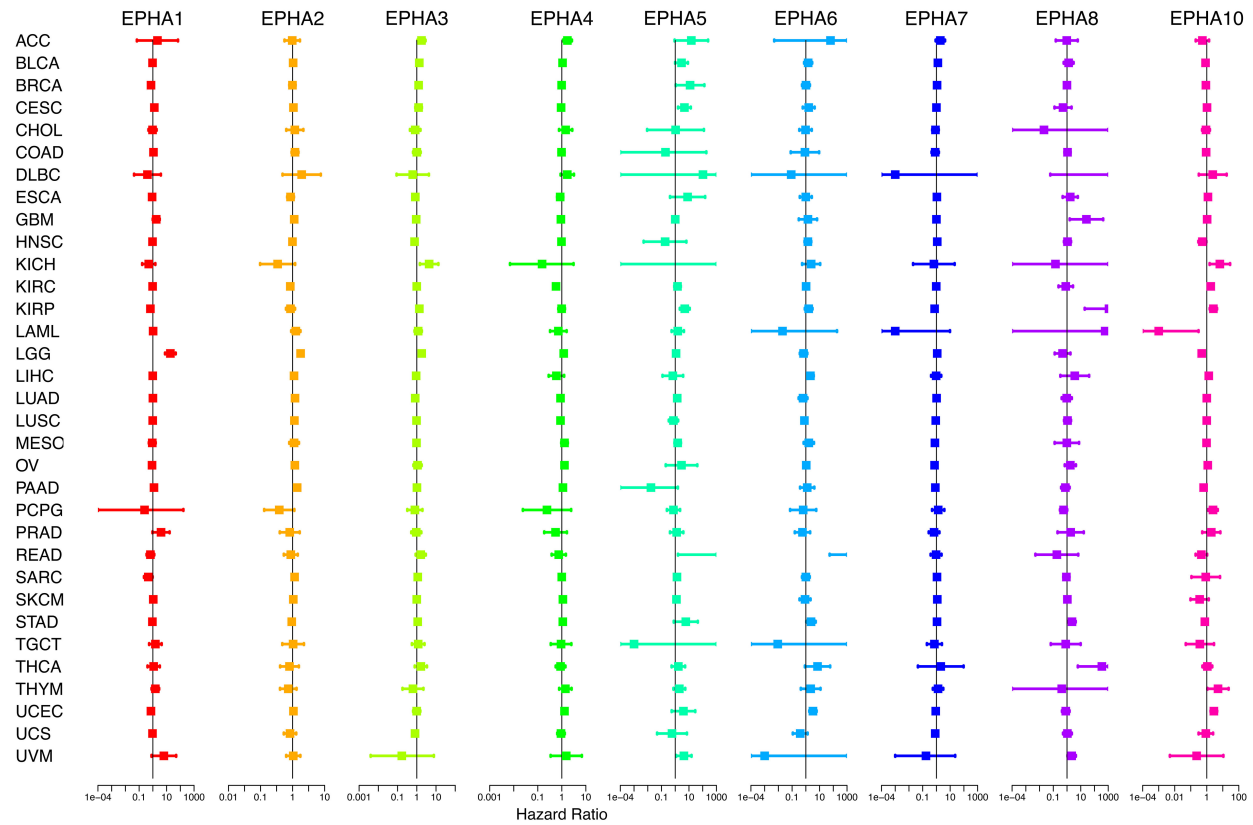

FIGURE 3
By applying COX analysis, we synthesized the prognosis risks associated with the nine genes across a pan-cancer context. The data underscored that EphA genes wielded the status of independent prognostic factors in various cancer types.

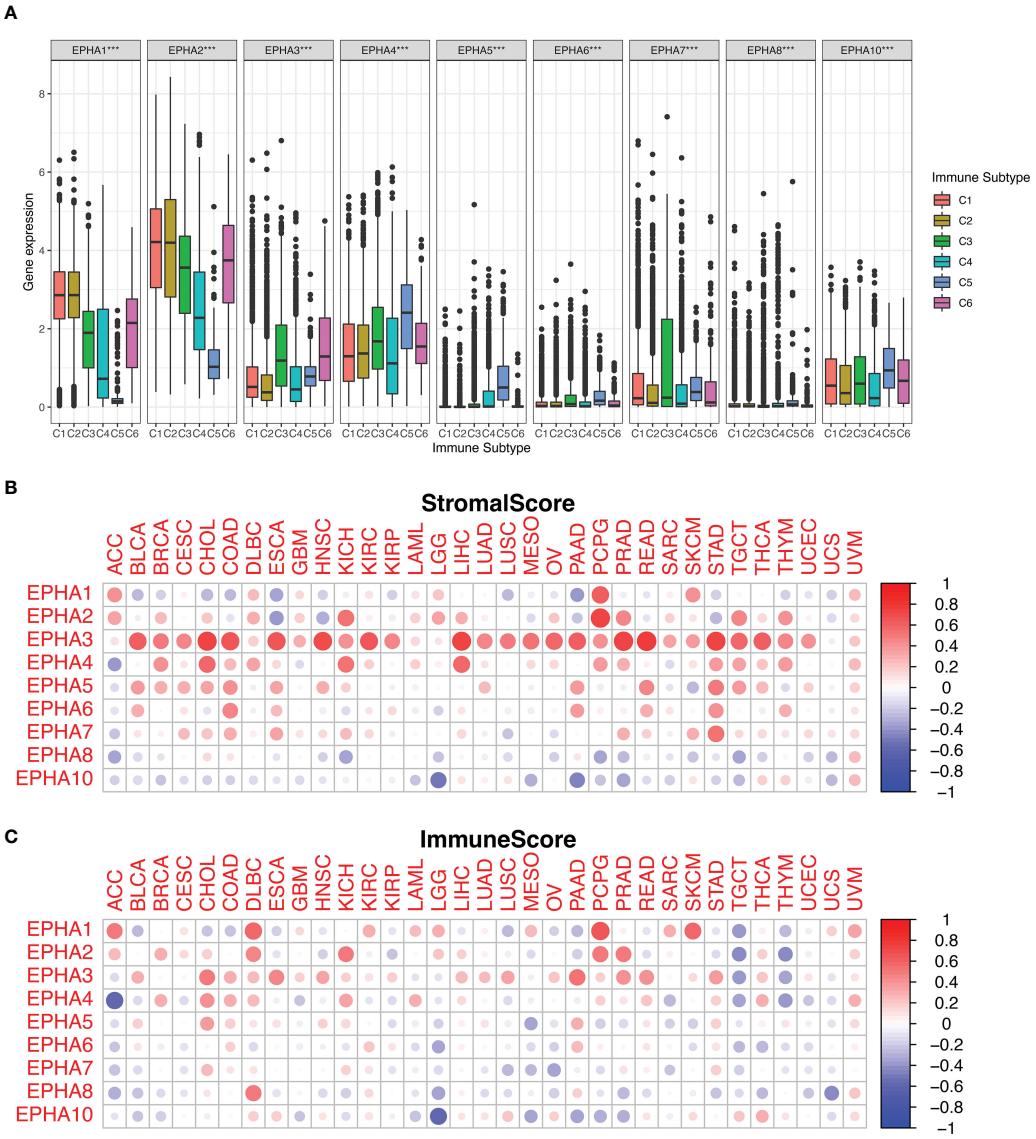

FIGURE 4
We investigated the correlation between EphA expression and immune infiltration across the pan-cancer landscape. The results depicted the significant roles played by all EphA genes within the TME **(A)**. Additionally, we harnessed the ESTIMATE algorithm to assess the stromal and immune scores attributed to EphA genes **(B, C)**. ***P < 0.001.

potentially be attributed to the intricate biological diversity and multifaceted molecular interactions inherent to the progression of tumors. The implications of EphAs on the immune dynamics of the TME hold the promise of guiding novel pathways for the development of treatment strategies.

Furthermore, we delved into the stromal and immune scores indicative of tumor growth and metastatic potential. Leveraging the ESTIMATE algorithm, EphA genes were subjected to a comprehensive analysis involving these scores (Figures 4B, C). EphA genes with high stromal scores suggested heightened complexity within the TME, possibly intensifying tumor malignancy. An illustration of this was found in the close association between EphA3 expression and elevated stromal score across diverse cancers, whereas EphA10 expression demonstrated an inverse pattern. The associations between distinct gene expression levels within the EphA family and the estimated scores across various tumors underscored the diverse impacts that these genes might exert on the TME.

Role of EphA genes in KIRP

Renal carcinoma ranks as the 13th most prevalent cancer worldwide, with an escalating incidence rate (25). Papillary renal cell carcinoma (KIRP), constituting 10% to 15% of kidney cancer cases, stands as the second most common subtype (26). In the metastatic context, the prognosis for KIRP patients remains bleak due to the absence of effective therapeutic options (27). The optimal treatment strategy for advanced KIRP continues to be a subject of debate. Nonetheless, recent clinical studies have unveiled promising outcomes for both molecularly targeted therapies and

immunotherapy within this subtype (28). Given the elevated risk association of most EphA genes with poor survival in KIRP patients, our research expanded to explore the interplay between EphA genes, diverse immune subtypes, stem cells, and the TME in KIRP. The connection between EphA gene expression and distinct immune subtypes in KIRP echoed the patterns observed across all 33 TCGA cancer types. Of particular note, EphA1, EphA 2, EphA 3, and EphA 7 exhibited significant associations with immune infiltration profiles in KIRP (Figure 5A). Subsequently, we delved into the correlation between EphA expression and stromal score, revealing positive associations for EphA3 and EphA6 ($P < 0.05$) in KIRP, in which EphA3 demonstrated the most robust correlation ($r = 0.49$) (Figure 5B). On the other hand, EphA2, EphA4, EphA5, EphA7 EphA 8, and EphA 10 did not display significant correlations with stromal scores, implying their potential origin from the tissue stroma in KIRP. Moreover, EphA3 exhibited correlations with the immune score, a metric assessing the presence of infiltrating immune cells ($P = 0.0011$) and tumor purity (Estimate score) ($P < 0.0001$).

Upon a deeper exploration of EphA3's role, pronounced connections surfaced between EphA3 expression and various

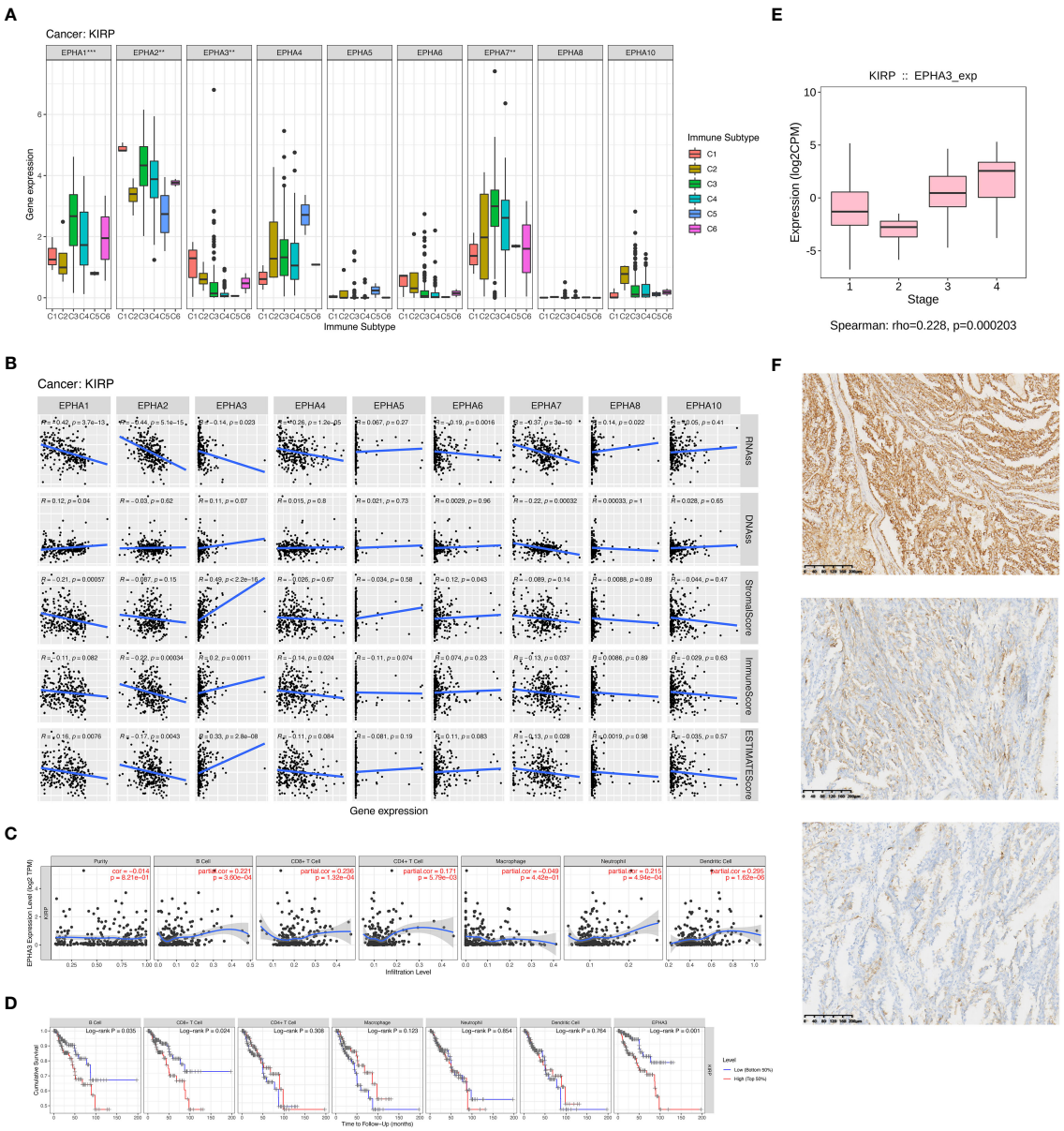

FIGURE 5
We delved into EphA's impact on immune infiltration through an examination of individual cancer types. The outcomes of our investigation demonstrated significant differences in immune subtypes among EphA genes in KIRP **(A)**. Subsequently, we investigated immune infiltration in KIRP to evaluate the effects of these genes **(B)**. We also found that EphA3 expression displayed correlations with immune cell infiltration specific to KIRP **(C, D)**. Further, EphA3 was found to be up-regulated in advanced-stage KIRP samples analyzed by TCGA datasets **(E)**. Finally, we evaluated the correlation between EphA3 expression and clinicopatho-logical parameters in KIRP by immunohistochemistry **(F)**. The pictures showed the different degrees of staining of EphA3 in KIRP:(up) strong EphA3 expression in KIRP; (center) moderate EphA3 expression in KIRP; and (down) weak EphA3 expression in KIRP (Magnification x400). **P < 0.01, ***P < 0.001.

immune cell types, such as $CD4^+$ T cells (R =0.171, P =5.79E-03), $CD8^+$ T cells (R =0.236, P =1.32E-04), B cells (R =0.221, P =3.60E-04), dendritic cells (R =0.295, P =1.62E-06), and neutrophils (R =0.215, P =4.94E-04). However, these correlations were notably absent for tumor purity (R=-0.014, P=8.21E-01) and macrophages (R =-0.049, P =4.42E-01) (Figure 5C). Leveraging the TIMER database, the Kaplan-Meier curves highlighted a substantial linkage between KIRP patients survival and EphA3 expression (P =0.001), as well as the infiltration of $CD8^+$ T cells (P =0.024) and B cells (P =0.035) (Figure 5D). Overall, our findings underscore the potential role of EphA3 in governing immune cell infiltration in KIRP. Alongside B cell and $CD8^+$ T cell infiltration, EphA3 emerges as a pivotal modulator influencing clinical outcomes for KIRP patients.

Further delving into the connection between EphA3 expression and immune cell infiltration, we uncovered EphA3's association with markers of various immune cell types, including B cells (CD19 and CD79A), monocytes (CD86 and CD115), M1 macrophages (INOS, IRF5, and COX2), Th2 cells (GATA3 and IL13), and Treg cells (FOXP3, CCR8, STAT5B, and TGFb) (Table 1). This revelation suggested that EphA3 may play a regulatory role as an immunomodulator in the renal cancer microenvironment.

The relationship between EphA3 protein expression and clinicopathologic parameters in KIRP

EphA3 was found to be up-regulated in advanced-stage KIRP samples analyzed by TCGA datasets (HR =0.228, P <0.001, Figure 5E). To further elucidate the association between EphA3 expression and KIRP, differences in the level of EphA3 protein expression between cancer cells and adjacent normal cells were compared in KIRP tissue specimens by immunohistochemistry. The high and low groups were defined based on the median EphA3 expression (Figure 5F). The result showed that the expression of EphA3 protein was significantly associated with metastases (TNM) stage (P =0.0017), tumor diameter (P <0.0001), and age (P =0.0030). No significant association between the expression of EphA3 and sex (P =0.8635) was found (Table 2).

TABLE 1 Correlations between EphA3 expression and related gene markers in KIRP.

Description	Gene markers	R	P
B cell	CD19	0.257	9.08E-06(***)
	CD79A	0.380	2.08E-11(***)
Monocyte	CD86	0.162	5.71E-03(**)
	CD115(CSF1R)	0.229	8.1E-05(***)
M1 Macrophage	INOS(NOS2)	0.253	1.35E-05(***)
	IRF5	-0.121	4.01E-02(*)
	COX2(PTGS2)	0.43	1.8E-14(***)
Th2	GATA3	0.447	1.14E-15(***)
	STAT6	0.056	3.42E-01
	STAT5A	0.095	1.07E-01
	IL13	0.157	7.48E-03(**)
Treg	FOXP3	0.279	1.37E-06(***)
	CCR8	0.336	4.27E-09(***)
	STAT5B	0.124	3.52E-02(*)
	TGFb(TGFB1)	0.36	2.51E-10(***)

*P < 0.05, **P < 0.01, ***P < 0.001.
KIRP, papillary renal cell cancer.

Discussion

This study offered an extensive pan-cancer analysis of EphA genes spanning 33 distinct cancer types using independent datasets from TCGA. The results emphasize the marked elevation in expression for the majority of EphA genes among cancer patients, except for EphA5, EphA6, and EphA8. Further, a thorough investigation into the association between the OS of patients and EphA expression levels was conducted. It was revealed that most of these genes hold prognostic significance within varied cancer types, often exerting bidirectional effects. EphA2, for example, correlated with a poor prognosis in COAD, DLBC, LGG, or PAAD cases, while heralding improved survival for patients with KICH and PCPG.

The TME stands as a pivotal determinant in tumorigenesis and tumor growth, offering a conducive setting for tumor proliferation and the dampening of immune responses (29, 30). Ephs and their corresponding ephrin ligands orchestrate intricate cell interactions during cellular growth processes, extending their influence to malignancies and the TME, thereby promoting cancer invasion, metastasis, and angiogenesis (24, 31). Prior studies have investigated six distinct types of immune infiltration (C1–C6) that may impact the proliferation of tumor cells in cancer patients (18).

TABLE 2 Expression of EphA3 protein in KIRP and the association with clinicopathologic parameters.

Parameter	Low expression (n=72)	High expression (n=65)	p-value
TNM Stage, n (%)			
I and II	64 (46.7%)	43 (31.4%)	0.0017
III and IV	8 (5.8%)	22 (16.1%)	
Sex, n (%)			
Female	33 (24.1%)	28 (20.4%)	0.8635
Male	39 (28.5%)	37 (27.0%)	
Age (years), n (%)			
<60	21 (15.3%)	36 (26.3%)	0.0030
≥60	51 (37.2%)	29 (21.2%)	
Tumor Diameter, cm			
<7	44 (32.1%)	16 (11.7%)	<0.0001
≥7	28 (20.4%)	49 (35.8%)	

Three scenarios of immune infiltration integrated, respectively, by poor cytotoxicity(C1–C2), intermediate cytotoxicity (C3–C4), and high cytotoxicity(C5–C6). Tumors with highly cytotoxic immunophenotype would be partially repressed by the immune system, resulting in less frequent progression to more advanced stages. Our findings consistently point towards robust connections between most members of the EphA gene family and infiltration within the TME. Particularly notable are the correlations of EphA1 and EphA2 with more aggressive subtypes of immune infiltration subtypes (C1 and C2), indicative of a poorer prognosis. Employing the ESTIMATE method, we further unearthed associations between EphA genes and infiltration of stromal and immune cells. This observation aligns with previous studies highlighting the role of EphA as an immunomodulator and pro-inflammatory factor (24, 32–34). These genes, thus, emerge as prospective candidates for treatment targets or predictive markers for the effectiveness of immune checkpoint modulators in cancer patients.

EphA's role exhibits divergence, potentially acting as either tumor-suppressive or tumor-promoting within the same tumor origin. For instance, the correlation pattern of these genes with immune infiltration subtypes in KIRP presented a parallel trend, with EphA3 demonstrating elevated expression in C1 and C2, thus implying a tumor-promoting function. Intriguingly, EphA3 demonstrated a robust correlation with stromal scores (r =0.49) in KIRP. Though these findings imply EphA3 is a promising target for anticancer treatment, further experimental validation is necessitated.

Elevated EphA3 expression is linked to poor prognosis in several malignancies including gastric cancer (35), colorectal cancer (36), and hepatocellular carcinoma (37). The study by Wang et al. suggested EphA3's tumor-suppressive role in kidney renal clear cell carcinoma (KIRC) (38). To date, there has been little published research investigating EphA3's role in the prognosis or therapeutic potential of KIRP. In our study, differential gene expression analysis accentuated significant down-regulation of EphA3 in KIRP samples compared to normal kidney samples (Figure 2). However, heightened EphA3 expression emerges as a risk factor for a poor prognosis in KIRP patients (Figure 3). This conflicting result adds complexity to our comprehension of EphA3's contribution to KIRP initiation and development. To deepen our under-standing, we analyzed the correlation between EphA3 and clinical stages using the sequencing data and clinical information from the TCGA database. The results reveal that EphA3 was up-regulated in advanced-stage KIRP samples (Figure 5E). Notably, further analysis of clinical samples showed that overexpression of EphA3 was associated with tumor diameter (P <0.0001) and TNM stage (P =0.0017) (Table 2).

EphA3 is the first receptor with dual significance, being recognized as a tumor antigen in lymphoblastic leukemia cells and, independently, in melanoma cells from a patient with an EphA3-reactive T cell immunological response (39). Recently, advancements have further illuminated the role of EphA3 as a binding partner to PD-L1, discovered during an extensive search for transmembrane receptors engaged with immunoglobulin superfamily members. The connection between EphA3/PD-L1 co-expression and overall PD-L1 expression is intricately linked to a CD8 T effector cell signature in urothelial carcinoma tissues, as unveiled through gene expression analyses (31).To delve deeper into the significance of EphA3 in KIRP, an exploration was undertaken using the TIMER databases to uncover its correlations with B cells, $CD8^+$ T cells, $CD4^+$ T cells, and neutrophil infiltration. The results established the affiliation of EphA3 expression with markers of B cells (CD19 and CD79A), monocytes (CD86 and CD115), M1 macrophages (INOS, IRF5, and COX2), Th2 cells (GATA3 and IL13), and Treg cells (FOXP3, CCR8, STAT5B, and TGFb) (Table 1). These insights further accentuate the alignment of EphA3 expression with immune infiltration in KIRP, validating its role as a modulator of immune evasion within the renal cancer microenvironment.

In summary, our findings cast light on the multifaceted contributions of EphA to immune response and the complex landscape of the TME, which is essential for promoting personalized anticancer treatments. A groundbreaking assertion is made that elevated EphA3 expression independently heightens the risk of poor prognosis in KIRP patients, while concurrently functioning as a regulator of the immune microenvironment as well as a viable biomarker for prognostic evaluation and the assessment of immunotherapy response in patients with kidney cancer.

It's imperative to acknowledge that the study carries certain limitations. First of all, the analysis of EphA genes leaned heavily on bioinformatics perspectives, lacking the validation provided by *in-vivo* or *in-vitro* experiments. More studies focusing on molecular and cellular basis are needed to facilitate high-throughput data analysis. Additionally, the inclusion of extensive data from diverse databases is essential to mitigate any potential information bias. Prospective studies investigating EphA gene expression in the context of immune cells across a wide range of cancers hold the potential to unveil novel insights, thereby opening new avenues for exploration in this intriguing domain.

Conclusion

In theory, it may be possible to enhance tumorimmune therapy by modifying EphA activity. However, how EphA controls tumor immunity is still largely a mystery. On the one hand, a large number of research papers evaluating the role of Eph receptors in immune responses have not yet been applied to cancer models. On the other hand, EphA receptor kinase inhibitors have been developed, but it remains unclear how they effect on the immune system. In summary, despite a great deal of research on Eph receptors in immunology and cancer biology, this family stands mostly understudied in the context of tumor immunity. Here, we delve deeply into the multifarious roles played by EphA genes play in the initiation and progression of diverse cancers, alongside their associations with patient prognosis and immune response. This gap in our current knowledge identifies a distinct opportunity for new discoveries that may advance our understanding of the tumor microenvironment and pave the way for novel immunotherapeutic targets.

Data availability statement

The datasets presented in this study can be found in online repositories. The names of the repository/repositories and accession number(s) can be found in the article/Supplementary Material.

Author contributions

ZC: Conceptualization, Investigation, Software, Writing – review & editing, Writing – original draft. CL: Writing – review & editing, Conceptualization, Data curation, Methodology, Supervision. XW: Formal analysis, Project administration, Resources, Validation, Visualization, Writing – original draft. YX: Resources, Writing – original draft, Funding acquisition, Writing – review & editing.

Funding

The author(s) declare financial support was received for the research, authorship, and/or publication of this article. The study was supported by the Tianjin Key Medical Discipline (Specialty) Construction Project (TJYXZDXK-012A).

Conflict of interest

The authors declare that the research was conducted in the absence of any commercial or financial relationships that could be construed as a potential conflict of interest.

Publisher's note

Supplementary material

The Supplementary Material for this article can be found online at: https://www.frontiersin.org/articles/10.3389/fonc.2024.1378087/full#supplementary-material

References

1. Bray F, Laversanne M, Sung H, Ferlay J, Siegel RL, Soerjomataram I, et al. Global cancer statistics 2022: GLOBOCAN estimates of incidence and mortality worldwide for 36 cancers in 185 countries. *CA Cancer J Clin*. (2024) 74:229–63. doi: 10.3322/caac.21834

2. Singh AK, McGuirk JP. CAR T cells: continuation in a revolution of immunotherapy. *Lancet Oncol*. (2020) 21:e168–e78. doi: 10.1016/S1470-2045(19)30823-X

3. Kennedy LB. Salama AKS. A review of cancer immunotherapy toxicity. *CA Cancer J Clin*. (2020) 70:86–104. doi: 10.3322/caac.21596

4. Srivastava S, Hanash S. Pan-cancer early detection: hype or hope? *Cancer Cell*. (2020) 38:23–4. doi: 10.1016/j.ccell.2020.05.021

5. Miao H, Wang B. Eph/ephrin signaling in epithelial development and homeostasis. *Int J Biochem Cell Biol*. (2009) 41:762–70. doi: 10.1016/j.biocel.2008.07.019

6. Zhou Y, Sakurai H. Emerging and diverse functions of the ephA2 noncanonical pathway in cancer progression. *Biol Pharm Bull*. (2017) 40:1616–24. doi: 10.1248/bpb.b17-00446

7. Andretta E, Cartón-García F, Martínez-Barriocanal Á, de Marcondes PG, Jimenez-Flores LM, Macaya I, et al. Investigation of the role of tyrosine kinase receptor EPHA3 in colorectal cancer. *Sci Rep*. (2017) 7:41576. doi: 10.1038/srep41576

8. Chen Z, Chen J, Ren D, Zhang J, Yang Y, Zhang H, et al. EPHA5 mutations predict survival after immunotherapy in lung adenocarcinoma. *Aging (Albany NY)*. (2020) 13:598–618. doi: 10.18632/aging.202169

9. Kikuchi S, Kaibe N, Morimoto K, Fukui H, Niwa H, Maeyama Y, et al. Overexpression of Ephrin A2 receptors in cancer stromal cells is a prognostic factor for the relapse of gastric cancer. *Gastric Cancer*. (2015) 18:485–94. doi: 10.1007/s10120-014-0390-y

10. Wang Y, Yu H, Shan Y, Tao C, Wu F, Yu Z, et al. EphA1 activation promotes the homing of endothelial progenitor cells to hepatocellular carcinoma for tumor neovascularization through the SDF-1/CXCR4 signaling pathway. *J Exp Clin Cancer Res*. (2016) 35:65. doi: 10.1186/s13046-016-0339-6

11. Youngblood VM, Kim LC, Edwards DN, Hwang Y, Santapuram PR, Stirdivant SM, et al. The ephrin-A1/EPHA2 signaling axis regulates glutamine metabolism in HER2-positive breast cancer. *Cancer Res*. (2016) 76:1825–36. doi: 10.1158/0008-5472.CAN-15-0847

12. Charmsaz S, Scott AM, Boyd AW. Targeted therapies in hematological Malignancies using therapeutic monoclonal antibodies against Eph family receptors. *Exp Hematol*. (2017) 54:31–9. doi: 10.1016/j.exphem.2017.07.003

13. Wilson K, Shiuan E, Brantley-Sieders DM. Oncogenic functions and therapeutic targeting of EphA2 in cancer. *Oncogene*. (2021) 40:2483–95. doi: 10.1038/s41388-021-01714-8

14. Buckens OJ, El Hassouni B, Giovannetti E, Peters GJ. The role of Eph receptors in cancer and how to target them: novel approaches in cancer treatment. *Expert Opin Investig Drugs*. (2020) 29:567–82. doi: 10.1080/13543784.2020.1762566

15. Shiuan E, Chen J. Eph receptor tyrosine kinases in tumor immunity. *Cancer Res*. (2016) 76:6452–7. doi: 10.1158/0008-5472.CAN-16-1521

16. Goldman MJ, Craft B, Hastie M, Repečka K, McDade F, Kamath A, et al. Visualizing and interpreting cancer genomics data via the Xena platform. *Nat Biotechnol*. (2020) 38:675–8. doi: 10.1038/s41587-020-0546-8

17. Yoshihara K, Shahmoradgoli M, Martínez E, Vegesna R, Kim H, Torres-Garcia W, et al. Inferring tumour purity and stromal and immune cell admixture from expression data. *Nat Commun*. (2013) 4:2612. doi: 10.1038/ncomms3612

18. Tamborero D, Rubio-Perez C, Muiños F, Sabarinathan R, Piulats JM, Muntasell A, et al. A pan-cancer landscape of interactions between solid tumors and infiltrating immune cell populations. *Clin Cancer Res*. (2018) 24:3717–28. doi: 10.1158/1078-0432.CCR-17-3509

19. Li T, Fu J, Zeng Z, Cohen D, Li J, Chen Q, et al. TIMER2.0 for analysis of tumor-infiltrating immune cells. *Nucleic Acids Res*. (2020) 48:W509–w14. doi: 10.1093/nar/gkaa407

20. Li T, Fan J, Wang B, Traugh N, Chen Q, Liu JS, et al. TIMER: a web server for comprehensive analysis of tumor-infiltrating immune cells. *Cancer Res*. (2017) 77:e108–e10. doi: 10.1158/0008-5472.CAN-17-0307

21. Siemers NO, Holloway JL, Chang H, Chasalow SD, Ross-MacDonald PB, Voliva CF, et al. Genome-wide association analysis identifies genetic correlates of immune infiltrates in solid tumors. *PloS One*. (2017) 12:e0179726. doi: 10.1371/journal.pone.0179726

22. Danaher P, Warren S, Dennis L, D'Amico L, White A, Disis ML, et al. Gene expression markers of Tumor Infiltrating Leukocytes. *J Immunother Cancer*. (2017) 5:18. doi: 10.1186/s40425-017-0215-8

23. Xiang YP, Xiao T, Li QG, Lu SS, Zhu W, Liu YY, et al. Y772 phosphorylation of EphA2 is responsible for EphA2-dependent NPC nasopharyngeal carcinoma growth by Shp2/Erk-1/2 signaling pathway. *Cell Death Dis*. (2020) 11:709. doi: 10.1038/s41419-020-02831-0

24. Janes PW, Vail ME, Ernst M, Scott AM. Eph receptors in the immunosuppressive tumor microenvironment. *Cancer Res*. (2021) 81:801–5. doi: 10.1158/0008-5472.CAN-20-3047

25. Siegel RL, Miller KD, Fuchs HE, Jemal A. Cancer statistics, 2022. *CA Cancer J Clin*. (2022) 72:7–33. doi: 10.3322/caac.21708

26. Akhtar M, Al-Bozom IA, Al Hussain T. Papillary renal cell carcinoma (PRCC): an update. *Adv Anat Pathol*. (2019) 26:124–32. doi: 10.1097/PAP.0000000000000220

27. Chandrasekar T, Klaassen Z, Goldberg H, Kulkarni GS, Hamilton RJ, Fleshner NE. Metastatic renal cell carcinoma: patterns and predictors of metastases-A contemporary population-based series. *Urol Oncol*. (2017) 35:661.e7–.e14. doi: 10.1016/j.urolonc.2017.06.060

28. Connor Wells J, Donskov F, Fraccon AP, Pasini F, Bjarnason GA, Beuselinck B, et al. Characterizing the outcomes of metastatic papillary renal cell carcinoma. *Cancer Med*. (2017) 6:902–9. doi: 10.1002/cam4.1048

29. Jiao S, Subudhi SK, Aparicio A, Ge Z, Guan B, Miura Y, et al. Differences in tumor microenvironment dictate T helper lineage polarization and response to immune checkpoint therapy. *Cell*. (2019) 179:1177–90.e13. doi: 10.1016/j.cell.2019.10.029

30. Quail DF, Joyce JA. Microenvironmental regulation of tumor progression and metastasis. *Nat Med*. (2013) 19:1423–37. doi: 10.1038/nm.3394

31. Verschueren E, Husain B, Yuen K, Sun Y, Paduchuri S, Senbabaoglu Y, et al. The immunoglobulin superfamily receptome defines cancer-relevant networks associated with clinical outcome. *Cell*. (2020) 182:329–44.e19. doi: 10.1016/j.cell.2020.06.007

32. Vail ME, Murone C, Tan A, Hii L, Abebe D, Janes PW, et al. Targeting EphA3 inhibits cancer growth by disrupting the tumor stromal microenvironment. *Cancer Res*. (2014) 74:4470–81. doi: 10.1158/0008-5472.CAN-14-0218

33. Zhang Z, Wu HX, Lin WH, Wang ZX, Yang LP, Zeng ZL, et al. EPHA7 mutation as a predictive biomarker for immune checkpoint inhibitors in multiple cancers. *BMC Med*. (2021) 19:26. doi: 10.1186/s12916-020-01899-x

34. Markosyan N, Li J, Sun YH, Richman LP, Lin JH, Yan F, et al. Tumor cell-intrinsic EPHA2 suppresses anti-tumor immunity by regulating PTGS2 (COX-2). *J Clin Invest*. (2019) 129:3594–609. doi: 10.1172/JCI127755

35. Lv XY, Wang J, Huang F, Wang P, Zhou JG, Wei B, et al. EphA3 contributes to tumor growth and angiogenesis in human gastric cancer cells. *Oncol Rep*. (2018) 40:2408–16. doi: 10.3892/or.2018.6586

36. Xi HQ, Zhao P. Clinicopathological significance and prognostic value of EphA3 and CD133 expression in colorectal carcinoma. *J Clin Pathol*. (2011) 64:498–503. doi: 10.1136/jcp.2010.087213

37. Lu CY, Yang ZX, Zhou L, Huang ZZ, Zhang HT, Li J, et al. High levels of EphA3 expression are associated with high invasive capacity and poor overall survival in hepatocellular carcinoma. *Oncol Rep*. (2013) 30:2179–86. doi: 10.3892/or.2013.2679

38. Wang X, Xu H, Cao G, Wu Z, Wang J. Loss of ephA3 protein expression is associated with advanced TNM stage in clear-cell renal cell carcinoma. *Clin Genitourin Cancer*. (2017) 15:e169–e73. doi: 10.1016/j.clgc.2016.07.028

39. Chiari R, Hames G, Stroobant V, Texier C, Maillère B, Boon T, et al. Identification of a tumor-specific shared antigen derived from an Eph receptor and presented to CD4 T cells on HLA class II molecules. *Cancer Res*. (2000) 60:4855–63.

frontiers | Frontiers in Oncology

TYPE Original Research
PUBLISHED 19 June 2024
DOI 10.3389/fonc.2024.1336106

OPEN ACCESS

EDITED BY
Valeria Visconte,
Cleveland Clinic, United States

REVIEWED BY
Luca Guarnera,
Policlinico Tor Vergata, Italy
Valentina Giudice,
University of Salerno, Italy

*CORRESPONDENCE
Na Hu
NaHu11091109@outlook.com

†These authors have contributed equally to this work

RECEIVED 01 December 2023
ACCEPTED 21 May 2024
PUBLISHED 19 June 2024

CITATION
Ma Y, Yue J, Gao L, Zhou J, Chen W, Su J, Yao J, Shi Q, Zhao X and Hu N (2024) Activation of non-classical Wnt signaling pathway effectively enhances HLA-A presentation in acute myeloid leukemia. *Front. Oncol.* 14:1336106. doi: 10.3389/fonc.2024.1336106

Activation of non-classical Wnt signaling pathway effectively enhances HLA-A presentation in acute myeloid leukemia

YuHan Ma[1†], JunShuai Yue[1†], Ling Gao[1], JingXin Zhou[1], Wei Chen[2], Jing Su[1], JinRong Yao[1], QiaoMei Shi[1], XiaoDong Zhao[1] and Na Hu[1*]

[1]Department of Hematology, The Affiliated Suqian First People's Hospital of Nanjing Medical University, Suqian, Jiangsu, China, [2]Department of Hematology, The Affiliated Hospital of Xuzhou Medical University, Xuzhou, Jiangsu, China

Objective: The escape from T cell-mediated immune surveillance is an important cause of death for patients with acute myeloid leukemia (AML). This study aims to identify clonal heterogeneity in leukemia progenitor cells and explore molecular or signaling pathways associated with AML immune escape.

Methods: Single-cell RNA sequencing (scRNA-seq) was performed to identified AML-related cellular subsets, and intercellular communication was analyzed to investigate molecular mechanisms associated with AML immune escape. Bulk RNA sequencing (RNA-seq) was performed to screen differentially expressed genes (DEGs) related to hematopoietic stem cell progenitors (HSC-Prog) in AML, and critical ore signaling pathways and hub genes were found by Gene Set Enrichment Analysis (GSEA), Gene Ontology (GO) and Kyoto Encyclopedia of Genes and Genomes (KEGG) enrichment analysis. The mRNA level of the hub gene was verified using quantitative real-time PCR (qRT-PCR) and the protein level of human leukocyte antigen A (HLA-A) using enzyme-linked immuno sorbent assay (ELISA).

Results: scRNA-seq analysis revealed a large heterogeneity of HSC-Prog across samples, and the intercellular communication analysis indicated a strong association between HSC-Prog and $CD8^+$-T cells, and HSC-Prog also had an association with HLA-A. Transcriptome analysis identified 1748 DEGs, enrichment analysis results showed that non-classical wnt signaling pathway was associated with AML, and 4 pathway-related genes (RHOA, RYK, CSNK1D, NLK) were obtained. After qRT-PCR and ELISA validation, hub genes and HLA-A were found to be down-regulated in AML and up-regulated after activation of the non-classical Wnt signaling pathway.

Conclusion: In this study, clonal heterogeneity of HSC-Prog cells in AML was identified, non-classical wnt signaling pathways associated with AML were identified, and it was verified that HLA-A could be upregulated by activation of non-classical wnt signaling, thereby increasing antigen presentation.

KEYWORDS

acute myeloid leukemia, HLA-A, immune escape, non-classical Wnt signaling pathway, scRNA-seq

1 Introduction

Acute myeloid leukemia (AML) is a hematologic malignancy that results from uncontrolled proliferation of hematopoietic stem cells (1). The vast majority of AML patients are elderly, with nearly a quarter of the remaining patients in children, and the 5-year overall survival, though better in pediatric patients under 5 years of age than in elderly patients, is generally low (2). Abnormal accumulation of immature myeloid cells in the patient's bone marrow and peripheral blood is detected as the most visual clinical manifestation for the diagnosis of AML (3). However, the excessive accumulation of immature myeloid cells directly leads to bone marrow failure and peripheral blood involvement, resulting in patient death (4).

Studies have confirmed that cytogenetic variants are associated with AML pathogenesis. After delving into the genetic mechanisms, researchers have gained a deeper understanding of the histopathology, immunophenotype, and clinical heterogeneity of AML. Genetic variants that occur frequently in AML have been found to predict better disease remission and prognostic survival (5). Aberrant gene expression has revealed genetic heterogeneity in AML and is expected to be a valid biomarker for disease diagnosis and treatment (6). However, although AML is one of the malignancies with the lowest mutational burden, there are several common mutations or translocations producing immunogenic proteins that can drive malignant phenotypes (7). These mechanisms can often change the immune microenvironment in AML, and contribute to tumor immune escape. It has been reported that hematopoietic stem cell progenitor cells (HSC-Prog) present antigens via HLA molecules to promote T cell-specific recognition, thus forming an immune surveillance mechanism to prevent AML onset. However, cancer cells can drive cancer malignancy by altering the expression of antigen-presenting molecules or cytokines to reduce activation of T cells, thereby preventing harmful signals from being recognized and cleared (8). Studies have shown that activation of the classical wnt signaling pathway is related to HLA downregulation, which can lead to poor tumor antigen presentation and immune escape (9). Wnt signaling pathways are generally classified as β-Catenin-dependent (classical) and β-Catenin-independent (non-classical), which interact to maintain proliferation and developmental homeostasis of hematopoietic stem cells. The abnormal activation of Wnt/β-catenin signaling pathway is an important reason for the accumulation of leukemia stem cells, which can cause and promote AML. The non-classical Wnt signaling pathway protein (wnt5a) acts as a tumor suppressor to prevent malignant proliferation of hematopoietic stem cells (10–12). Therefore, this study will explore the relationship between non-classical wnt signaling pathways and HLA in AML.

Healthy hematopoietic stem cells (HSCs) have the ability to differentiate into bloodstream and immune cell lineages, but this ability is inhibited upon the occurrence of AML, resulting in abnormal proliferation of HSCs or HSC-Prog (13). Therefore, it is necessary to understand the differentiation direction and proliferation status of HSCs or HSC-Prog in AML. Using scRNA-seq method to analyze the cell hierarchy of bone marrow samples has become a new way to investigate the heterogeneity of AML cell clones recently (14). A report by Beneyto-Calabuig S et al. has used scRNA-seq to reveal the differentiation landscape of HSCs in AML and showed that patients were unable to produce sufficient numbers of healthy mature leukocytes due to the differentiation blockage of leukemia progenitor cells (15). In this study, referring to the recently published literature (16), scRNA-seq was performed to analyze the immune microenvironment of peripheral blood mononuclear cells (PBMCs) and identify the molecular mechanisms associated with clonal heterogeneity of leukemia progenitor cells, providing a new direction for immunotherapy in AML patients with genetic abnormalities.

2 Materials and methods

2.1 Data sources

The GSE235857 dataset was obtained from the Gene Expression Omnibus (GEO), and scRNA-seq was performed to analyze the collected PBMCs from AML patients or healthy donors, including 6 healthy samples (HL2-7: GSM7510825, GSM7510826, GSM7510827, GSM7510828, GSM7510829, and GSM7510830) and 6 AML samples (AML1-3, AML3B, and AML4-5: GSM7510831, GSM7510832, GSM7510833, GSM7510834, GSM7510835, and GSM7510836). Protein expression data of HLA-A in single cells were acquired from the Human Protein Atlas (https://www.proteinatlas.org/).

2.2 ScRNA-seq data analysis

The scRNA-seq datasets of 12 cases in GSE235857 were preprocessed using the Seurat (v4.3.0.1), and the single-cell datasets were debatched using the Harmony after merging the scRNA-seq datasets of 6 healthy samples and 6 AML samples. Following the normalization of the data, genes with highly variable expression from cell to cell were identified. The principal components (PCs) were subsequently calculated using the RunPCA in Seurat, and then corrected for batch effect using Harmony. The neighboring cells in the top 30 PCs were determined using the FindNeighbors function, grouped using the FindClusters function, and visualized using Uniform Manifold Approximation and Projection (UMAP). Cell types were identified based on the marker genes used for cell annotations collected from the CellMarker 2.0 database. The CellChat was used to infer the relations between ligand-receptor interactions and Intercellular communication.

2.3 Differential expression genes analysis

The Findmarker function was utilized to analyze the differences between the sample GSM7510831 (AML1) with the largest proportion of HSC-Prog and other samples (11 cases except GSM7510831). $|\text{Fold Change}| > 1.2$ and $P < 0.05$ were set as the threshold, and those meeting the conditions were defined as DEGs.

2.4 Gene set enrichment analysis

GSEA was performed to analyze pathways enriched by DEGs between GSM7510831 and other samples. The hub genes of critical pathway were selected for GO and KEGG enrichment analysis. A pathway of $P<0.05$ was significant.

2.5 Cell culture

MOLM-13 human AML cells (CL-0681), HL-60 cells (CL-0110), THP-1 cells (CL-0233) and human bone marrow HSC (CP-H262) were purchased from Procell Life Science &Technology Co., Ltd., Wuhan, China. According to the manufacturer's instructions, MOLM-13 human AML cells (AML group) were cultured in medium containing RPMI-1640 + 10% FBS +1% P/S, and human bone marrow HSC (HL group) was cultured in human bone marrow hematopoietic stem cell complete medium (Procell, CM-H262) at 37°C in an atmosphere of 5% CO_2. In addition, MOLM-13 human AML cells were treated with Wnt5a agonists (Foxy-5, HY-P1416, MCE) or inhibitors (Box5, HY-123071, MCE), respectively, and placed in medium culture for follow-up experiments.

2.6 Quantitative real-time PCR

Total RNA was extracted using Trizol reagent, according to the manufacturer's instructions. RNA was reverse transcribed to cDNA and subsequently qRT-PCR was performed on the Applied Biosystems 7500 Fast Real-Time PCR System. Glyceraldehyde-3-phosphate dehydrogenase (GAPDH) was used as the internal control gene. The primer sequences used were shown in Table 1.

2.7 Enzyme-linked immuno sorbent assay

Protein levels of Anti-HLA Class I antibodies (abcam, ab23755) were measured using an ELISA kit that can be used to detect antigenic determinants shared by HLA-A, B, and C. The processed cells were collected, and the supernatant was taken after centrifugation, followed by the addition of biotin-labeled antibody. The horseradish peroxide conjugate was then added and incubated at 37°C for 30 min. The optical density (OD) value was measured at 450 nm with an enzyme marker to calculate the sample concentration.

2.8 Statistical analysis

All analyses in this study were calculated using Graphpad Prism and data were expressed as mean ± standard deviation (SD). Unpaired t-tests were used to calculate significant differences between the two groups. $P<0.05$ was statistically significant.

TABLE 1 qRT-PCR primers.

Gene	Forward (5′-3′)	Reverse (5′-3′)
ROHA	GAGCCGGTGAA ACCTGAAGA	TTCCCACGTC TAGCTTGCAG
RYK	ATTTCCTGCAC TTCACCTGG	CTTTGGCCTCC AAAAGAGTG
CSNK1D	AAGTCACGTTG TCTCGAAGCATGG	TGAAGCCAAGC CGCAAGGTAAC
NLK	ATCATCAGCACTCGCATC	GACCAGACAA CACCAAAGC
GAPDH	CATGACCACAGT CCATGCCATCACT	TGAGGTCCAC CACCTGTTGCTGTA

3 Results

3.1 AML cell data pre-processing

Ineligible cells in the GSE235857 dataset were filtered out, obtaining 91,772 cells and 22,032 genes (Figures 1A, B). The data were then standardized to obtain 2000 highly variable genes (Figure 1C). All samples and genes were processed with principal component analysis (PCA), and the top 30 PCs were selected for subsequent analysis (Figure 1D).

3.2 Identification of critical cellular subsets of AML

Cells with similar gene expression patterns were classified into one class by UMAP, identifying 33 cellular subsets. The UMAP plots demonstrated the clustering of cellular subsets in each sample, which was similar in all samples except AML1 (Figure 2A). The 33 cellular subsets were determined as 19 cell types by the expression level of marker genes (Figures 2B, C), which were B cells, Basophil, $CD14^+$-monocytes, $CD16^+$-monocytes, $CD4^+$-Tcm, $CD4^+$-Tn, $CD4^+$-Treg, $CD8^+$-Teff, $CD8^+$-Tem, CD8+-Tn, cDC, Ery, GMP, HSC-Prog, Megakaryocyte, Neutrophil, natural killer cells, pDC, Plasma cell. Each cell had a different proportion in different samples, and this study found HSC-Prog was extremely high in AML1 but low in other samples (Figure 2D).

3.3 Cellular communication analysis of HSC-Prog signaling interactions

Cellular communication analysis was performed, and focused on the communication between HSC-Prog and other cellular subsets as different ligand-receptor interaction pairs were enriched in different cellular communication. There were significant differences in the communication between HSC-Prog and $CD4^+$-T or $CD8^+$-T. The interaction pairs between HLA-II molecules and CD4 were only enriched in HSC-Prog-$CD4^+$-T, and the probability was relatively small. However, the interaction pairs between HLA-I molecules and CD8A/B were only enriched in HSC-Prog-$CD8^+$-T, and the most

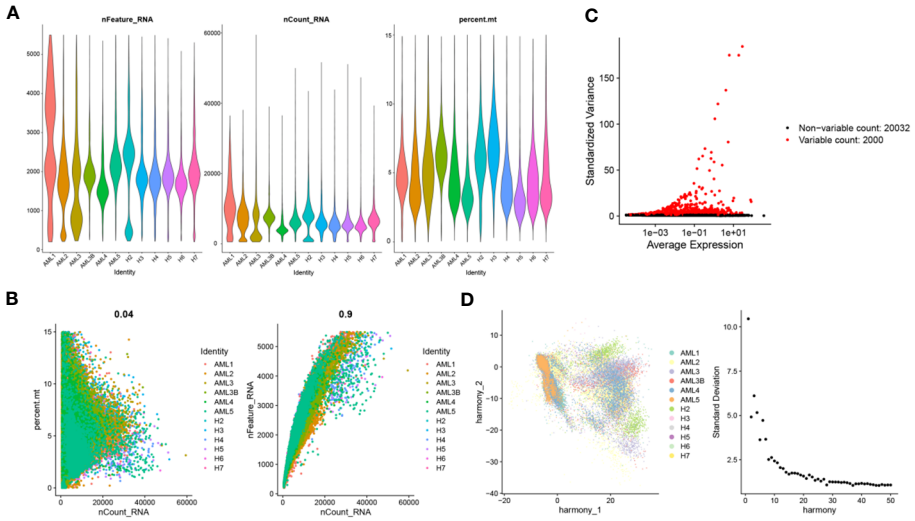

FIGURE 1
Cell quality control and classification. **(A)** Identification of 91772 cells and 22032 genes after quality control analysis of scRNA-seq for AML; **(B)** Scatterplots of the relationship between the number of sequences and the proportion of mitochondria and the number of genes before quality control, respectively; **(C)** Characteristic variance plot of gene expression profiles in the sample; **(D)** PCA results.

significant interaction pairs were HLA-A/CD8B and HLA-B/CD8B in HSC-Prog/$CD8^+$-Tn (Figure 3A). Subsequent studies have found that there are different degrees of interaction between various cell subsets, the more significant are neutrophil-CD8 +T cells, HSC-PROg-CD8 +T cells, CD16+ monocyte-CD8 +T cells and so on. In addition, we found that HSC-Prog interacted with different $CD8^+$-T or $CD4^+$-T cellular subsets, but the signaling interactions between HSC-Prog and $CD8^+$-T cells were stronger compared with $CD4^+$-T cellular subsets (Figure 3B).

3.4 Identification of hub genes in AML cells by bulk RNA-seq

A total of 1748 DEGs were identified by differential gene expression analysis, including 964 up-regulated and 784 down-regulated genes (Figure 4A). Subsequently, a significant signaling pathway, Wnt signaling pathway, was obtained by GSEA, and 10 hub genes associated with this pathway were obtained (Figure 4B). GO function and KEGG Pathway enrichment analysis were conducted based on core genes, and a significantly enriched signaling pathway was found in the biological process: non –canonical Wnt signaling pathway (Figures 4C–F). At the same time, we noticed that the four genes RHOA, RYK, CSNK1D and NLK in the HSC-Prog cells of the AML1 sample were significantly enriched in the non-classical Wnt signaling pathway, and as downstream genes of this pathway, the expression levels of these genes showed a significant downward trend (Figure 4A). It indicates that non-classical Wnt signaling pathway may be a potential key signaling pathway.

3.5 Activation of non-classical Wnt signaling pathway increased protein levels of HLA-A

The results of qRT-PCR showed that the mRNA levels of RHOA, RYK and NLK downstream molecules of non-classical wnt signaling pathway in AML group were significantly lower than those in HL group, while the mRNA levels of CSNK1D were not significantly different. However, compared with AML group, the levels of RHOA, RYK, and NLK in Foxy-5+AML group were significantly increased, while the levels of RHOA, RYK, and NLK in Box5+AML group were not significantly different (Figures 5A–D). ELISA results showed that HLA-A protein level in AML group was significantly decreased compared with HL group. Compared with AML group, the protein level of HLA-A in Foxy-5+AML group was also significantly increased, but there was no significant difference in the protein level of HLA-A in Box5+AML group (Figure 5E). In addition, since TP53 mutations were detected in AML1 patients, to rule out the effect of this factor, we conducted experiments with non-TP53 mutated cell lines (HL-60) and TP53 mutated cell lines (THP-1). By comparing the expression of key genes and HLA-A, it was found that the occurrence of TP53 mutations was not associated with abnormal changes in the non-classical wnt signaling pathway (Supplementary Figure 2). Figure 5F presented the protein expression levels of HLA-A in various cells from the bone marrow, and it was found that the protein levels of HLA-A were generally higher in myeloid cells such as eosinophils, basophils, neutrophils, and monocytes (Figure 5F).

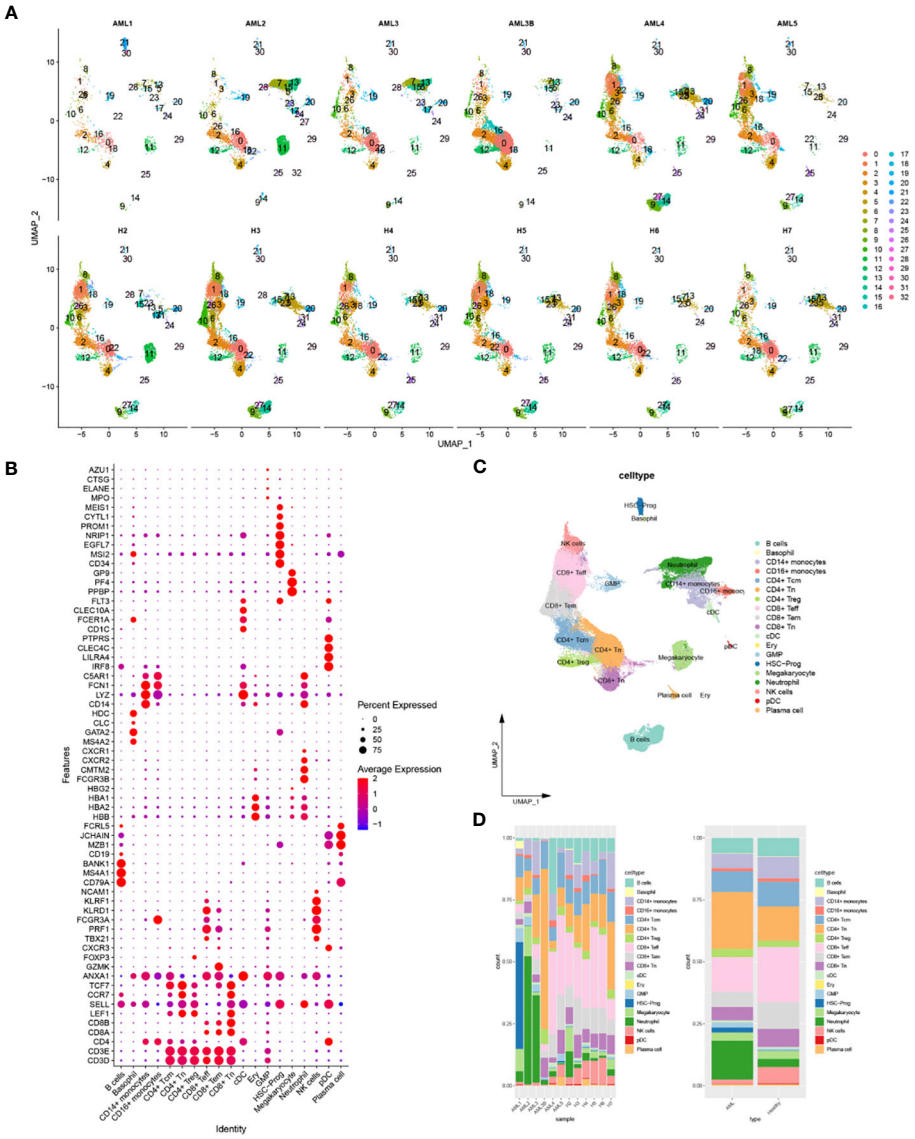

FIGURE 2
Identification of 19 cellular subsets and their intercellular communication based on scRNA-seq data. **(A)** Classification of cellular subsets in each sample; **(B)** Bubble plot of the expression level of the markers used for cell annotation; **(C)** The UMAP plot of the cell annotation results; **(D)** Stacked plot of the proportion of different cells in AML samples or healthy samples.

4 Discussion

As a rapidly progressive malignancy, AML generally presents with a deficiency of red blood cells, platelets, and granulocytes, resulting in the inability of patients to develop adequate immunity (17). Researches and advances in novel molecularly targeted therapies have brought new hope to AML patients. A number of molecules have been proved to mutate in AML and are associated with poor prognosis. Several clinical trials have indicated clinical outcomes of patients can be improved by administering molecularly targeted therapies (18–20). Besides, the administration of immune checkpoint inhibitors to prevent tumor immune escape has also become an important tool in AML treatment (21). This study focused on exploring the molecular mechanisms associated with tumor immune escape in AML, combining scRNA-seq and Bulk RNA-seq to investigate signaling with AML cells.

Resistance often occurs in the treatment of AML with immune checkpoint inhibitors, and the underlying cause of this phenomenon is that AML cells evade T cell surveillance by aberrantly regulating the antigen presentation of major histocompatibility complex (MHC)-I molecules (22). The gene cluster encoded by human MHC is known as HLA, and HLA-I molecules include HLA-A, HLA-B, and HLA-C. Cellular communication analysis of single cells reflected that HLA-A played an important role in the connection between HSC-Prog cells and $CD8^+$-T cells. Peptides produced by HLA-I molecules have been reported to be recognized by tumor-specific $CD8^+$-T cells, thereby activating T cells to produce immune responses. Immune checkpoint inhibitors, on the other hand, produce

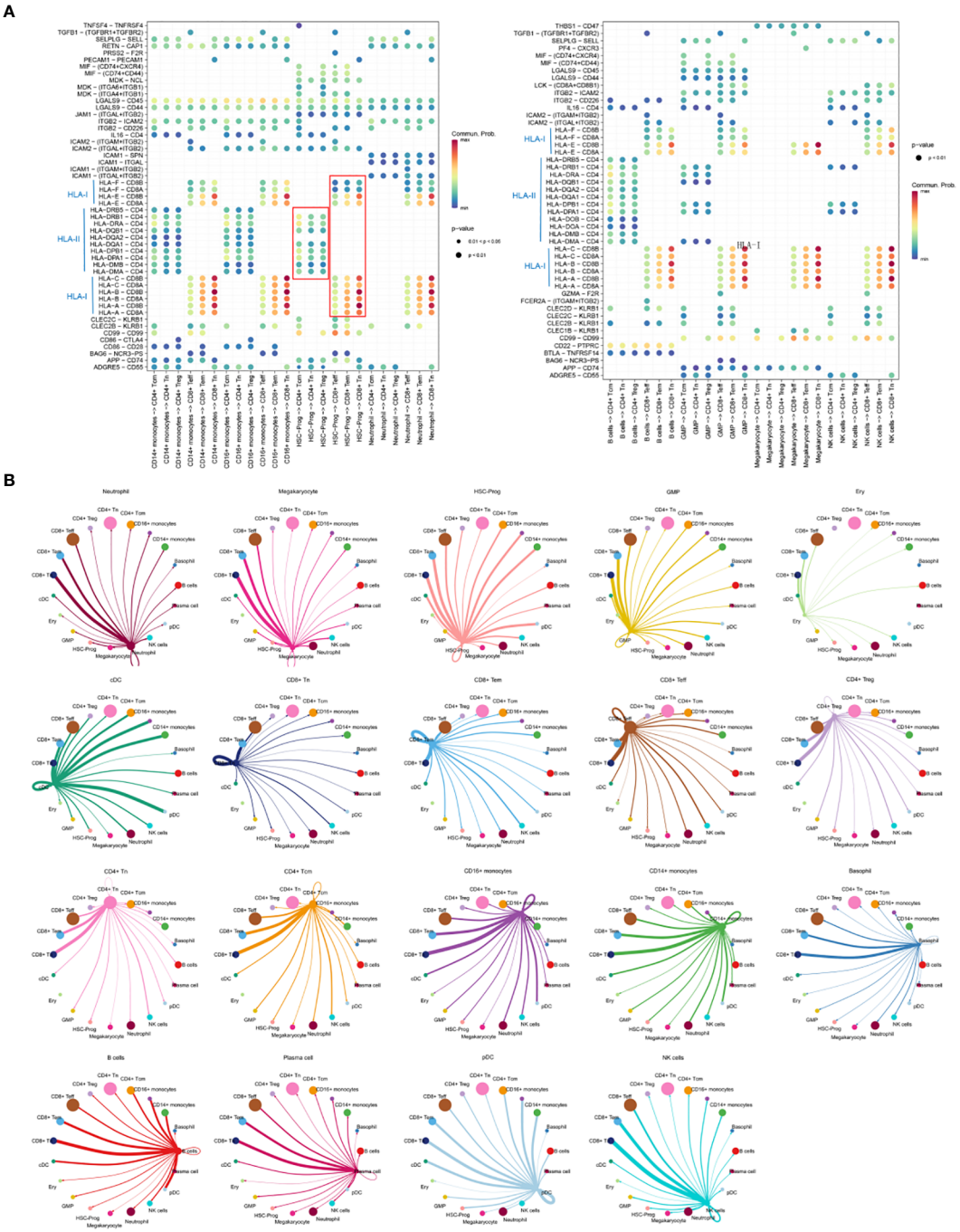

FIGURE 3
Cellular communication between HSC-Prog and other cellular subsets. **(A)** Interactions probabilities of ligand-receptor signaling associated with intercellular communication; **(B)** Cellular communication diagram.

efficacy by increasing T cell recognition of HLA-I molecules on the tumor surface (23). However, tumors during drug resistance downregulate the HLA-I molecule-mediated endogenous antigen presentation pathway, reduce T cell infiltration, and allow tumor cells to evade host immune surveillance (24, 25). Thus, it can be determined that AML cells can inhibit the expression of HLA-A by restricting the antigen presentation pathway, thereby avoiding anti-tumor immune responses after the activation of cytotoxic $CD8^+$-T cells.

Subsequently, the results of Bulk RNA-seq analysis illustrated that the non-classical Wnt signaling pathway was associated with HSC-Prog. Wnt signaling consists of one canonical cascade: the Wnt/β-catenin signaling pathway, and two atypical cascades: the planar cellular polarity (PCP) pathway and the $Ca2^+$ pathway (26). In leukemia cells, β-catenin expression increases and activates the classical Wnt signaling pathway (27). When the drug resistance-related Wnt/β-catenin signaling pathway is activated, IFNγ and NFκB signaling are inhibited in tumor cells, and down-regulate

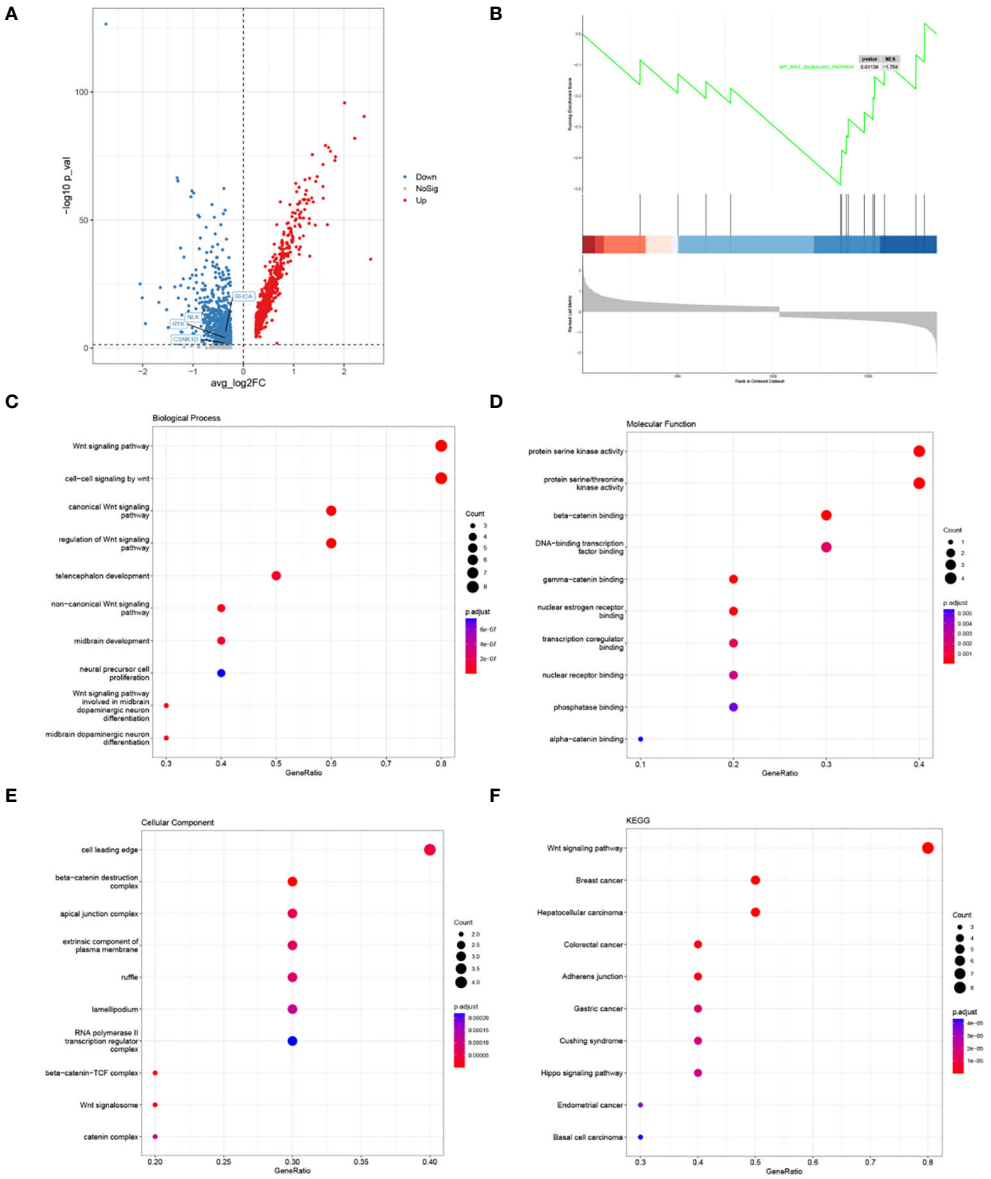

FIGURE 4
Results of HSC-Prog-based differential gene expression analysis and enrichment analysis. **(A)** Results of differential gene expression analysis of AML1 and other samples; **(B)** Enriched signaling pathways by GSEA; the top 10 hub genes; **(C)** Biological processes, **(D)** Molecular functions, and **(E)** Cellular components; **(F)** The top 10 KEGG pathways for hub genes.

the expression of MHC-I molecules (28, 29). In contrast, the atypical Wnt signaling pathway has been shown to inhibit the classical Wnt/β-catenin signaling pathway (30). $Ca2^{+}$ signaling related Wnt5a, and PCP signaling related Frizzled-6 (Fzd6) can inhibit the expression of β-catenin (31, 32). The qRT-PCR and ELISA results of this study reflected that the hub genes RHOA, RYK, NLK and MHC-I molecules HLA-A of the atypical Wnt signaling pathway were down-regulated in leukemia cells. The mRNA levels of RHOA, RYK, NLK and HLA-A protein levels increased significantly after Wnt5a agonist treatment. In this process, the expression of CSNK1D was not greatly affected, and it was speculated that the possible reason was that CSNK1D was involved in phosphorylation of DVL, a hub gene of the non-classical Wnt signaling pathway, but without being directly regulated by the pathway (33). In conclusion, although the non-classical Wnt signaling pathway may be in an inactivated state in AML cells, the stimulation of non-classical Wnt signaling pathway may inhibit the classical Wnt/β-catenin signaling pathway, thereby increasing the expression of HLA-A.

In summary, scRNA-seq and Bulk RNA-seq methods revealed the differentiation mechanisms of leukemia cells and identified a molecular and signaling mechanism associated with leukemia immune escape. It was verified by *in vitro* experiments that stimulation of the non-classical Wnt signaling pathway may inhibit the canonical Wnt/β-catenin signaling pathway, and up-regulate the expression of HLA-A, thereby increasing T cell antigen presentation recognition. However, there are certain limitations to this study. In subsequent studies, more experiments need to be

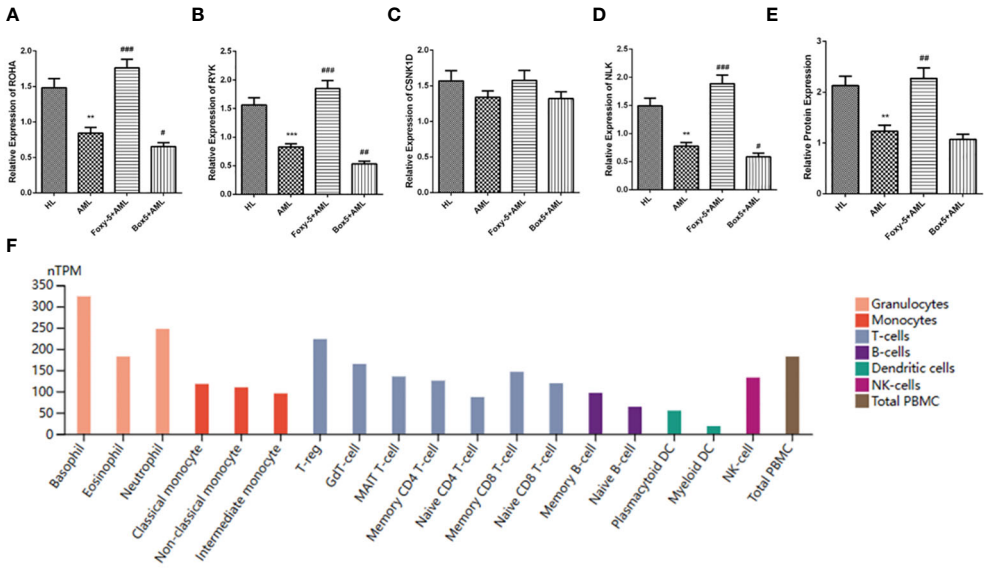

FIGURE 5
Identification of hub gene expression. **(A–D)** The relative expression levels of RHOA, RYK, CSNK1D and NLK in HL group, AML group, Foxy-5+AML group and Box5+AML group were detected by qRT-PCR; **(E)** HLA-A protein levels in HL group, AML group, Foxy-5+AML group and Box5+AML group were detected by ELISA; **(F)** Protein levels of HLA-A in various cells from bone marrow. Notes: Compared with HL, ** means $P<0.01$, *** means $P<0.001$; Compared with AML group, # means $P<0.05$, ## means $P<0.01$ and ### means $P<0.001$.

added to verify the infiltration of T cells after activation of the non-classical Wnt signaling pathway, and to deeply explore whether the hub genes of the non-classical Wnt signaling pathway can directly regulate HLA-A to increase antigen presentation.

Data availability statement

The datasets presented in this study can be found in online repositories. The names of the repository/repositories and accession number(s) can be found in the article/Supplementary Material.

Author contributions

YM: Conceptualization, Data curation, Formal analysis, Writing – original draft, Writing – review & editing. JSY: Conceptualization, Data curation, Formal analysis, Writing – original draft, Writing – review & editing. LG: Funding acquisition, Writing – original draft. JZ: Investigation, Writing – original draft. WC: Methodology, Writing – review & editing. JS: Project administration, Writing – review & editing. JRY: Methodology, Writing – review & editing. QS: Project administration, Writing – review & editing. XZ: Resources, Writing – review & editing. NH: Funding acquisition, Writing – review & editing.

Funding

The author(s) declare financial support was received for the research, authorship, and/or publication of this article. This work was supported by Suqian Sci & Tech Program (Grant No. M202111).

Conflict of interest

The authors declare that the research was conducted in the absence of any commercial or financial relationships that could be construed as a potential conflict of interest.

Publisher's note

Supplementary material

The Supplementary Material for this article can be found online at: https://www.frontiersin.org/articles/10.3389/fonc.2024.1336106/full#supplementary-material

References

1. Stubbins RJ, Francis A, Kuchenbauer F, Sanford D. Management of acute myeloid leukemia: A review for general practitioners in oncology. *Curr Oncol.* (2022) 29:6245–59. doi: 10.3390/curroncol29090491

2. Yang X, Wang J. Precision therapy for acute myeloid leukemia. *J Hematol Oncol.* (2018) 11:3. doi: 10.1186/s13045-017-0543-7

3. Döhner H, Weisdorf DJ, Bloomfield CD. Acute myeloid leukemia. *N Engl J Med.* (2015) 373:1136–52. doi: 10.1056/NEJMra1406184

4. Estey EH. Acute myeloid leukemia: 2019 update on risk-stratification and management. *Am J Hematol.* (2018) 93:1267–91. doi: 10.1002/ajh.25214

5. Padmakumar D, Chandraprabha VR, Gopinath P, Vimala Devi ART, Anitha GRJ, Sreelatha MM, et al. A concise review on the molecular genetics of acute myeloid leukemia. *Leuk Res.* (2021) 111:106727. doi: 10.1016/j.leukres.2021.106727

6. Liu X, Ye Q, Zhao XP, Zhang PB, Li S, Li RQ, et al. RAS mutations in acute myeloid leukaemia patients: A review and meta-analysis. *Clin Chim Acta.* (2019) 489:254–60. doi: 10.1016/j.cca.2018.08.040

7. Alexandrov LB, Nik-Zainal S, Wedge DC, Aparicio SA, Behjati S, Biankin AV, et al. Signatures of mutational processes in human cancer. *Nature.* (2013) 500:415–21. doi: 10.1038/nature12477

8. Vago L, Gojo I. Immune escape and immunotherapy of acute myeloid leukemia. *J Clin Invest.* (2020) 130(4):1552–64. doi: 10.1172/JCI129204

9. Yang W, Li Y, Gao R, Xiu Z, Sun T. MHC class I dysfunction of glioma stem cells escapes from CTL-mediated immune response via activation of Wnt/β-catenin signaling pathway. *Oncogene.* (2020) 39:1098–111. doi: 10.1038/s41388-019-1045-6

10. Staal FJ, Famili F, Garcia Perez L, Pike-Overzet K. Aberrant wnt signaling in leukemia. *Cancers.* (2016) 8:78. doi: 10.3390/cancers8090078

11. Grainger S, Traver D, Willert K. Wnt signaling in hematological Malignancies. *Prog Mol Biol Trans Sci.* (2018) 153:321–41. doi: 10.1016/bs.pmbts.2017.11.002

12. Yan H, Wang Z, Sun Y, Hu L, Bu P. Cytoplasmic NEAT1 suppresses AML stem cell self-renewal and leukemogenesis through inactivation of wnt signaling. *Advanced Sci (Weinheim Baden-Wurttemberg Germany).* (2021) 8:e2100914. doi: 10.1002/advs.202100914

13. Yamashita M, Dellorusso PV, Olson OC, Passegué E. Dysregulated haematopoietic stem cell behaviour in myeloid leukaemogenesis. *Nat Rev Cancer.* (2020) 20:365–82. doi: 10.1038/s41568-020-0260-3

14. Crinier A, Dumas PY, Escalière B, Piperoglou C, Gil L, Villacreces A, et al. Single-cell profiling reveals the trajectories of natural killer cell differentiation in bone marrow and a stress signature induced by acute myeloid leukemia. *Cell Mol Immunol.* (2021) 18:1290–304. doi: 10.1038/s41423-020-00574-8

15. Beneyto-Calabuig S, Merbach AK, Kniffka JA, Antes M, Szu-Tu C, Rohde C, et al. Clonally resolved single-cell multi-omics identifies routes of cellular differentiation in acute myeloid leukemia. *Cell Stem Cell.* (2023) 30:706–721.e708. doi: 10.1016/j.stem.2023.04.001

16. Hu X, Cao D, Zhou Z, Wang Z, Zeng J, Hong WX. Single-cell transcriptomic profiling reveals immune cell heterogeneity in acute myeloid leukaemia peripheral blood mononuclear cells after chemotherapy. *Cell Oncol (Dordr).* (2024) 47:97–112. doi: 10.1007/s13402-023-00853-2

17. Thomas D, Majeti R. Biology and relevance of human acute myeloid leukemia stem cells. *Blood.* (2017) 129:1577–85. doi: 10.1182/blood-2016-10-696054

18. Singh Mali R, Zhang Q, DeFilippis RA, et al. Venetoclax combines synergistically with FLT3 inhibition to effectively target leukemic cells in FLT3-ITD+ acute myeloid leukemia models. *Haematologica.* (2021) 106:1034–1046. doi: 10.3324/haematol.2019.244020

19. Ma J, Zhao S, Qiao X, et al. Inhibition of Bcl-2 Synergistically Enhances the Antileukemic Activity of Midostaurin and Gilteritinib in Preclinical Models of FLT3-Mutated Acute Myeloid Leukemia. *Clin Cancer Res.* (2019) 25:6815–26. doi: 10.1158/1078-0432.CCR-19-0832

20. Tallman MS, Wang ES, Altman JK, et al. Acute Myeloid Leukemia, Version 3.2019, NCCN Clinical Practice Guidelines in Oncology. *J Natl Compr Canc Netw.* (2019) 17:721–749. doi: 10.6004/jnccn.2019.0028

21. Bewersdorf JP, Abdel-Wahab O. Translating recent advances in the pathogenesis of acute myeloid leukemia to the clinic. *Genes Dev.* (2022) 36:259–77. doi: 10.1101/gad.349368.122

22. Chen X, Lu Q, Zhou H, Liu J, Nadorp B, Lasry A, et al. A membrane-associated MHC-I inhibitory axis for cancer immune evasion. *Cell.* (2023) 186:3903–3920.e3921. doi: 10.1016/j.cell.2023.07.016

23. Taylor BC, Balko JM. Mechanisms of MHC-I downregulation and role in immunotherapy response. *Front Immunol.* (2022) 13:844866. doi: 10.3389/fimmu.2022.844866

24. Neefjes J, Jongsma ML, Paul P, Bakke O. Towards a systems understanding of MHC class I and MHC class II antigen presentation. *Nat Rev Immunol.* (2011) 11:823–36. doi: 10.1038/nri3084

25. Yu J, Wu X, Song J, Zhao Y, Li H, Luo M, et al. Loss of MHC-I antigen presentation correlated with immune checkpoint blockade tolerance in MAPK inhibitor-resistant melanoma. *Front Pharmacol.* (2022) 13:928226. doi: 10.3389/fphar.2022.928226

26. Zhan T, Rindtorff N, Boutros M. Wnt signaling in cancer. *Oncogene.* (2017) 36:1461–73. doi: 10.1038/onc.2016.304

27. Polakis P. Wnt signaling in cancer. *Cold Spring Harb Perspect Biol.* (2012) 4. doi: 10.1101/cshperspect.a008052

28. Jongsma MLM, Neefjes J, Spaapen RM. Playing hide and seek: Tumor cells in control of MHC class I antigen presentation. *Mol Immunol.* (2021) 136:36–44. doi: 10.1016/j.molimm.2021.05.009

29. Dholakia J, Scalise CB, Katre AA, Goldsberry WN, Meza-Perez S, Randall TD, et al. Sequential modulation of the Wnt/β-catenin signaling pathway enhances tumor-intrinsic MHC I expression and tumor clearance. *Gynecol Oncol.* (2022) 164:170–80. doi: 10.1016/j.ygyno.2021.09.026

30. Mikels AJ, Nusse R. Purified Wnt5a protein activates or inhibits beta-catenin-TCF signaling depending on receptor context. *PloS Biol.* (2006) 4:e115. doi: 10.1371/journal.pbio.0040115

31. Abidin BM, Owusu Kwarteng E, Heinonen KM. Frizzled-6 regulates hematopoietic stem/progenitor cell survival and self-renewal. *J Immunol.* (2015) 195:2168–76. doi: 10.4049/jimmunol.1403213

32. Chattopadhyay S, Chaklader M, Law S. Aberrant wnt signaling pathway in the hematopoietic stem/progenitor compartment in experimental leukemic animal. *J Cell Commun Signal.* (2019) 13:39–52. doi: 10.1007/s12079-018-0470-6

33. Xu P, Ianes C, Gärtner F, Liu C, Burster T, Bakulev V, et al. Structure, regulation, and (patho-)physiological functions of the stress-induced protein kinase CK1 delta (CSNK1D). *Gene.* (2019) 715:144005. doi: 10.1016/j.gene.2019.144005

frontiers | Frontiers in Oncology

TYPE Original Research
PUBLISHED 26 July 2024
DOI 10.3389/fonc.2024.1433874

OPEN ACCESS

EDITED BY
Vinay Kumar,
The Pennsylvania State University,
United States

REVIEWED BY
Manish Shukla,
Penn State Milton S. Hershey Medical Center,
United States
Sudha Varadaraj,
University of Texas Southwestern Medical Center, United States

*CORRESPONDENCE
Yan Zhang
zhangyan_china@163.com
Xinhua Gu
1173421755@qq.com

†These authors contributed equally to these work

RECEIVED 16 May 2024
ACCEPTED 04 July 2024
PUBLISHED 26 July 2024

CITATION
Zhang Y, Cao J, Yuan Z, Zuo H, Yao J, Tu X and Gu X (2024) Construction and validation of prognostic signatures related to mitochondria and macrophage polarization in gastric cancer.
Front. Oncol. 14:1433874.
doi: 10.3389/fonc.2024.1433874

Construction and validation of prognostic signatures related to mitochondria and macrophage polarization in gastric cancer

Yan Zhang[1*†], Jian Cao[2†], Zhen Yuan[1], Hao Zuo[1], Jiacong Yao[3], Xiaodie Tu[3] and Xinhua Gu[1*]

[1]Department of Gastrointestinal Surgery, Suzhou Municipal Hospital, Affiliated Suzhou Hospital of Nanjing Medical University, Gusu School of Nanjing Medical University, Suzhou, China, [2]Department of Gastroenterology, Suzhou Municipal Hospital, Affiliated Suzhou Hospital of Nanjing Medical University, Gusu School of Nanjing Medical University, Suzhou, China, [3]Alliance Biotechnology Company, Hangzhou, China

Background: Increasing evidence reveals the involvement of mitochondria and macrophage polarisation in tumourigenesis and progression. This study aimed to establish mitochondria and macrophage polarisation-associated molecular signatures to predict prognosis in gastric cancer (GC) by single-cell and transcriptional data.

Methods: Initially, candidate genes associated with mitochondria and macrophage polarisation were identified by differential expression analysis and weighted gene co-expression network analysis. Subsequently, candidate genes were incorporated in univariateCox analysis and LASSO to acquire prognostic genes in GC, and risk model was created. Furthermore, independent prognostic indicators were screened by combining risk score with clinical characteristics, and a nomogram was created to forecast survival in GC patients. Further, in single-cell data analysis, cell clusters and cell subpopulations were yielded, followed by the completion of pseudo-time analysis. Furthermore, a more comprehensive immunological analysis was executed to uncover the relationship between GC and immunological characteristics. Ultimately, expression level of prognostic genes was validated through public datasets and qRT-PCR.

Results: A risk model including six prognostic genes (GPX3, GJA1, VCAN, RGS2, LOX, and CTHRC1) associated with mitochondria and macrophage polarisation was developed, which was efficient in forecasting the survival of GC patients. The GC patients were categorized into high-/low-risk subgroups in accordance with median risk score, with the high-risk subgroup having lower survival rates. Afterwards, a nomogram incorporating risk score and age was generated, and it had significant predictive value for predicting GC survival with higher predictive accuracy than risk model. Immunological analyses revealed showed higher levels of M2 macrophage infiltration in high-risk subgroup and the strongest positive correlation between risk score and M2 macrophages. Besides, further analyses demonstrated a better outcome for immunotherapy in low-risk patients. In single-cell and pseudo-time analyses, stromal cells were identified as key cells, and a relatively complete developmental trajectory existed for stromal C1 in three subclasses. Ultimately, expression analysis revealed that the expression trend of

RGS2, GJA1, GPX3, and VCAN was consistent with the results of the TCGA-GC dataset.

Conclusion: Our findings demonstrated that a novel prognostic model constructed in accordance with six prognostic genes might facilitate the improvement of personalised prognosis and treatment of GC patients.

KEYWORDS

gastric cancer, mitochondria, macrophage polarization, single-cell data, prognostic signature

1 Introduction

Gastric cancer is one of the most common malignancies in the world. Gastric cancer is a complex disease, and its etiology is not fully understood at present. Helicobacter pylori infection, environmental factors, genetic factors, etc. may be related to the occurrence of gastric cancer. About 950,000 new cases of gastric cancer are reported every year around the world, with nearly 700,000 deaths (1). At present, there are still many deficiencies in the diagnosis and treatment of gastric cancer. Due to the unobvious early symptoms of gastric cancer, many patients are in the middle and late stages when they are found, which greatly reduces the success rate of treatment. At present, laparoscopic surgery, and even robotic surgery, have been widely used in the treatment of gastric cancer patients, which is the most important treatment method for gastric cancer. However, due to the physical condition, disease progression and other reasons, surgical treatment often cannot achieve radical results (2). In addition, there are great limitations in the chemotherapy of gastric cancer. The selectivity of chemotherapy drugs is not strong, which may cause damage to normal cells of patients and produce side effects. For gastric cancer patients who have metastasis, the effect of chemotherapy is not ideal (3). Although targeted therapy and immunotherapy for gastric cancer have made some progress, they are still in the exploratory stage, and their efficacy and safety need further verification and improvement (4). Currently, liquid biopsy is playing an increasingly important role in the diagnosis and treatment of gastric cancer (5). It is necessary to find more reliable biomarkers to predict the prognosis of gastric cancer and explore more potential therapeutic targets.

Mitochondrial function and macrophage polarization processes are associated with a variety of tumors, including gastric cancer. Mitochondria are important organelles in cells that can participate in the metabolism of various substances, including carbohydrates, fats, and proteins. Mitochondria maintain the normal physiological functions of cells through oxidative phosphorylation. Abnormal mitochondrial function may lead to metabolic abnormalities in the body. Tumor cells often have various abnormalities in mitochondrial function, such as changes in mitochondrial metabolic pathways and dysregulation of mitochondrial autophagy. These abnormalities can lead to disturbed energy metabolism and uncontrolled growth of tumor cells (6). Mitochondria contain mitochondrial DNA (mtDNA), which is the genetic material in mitochondria and is double-stranded and circular. mtDNA carries its own genetic information, including 37 genes, which encode certain proteins and RNAs within the mitochondria. Many studies have found mitochondrial DNA mutations in various malignant tumors. Abnormal proteins produced by mutated mitochondrial DNA can not only help tumor cells proliferate, but also enable them to migrate and invade distal organs (7). Abnormal copies of mitochondrial genes are often associated with poor prognosis for patients (8). In addition to mtDNA, there are also a large number of mitochondrial-related genes in the genome, which are closely related to mitochondrial function. Mutations in these genes often cause abnormal mitochondrial function in tumor cells (9). Therefore, further research on mitochondria may not only help us understand the physiological and pathological processes of various tumors such as gastric cancer, but also provide new ideas and methods for cancer treatment.

Macrophage polarization refers to the process that macrophages exhibit different functional and phenotypic characteristics under different stimuli. It is a complex cellular process that involves various signaling pathways and molecular regulatory mechanisms (10). Macrophages can be divided into M1 macrophages and M2 macrophages, and can be further divided into various subtypes. Macrophage polarization is a complex process involving various regulatory mechanisms, including inflammatory factors and anti-inflammatory factors, as well as various genes involved in the process of macrophage polarization (11, 12). Currently, macrophage polarization-related genes have been successively discovered, such as IRF5 and STAT1, which activate innate immune responses by inducing the expression of cytokines (13); STAT3 plays an important role in controlling macrophage

proliferation and differentiation (14). Macrophage polarization also plays an important role in tumors. In the tumor microenvironment, M1 macrophages have the characteristics of killing tumor cells, producing inflammatory factors and anti-tumor immune responses, while M2 macrophages are more involved in tissue repair and immunosuppression (15). Studies have shown that in gastric cancer tissue, the number of M2 macrophages is significantly increased, while the number of M1 macrophages is decreased. This polarization imbalance can promote tumor growth and immunosuppression, providing favorable conditions for the development of gastric cancer (16). Cytokines, growth factors, and chemical substances released by tumor cells, as well as abnormal tumor microenvironments, can regulate the process of macrophage polarization. These factors can affect the signal transduction pathway of macrophages, thereby changing the function and polarization state of macrophages (17). Therefore, regulating tumor-associated macrophage polarization may become a new strategy for tumor treatment. Some drugs can inhibit the polarization of M2 macrophages, thereby enhancing the anti-tumor function of macrophages (18).

There is a close relationship between mitochondrial dysfunction and macrophage polarization in tumors. Mitochondrial dysfunction can promote the polarization of tumor-associated macrophages (TAMs). Mitochondrial damage-associated molecular patterns (DAMPs) released by tumor cells can activate macrophages and induce their polarization towards pro-inflammatory (M1) or anti-inflammatory (M2) phenotypes (19). Macrophage polarization can also affect mitochondrial function in tumor cells. For example, M1-type TAMs can release reactive oxygen species (ROS) and other oxidative stress molecules, leading to mitochondrial damage and energy metabolism disorders in tumor cells; while M2-type TAMs can secrete growth factors and anti-inflammatory factors to promote tumor cell growth and survival (20). In summary, there is an interactive and regulatory relationship between mitochondrial dysfunction and macrophage polarization in tumors. Mitochondrial dysfunction can promote the polarization of TAMs, while macrophage polarization can also affect mitochondrial function and biological behavior of tumor cells.

Currently, there are still limited reports on the relationship between mitochondrial and macrophage polarization-related genes in tumors. There is even less literature on prognostic genes related to these two functions and their underlying molecular mechanisms in gastric cancer. This study identified prognostic genes related to mitochondrial and macrophage polarization in gastric cancer patients based on public database data, including transcriptome data and single-cell data, and constructed a prognostic model. In addition, based on the prognostic model, we further explored the biological pathways involved in prognostic genes and their relationships with clinical features and tumor immune microenvironment. In summary, this study identified prognostic genes related to mitochondrial and macrophage polarization in gastric cancer and validated them in clinical samples. By exploring the key genes underlying the intrinsic relationship between the two, we provide a new perspective for understanding the pathogenesis and development of gastric cancer, and also provide new ideas and methods for tumor treatment.

2 Materials and methods

2.1 Data collection

TCGA database provided the mRNA expression profiles and accompanying clinical data of 375 stomach adenocarcinoma tumor tissue samples (GC samples) and 32 paraneoplastic tissue samples (normal samples), and this set of data was referred to as the TCGA-GC dataset. Meanwhile, GEO database (http://www.ncbi.nlm.nih.gov/geo/) provided GC-related original microarray data, specifically, the GSE15459 dataset with 191 GC samples, and the GSE13911 dataset which contained 38 GC samples and 31 normal samples, as well as both datasets were based on the GPL570 platform (21, 22). Similarly, the GSE183904 dataset comprised high-throughput sequencing data from 26 GC tissue samples, 10 normal tissue samples and four peritonium tissue samples for single-cell data analysis (23). There was no significant statistical difference in basic information such as the age and gender of patients in the above-mentioned datasets. Furthermore, a total of 1,136 mitochondria-related genes (MRGs) (Supplementary Table 1) and 35 macrophage polarization-related genes (MPRGs) (Supplementary Table 2) were collected by accessing MitoCarta3.0 database (https://www.broadinstitute.org/mitocarta) and Molecular Signatures Database (MsigDB, http://www.broadinstitute.org/gsea/msigdb/index.jsp), respectively.

2.2 Differential expression analysis

In order to acquire the differentially expressed genes 1 (DEGs1) between GC and normal groups in single-cell sequencing data (GSE183904), the 'FindMarker'-function divided in 'Seurat'-package (v 4.3.0) (24) was utilized to carry out differential expression analysis, and the screening condition was adj.P<0.05. Meanwhile, DEGs2 between GC and normal groups in TCGA-GC were identified via 'DESeq2'-package (v 1.36.0) (25), with the filtering conditions of adj.P<0.05 and $|\log_2\text{FoldChange(FC)}|$>0.5. The 'ggplot2'-package (v 3.4.1) (26) and 'ComplexHeatmap'-package (v 2.12.1) (27) were utilized to create the volcano map and heat map of DEGs2, respectively.

2.3 Weighted gene co-expression network analysis(WGCNA)

In our study, based on MRGs and MPRGs as background gene sets, the MRGs score and MPRGs score for each sample of TCGA-GC were calculated via 'GSVA'-package (v 1.38.2) (28), followed by a rank-sum test to compare the differences in MPRGs score and MRGs score between GC and normal groups (P<0.05). Subsequently, depending on the expression data of the GC samples in TCGA-GC dataset, WGCNA was implemented via the 'WGCNA'-package (v 1.72–1) (29) to identify the module and module genes that were most relevant to the MRGs score and MRGs score. To begin with, the GC samples were clustered and outlier samples were removed to determine the accuracy of

subsequent analyses. Next, the optimal soft threshold was determined at R^2 crossing the threshold 0.80 (red line) and mean connectivity also tending to 0 for ensuring that interactions between genes maximally matched the scale-free distribution. The systematic clustering tree was obtained by utilizing the adjacency connection and gene similarity, and following that, the co-expression network was constructed according to the guidelines of the hybrid dynamic tree cutting algorithm (minModuleSize=50 and mergeCutHeight=0.5). Ultimately, a module-trait heatmap was created to further determine the key module in GC that was most significant with MRGs score and MPRGs score by comparing the correlation coefficient and *P*-value ($P<0.05$). The genes contained in key module were defined as key module genes highly correlated with the MRGs score and MPRGs score.

2.4 Screening of candidate genes and functional annotation analysis

The intersections of DEGs1, DEGs2, and key module genes were taken utilizing 'ggVennDiagram'-package (v 1.2.2) (30), and the intersecting genes were called candidate genes for follow-up analysis. Furthermore, in order to further reveal the biological functions exerted by the candidate genes, enrichment analysis was undertaken. Specifically, enrichment analyses on the basis of Gene Ontology (GO) and Kyoto Encyclopedia of Genes and Genomes (KEGG) databases were implemented via 'clusterProfiler'-package (v 4.4.4) (31) and 'org.Hs.eg.db'-package (v 3.15.0) (32) with a significance of $P<0.05$.

2.5 Creation and validation of risk model

To begin with, the 'survival'-package (v 3.3–1) (33) was applied to carry out univariate Cox regression analysis on the basis of candidate gene expression in 351 GC samples with survival data from TCGA-GC dataset, and prognosis-related genes in GC were acquired with HR≠1 and $P<0.05$ as filter conditions. Subsequently, prognosis-related genes that passed the PH test ($P>0.05$) were subject to LASSO analysis via 'glmnet'-package (v 4.1–6) (34), followed by identifying prognostic genes in GC based on $lambda_{min}$ value. What's more, risk model was created, and the risk score of GC patient was computed on the basis of the expression levels of prognostic genes and their coefficients with the following formula:

$$risk\ \ score = \sum_{i=1}^{n}(Coefi * Expi)$$

In TCGA-GC dataset, the GC sample was classified into two risk subgroups (high- and low-risk subgroups) in accordance with median risk score. Next, analyses of risk curves, survival status, and prognostic signature gene expression were completed depending on survival and expression data of samples in two risk subgroups. Following this, Kaplan-Meier (KM) survival analysis was achieved via 'survminer'-package (v 0.4.9) with the aim of comparing the survival differences ($P<0.05$) between the two risk subgroups. Meanwhile, receiver operating characteristic (ROC) curves at 1-, 3- and 5-years were displayed utilizing 'survivalROC'-package (v 1.0.3) (35), and the precision of risk model in forecasting the prognosis of GC on the basis of area under curve (AUC) value was evaluated. In general, AUC value greater than 0.6 indicated favorable performance of the risk model. Ultimately, the same approaches were employed in GSE15459 dataset to validate the generalisability of the risk model to predict GC prognosis.

2.6 Clinical correlation analysis

According to 351 GC samples with clinical data in TCGA-GC dataset, the number of patients with different clinical subgroups was compared between high- and low-risk subgroups with the use of the chi-square test to explore the association between risk score and GC clinical characteristics. Specifically, the clinical characteristics included age, gender, vital status, overall survival (OS), pathologic-M/N/T, pathologic-stage and grade. Subsequently, based on the clinical characteristics associated with the risk scores, comparison of risk scores between different clinical subgroups was undertaken by rank sum test (two subgroups) and ANOVA test (three and more subgroups), followed by visualization of the results using box plots and Sankey diagrams. Eventually, the expression level analysis of prognostic genes were achieved between different clinical subgroups.

2.7 Independent prognostic analysis and nomogram creation

By combining risk score with seven conventional clinical characteristics (age, gender, grade, pathologic-M/N/T, and pathologic-stage), univariate and multivariate Cox regression analyses ($P<0.05$) as well as proportional hazard (PH) hypothesis test ($P>0.05$) were performed in the TCGA-GC dataset to further assess the possibility of utilizing them as independent prognostic indicators for GC. After selecting the independent prognostic indicators, we created a nomogram of 1, 3, and 5-year survival via 'rms'-package (v 6.5–0) (36). What's more, the ROC and calibration curves were generated to determine the predictive efficacy of this nomogram.

2.8 Gene set enrichment analysis (GSEA)

GSEA was accomplished with the aim of uncovering biological pathway differences between the two risk subgroups. To begin with, differential expression analysis was performed between two risk subgroups in TCGA-GC dataset, and DEGs were sorted in accordance with log2FC. Next, based on the KEGG database, GSEA-KEGG was carried out on the sorted genes via 'clusterProfiler'-package (v 4.4.4) (31), with thresholds of adj.$P<0.05$ and $|NES|>1$.

2.9 Tumor immune microenvironment (TIME) analysis

In an attempt to elucidate the association between risk score and immunological characteristics, a more comprehensive immunological analysis was accomplished. Firstly, the abundance of individual immune cells for each sample was obtained through calculating the scores of 22 immune cells in TCGA-GC dataset utilizing CIBERSORT algorithm, followed by a rank-sum test to analyze the differences in immune cell scores between two risk subgroups (P<0.05). Subsequently, Spearman correlation analysis was executed between risk score and differential immune cells as well as between prognostic genes and differential immune cells, respectively, so as to uncover the relationship between them.

Furthermore, immune checkpoint genes (ICGs) play a critical role in the TIME. Therefore, this work compared the ICG expression discrepancy between two risk subgroups on the basis of 43 ICGs obtained from published literature (37). The Spearman correlation analysis between prognostic genes and differential ICGs was also performed. What's more, tumor immune dysfunction and exclusion (TIDE) score was calculated for each GC sample in TCGA-GC dataset through accessing TIDE database (http://tide.dfci.harvard.edu), and differences between two risk subgroups were compared by a rank-sum test to predict treatment response to immune checkpoint inhibitors.

Meanwhile, immunity, stromal, and ESTIMATE scores were computed through ESTIMATE method for all GC samples from TCGA-GC dataset with the aim of comparing the differences in each score between two risk subgroups (P<0.05).

2.10 Chemotherapy drug sensitivity, MSI, TMB, and CNV analyses

In TCGA-GC dataset, the 50% inhibitory concentration (IC50) values of 138 chemotherapeutic drugs for each GC sample were obtained via the 'pRRophetic'-package (v 0.5) (38), and these 138 agents were retrieved from genomics of drug sensitivity in cancer (GDSC) database (https://www.cancerrxgene.org/). Next, IC50 values of 138 chemotherapeutic agents were subjected to the rank-sum test to identify agents that differed markedly between two risk subgroups. Meanwhile, the fold change (FC) was calculated, followed by classifying the agents into three groups based on P value and FC, namely sensitive low-risk (P<0.05 and FC>0.2), sensitive high-risk (P<0.05 and FC<-0.2), and no sensitive. Subsequently, the top five agents of sensitive high-risk/sensitive low-risk were selected for correlation analysis with the risk score.

In the meantime, on the basis of microsatellite instability (MSI) data in GC patients gained from cBiPortal database (https://www.cbioportal.org/), GC samples with MSI score>0.3 were defined as the MSI group, and GC samples with MSI score<0.3 were defined as the MSS (microsatellite stable) group in TCGA-GC dataset. Subsequently, the difference in risk score between MSI and MSS groups was compared, and Spearman correlation analysis was performed between MSI score and risk score. More importantly, the top five agents of sensitive high-risk/sensitive low-risk were selected for correlation analysis with MSI score.

Additionally, tumor mutation burden (TMB) and copy number variation (CNV) data for GC samples were derived from the cBiPortal and UCSC Xena (https://xena.ucsc.edu/) databases, respectively. Next, the differences in TMB and CNV between two risk subgroups were compared via rank-sum test (P<0.05), followed by Spearman correlation analysis between them and risk score.

2.11 Single-cell data analysis and pseudo-time analysis

Single-cell sequencing data (GSE183904) were imported into R software and analyzed using the 'Seurat'-package (v 4.3.0) (24). Initially, the data were filtered using the 'CreateSeuratObject'-function with the following filtering criteria: (1) genes expressed in fewer than 3 cells were eliminated; (2) cells with a total gene count greater than 200 were retained. Secondly, the percentage of mitochondrial genes was computed via 'PercentageFeatureSet'-function, and cells with a percentage less than 10% were retained to ensure that low quality cells were excluded. For downstream analysis, data were normalized utilizing 'NormalizeData'-function, and 'FindVariableFeatures'-function was adopted to identify top 2,000 highly variable genes after quality control (QC) with the 'vst' method. Immediately thereafter, multiple samples were combined and canonical correlation analysis was implemented to remove batch effects. Based on these 2,000 genes, principal component analysis (PCA) was implemented for dimensionality reduction, and then the cells were clustered using 'FindNeighbors' and 'FindClusters'-functions to yield cell clusters. Additionally, 'FindAllMarkers'-function was applied to discover the significant marker genes for each cell cluster by setting the parameters min.pct=0.25, only.pos=TRUE, and logfc.threshold=0.7. What's more, to identify cell subpopulations, cell clusters were annotated according to the CellMarker database (http://biocc.hrbmu.edu.cn/CellMarker/), and marker genes in different cell subpopulations were displayed.

Further, the expression level of prognostic genes in each cell subpopulation was demonstrated, and cell subpopulation with higher expression of prognostic genes and with expression of each gene was utilized as the key cell for subsequent analyses. Immediately thereafter, the identified key cell was analyzed for functional enrichment via 'ReactomeGSA'-package (v 1.4.2) (39). Eventually, based on key cells, unsupervised cluster analysis was implemented via 'FindNeighbors' and 'FindClusters' functions to identify subclasses of key cells, followed by pseudo-time analysis of these subclasses via 'monocle3'-package (v 1.0.0) (40).

2.12 Chromosomal localization and subcellular localization analyses

The subcellular localization analysis was performed using the 'RCircos'-package (v 1.2.2) (41) for determining the location of prognostic genes on human chromosomes. Simultaneously, the

function of prognostic genes was closely linked to their location in the cell, so it was important to know the subcellular location of these genes. In this study, the subcellular localization of prognostic genes was predicted by visiting the online website mRNALocater (http://bio-bigdatacn/mRNALocater).

2.13 Regulatory network analysis

To uncover the molecular regulatory mechanisms of prognostic genes in GC, lncRNA-miRNA-mRNA regulatory network was established. Initially, miRWalk database(http://mirwalk.umm.uni-heidelberg.de/) was employed to forecast miRNAs that could target prognostic genes. Later on, upstream lncRNAs of miRNAs were predicted by accessing starBase database (http://starbase.sysu.edu.cn/), with the filtering conditions of clipExpNum≥2, degraExpNum≥2, and pancancerNum≥2. The lncRNA-miRNA-mRNA network was generated with the help of Cytoscape software (v 3.9.1) (42).

2.14 Expression level analysis and validation

In TCGA-GC and GSE13911 datasets, expression level of prognostic genes in GC and normal samples was analyzed. Subsequently, expression analysis of prognostic genes was finished through quantitative real time polymerase chain reaction (qRT-PCR). Ten clinical gastric tissue samples were collected from Suzhou Municipal Hospital, Affiliated Suzhou Hospital of Nanjing Medical University, including five GC patients and five paraneoplastic patients. The experiment was approved by the Ethics Committee of Gusu School, Nanjing Medical University.

Total RNA was isolated from gastric tissue using TRIzol reagent, followed by reverse transcription to synthesize complementary DNA (cDNA) using SweScript First Strand cDNA synthesis kit. The qRT-PCR was run for 40 cycles under the following conditions, 95°C for 1 min, 95°C for 20 s, 55°C for 20 s, and 72°C for 30 s. GAPDH served as the internal reference gene for biomarkers, and the relative expression levels of prognostic genes were quantified using the $2^{-\Delta\Delta CT}$ method. Primers were shown in Table 1.

2.15 Statistical analysis

In the present work, all statistical analyses involved were performed by R program (v 4.2.1). Discrepancies between groups were completed by rank sum test (two subgroups) or ANOVA test (three and more subgroups). *P*-value<0.05 was deemed statistically meaningful unless otherwise stated.

3 Results

3.1 Key module genes correlated with MRGs and MPRGs scores were obtained through WGCNA

In TCGA-GC dataset, there were remarkable differences in MRGs score and MPRGs score between GC and normal groups ($P<0.05$), and both MRGs and MPRGs scores were lower in GC samples than in normal samples (Figure 1A). Subsequently, WGCNA was implemented to excavate the modules and module genes that related to MRGs score and MPRGs score. After the cluster analysis of the samples, no outlier samples were observed (Figure 1B). Also, the soft threshold of 14 was chosen to construct the co-expression network, at which point interactions between genes maximally matched the scale-free distribution (Figure 1C). In the process of constructing the co-expression network, five modules were created with the systematic clustering tree and dynamic tree cutting algorithms (Figures 1D, E). The module MEbrown demonstrated the strongest association with MRGs score and MPRGs score, with a negative correlation with MRGs score (cor=-0.69 and $P<0.001$) and a positive association with MPRGs score (cor=0.32 and $P<0.001$). Ultimately, a total of 3,110 genes contained in module MEbrown were identified as key module genes highly linked to MRGs score and MPRGs score.

3.2 Candidate genes were strongly associated with immune responses and cytokines

Through differential expression analysis, a total of 1,628 DEGs1 in GSE183904 dataset and 7,704 DEGs2 (3,625 up-regulated and

TABLE 1 Primers used in PCR experiments.

Gene	Forward Primer	Reverse Primer
RGS2	ATTCAGCCTGGGTGTTCAGG	AGACACCACGTTCAGACCAC
GJA1	CAGCCACTAGCCATTGTGGA	GGCTGTTGAGTACCACCTCC
GPX3	AGAAGTCGAAGATGGACTGCC	GGGAAAGCCCAGAATGACCA
LOX	GTGGGCGAAGGTACAGCATA	TGACAACTGTGCCATTCCCA
VCAN	TCGAGGAGGCTGCAAAAGAG	TGCAGCGATCAGGTCGTTTA
CTHRC1	GGGAGGTGGTGGACCTGTAT	GTCCTTCCACGCAATTTTCC
GAPDH	CGAAGGTGGAGTCAACGGATTT	ATGGGTGGAATCATATTGGAAC

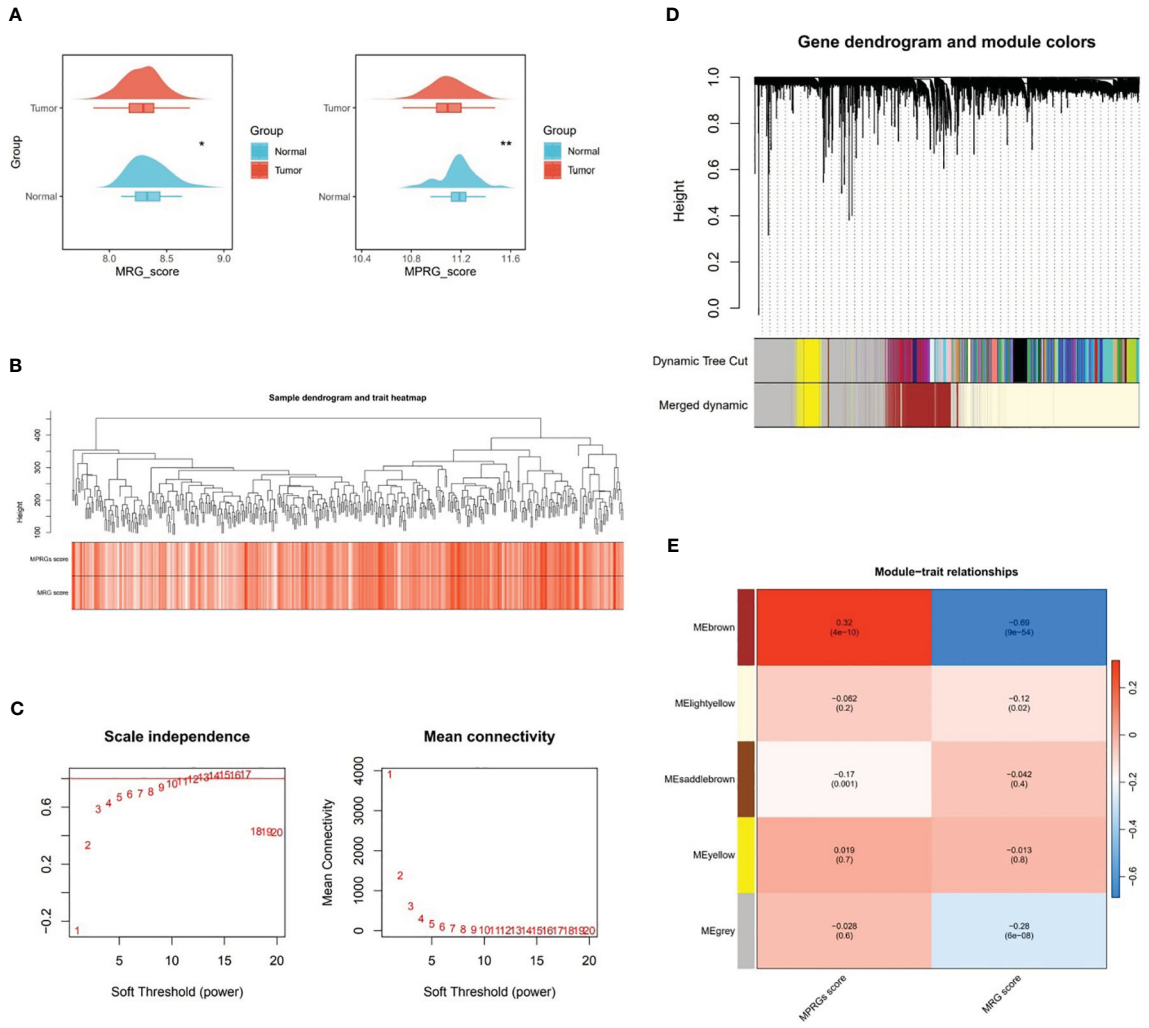

FIGURE 1
Key modular genes correlated with MRGs and MPRGs scores obtained through WGCNA. **(A)** MRGs and MPRGs scores between gastric cancer (GC) group and normal group in TCGA-GC dataset, **(B)** Sample dendrogram and trait heatmap, **(C)** Scale independence and mean connectivity among genes, **(D)** Gene dendrogram and module colors, **(E)** Trait relationships of different colored modules. * indicates p<0.05, ** indicates p<0.01.

4,079 down-regulated) in TCGA-GC dataset were mined (Figures 2A, B). Subsequently, the Venn diagram demonstrated that 292 candidate genes were acquired through fetching the intersections of 1,628 DEGs1, 7,704 DEGs2 and 3,110 key module genes (Figure 2C).

Further, 292 candidate genes were significantly enriched into 800 GO items [699 biological processes (BPs), 60 cellular components (CCs), and 41 molecular functions (MFs)] and 14 KEGG pathways (P<0.05). The important GO-BP categories were primarily connected with immune responses and cytokines, such as "leukocyte migration", "leukocyte mediated immunity", "cell chemotaxis", "leukocyte activation involved in immune response", etc (Figure 2D). The candidate genes were highly enriched in the "endoplasmic reticulum lumen", "collagen trimer" and "basement membrane" in GO-CC analysis (Figure 2D). In GO-MF category, they showed concentration in "growth factor binding", "immunoglobulin binding", "transforming growth factor beta binding", etc (Figure 2D). Meanwhile, KEGG analysis elucidated that candidate genes were engaged in "PI3K-Akt signaling pathway", "Phagosome", "ECM-receptor interaction", and other signaling pathways (Figure 2E). These findings strongly revealed that immune responses and cytokines were highly relevant to the pathogenesis and progression of GC.

3.3 Risk model was effective in predicting prognosis of GC

After incorporating 292 candidate genes into univariate Cox regression analysis and PH hypothesis test, totally 101 genes were identified that were significantly associated with prognosis in TCGA-GC dataset (Supplementary Figure 1). Immediately, with respect to the LASSO regression analysis, the model was optimal when $lambda_{min}$ was equal to 0.08366, and six prognostic genes (GPX3, GJA1, VCAN, RGS2, LOX, and CTHRC1) were chosen to create risk model (Figure 3A). On the basis of the coefficients of these six genes

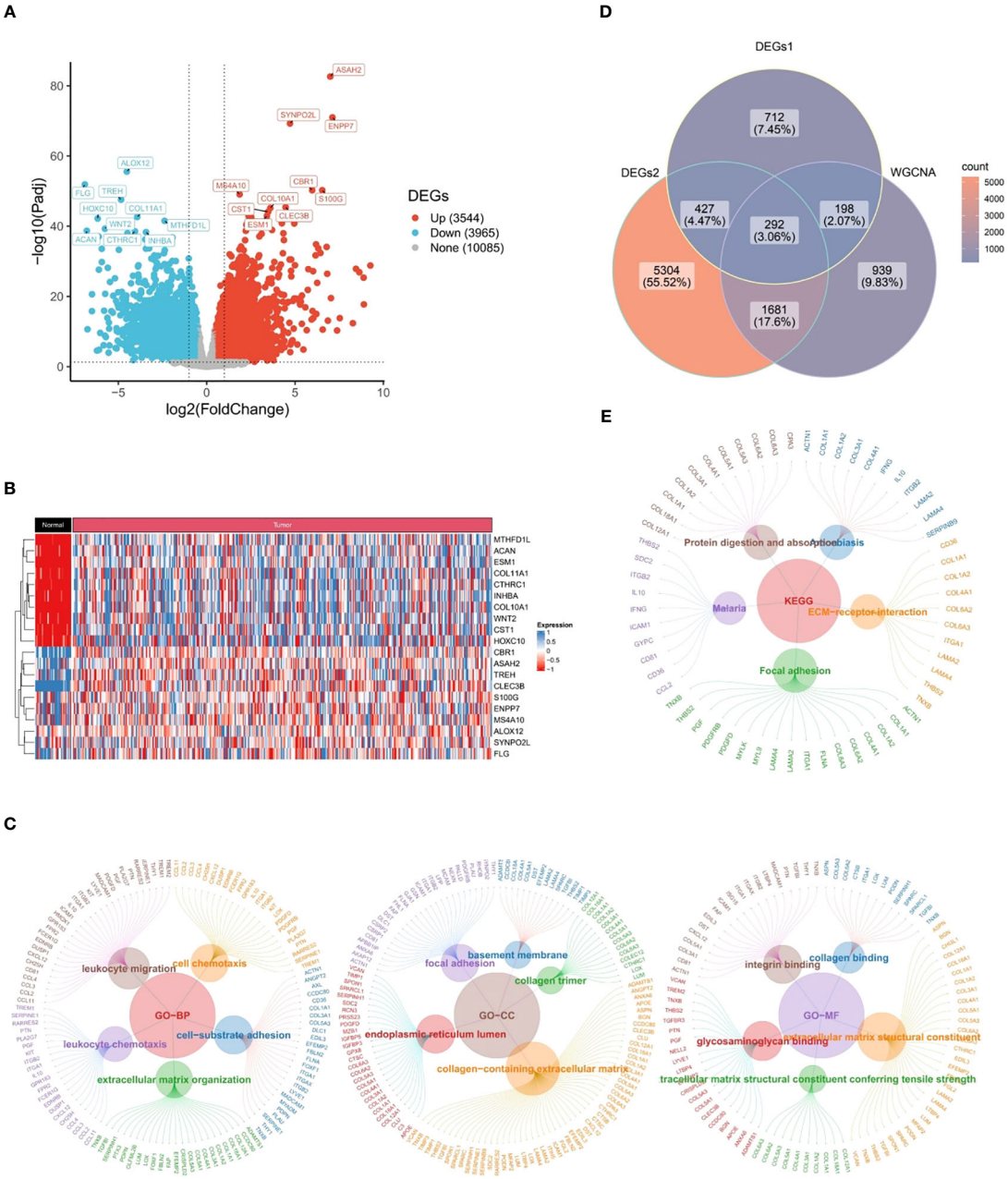

FIGURE 2
Candidate genes closely related to immune response and cytokines. **(A)** 1,628 differentially expressed genes (DEGs1) in GSE183904 dataset, **(B)** 7,704 differentially expressed genes (DEGs2) in TCGA-GC dataset, **(C)** Venn diagram obtained by intersecting DEGs1, DEGs2, and key modular genes, **(D)** Go functional enrichment analysis of candidate genes, **(E)** KEGG enrichment analysis of candidate genes.

in LASSO analysis, we computed risk score by following the formula below: Risk score = GPX3*0.145 + GJA1*0.071 + VCAN*0.005 + RGS2*0.072 + LOX*(-0.025) + CTHRC1*0.110. In TCGA-GC dataset, the GC patients were categorized into two risk subgroups (low- and high-risk subgroups) in accordance with median risk score. As demonstrated in Figure 3B, the K-M curve revealed that the survival rate of high-risk patients was markedly lower than that of low-risk patients (P<0.001). In ROC analysis, AUC values for 1-, 3-, and 5-year were 0.650, 0.614, and 0.731, correspondingly, which implied that risk model was stable and effective in forecasting the prognosis of GC patients (Figure 3B). In order to evaluate the robust prediction value of risk model, these were additionally further validated in GSE15459 dataset. The results indicated that the significant prognostic value was P=0.013, and AUC values at 1-, 3-, and 5-year survival were 0.613, 0.623, and 0.644, correspondingly (Figure 3C). The relationships of risk score with survival time and survival status, as well as the heat map of expressions of the six prognostic genes, were illustrated in Figures 3D, E. Obviously, with increasing risk score, the survival time of the patient decreased and the number of deaths rose at the same time.

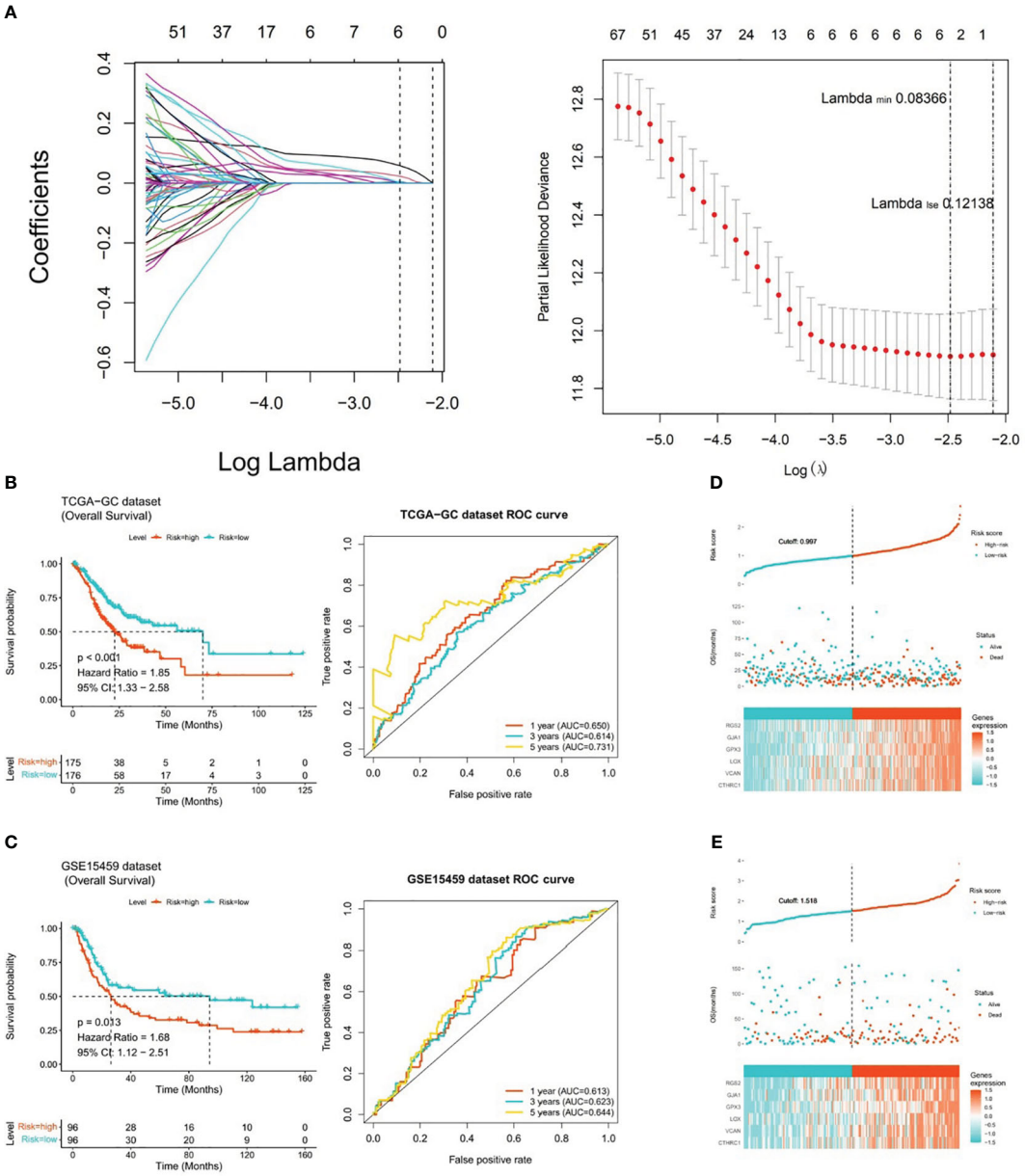

FIGURE 3
Risk model for predicting the prognosis of gastric cancer. **(A)** Six prognostic genes (GPX3, GJA1, VCAN, RGS2, LOX, and CTHRC1) selected by LASSO regression analysis to construct the risk model, **(B)** K-M curve and ROC analysis between high-risk and low-risk patients in TCGA-GC dataset (P<0.001), **(C)** K-M curve and ROC analysis between high-risk and low-risk patients in GSE15459 dataset (P=0.013), **(D)** Heatmap of the expression of six prognostic genes in patients from TCGA-GC dataset, **(E)** Heatmap of the expression of six prognostic genes in patients from GSE15459 dataset.

3.4 Association analysis of risk score with GC clinical characteristics

In TCGA-GC dataset, the relationship between risk score and various clinical characteristics was further investigated to reveal the effect of risk score in GC progression. Firstly, clinical characteristics of the two risk subgroups were compared, and the differences in vital status (P=0.001), OS (P=0.029), pathologic-T (P=0.007) and grade (P=0.017) between two risk subgroups were statistically significant (Table 2). Among them, there were marked discrepancies in risk scores of patients with different pathologic-T and grade, and pathologic-TX and grade-3 were associated with higher risk score (Figure 4A). Meanwhile, the Sankey plot also demonstrated that the majority of T1 and G2 patients flowed to the low-risk subgroup (Figure 4B). What's more, it was discovered that the expression of six prognostic genes had a gradual upward trend during the period from pathologic-T1 to TX (P<0.05), and the same trend was noted for the remaining five genes, except for CTHRC1, during the period from grade-1 to grade-X (P<0.05) (Figure 4C).

TABLE 2 Clinical characteristics of the two risk subgroups.

	Total	Risk		*Pvalue*
		high	low	
age(year)				
Mean (SD)	65.5 (±10.6)	65.3 (±10.9)	65.8 (±10.4)	0.73
gender				
FEMALE	124 (35.3%)	62 (35.4%)	62 (35.2%)	1
MALE	227 (64.7%)	113 (64.6%)	114 (64.8%)	
vital_status				
Alive	209 (59.5%)	89 (50.9%)	120 (68.2%)	0.001
Dead	142 (40.5%)	86 (49.1%)	56 (31.8%)	
OS(Months)				
Mean (SD)	612.0 (±548.5)	533.9 (±458.2)	689.6 (±617.0)	0.029
pathologic_M				
M0	313 (89.2%)	151 (86.3%)	162 (92.0%)	0.18
M1	22 (6.3%)	13 (7.4%)	9 (5.1%)	
MX	16 (4.6%)	11 (6.3%)	5 (2.8%)	
pathologic_N				
N0	103 (29.4%)	46 (26.4%)	57 (32.4%)	0.26
N1	95 (27.1%)	45 (25.9%)	50 (28.4%)	
N2	72 (20.6%)	36 (20.7%)	36 (20.5%)	
N3	71 (20.3%)	40 (23.0%)	31 (17.6%)	
NX	9 (2.6%)	7 (4.0%)	2 (1.1%)	
pathologic_T				
T1	18 (5.1%)	3 (1.7%)	15 (8.5%)	0.007
T2	74 (21.1%)	39 (22.3%)	35 (19.9%)	
T3	161 (45.9%)	77 (44.0%)	84 (47.7%)	
T4	94 (26.8%)	52 (29.7%)	42 (23.9%)	
TX	4 (1.1%)	4 (2.3%)	0 (0.0%)	
pathologic_stage				
Stage I	48 (14.2%)	19 (11.4%)	29 (16.9%)	0.54
Stage II	109 (32.2%)	54 (32.5%)	55 (32.0%)	
Stage III	147 (43.5%)	75 (45.2%)	72 (41.9%)	
Stage IV	34 (10.1%)	18 (10.8%)	16 (9.3%)	
Grade				
G1	9 (2.6%)	5 (2.9%)	4 (2.3%)	0.017
G2	126 (35.9%)	49 (28.0%)	77 (43.8%)	
G3	207 (59.0%)	117 (66.9%)	90 (51.1%)	
GX	9 (2.6%)	4 (2.3%)	5 (2.8%)	

Red value means p<0.05.

3.5 An effective nomogram was created in GC

By combining conventional clinical characteristics with risk score in TCGA-GC dataset, univariate Cox analysis manifested that risk score, age, pathologic-M, pathologic-N, pathologic-T, and pathologic-stage were all markedly associated with OS in GC (P<0.05) (Figure 5A). On the basis of PH hypothesis test and multivariate Cox analysis, risk score and age were detected as independent prognostic indicators for predicting the prognosis of GC patients (Figure 5B). Subsequently, a nomogram integrating risk score and age for predicting GC prognosis was constructed (Figure 5C). The calibration curve suggested that the predicted and actual values of nomogram were roughly the same (Figure 5D). Meanwhile, AUC values at 1-, 3-, and 5-years were 0.664, 0.644, and 0.737, correspondingly (Figure 5E). In summary, the nomogram constructed in accordance with risk score and age had significant predictive value for predicting GC survival with higher predictive accuracy than risk model.

3.6 Differences in biological pathways between two risk subgroups were clarified

The GSEA was conducted in TCGA-GC dataset to determine the most markedly enriched pathways between two risk subgroups. It was noted that genes from high-risk patients were markedly enriched in the "cell adhesion molecules", "ECM-receptor interaction", "cGMP-PKG signaling pathway", "Calcium signaling pathway pathways", etc (Figure 6A). However, genes in low-risk subgroup were markedly enriched in the following pathways, namely, "RIG-I-like receptor signaling pathway", "cell cycle", "oxidative phosphorylation pathway", etc (Figure 6B). These analyses suggested that risk score was highly correlated with these biological pathways, providing insight valuable for understanding the potential molecular mechanisms of GC.

3.7 Risk score was associated with immunological features in GC

The CIBERSORT program was adopted to estimate the score of immune cells between the two risk subgroups, and the results revealed that resting-memory $CD4^+$ T cells, M0 macrophages, M1 macrophages, and M2 macrophages were more enriched in samples of TCGA-GC dataset (Figure 6C). Further, it was noted that in case of statistical differences (P<0.05), the infiltration levels of naive B cells, M2 macrophages, monocytes, resting dendritic cells, and resting mast cells were higher in GC samples from high-risk subgroups, whereas the infiltration levels of activated-memory $CD4^+$ T cells, follicular helper T cells, regulatory T cells (Tregs), and activated mast cells were higher in GC samples from low-risk subgroups (Figure 6D). The strongest positive correlation (cor=0.31 and P<0.001) between risk score and M2 macrophages was observed in the correlation study (Figure 6E). Simultaneously, it

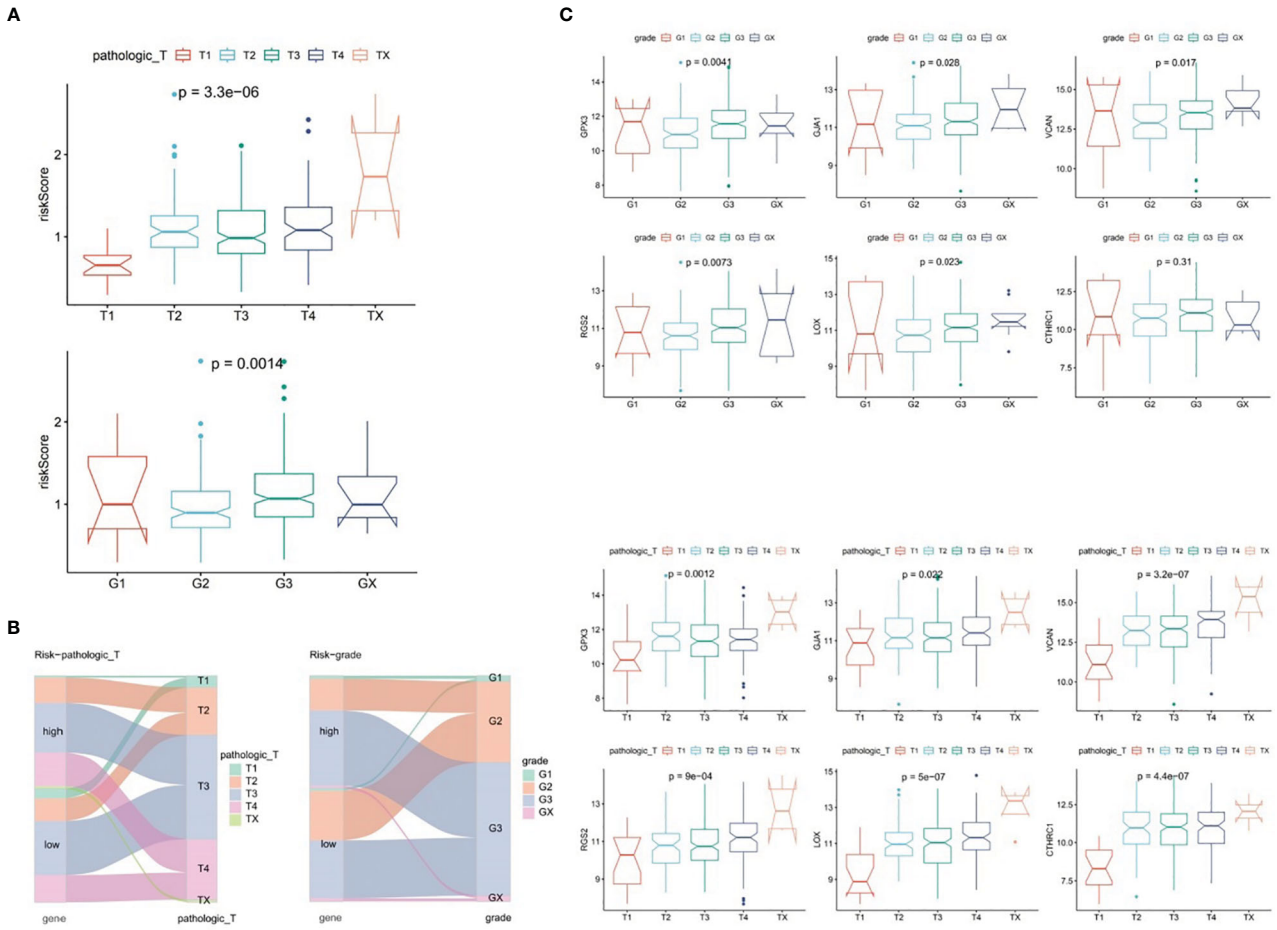

FIGURE 4
Correlation analysis of risk scores with clinical characteristics of gastric cancer in the TCGA-GC dataset. **(A)** Differences in risk scores among patients with different pathological T stages and grades, **(B)** Representation of patient flow into different subgroups through Sankey diagram, **(C)** Expression profiles of six prognostic genes between patients with pathological T1 to TX stages and grades 1 to X.

was also clear that there was significant correlations between prognostic genes and differential immune cells, in which the strongest positive association was found between CTHRC1 and M2 macrophages (cor=0.32 and P<0.001), and the strongest negative association was found between RGS2 and Tregs (cor=-0.31 and P<0.001) (Figure 6F).

From Figure 7A, it could be observed that there were differences in 28 ICGs (BTLA, BTN2A1, BTN2A2, etc.) levels between the two risk subgroups, and all of these 28 ICGs levels were lower in high-risk subgroup compared to the low-risk group. Besides, there were multiple positive correlations between six prognostic genes and these 28 ICGs, among which TNFSF4 and CD200 were more strongly correlated with prognostic genes (Figure 7B). Further analyses demonstrated a marked difference in TIDE score between two risk subgroups and a notable positive association between TIDE score and risk score (cor=0.57 and P<0.001), predicting a better outcome for immunotherapy in low-risk patients (Figure 7C). Ultimately, ESTIMATE algorithm demonstrated higher immune, stromal, and ESTIMATE scores (P<0.001) in high-risk subgroup compared to the low-risk subgroup (Figure 7D), in other words, there was marked positive correlations between them and the risk score (stromal score: cor=0.7, immune score: cor=0.26, ESTIMATE score: cor=0.53; all P<0.001) (Figure 7D).

3.8 The relationship of risk score with chemotherapy agents, MSI, TMB, and CNV

Among 138 chemotherapy agents, five agents (AZD6244, CCT018159, Mitomycin.C, etc.) belonged to sensitive low-risk group and 30 agents (AP.24534, Midostaurin, etc.) belonged to sensitive high risk group (Figures 8A, B). Of these, CCT018159 was markedly positively associated with risk score, as well as DMOG, BMS.754807, BX.795, Midostaurin, and AP.24534 were significantly negatively linked to risk score (P<0.05 and |cor|>0.3) (Figure 8C). These findings could provide a reliable reference for clinical treatment. Subsequently, with respect to the MSI analysis, patients in MSS group had a higher risk score than those in MSI group, and MSI score was markedly negatively linked to risk score (P<0.001 and cor=-0.31) (Figure 8D). Interestingly, it was noticed that the chemotherapeutic agent DMOG was significantly positively associated with MSI score, while the chemotherapeutic agent

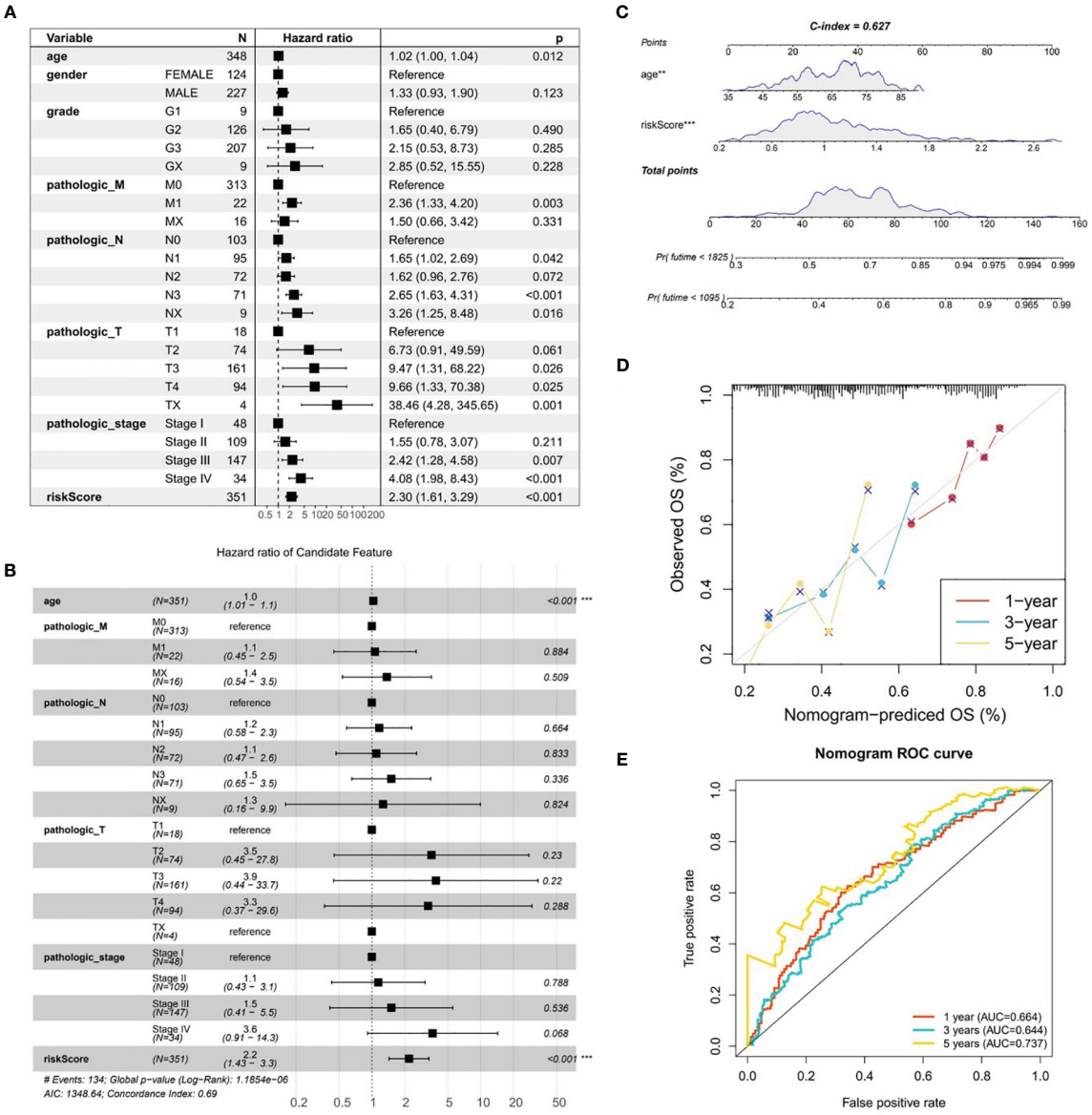

FIGURE 5
Analysis of gastric cancer in the TCGA-GC dataset combining risk scores and traditional clinical features. **(A)** Univariate Cox analysis of risk scores and traditional clinical features associated with overall survival in gastric cancer, **(B)** Independent prognostic indicators for predicting the prognosis of gastric cancer patients obtained through PH hypothesis testing and multivariate Cox analysis, **(C)** Nomogram constructed by combining risk scores and age for predicting the prognosis of gastric cancer, **(D)** Calibration curve of the nomogram, **(E)** ROC curve of the nomogram.

CCT018159 was significantly negatively associated with MSI score (P<0.05 and |cor|>0.3) (Figure 8E).

Further, our data revealed that TMB and CNV were markedly lower in high-risk patients than in low-risk patients, and risk score was remarkably negatively linked to TMB and CNV in GC (Figures 8F, G).

3.9 Stromal cells were identified as key cells

In the samples of GSE183904 dataset, totally 130,770 cells and 25,504 genes were identified after QC for downstream analysis. After PCA dimensional reduction and unsupervised cluster analysis, 35 distinct cell clusters were identified (Figure 9A). Subsequently, cell annotation yielded six cell subpopulations, namely, lymphoid cell, epithelial cell, plasma cell, myeloid cell, stromal cell, and endothelial cell (Figure 9B). Meanwhile, Figure 9C revealed that the expression of the respective corresponding significant marker genes was higher in six cell subpopulations, for example, PECAM1, PLVAP, VWF, and CDH5 were highly expressed in endothelial cell, as well as FCER1G and SPARC had higher expression in myeloid cell and stromal cell, respectively. Besides, the proportion of these six cell subpopulations could be observed for the sample in GSE183904 dataset from Figure 9D, where lymphoid cell content was highest in all samples.

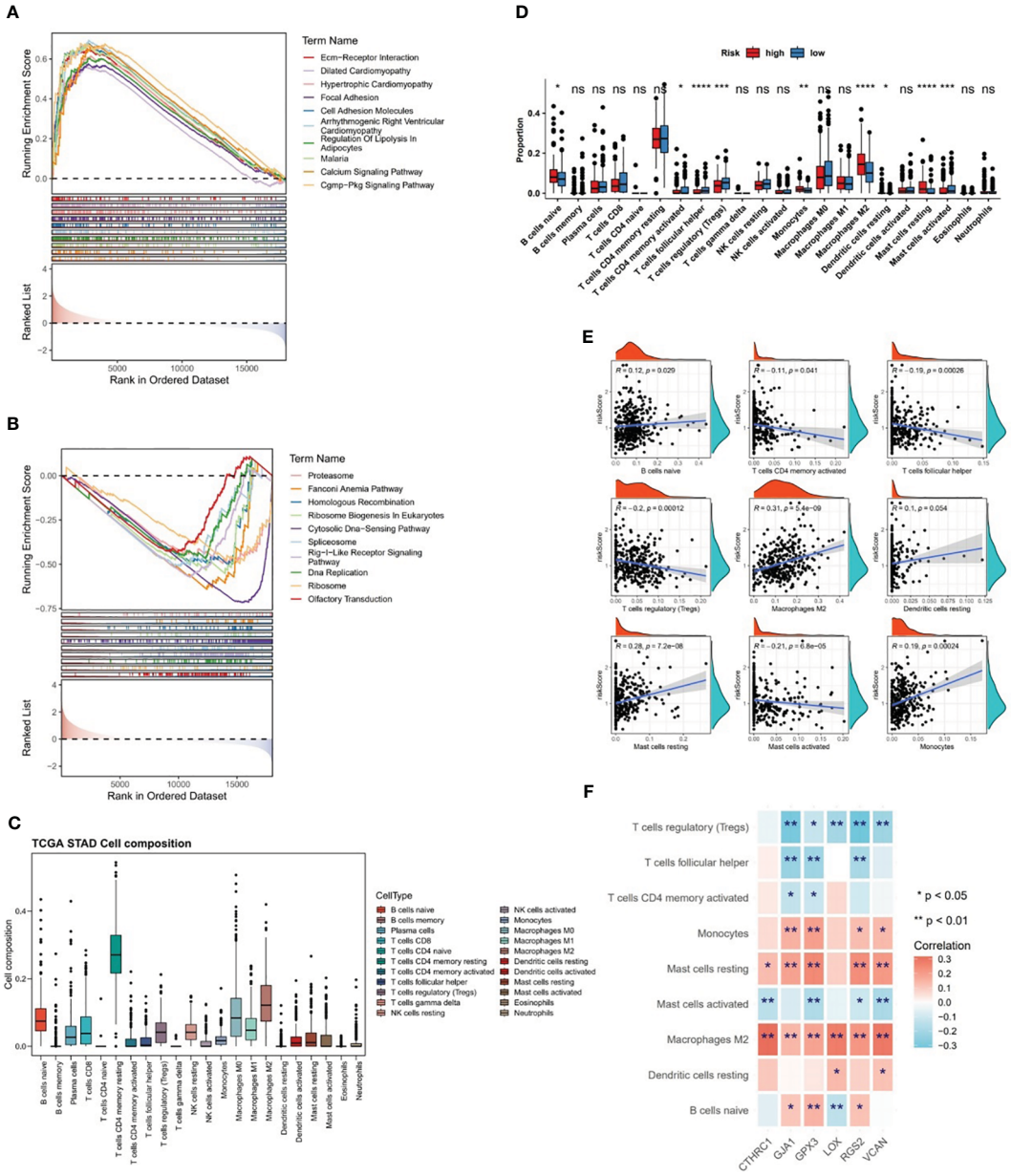

FIGURE 6
Differences in biological pathways and immune characteristics between two risk subgroups in the TCGA-GC dataset. **(A, B)** Gene Set Enrichment Analysis (GSEA) for the high-risk subgroup **(A)** and the low-risk subgroup **(B)**, **(C, D)** Analysis of different infiltration levels of immune cells between the two risk subgroups using the CIBERSORT program, **(E)** Correlation study between risk scores and different immune cells, **(F)** Correlation study between prognostic genes and different immune cells. * represent p<0.05, ** represent p<0.01, *** represent p<0.001, **** represent p<0.0001, ns represent no significant different.

The expression discrepancies of the six prognostic genes were analyzed in six different cell subpopulations to further explore the expression of these genes at the cellular level. As demonstrated in Figure 9E and Supplementary Figure 2, the cells with more expression of the prognostic genes were stromal cell, myeloid cell, and endothelial cell, and all six genes were expressed in stromal cell, so stromal cell was employed as the key cell for subsequent analyses in this study. ReactomeGSA enrichment analysis demonstrated that stromal cells were primarily engaged in “ATP sensitive potassium channels”, “FMO oxidizes nucleophiles”, “regulation of thyroid hormone activity”, etc (Figure 9F). Further, stromal cells was divided into three subclasses (stromal C1, stromal C2, and stromal C3), and it was noted that a relatively complete developmental trajectory existed for stromal C1 in pseudo-time analysis (Figure 9G).

3.10 Chromosomal localization, subcellular localization, and potential regulatory analyses were completed

The results of chromosomal localization analysis indicated that GPX3, LOX, and VCAN were all located in chromosomes 5, as well

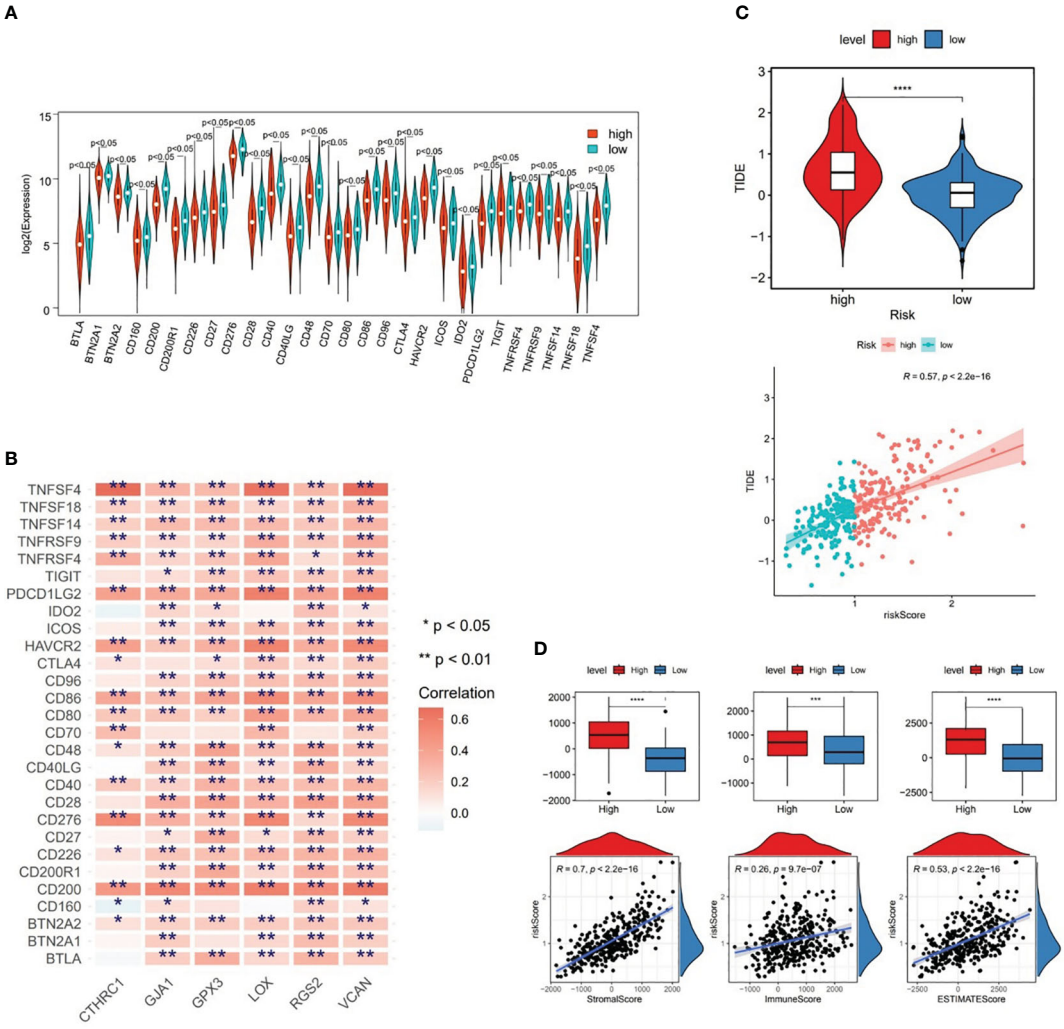

FIGURE 7
Differences in immune cell infiltration between two risk subgroups in the TCGA-GC dataset. **(A)** Immune cell gene (ICG) levels between the two risk subgroups, **(B)** Correlation analysis between six prognostic genes and immune cell genes, **(C)** TIDE scores between the two risk subgroups, **(D)** Immune score, stromal score, and ESTIMATE score between the two risk subgroups. * represent p<0.05, ** represent p<0.01, *** represent p<0.001, **** represent p<0.0001.

as RGS2, GJA1, and CTHRC1 in chromosomes 1, 6, and 8, respectively (Figure 10A). Meanwhile, the six prognostic genes were entered into the mRNALocater database to analyze their subcellular localisation, and the results revealed that GPX3, LOX, and CTHRC1 were preferably expressed in cytoplasm, whereas GJA1, VCAN, and RGS2 were preferably expressed in nucleus (Figure 10B).

Furthermore, the potential regulatory mechanisms of prognostic genes were elucidated by constructing a lncRNA-miRNA-mRNA network, as demonstrated in Figure 10C. It could be observed that the lncRNA-miRNA-mRNA network included 73 nodes (6 mRNA, 50 miRNA, and 17 lncRNA) and 133 edges, as well as the multiple relationship pairs were found in network. Obviously, lncRNAs (LINC01001, AC138035.1, and AC240565.2) could simultaneously regulate prognostic genes (VCAN, CTHRC1, and GPX3) via both hsa-let-7 family members (hsa-let-7a-5p, hsa-let-7b-5p, and hsa-let-7d-5p), as well as hsa-miR-200c-3p was identified as a regulator of LOX.

3.11 Experimental verification of prognostic genes expression in GC

In TCGA-GC dataset, the expression of the GJA1, VCAN, LOX, and CTHRC1 was markedly higher in GC samples than in normal samples, whereas GPX3 and RGS2 were markedly lower in the GC samples (Figure 11A). Besides, the expression of six prognostic genes was validated in GSE13911 dataset, and the results were presented in Figure 11B. Except for GJA1, the expression trends of the remaining five genes were consistent with the TCGA-GC dataset, and the expression of GPX3, LOX, and CTHRC1 had markedly difference between GC and normal samples (P<0.05).

With the purpose of verifying demonstrate the expression of prognostic genes in GC samples, qRT-PCR was performed on the GC tumor and the paraneoplastic normal tissues. As shown in Figure 11C, RGS2, GJA1, GPX3, and LOX were less expressed in

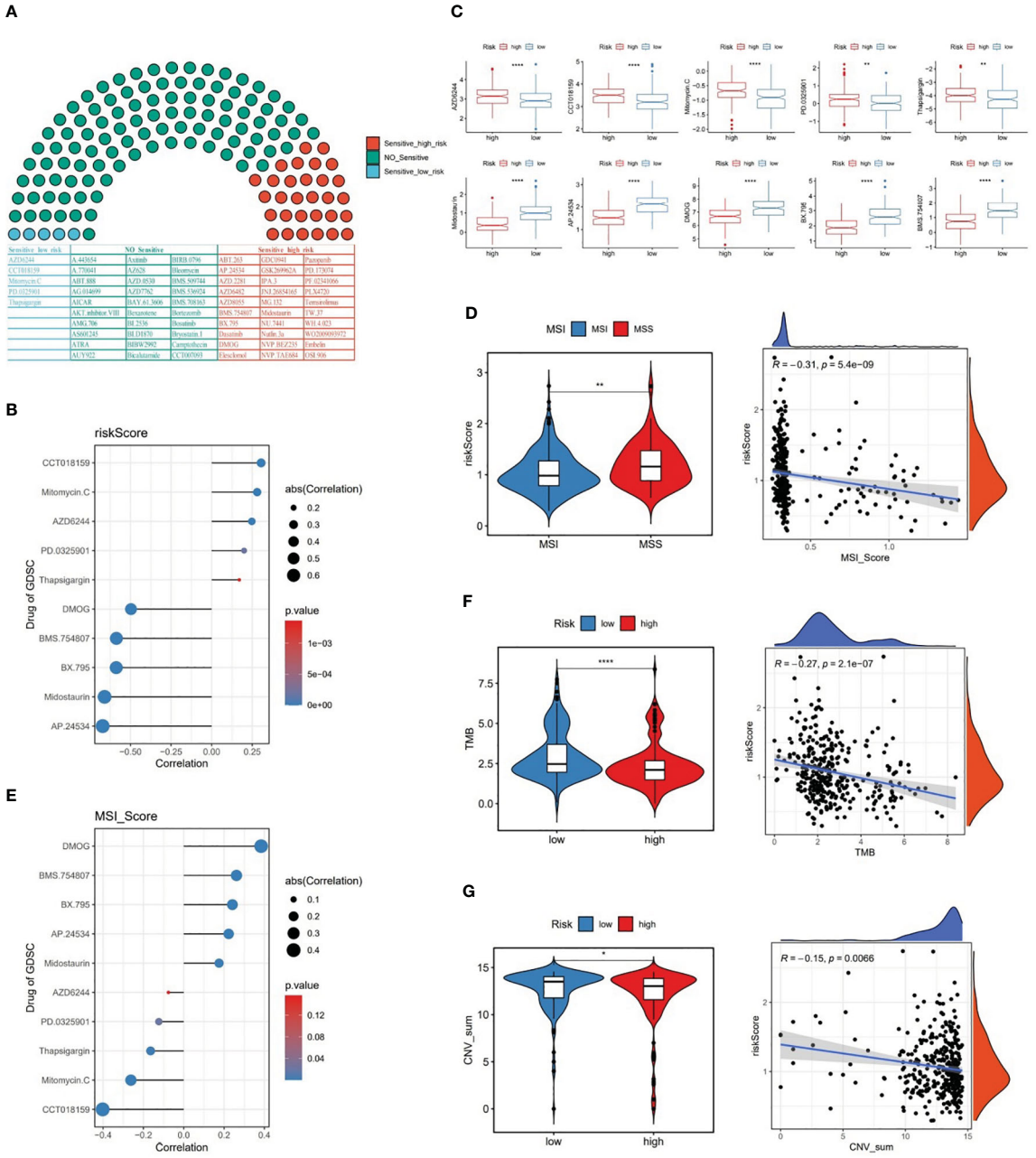

FIGURE 8
The relationship between risk score and chemotherapy drugs, MSI, TMB, and CNV. **(A)** Likelihood of sensitivity to different chemotherapy drugs, **(B)** Correlation between risk score and chemotherapy drugs, **(C)** Chemotherapy drug scores between the two risk subgroups, **(D)** MSI scores between the two risk subgroups and the correlation between MSI score and risk score, **(E)** Correlation between MSI score and chemotherapy drugs, **(F)** TMB scores between the two risk subgroups and the correlation between TMB score and risk score, **(G)** CNV scores between the two risk subgroups and the correlation between CNV score and risk score. * represent p<0.05, ** represent p<0.01, **** represent p<0.0001.

gastric cancer tissues than in paracancerous tissues (P<0.05). The expression trend of VCAN was opposite (P<0.05), while CTHRC1 had no difference in expression between GC and paracancerous samples (P>0.05).

4 Discussion

Gastric cancer is a common malignant tumor of the digestive tract worldwide, and its pathogenesis involves various factors. In recent years, with the development of molecular biology, the role of mitochondrial function and macrophage polarization in gastric cancer has gradually attracted attention. Current studies have shown that mitochondrial function is closely related to the progression of gastric cancer (43), while macrophage polarization also plays an important role in the immune microenvironment of gastric cancer (44). However, the relationship between mitochondrial function and macrophage polarization in gastric cancer and the underlying genetic regulatory mechanisms remain

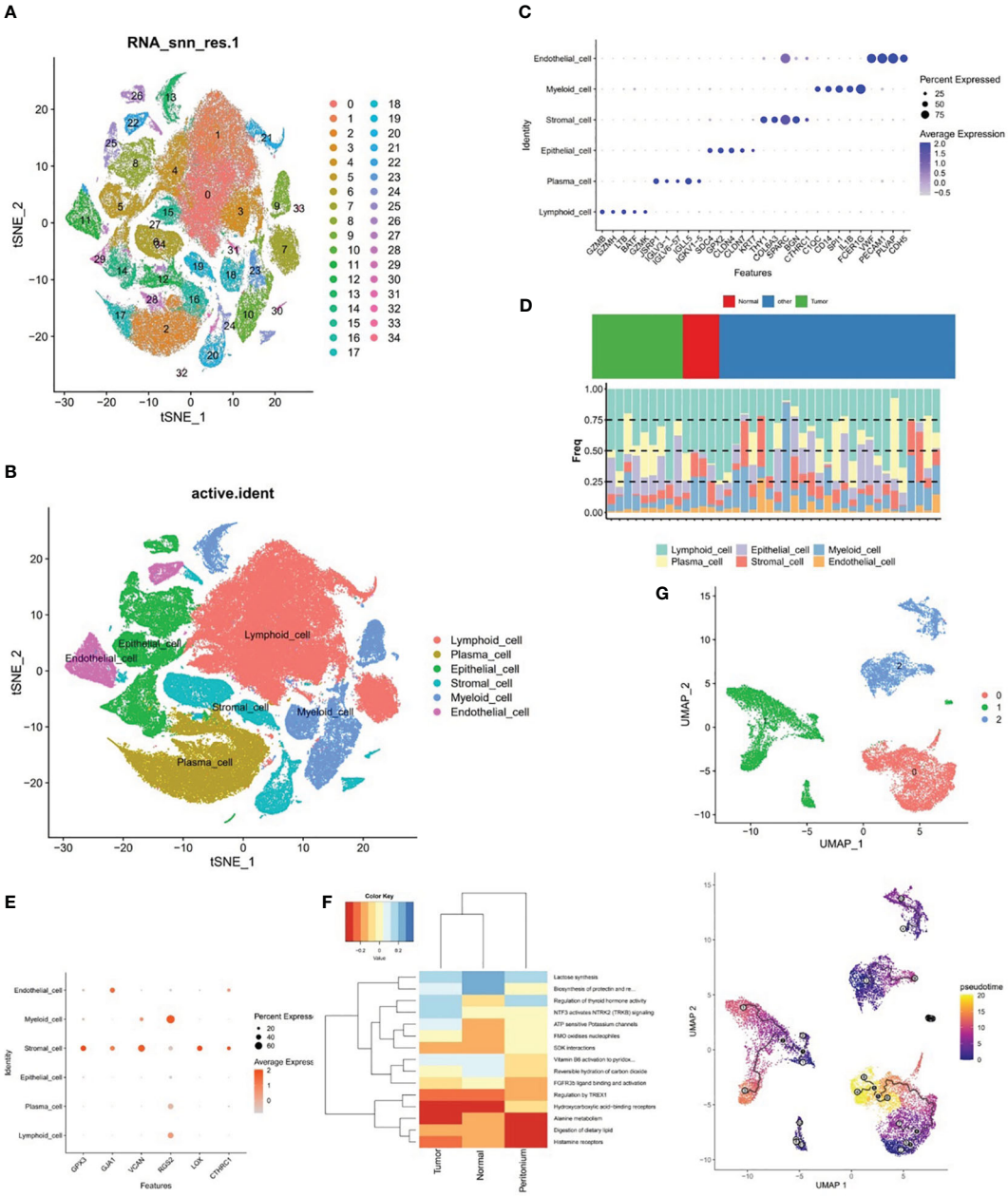

FIGURE 9
The relationship between stromal cells and prognostic genes. **(A, B)** Cell clusters in the GSE183904 dataset, **(C)** Significant marker genes corresponding to each of the six cell subsets. **(D)** Proportions of the six cell subsets, **(E)** Expression differences of six prognostic genes in six different cell subsets, **(F)** ReactomeGSA enrichment analysis of stromal cells in different tissues, **(G)** Pseudo-time analysis of three stromal cell subclasses.

unclear. This study aims to identify genes related to mitochondrial function and macrophage polarization in gastric cancer through bioinformatics analysis and biological sample validation, providing new ideas for the diagnosis and treatment of gastric cancer.

In this study, we first collected gene expression data from gastric cancer patients and screened out genes related to mitochondrial function and macrophage polarization using bioinformatics methods. We selected data of 375 cases of gastric cancer and 32 adjacent tissues from the TCGA dataset, as well as data from the GSE183904 dataset with complete single-cell sequencing data to identify related differentially expressed genes and establish the model. We also selected the larger sample-sized GSE15459 dataset and GSE13911 dataset for validation. To avoid potential selection bias, we used the data of all patients in the datasets for analysis. Then, we used bioinformatics tools to perform functional annotation and pathway analysis on these genes to reveal their possible mechanisms in gastric cancer. Through analysis, we identified a group of genes closely related to mitochondrial function and macrophage polarization in gastric cancer. These genes are mainly involved in biological processes such as energy metabolism, oxidative stress, and immune response. In addition, we also found that these genes are closely related to the prognosis of

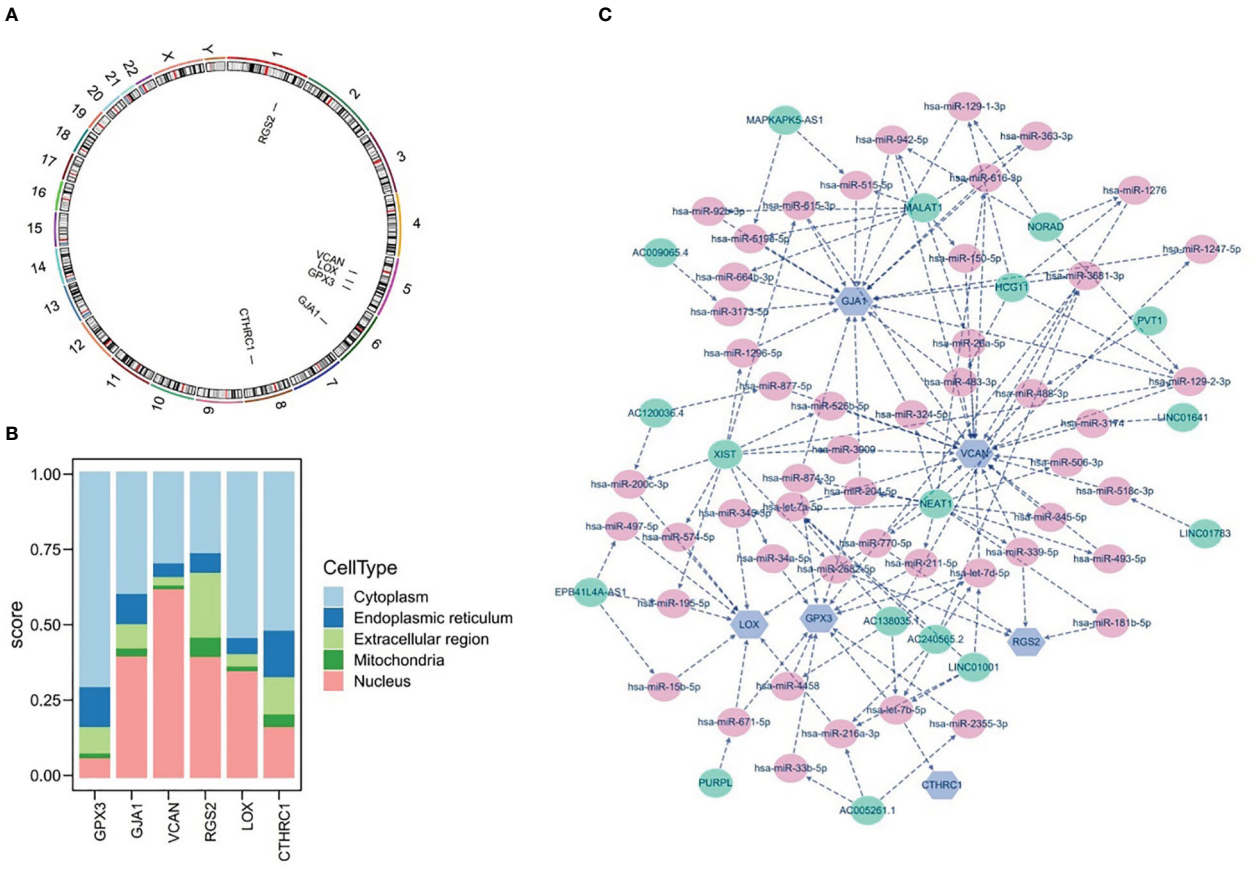

FIGURE 10
Chromosome Localization, subcellular Localization, and potential regulatory analysis. **(A)** Chromosome localization analysis of six prognostic genes, **(B)** subcellular localization of six prognostic genes, **(C)** lncRNA-miRNA-mRNA network of six prognostic genes.

gastric cancer, suggesting that they may be potential targets for gastric cancer treatment.

Glutathione peroxidase 3 (GPX3), the only known extracellular glycosylated enzyme in the glutathione peroxidase family, is a protein that contains a selenocysteine residue. It plays an important role in cellular defense mechanisms by resisting stress signals and scavenging reactive oxygen species, thereby maintaining the genetic integrity of cells (45). GPX3 can induce mitochondrial-related apoptosis through the AMPK/ERK1/2 pathway (46). GPX3 is also correlated with macrophage infiltration in tumors (47). In various tumors, the GPX3 promoter is hypermethylated or its allele is lost, leading to low expression (48, 49). Low expression of GPX3 is closely related to the occurrence, development, and prognosis of tumors such as gastric cancer (50).

Regulator of G protein signalling 2 (RGS2) is involved in cell cycle, transmembrane receptor protein tyrosine kinase signaling pathway, and regulation of G protein-coupled receptor protein signaling pathway, with a negative regulatory function in signal transduction (51). Studies have shown that the RGS2 gene also plays a certain role in cancer. In gastric cancer, the RGS2 gene is considered a new tumor biomarker. Fatty acid metabolism is related to the changes in the immune microenvironment of gastric cancer, and the RGS2 gene may participate in this process by regulating the G protein signaling pathway (52). Additionally, the RGS2 gene exhibits abnormal expression in prostate cancer. During the progression of prostate cancer, the downregulation of RGS2 expression is associated with hypoxia and is related to the regulation and influence of tumor phenotypes (53).

Versican, the protein encoded by the VCAN gene, is an important extracellular matrix protein involved in biological processes such as cell adhesion, migration, proliferation, and signaling. Research has shown that the VCAN gene is negatively regulated by methylation, leading to its high expression in cancer tissues (54). In gastric cancer, VCAN is overexpressed and can predict the response to adjuvant chemotherapy, adjuvant radiotherapy and immunotherapy (55).

The CTHRC1 gene encodes collagen triple helix repeat protein 1, which plays an important role in various biological processes, including inhibiting collagen deposition, promoting cell migration, and accelerating vascular repair. In recent years, the role of CTHRC1 in cancer research has gradually emerged, especially in gastric cancer, hepatocellular carcinoma, colorectal cancer, esophageal cancer, and other cancers (56). The expression of CTHRC1 protein in gastric cancer tissues is significantly higher than that in adjacent tissues, and there is a certain correlation between the expression of CTHRC1 protein and the prognosis of gastric cancer patients. CTHRC1 increases the expression of CXCR4 by up-regulating the expression of HIF-1α, ultimately

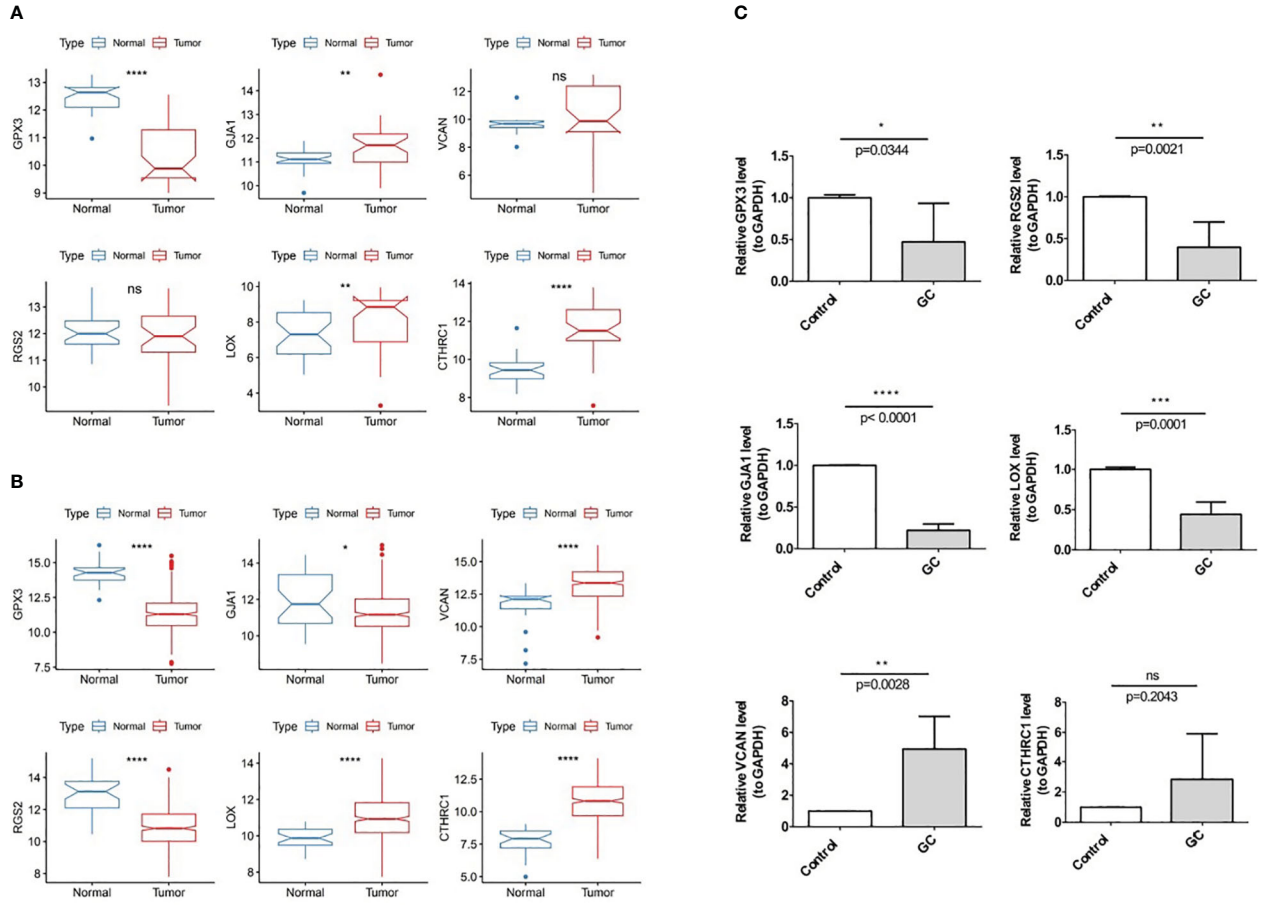

FIGURE 11
Experimental validation of prognostic gene Expression in GC, **(A)** Expression of six prognostic genes in the TCGA-GC dataset, **(B)** Expression of six prognostic genes in the GSE13911 dataset, **(C)** Expression of six prognostic genes in GC tumor tissues and adjacent normal tissues. * represent p<0.05, ** represent p<0.01, *** represent p<0.001, **** represent p<0.0001, ns represent no significant different.

promoting cell migration and invasion (57). In colon cancer, CTHRC1 remodels infiltrating macrophages through interaction with TGF-β receptors, promoting liver metastasis of colorectal cancer cells (58).

The gene for Gap Junction Alpha-1 (GJA1), also known as Connexin43 (Cx43), is a key gap junction protein necessary for the propagation of action potentials between adjacent cells (59). The GJA1 gene also plays a role in cancer. In breast cancer, the expression of GJA1 is related to tumor subtype (60). In colorectal cancer, the loss of GJA1 expression is positively correlated with patient metastasis and poor prognosis. Overexpression of GJA1 can inhibit the progression of colorectal cancer and enhance cancer cell sensitivity to 5-fluorouracil (5-FU) (61). The function of the GJA1 gene in gastric cancer is still unclear. Some studies have shown that the expression level of GJA1 protein is low in gastric cancer tissue, and its low expression is associated with the progression and poor prognosis of gastric cancer (62), which is consistent with our analysis results but inconsistent with the results of the TCGA database. This suggests that the role of the GJA1 gene in the occurrence and development of gastric cancer may be complex. Currently, the specific mechanism of GJA1 in gastric cancer still requires further investigation to provide new ideas and methods for the diagnosis and treatment of gastric cancer.

LOX is a copper-dependent monoamine oxidase that participates in the covalent cross-linking of collagen and elastin in the extracellular matrix, thereby maintaining the normal structure and function of the extracellular matrix (63). LOX can affect VEGF induction, HIF-1α activation, and other mechanisms, playing an important role in the occurrence, development, invasion, and metastasis of various tumor (64). In gastric cancer, the downregulation of LOX expression can downregulate the expression of MMP-2 and MMP-9 in cancer cells (65). Literature shows that the expression level of LOX in gastric cancer is usually high, which is consistent with the results of TCGA and GEO databases (66). However, our verification results may be limited by the sample size and show opposite results, which can be further verified with more samples in the future.

This study revealed the potential mechanism of mitochondrial function and macrophage polarization-related genes in gastric cancer through bioinformatics analysis, and verified the expression of these genes in gastric cancer tissues by qRT-PCR, providing new ideas for the diagnosis and treatment of gastric

cancer. Gene diagnosis is playing an increasingly important role in clinical work. Currently, samples from patients after surgery are often subject to genetic analysis. Therefore, in future work, it is highly feasible to apply the nomogram composed of these genes for clinical diagnosis, prognosis determination and clinical decision-making. The target genes screened in this study have not yet been functionally validated at the cellular level. These genes may not only function in tumor cells but also play important roles in stromal cells and affect the behavior of tumor cells. Stromal cells in tumors may impact aspects such as tumor occurrence, development, metastasis, and treatment response through means like growth factor signal transduction, influencing the function of immune cells in the tumor microenvironment, and providing nutrients for tumor cells. In the future, we will further validate the functions of these genes through cellular and animal experiments, focusing on exploring their mechanisms in mitochondrial function and macrophage polarization in gastric cancer, in order to more comprehensively understand the pathogenesis and treatment of gastric cancer.

Data availability statement

The original contributions presented in the study are included in the article/Supplementary Material. Further inquiries can be directed to the corresponding authors.

Ethics statement

The studies involving humans were approved by Gusu School, Nanjing Medical Universtiy. The studies were conducted in accordance with the local legislation and institutional requirements. The participants provided their written informed consent to participate in this study.

Author contributions

YZ: Conceptualization, Writing – original draft, Writing – review & editing. JC: Data curation, Writing – original draft. ZY: Formal analysis, Writing – original draft. HZ: Investigation, Writing – original draft. JY: Methodology, Writing – original draft. XT: Software, Writing – original draft. XG: Project administration, Writing – review & editing.

Funding

The author(s) declare financial support was received for the research, authorship, and/or publication of this article. Suzhou Medical Key Discipline (SZXK202109), Suzhou Clinical Key Disease Project (LCZX202111), Nanjing Medical University Gusu School Research Project (GSKY20210233), Suzhou Promoting Health through Science and Education Research Project (KJXW2021028).

Conflict of interest

Authors JY and XT was employed by the company Alliance Biotechnology Company, China.

The remaining authors declare that the research was conducted in the absence of any commercial or financial relationships that could be construed as a potential conflict of interest.

Publisher's note

Supplementary material

The Supplementary Material for this article can be found online at: https://www.frontiersin.org/articles/10.3389/fonc.2024.1433874/full#supplementary-material

SUPPLEMENTARY FIGURE 1
Genes significantly associated with prognosis obtained through univariate Cox regression analysis and PH assumption testing.

SUPPLEMENTARY FIGURE 2
Expression differences of six prognostic genes across six different cell subpopulations.

SUPPLEMENTARY TABLE 1
1,136 Mitochondrial-Related Genes (MRGs).

SUPPLEMENTARY TABLE 2
35 Macrophage Polarization-Related Genes (MPRGs).

References

1. Sung H, Ferlay J, Siegel RL, Laversanne M, Soerjomataram I, Jemal A, et al. Global cancer statistics 2020: GLOBOCAN estimates of incidence and mortality worldwide for 36 cancers in 185 countries. *CA Cancer J Clin*. (2021) 71:209–49. doi: 10.3322/caac.21660

2. Shibasaki S, Suda K, Hisamori S, Obama K, Terashima M, Uyama I. Robotic gastrectomy for gastric cancer: systematic review and future directions. *Gastric Cancer*. (2023) 26:325–38. doi: 10.1007/s10120-023-01389-y

3. Guan WL, He Y, Xu RH. Gastric cancer treatment: recent progress and future perspectives. *J Hematol Oncol*. (2023) 16:57. doi: 10.1186/s13045-023-01451-3

4. Patel TH, Cecchini M. Targeted therapies in advanced gastric cancer. *Curr Treat Options Oncol*. (2020) 21:70. doi: 10.1007/s11864-020-00774-4

5. Guo X, Peng Y, Song Q, Wei J, Wang X, Ru Y, et al. A liquid biopsy signature for the early detection of gastric cancer in patients. *Gastroenterology*. (2023) 165:402–413 e13. doi: 10.1053/j.gastro.2023.02.044

6. Liu Y, Chen C, Wang X, Sun Y, Zhang J, Chen J, et al. An epigenetic role of mitochondria in cancer. *Cells*. (2022) 11(16). doi: 10.3390/cells11162518

7. Kopinski PK, Singh LN, Zhang S, Lott MT, Wallace DC. Mitochondrial DNA variation and cancer. *Nat Rev Cancer*. (2021) 21:431–45. doi: 10.1038/s41568-021-00358-w

8. Cai X, Liang C, Zhang M, Dong Z, Weng Y, Yu W. Mitochondrial DNA copy number and cancer risks: A comprehensive Mendelian randomization analysis. *Int J Cancer*. (2024) 154:1504–13. doi: 10.1002/ijc.34833

9. Li Y, Sundquist K, Zhang N, Wang X, Sundquist J, Memon AA. Mitochondrial related genome-wide Mendelian randomization identifies putatively causal genes for multiple cancer types. *EBioMedicine*. (2023) 88:104432. doi: 10.1016/j.ebiom.2022.104432

10. Shapouri-Moghaddam A, Mohammadian S, Vazini H, Taghadosi M, Esmaeili SA, Mardani F, et al. Macrophage plasticity, polarization, and function in health and disease. *J Cell Physiol*. (2018) 233:6425–40. doi: 10.1002/jcp.26429

11. Zhang G, Yang L, Han Y, Niu H, Yan L, Shao Z, et al. Abnormal macrophage polarization in patients with myelodysplastic syndrome. *Mediators Inflamm*. (2021) 2021:9913382. doi: 10.1155/2021/9913382

12. Mehla K, Singh PK. Metabolic regulation of macrophage polarization in cancer. *Trends Cancer*. (2019) 5:822–34. doi: 10.1016/j.trecan.2019.10.007

13. Lawrence T, Natoli G. Transcriptional regulation of macrophage polarization: enabling diversity with identity. *Nat Rev Immunol*. (2011) 11:750–61. doi: 10.1038/nri3088

14. Xia T, Zhang M, Lei W, Yang R, Fu S, Fan Z, et al. Advances in the role of STAT3 in macrophage polarization. *Front Immunol*. (2023) 14:1160719. doi: 10.3389/fimmu.2023.1160719

15. Kerneur C, Cano CE, Olive D. Major pathways involved in macrophage polarization in cancer. *Front Immunol*. (2022) 13:1026954. doi: 10.3389/fimmu.2022.1026954

16. Li W, Zhang X, Wu F, Zhou Y, Bao Z, Li H, et al. Gastric cancer-derived mesenchymal stromal cells trigger M2 macrophage polarization that promotes metastasis and EMT in gastric cancer. *Cell Death Dis*. (2019) 10:918. doi: 10.1038/s41419-019-2131-y

17. Hu X, Ma Z, Xu B, Li S, Yao Z, Liang B, et al. Glutamine metabolic microenvironment drives M2 macrophage polarization to mediate trastuzumab resistance in HER2-positive gastric cancer. *Cancer Commun (Lond)*. (2023) 43:909–37. doi: 10.1002/cac2.12459

18. Liang S, Cai J, Li Y, Yang R. 1,25–Dihydroxy–Vitamin D3 induces macrophage polarization to M2 by upregulating T–cell Ig–mucin–3 expression. *Mol Med Rep*. (2019) 19:3707–13. doi: 10.3892/mmr

19. Van den Bossche J, Saraber DL. Metabolic regulation of macrophages in tissues. *Cell Immunol*. (2018) 330:54–9. doi: 10.1016/j.cellimm.2018.01.009

20. Dubey S, Ghosh S, Goswami D, Ghatak D, De R. Immunometabolic attributes and mitochondria-associated signaling of Tumor-Associated Macrophages in tumor microenvironment modulate cancer progression. *Biochem Pharmacol*. (2023) 208:115369. doi: 10.1016/j.bcp.2022.115369

21. Subhash VV, Yeo MS, Wang L, Tan SH, Wong FY, Thuya WL, et al. Anti-tumor efficacy of Selinexor (KPT-330) in gastric cancer is dependent on nuclear accumulation of p53 tumor suppressor. *Sci Rep*. (2018) 8:12248. doi: 10.1038/s41598-018-30686-1

22. D'Errico M, de Rinaldis E, Blasi MF, Viti V, Falchetti M, Calcagnile A, et al. Genome-wide expression profile of sporadic gastric cancers with microsatellite instability. *Eur J Cancer*. (2009) 45:461–9. doi: 10.1016/j.ejca.2008.10.032

23. Kumar V, Ramnarayanan K, Sundar R, Padmanabhan N, Srivastava S, Koiwa M, et al. Single-cell atlas of lineage states, tumor microenvironment, and subtype-specific expression programs in gastric cancer. *Cancer Discov*. (2022) 12:670–91. doi: 10.1158/2159-8290.CD-21-0683

24. Ritchie ME, Phipson B, Wu D, Hu Y, Law CW, Shi W, et al. limma powers differential expression analyses for RNA-sequencing and microarray studies. *Nucleic Acids Res*. (2015) 43:e47. doi: 10.1093/nar/gkv007

25. Love MI, Huber W, Anders S. Moderated estimation of fold change and dispersion for RNA-seq data with DESeq2. *Genome Biol*. (2014) 15:550. doi: 10.1186/s13059-014-0550-8

26. Gustavsson EK, Zhang D, Reynolds RH, Garcia-Ruiz S, Ryten M. ggtranscript: an R package for the visualization and interpretation of transcript isoforms using ggplot2. *Bioinformatics*. (2022) 38:3844–6. doi: 10.1093/bioinformatics/btac409

27. Gu Z, Eils R, Schlesner M. Complex heatmaps reveal patterns and correlations in multidimensional genomic data. *Bioinformatics*. (2016) 32:2847–9. doi: 10.1093/bioinformatics/btw313

28. Hanzelmann S, Castelo R, Guinney J. GSVA: gene set variation analysis for microarray and RNA-seq data. *BMC Bioinf*. (2013) 14:7. doi: 10.1186/1471-2105-14-7

29. Langfelder P, Horvath S. WGCNA: an R package for weighted correlation network analysis. *BMC Bioinf*. (2008) 9:559. doi: 10.1186/1471-2105-9-559

30. Gao CH, Yu G, Cai P. ggVennDiagram: an intuitive, easy-to-use, and highly customizable R package to generate venn diagram. *Front Genet*. (2021) 12:706907. doi: 10.3389/fgene.2021.706907

31. Yu G, Wang LG, Han Y, He QY. clusterProfiler: an R package for comparing biological themes among gene clusters. *OMICS*. (2012) 16:284–7. doi: 10.1089/omi.2011.0118

32. Qing J, Li C, Hu X, Song W, Tirichen H, Yaigoub H, et al. Differentiation of T helper 17 cells may mediate the abnormal humoral immunity in igA nephropathy and inflammatory bowel disease based on shared genetic effects. *Front Immunol*. (2022) 13:916934. doi: 10.3389/fimmu.2022.916934

33. Ramsay IS, Ma S, Fisher M, Loewy RL, Ragland JD, Niendam T, et al. Model selection and prediction of outcomes in recent onset schizophrenia patients who undergo cognitive training. *Schizophr Res Cognit*. (2018) 11:1–5. doi: 10.1016/j.scog.2017.10.001

34. Li Y, Lu F, Yin Y. Applying logistic LASSO regression for the diagnosis of atypical Crohn's disease. *Sci Rep*. (2022) 12:11340. doi: 10.1038/s41598-022-15609-5

35. Heagerty PJ, Lumley T, Pepe MS. Time-dependent ROC curves for censored survival data and a diagnostic marker. *Biometrics*. (2000) 56:337–44. doi: 10.1111/j.0006-341X.2000.00337.x

36. Ma X, Cheng J, Zhao P, Li L, Tao K, Chen H. DNA methylation profiling to predict recurrence risk in stage Iota lung adenocarcinoma: Development and validation of a nomogram to clinical management. *J Cell Mol Med*. (2020) 24:7576–89. doi: 10.1111/jcmm.15393

37. Zhang J, Han X, Lin L, Chen J, Wang F, Ding Q, et al. Unraveling the expression patterns of immune checkpoints identifies new subtypes and emerging therapeutic indicators in lung adenocarcinoma. *Oxid Med Cell Longev*. (2022) 2022:3583985. doi: 10.1155/2022/3583985

38. Jiang HZ, Yang B, Jiang YL, Liu X, Chen DL, Long FX, et al. Development and validation of prognostic models for colon adenocarcinoma based on combined immune-and metabolism-related genes. *Front Oncol*. (2022) 12:1025397. doi: 10.3389/fonc.2022.1025397

39. Jiang A, Wang J, Liu N, Zheng X, Li Y, Ma Y, et al. Integration of single-cell RNA sequencing and bulk RNA sequencing data to establish and validate a prognostic model for patients with lung adenocarcinoma. *Front Genet*. (2022) 13:833797. doi: 10.3389/fgene.2022.833797

40. Cao J, Spielmann M, Qiu X, Huang X, Ibrahim DM, Hill AJ, et al. The single-cell transcriptional landscape of mammalian organogenesis. *Nature*. (2019) 566:496–502. doi: 10.1038/s41586-019-0969-x

41. Zhang H, Meltzer P, Davis S. RCircos: an R package for Circos 2D track plots. *BMC Bioinf*. (2013) 14:244. doi: 10.1186/1471-2105-14-244

42. Shannon P, Markiel A, Ozier O, Baliga NS, Wang JT, Ramage D, et al. Cytoscape: a software environment for integrated models of biomolecular interaction networks. *Genome Res*. (2003) 13:2498–504. doi: 10.1101/gr.1239303

43. Chen X, Wei C, Huang L, Syrigos K, Li Y, Li P. Non-coding RNAs regulate mitochondrial dynamics in the development of gastric cancer. *Front Mol Biosci*. (2023) 10:1107651. doi: 10.3389/fmolb.2023.1107651

44. Zheng HC, Xue H, Zhang CY. REG4 promotes the proliferation and anti-apoptosis of cancer. *Front Cell Dev Biol*. (2022) 10:1012193. doi: 10.3389/fcell.2022.1012193

45. Chang C, Worley BL, Phaeton R, Hempel N. Extracellular glutathione peroxidase GPx3 and its role in cancer. *Cancers (Basel)*. (2020) 12(8). doi: 10.3390/cancers12082197

46. Li Y, Zhou Y, Liu D, Wang Z, Qiu J, Zhang J, et al. Glutathione Peroxidase 3 induced mitochondria-mediated apoptosis *via* AMPK /ERK1/2 pathway and resisted autophagy-related ferroptosis *via* AMPK/mTOR pathway in hyperplastic prostate. *J Transl Med*. (2023) 21:575. doi: 10.1186/s12967-023-04432-9

47. Pei J, Tian X, Yu C, Luo J, Zhang J, Hua Y, et al. GPX3 and GSTT1 as biomarkers related to oxidative stress during renal ischemia reperfusion injuries and their relationship with immune infiltration. *Front Immunol*. (2023) 14:1136146. doi: 10.3389/fimmu.2023.1136146

48. Ragavi R, Muthukumaran P, Nandagopal S, Ahirwar DK, Tomo S, Misra S, et al. Epigenetics regulation of prostate cancer: Biomarker and therapeutic potential. *Urol Oncol*. (2023) 41:340–53. doi: 10.1016/j.urolonc.2023.03.005

49. Qu Y, Dang S, Hou P. Gene methylation in gastric cancer. *Clin Chim Acta*. (2013) 424:53–65. doi: 10.1016/j.cca.2013.05.002

50. He Q, Chen N, Wang X, Li P, Liu L, Rong Z, et al. Prognostic value and immunological roles of GPX3 in gastric cancer. *Int J Med Sci*. (2023) 20:1399–416. doi: 10.7150/ijms.85253

51. Xu Q, Yao M, Tang C. RGS2 and female common diseases: a guard of women's health. *J Transl Med*. (2023) 21:583. doi: 10.1186/s12967-023-04462-3

52. Yang S, Sun B, Li W, Yang H, Li N, Zhang X. Fatty acid metabolism is related to the immune microenvironment changes of gastric cancer and RGS2 is a new tumor biomarker. *Front Immunol*. (2022) 13:1065927. doi: 10.3389/fimmu.2022.1065927

53. Linder A, Hagberg Thulin M, Damber JE, Welen K. Analysis of regulator of G-protein signalling 2 (RGS2) expression and function during prostate cancer progression. *Sci Rep*. (2018) 8:17259. doi: 10.1038/s41598-018-35332-4

54. Luo HL, Chang YL, Liu HY, Wu YT, Sung MT, Su YL, et al. VCAN hypomethylation and expression as predictive biomarkers of drug sensitivity in upper urinary tract urothelial carcinoma. *Int J Mol Sci*. (2023) 24(8). doi: 10.3390/ijms24087486

55. Song J, Wei R, Huo S, Liu C, Liu X. Versican enrichment predicts poor prognosis and response to adjuvant therapy and immunotherapy in gastric cancer. *Front Immunol*. (2022) 13:960570. doi: 10.3389/fimmu.2022.960570

56. Mei D, Zhu Y, Zhang L, Wei W. The role of CTHRC1 in regulation of multiple signaling and tumor progression and metastasis. *Mediators Inflamm*. (2020) 2020:9578701. doi: 10.1155/2020/9578701

57. Ding X, Huang R, Zhong Y, Cui N, Wang Y, Weng J, et al. CTHRC1 promotes gastric cancer metastasis *via* HIF-1alpha/CXCR4 signaling pathway. *BioMed Pharmacother*. (2020) 123:109742. doi: 10.1016/j.biopha.2019.109742

58. Zhang XL, Hu LP, Yang Q, Qin WT, Wang X, Xu CJ, et al. CTHRC1 promotes liver metastasis by reshaping infiltrated macrophages through physical interactions with TGF-beta receptors in colorectal cancer. *Oncogene*. (2021) 40:3959–73. doi: 10.1038/s41388-021-01827-0

59. Whisenant CC, Shaw RM. Internal translation of Gja1 (Connexin43) to produce GJA1-20k: Implications for arrhythmia and ischemic-preconditioning. *Front Physiol*. (2022) 13:1058954. doi: 10.3389/fphys.2022.1058954

60. Busby M, Hallett MT, Plante I. The complex subtype-dependent role of connexin 43 (GJA1) in breast cancer. *Int J Mol Sci*. (2018) 19(3). doi: 10.3390/ijms19030693

61. Han Y, Wang H, Chen H, Tan T, Wang Y, Yang H, et al. CX43 down-regulation promotes cell aggressiveness and 5-fluorouracil-resistance by attenuating cell stiffness in colorectal carcinoma. *Cancer Biol Ther*. (2023) 24:2221879. doi: 10.1080/15384047.2023.2221879

62. Lerotic I, Vukovic P, Hrabar D, Misir Z, Kruljac I, Pavic T, et al. Expression of NEDD9 and connexin-43 in neoplastic and stromal cells of gastric adenocarcinoma. *Bosn J Basic Med Sci*. (2021) 21:542–8. doi: 10.17305/bjbms.2020.5379

63. Laczko R, Csiszar K. Lysyl oxidase (LOX): functional contributions to signaling pathways. *Biomolecules*. (2020) 10(8). doi: 10.3390/biom10081093

64. Murdocca M, De Masi C, Pucci S, Mango R, Novelli G, Di Natale C, et al. LOX-1 and cancer: an indissoluble liaison. *Cancer Gene Ther*. (2021) 28:1088–98. doi: 10.1038/s41417-020-00279-0

65. Zhao L, Niu H, Liu Y, Wang L, Zhang N, Zhang G, et al. LOX inhibition downregulates MMP-2 and MMP-9 in gastric cancer tissues and cells. *J Cancer*. (2019) 10:6481–90. doi: 10.7150/jca.33223

66. Wang F, Li H, Zhang J, Fan J, Xu J. A comprehensive analysis of the expression and the prognosis for LOX-1 in multiple cancer types. *Biotechnol Genet Eng Rev*. (2023), 1–23. doi: 10.1080/02648725.2023.2199477

frontiers | Frontiers in Oncology

TYPE Mini Review
PUBLISHED 05 August 2024
DOI 10.3389/fonc.2024.1456631

OPEN ACCESS

EDITED BY
Zhi Sheng,
University of South Alabama, United States

REVIEWED BY
Sanjeev Das,
National Institute of Immunology (NII), India
Seema Singh,
University of South Alabama, United States

*CORRESPONDENCE
Romi Gupta
romigup@uab.edu

RECEIVED 28 June 2024
ACCEPTED 22 July 2024
PUBLISHED 05 August 2024

CITATION
Kumar R and Gupta R (2024) Epigenetic regulation of NKG2D ligand and the rise of NK cell-based immunotherapy for cancer treatment.
Front. Oncol. 14:1456631.
doi: 10.3389/fonc.2024.1456631

Epigenetic regulation of NKG2D ligand and the rise of NK cell-based immunotherapy for cancer treatment

Raj Kumar[1] and Romi Gupta[1,2]*

[1]Department of Biochemistry and Molecular Genetics, The University of Alabama at Birmingham, Birmingham, AL, United States, [2]O'Neal Comprehensive Cancer Center, The University of Alabama at Birmingham, Birmingham, AL, United States

Epigenetic modifications influence gene expression and effects cancer initiation and progression. Therefore, they serve as diagnostic and prognostic biomarkers and potential therapeutic targets. Natural Killer (NK) cells, integral to the innate immune system, exhibit anti-tumor effect by recognizing and eliminating cancerous cells through the balance of activating and inhibitory ligands. Understanding the epigenetic regulation of NK cell ligands offers insights into enhancing NK cell-mediated tumor eradication. This review explores the epigenetic modifications governing the expression of activating NKG2D ligands and discusses clinical trials investigating NK cell-based immunotherapies, highlighting their potential as effective cancer treatment strategies. Case studies examining the safety and effectiveness of NK cell therapies in different cancer types, such as acute myeloid leukemia (AML) and non-small cell lung cancer (NSCLC), demonstrate promising outcomes with minimal toxicity. These findings underscore the therapeutic prospects of epigenetic modulation of NKG2D ligands and NK cell-based immunotherapies as effective cancer treatment strategies. Future research in the advancement of personalized medicine approaches and novel combination therapies with NK cell will further improve treatment outcomes and provide new therapeutic options for treating patients with various types of cancer.

KEYWORDS

epigenetics, NK cell, acetylation, methylation, clinical trial

Introduction

Epigenetic changes regulating gene expression are those that are independent of alterations in the DNA sequence. These changes can be regulated by numerous factors (1). Epigenetic regulators mediating epigenetic changes have been shown to play a pivotal role in cancer initiation and progression by regulating the expression of tumor suppressor genes (TSGs) and oncogenes (2). Moreover, these epigenetic changes impact DNA repair

mechanisms, potentially leading to genomic instability and driving tumorigenesis (3, 4). They also contribute to maintaining the stemness of cancer cells (5) and regulate responses to therapy (6). Therefore, they are used as biomarkers for cancer diagnosis and prognosis and represent promising targets for cancer therapy. Understanding the role of epigenetic regulators and epigenetic modifications in cancer development is essential for unraveling the complexity of the disease and developing effective targeted therapeutic strategies.

Natural Killer (NK) cells is a kind of white blood cell and represents crucial components of the immune system. NK cells are a part of the innate immune system and play an important role in regulating the immune response to viral infections, as well as in recognizing and destroying infected or abnormal cells, such as cancer cells (7). NK cells possess the ability to identify and target cancer cells without prior sensitization (8). They express receptors that recognize specific ligands on cancer cells and, upon recognition, release cytotoxic granules that induce apoptosis, thereby eradicating cancer cells (9).

Cancer cells express both activating and inhibitory ligands, and the balance of these ligands interacting with receptors on the surface of NK cells determines the fate of cancer cells (10). Activating ligands include Natural Killer Group 2D (NKG2D) ligands e.g., Major histocompatibility complex (MHC) class I chain-related protein A (MICA), MHC class I chain-related protein B (MICB), UL16 binding proteins (ULBPs), trigger NK cell activation and promote cytotoxicity upon their expression (11). Another group of activating ligands include DNAX accessory molecule- 1 (DNAM-1) ligands e.g., Nectin-2 (CD112), PVR or cluster of differentiation155 (CD155). DNAM-1 is expressed on NK cells and serve as an activating receptor. It specifically interacts with DNAM-1 ligands expressed on cancer cells and promotes NK cell-mediated cytotoxicity by producing cytokines (12). Inhibitory ligands, for example MHC class I molecules upon interacting with inhibitory receptors on NK cells leads to transmitting signals that prevent NK cell activation and killing of self-cells (13). Thus, the balance between the expression of activating and inhibitory ligands determines NK cell responsiveness to cancer cells. Additionally, NK cells play a role to modulate the overall immune response. It interacts with other immune cells such as macrophages, dendritic cells, and T cells and contributes to the overall regulation of the immune system's function (14).

Given the important role that NK cells play, potential therapeutic applications of NK cells in cancer treatment are being explored (7). Several clinical trials are ongoing to develop novel therapies based on NK cells for effective cancer treatment. Additionally, previous studies have provided understanding into the epigenetic mechanisms that play a critical role in regulating the expression of NK cell ligands (15–17), affecting NK cell-mediated tumor cell eradication. This article discusses the role of epigenetic modifications that regulate the expression of activating NKG2D ligands and reviews various clinical trials with NK cells, highlighting the effectiveness of NK cell-based immunotherapy as a successful and promising therapeutic strategy for cancer treatment.

Epigenetic modifications regulating the expression of activating NKG2D

Epigenetic modifications are crucial for regulating gene expression, including the expression of NKG2D ligands (15–17). This section provides a review of various epigenetic modifications that regulate NKG2D ligand expression. The concept of epigenetic regulation of NKG2D ligands and its role in NK-cell mediated antitumor response to eliminate tumor cells was conceived long ago. In a study published in 2011, authors showed that the epigenetic drugs hydralazine, a DNA methylation inhibitor and valproic acid, an inhibitor that belong to class I histone deacetylases (HDACs) and regulator of DNA methylation and demethylation of histones (18) increased the expression of MICA and MICB NKG2D ligands on the target cells. It was via increasing the H3K4 methylation mark at the promoter region of MICA and MICB genes. The increase in expression of MICA and MICB led to an increase in NK cell-mediated cytotoxicity, leading to tumor growth suppression (19).

Since then, several studies have reported that epigenetic modification play an imminent role in regulating the expression of NKG2D ligand. Histone acetylation is a type of posttranslational modification regulated by histone acetyl transferases (HATs) that functions as acetyltransferases and aid in transferring the acetyl moiety of acetyl-CoA to lysine (K) residues on histone. In contrast, HDACs function as deacetylases and remove the acetyl moiety (20). Epigenetic modification involving acetylation is reversible (20). Previous studies as described below have demonstrated that histone acetylation regulates NKG2D ligand expression such as MICA, MICB, and ULBPs, which are critical for the activation of natural killer (NK) cells and immune surveillance against cancer cells. In a study published by Cho et al., authors found that treatment of lung cancer cells with a selective HDAC1/2 inhibitor FK228, also known as Romidepsin, led to the induction NKG2D ligands expression both at mRNA and protein level (21). This resulted in increased cytotoxicity of NCI-H23 cells to NK cells (21). Similar results were obtained when the expression of both HDAC1 or HDAC2 was inhibited, suggesting that suppressing HDAC1 and HDAC2 expression both genetically and pharmacologically leads to activation of NKG2D ligands and facilitate NK cell-mediated anti-tumor effects in lung cancer (21).

In another study published by Mormino et.al., authors demonstrated that histone deacetylase HDAC8 regulate the expression of NKG2D ligands. They further showed that pharmacological inhibition of HDAC8 using the small molecule inhibitor PCI-34051 led to the upregulation of ULBP1, H60A, and RAE1 NKG2D ligands in glioma cells by significantly increasing H3K4me3 levels, resulting in an increase in NK-mediated cytotoxicity (22). Similar observations were made in other cancer types where authors reported that treatment of Panc89 (a pancreatic carcinoma cell line) and PC-3 (a prostate carcinoma cell line) with Valproic acid (VPA), a histone deacetylase inhibitor, significantly enhanced the expression and/or release of the several NKG2D ligands such as ULBP-2, MICA, MICB (23).

Additionally, interesting results were obtained in non-small cell lung cancer (NSCLC) cell line NCI-H23 cells, where ionizing radiation and HDAC inhibitors (Apicidin, SAHA, or TSA) in combination synergistically increased both the expressions of NKG2D ligands and sensitivity of NSCLC cell line to NK cells-NK-92, enhancing tumor eardication (24). Moreover, in colon carcinoma and sarcoma cells, treatment with HDAC inhibitor Entinostat, a class I HDAC1 and HDAC3 inhibitor, led to increase in expression of NKG2D ligand MICA and MICB, enhancing cytotoxicity of NK cells against tumor cells (25). Thus, several studies have confirmed that histone acetylation/deacetylation plays a crucial role in regulating the expression of NKG2D ligand and NK cell mediated tumor clearance in multiple cancer types.

Apart from histone acetylation, histone methylation has also been shown to regulate the expression of NKG2D ligands. In a previous study by Bugide et al., it was demonstrated that Enhancer of zeste homolog 2 (EZH2), which functions as histone-lysine N-methyltransferase, serves as a transcriptional repressor of NKG2D ligands. Pharmacological or genetic inhibition of EZH2 led to an increase in the expression of NKG2D ligands and enhanced eradication of hepatocellular carcinoma (HCC) cell (16). Furthermore, Bugide et al. in another study showed that histone deacetylase 10 (HDAC10) promotes EZH2 recruitment to the chemokine (C-X-C motif) ligand 10 (CXCL10) promoter, resulting in its transcriptional repression. They further demonstrated that CXCL10 is required and sufficient to stimulate NK cell migration and this phenomenon is conserved in EZH2-dependent cancers besides HCC (17).

In a different study performed in acute myeloid leukemia (AML), screening was performed with 70 small molecular drugs in NB4 cell line, an acute promyelocytic leukemia cell line. This screening with small molecular inhibitor showed that lysine-specific demethylase 1 (LSD1) inhibitor tranylcypromine (2-PCPA) hydrochloride significantly up-regulated ULBP2/5/6 expression in the NB4 cells and increased sensitivity of NB4 cells to NK-dependent killing. LSD1 functions to demethylate mono- or di-methyl-lysine 4 or 9 of histone H3 (H3K4me1/me2 and H3K9me1/me2, respectively) by interacting with different proteins (26). This study also demonstrated significant reduction in tumor growth upon combination with human NK cells and LSD1 inhibition (27). These results highlight that methylation regulates NKG2D ligands expression, contributing to immune evasion in acute myeloid leukemia (AML).

Bromodomain and extra-terminal (BET) proteins serve as epigenetic readers of acetylated histones and are also been known to regulate the expression of NKG2D ligands. For example, previous studies have shown that inhibition of BET proteins by JQ1 and I-BET151 or selective BRD4-degrader proteolysis targeting chimera (PROTAC) (ARV-825) leads to an increase in the expression of NKG2D ligand MICA in multiple myeloma (MM) cell lines [RPMI-8226, U266, ARP-1, JJN3, SKO-007(J3)] isolated from MM patients and $CD138^{+}$ MM cells. Increased expression of NKG2D ligand MICA resulted in increased NK cell-mediated cytotoxicity (28). These studies collectively confirm that various epigenetic mechanisms regulate the expression of multiple NKG2D ligand in different cancer cell types, and modulating these mechanisms offers the possibility of enhancing NK-cell based therapy for cancer treatment.

Clinical trials with NK-cells for cancer therapy

Based on the potential of NK cells to eradicate cancer cells, several clinical trials are testing their effectiveness in cancer therapy. In this phase I clinical trial, the safety and efficacy of NK cells in combination with IgG1 antibodies were examined for the treatment of advanced colorectal or gastric cancers. Adoptive NK cell therapy was utilized alongside trastuzumab- or cetuximab-based chemotherapy for the treatment. After 3 days of administration of IgG1 antibody, patients were administered NK cells three times at triweekly intervals. It was observed that there were no severe adverse effects and the combination therapy was well tolerated. Among the six tested patients, four displayed stable disease (SD) while two showed progressive disease. Notably, three out of four patients with stable disease showed a positive response to the combination therapy, with an overall decrease in tumor size. These outcomes indicate the effectiveness of this combination therapy in treating advanced colorectal or gastric patients, who have been prior treated (29).

Another clinical trial was performed in non-small-cell lung cancer (NSCLC) patients with positive epidermal growth factor receptor (EGFR) mutation. The goal of this trial was to manage acquired resistance (advanced NSCLC) to gefitinib and also extend progression free survival (PFS) in the patient. Here, the effectiveness and safety of allogenic CD8 + CD56+ Natural Killer T (NKT) cell immunotherapy in combination with gefitinib for patients with advanced NSCLC with EGFR mutations was explored (30). The results of this trial showed that the treatment used in this study could effectively delay gefitinib resistance also and enhance anti-tumor immune response leading to better clinical outcome (31). Thus, the success of this trial provides the hope for testing NKT cell immunotherapy in context of other EGFR-tyrosine kinase inhibitors (TKIs) and various other types of tumors.

In a separate phase I/IIa clinical trial in patients with stage IV non-small-cell lung cancer, the safety and efficacy of natural killer (NK) cell therapy (SNK01), which were ex vivo activated and expanded were evaluated in combination with pembrolizumab. In this trial, 18 patients with advanced non-small cell lung cancer, who previously failed frontline platinum-based therapy were randomized to receive either pembrolizumab as monotherapy or pembrolizumab in combination with SNK01. The study observed that the objective response rate (ORR) and the 1-year survival rate was higher in patients who received NK combination therapy with pembrolizumab than those who received pembrolizumab as monotherapy (ORR, 41.7% vs. 0%; 1-year survival rate, 66.7% vs. 50.0%). Additionally, the median progression-free survival (PFS) was higher in the SNK01 and pembrolizumab combination group (6.2 months vs. 1.6 months, p=0.001). These results confirm that NK cell combination therapy can be safely used for the treatment of stage IV NSCLC patients who did not respond to platinum-based therapy with least toxicity (32). Based on the success of this trial, another follow-up 2-year study was conducted to determine the long-term effectiveness of the combination therapy. In this study, 20 patients with advanced NSCLC

who did not respond to prior frontline platinum-based therapy were included. Patients either received pembrolizumab alone in combination with low-dose (2×10^9cells/dose) or high-dose of SNK01 (4×10^9cells/dose), or just pembrolizumab alone as monotherapy. The results obtained were promising and showed that the 2-year survival rate was higher in the combination group compared to when pembrolizumab was used as monotherapy (58.3% versus 16.7%). They also found that although the median progression-free survival was significantly higher in patients who received pembrolizumab in combination with SNK01 than the ones who receives only pembrolizumab, overall survival, and progression-free survival did not differ between the patients who received low doses or high doses of NK cells (33).

In another trial (NCT03958097), the safety of PD-1 antibody in combination with autologous NK cells was tested for the treating non-small-cell lung cancer patients of stage IIIB/IIIC or IV who did not respond to the first-line platinum-based chemotherapy. In this research, 20 patients received both PD-1 antibody (sintilimab) and NK cells, with a median follow-up time of 22.6 months. The results showed that autologous NK in combination with sintilimab effectively promoted antitumor activity and displayed least toxicity. Thus, this trial suggested that NK cells in combination with sintilimab can be used for treating advanced, mutation-negative NSCLC patients who did not respond to the first-line treatment (34).

In another promising phase I clinical trial, fludarabine/cytarabine followed by 6 infusions of NK cells expanded from haploidentical donors was used to treat 12 patients (median age 60 years) with refractory AML (median 5 lines of prior therapy, median bone marrow blast count of 47%). In this trial, neither graft-versus-host disease (GVHD), nor any toxicity was observed in patients. Results from this study further showed that 7 out of 12 patients (58.3%) achieved response and complete remission (CR) with/without count recovery with 48 days as median time for the best response. The other 5 responding patients got haploidentical transplant from the same donor and were monitored for 52 months. The one-year overall survival (OS) for all 12 patients was observed to be 41.7%, with better outcome noted for patients who achieved a complete response with incomplete count recovery (57.14%), and for those patients who responded and underwent transplantation (60%). In conclusion, in this trial, significant response was observed in refractory AML patients with ex vivo expanded NK-cell administration without adverse effects (35).

Thus, the success of these clinical trials demonstrates that NK-cell based immunotherapies have the potential to serve as effective cancer treatment strategies either alone or in combination with other anti-cancer agents with minimal toxicity.

Future direction of NK cell therapy

Future directions in NK cell therapy research hold promise for advancing cancer treatment through personalized medicine approaches and novel combination therapies. Similar to CAR-T cells, chimeric antigen receptor (CAR) NK cells engineered to express receptors targeting specific antigens on cancer cells will be a significant progress in this direction. Further future research focusing on optimizing CAR constructs for enhanced specificity, persistence, and efficacy against various cancers can also provide significant benefit in area of cancer therapy. Moreover, tailoring NK cells through genetic editing techniques like CRISPR/Cas9 will offer new opportunities to enhance their targeting capabilities and improve immune recognition of cancer cells. Finally, developing methods to expand and activate NK cells from patients' own immune cells could enhance efficacy and reduce immune rejection in clinical settings.

Studies have also suggested that combination therapy, whereby combining NK cells with immune checkpoint inhibitors like pembrolizumab or nivolumab, could enhance anti-tumor immune responses. Additionally, conducting trials to explore the synergistic effects of NK cell therapy with cytokines (e.g., IL-2, IL-15) or other immune stimulants to boost NK cell activity and sustain anti-tumor responses will provide beneficial outcomes. Exploring epigenetic modulators to augment NK cell cytotoxicity by enhancing NKG2D ligand expression or reducing immune evasion mechanisms in tumors will be yet another way to enhance the efficacy of NK cell-based therapy. Thus, future trials are certainly needed to explore optimal dosing of the combination agents to achieve higher efficacy with minimum toxicity in patients.

In conclusion, future research directions aimed at advancing personalized medicine approaches and novel combination therapies will help in improving treatment outcomes and providing new therapeutic options for treating patients with various types of cancer.

Conclusion

In conclusion, epigenetic changes, by regulating gene expression, play an important role in cancer initiation, progression, and determining therapeutic responses. Moreover, epigenetic modifications play key role in regulating NKG2D ligands expression, influencing NK cell-mediated tumor cell eradication. By modulating epigenetic mechanisms, novel therapeutic strategies can be developed to enhance NK cell activity and improve cancer treatment outcomes. Current clinical trials exploring NK cell-based immunotherapy have shown encouraging results, demonstrating both safety and efficacy across various cancer types. Therefore, future treatments employing the combination of epigenetic modulators with NK cell-based immunotherapy will hold great promise and may discover new avenues for personalized and targeted therapeutic approaches. Continued research and clinical trials to advance personalized medicine approaches and novel combination therapies with NK cell holds will undoubtedly lead to further advancements in cancer therapy and improve patient outcomes.

Author contributions

RK: Writing – review & editing. RG: Writing – original draft, Writing – review & editing, Funding acquisition, Project administration.

Funding

The author(s) declare financial support was received for the research, authorship, and/or publication of this article. We would like to acknowledge the grants received from the National Institutes

of Health: R03CA292128 (RG), R03CA230815 (RG), R03CA248913 (RG), and R01CA233481 (RG).

Conflict of interest

The authors declare that the research was conducted in the absence of any commercial or financial relationships that could be construed as a potential conflict of interest.

Publisher's note

References

1. Hamilton JP. Epigenetics: principles and practice. *Dig Dis*. (2011) 29:130–5. doi: 10.1159/000323874

2. Yang J, Xu J, Wang W, Zhang B, Yu X, Shi S. Epigenetic regulation in the tumor microenvironment: molecular mechanisms and therapeutic targets. *Signal Transduct Target Ther*. (2023) 8:210. doi: 10.1038/s41392-023-01480-x

3. Janssen A, Colmenares SU, Karpen GH. Heterochromatin: guardian of the genome. *Annu Rev Cell Dev Biol*. (2018) 34:265–88. doi: 10.1146/annurev-cellbio-100617-062653

4. Fernandez A, O'leary C, O'byrne KJ, Burgess J, Richard DJ, Suraweera A. Epigenetic mechanisms in DNA double strand break repair: A clinical review. *Front Mol Biosci*. (2021) 8:685440. doi: 10.3389/fmolb.2021.685440

5. Wainwright EN, Scaffidi P. Epigenetics and cancer stem cells: unleashing, hijacking, and restricting cellular plasticity. *Trends Cancer*. (2017) 3:372–86. doi: 10.1016/j.trecan.2017.04.004

6. Cheng Y, He C, Wang M, Ma X, Mo F, Yang S, et al. Targeting epigenetic regulators for cancer therapy: mechanisms and advances in clinical trials. *Signal Transduct Target Ther*. (2019) 4:62. doi: 10.1038/s41392-019-0095-0

7. Vivier E, Rebuffet L, Narni-Mancinelli E, Cornen S, Igarashi RY, Fantin VR. Natural killer cell therapies. *Nature*. (2024) 626:727–36. doi: 10.1038/s41586-023-06945-1

8. Miyazato K, Hayakawa Y. Pharmacological targeting of natural killer cells for cancer immunotherapy. *Cancer Sci*. (2020) 111:1869–75. doi: 10.1111/cas.14418

9. Liu S, Galat V, Galat Y, Lee YKA, Wainwright D, Wu J. NK cell-based cancer immunotherapy: from basic biology to clinical development. *J Hematol Oncol*. (2021) 14:7. doi: 10.1186/s13045-020-01014-w

10. Khan M, Arooj S, Wang H. NK cell-based immune checkpoint inhibition. *Front Immunol*. (2020) 11:167. doi: 10.3389/fimmu.2020.00167

11. Mistry AR, O'Callaghan CA. Regulation of ligands for the activating receptor NKG2D. *Immunology*. (2007) 121:439–47. doi: 10.1111/j.1365-2567.2007.02652.x

12. Focaccetti C, Benvenuto M, Pighi C, Vitelli A, Napolitano F, Cotugno N, et al. DNAM-1-chimeric receptor-engineered NK cells, combined with Nutlin-3a, more effectively fight neuroblastoma cells in *vitro*: a proof-of-concept study. *Front Immunol*. (2022) 13:886319. doi: 10.3389/fimmu.2022.886319

13. Elliott JM, Yokoyama WM. Unifying concepts of MHC-dependent natural killer cell education. *Trends Immunol*. (2011) 32:364–72. doi: 10.1016/j.it.2011.06.001

14. Malhotra A, Shanker A. NK cells: immune cross-talk and therapeutic implications. *Immunotherapy*. (2011) 3:1143–66. doi: 10.2217/imt.11.102

15. Fernandez-Sanchez A, Baragano Raneros A, Carvajal Palao R, Sanz AB, Ortiz A, Ortega F, et al. DNA demethylation and histone H3K9 acetylation determine the active transcription of the NKG2D gene in human CD8+ T and NK cells. *Epigenetics*. (2013) 8:66–78. doi: 10.4161/epi.23115

16. Bugide S, Green MR, Wajapeyee N. Inhibition of Enhancer of zeste homolog 2 (EZH2) induces natural killer cell-mediated eradication of hepatocellular carcinoma cells. *Proc Natl Acad Sci U.S.A*. (2018) 115:E3509–18. doi: 10.1073/pnas.1802691115

17. Bugide S, Gupta R, Green MR, Wajapeyee N. EZH2 inhibits NK cell-mediated antitumor immunity by suppressing CXCL10 expression in an HDAC10-dependent manner. *Proc Natl Acad Sci U.S.A*. (2021) 118. doi: 10.1073/pnas.2102718118

18. Mello MLS. Sodium valproate-induced chromatin remodeling. *Front Cell Dev Biol*. (2021) 9:645518. doi: 10.3389/fcell.2021.645518

19. Chavez-Blanco A, De La Cruz-Hernandez E, Dominguez GI, Rodriguez-Cortez O, Alatorre B, Perez-Cardenas E, et al. Upregulation of NKG2D ligands and enhanced natural killer cell cytotoxicity by hydralazine and valproate. *Int J Oncol*. (2011) 39:1491–9. doi: 10.3892/ijo.2011.1144

20. Wapenaar H, Dekker FJ. Histone acetyltransferases: challenges in targeting bi-substrate enzymes. *Clin Epigenet*. (2016) 8:59. doi: 10.1186/s13148-016-0225-2

21. Cho H, Son WC, Lee YS, Youn EJ, Kang CD, Park YS, et al. Differential effects of histone deacetylases on the expression of NKG2D ligands and NK cell-mediated anticancer immunity in lung cancer cells. *Molecules*. (2021) 26. doi: 10.3390/molecules26133952

22. Mormino A, Cocozza G, Fontemaggi G, Valente S, Esposito V, Santoro A, et al. Histone-deacetylase 8 drives the immune response and the growth of glioma. *Glia*. (2021) 69:2682–98. doi: 10.1002/glia.24065

23. Bhat J, Dubin S, Dananberg A, Quabius ES, Fritsch J, Dowds CM, et al. Histone deacetylase inhibitor modulates NKG2D receptor expression and memory phenotype of human gamma/delta T cells upon interaction with tumor cells. *Front Immunol*. (2019) 10:569. doi: 10.3389/fimmu.2019.00569

24. Son CH, Keum JH, Yang K, Nam J, Kim MJ, Kim SH, et al. Synergistic enhancement of NK cell-mediated cytotoxicity by combination of histone deacetylase inhibitor and ionizing radiation. *Radiat Oncol*. (2014) 9:49. doi: 10.1186/1748-717X-9-49

25. Zhu S, Denman CJ, Cobanoglu ZS, Kiany S, Lau CC, Gottschalk SM, et al. The narrow-spectrum HDAC inhibitor entinostat enhances NKG2D expression without NK cell toxicity, leading to enhanced recognition of cancer cells. *Pharm Res*. (2015) 32:779–92. doi: 10.1007/s11095-013-1231-0

26. Majello B, Gorini F, Sacca CD, Amente S. Expanding the role of the histone lysine-specific demethylase LSD1 in cancer. *Cancers (Basel)*. (2019) 11. doi: 10.3390/cancers11030324

27. Liu M, Du M, Yu J, Qian Z, Gao Y, Pan W, et al. CEBPA mutants down-regulate AML cell susceptibility to NK-mediated lysis by disruption of the expression of NKG2D ligands, which can be restored by LSD1 inhibition. *Oncoimmunology*. (2022) 11:2016158. doi: 10.1080/2162402X.2021.2016158

28. Abruzzese MP, Bilotta MT, Fionda C, Zingoni A, Soriani A, Vulpis E, et al. Inhibition of bromodomain and extra-terminal (BET) proteins increases NKG2D ligand MICA expression and sensitivity to NK cell-mediated cytotoxicity in multiple myeloma cells: role of cMYC-IRF4-miR-125b interplay. *J Hematol Oncol*. (2016) 9:134. doi: 10.1186/s13045-016-0362-2

29. Ishikawa T, Okayama T, Sakamoto N, Ideno M, Oka K, Enoki T, et al. Phase I clinical trial of adoptive transfer of expanded natural killer cells in combination with IgG1 antibody in patients with gastric or colorectal cancer. *Int J Cancer*. (2018) 142:2599–609. doi: 10.1002/ijc.31285

30. Yu W, Ye F, Yuan X, Ma Y, Mao C, Li X, et al. A phase I/II clinical trial on the efficacy and safety of NKT cells combined with gefitinib for advanced EGFR-mutated non-small-cell lung cancer. *BMC Cancer*. (2021) 21:877. doi: 10.1186/s12885-021-08590-1

31. Yu W, Yuan X, Ye F, Mao C, Li J, Zhang M, et al. Role of allogeneic natural killer T cells in the treatment of a patient with gefitinib-sensitive lung adenocarcinoma. *Immunotherapy*. (2022) 14:1291–6. doi: 10.2217/imt-2022-0178

32. Kim EJ, Cho YH, Kim DH, Ko DH, Do EJ, Kim SY, et al. A phase I/IIa randomized trial evaluating the safety and efficacy of SNK01 plus pembrolizumab in patients with stage IV non-small cell lung cancer. *Cancer Res Treat*. (2022) 54:1005–16. doi: 10.4143/crt.2021.986

33. Park HJ, Kim YM, Jung JS, Ji W, Lee JC, Choi CM. Two-year efficacy of SNK01 plus pembrolizumab for non-small cell lung cancer: Expanded observations from a phase I/IIa randomized controlled trial. *Thorac Cancer*. (2022) 13:2050–6. doi: 10.1111/1759-7714.14523

34. Jia L, Chen N, Chen X, Niu C, Liu Z, Ma K, et al. Sintilimab plus autologous NK cells as second-line treatment for advanced non-small-cell lung cancer previous treated with platinum-containing chemotherapy. *Front Immunol*. (2022) 13:1074906. doi: 10.3389/fimmu.2022.1074906

35. Ciurea SO, Kongtim P, Srour S, Chen J, Soebbing D, Shpall E, et al. Results of a phase I trial with Haploidentical mbIL-21 ex vivo expanded NK cells for patients with multiply relapsed and refractory AML. *Am J Hematol*. (2024) 99:890–9. doi: 10.1002/ajh.27281

frontiers | Frontiers in Oncology

TYPE Systematic Review
PUBLISHED 07 August 2024
DOI 10.3389/fonc.2024.1361530

OPEN ACCESS

EDITED BY
Sam Hanash,
University of Texas MD Anderson Cancer Center, United States

REVIEWED BY
Shengshan Xu,
Jiangmen Central Hospital, China
Carmen Rubio,
Manuel Velasco Suárez National Institute of Neurology and Neurosurgery, Mexico

*CORRESPONDENCE
Yina Yu
yuyinayuyina@163.com

RECEIVED 05 February 2024
ACCEPTED 17 July 2024
PUBLISHED 07 August 2024

CITATION
Lv K, Du X, Chen C and Yu Y (2024) Research hotspots and trend of glioblastoma immunotherapy: a bibliometric and visual analysis. *Front. Oncol.* 14:1361530. doi: 10.3389/fonc.2024.1361530

Research hotspots and trend of glioblastoma immunotherapy: a bibliometric and visual analysis

Keren Lv[1], Xue Du[2], Chunbao Chen[3] and Yina Yu[1]*

[1]Department of Hematology, The First Affiliated Hospital of Zhejiang Chinese Medical University, Hangzhou, Zhejiang, China, [2]Yaan People's Hospital, Sichuan University West China Hospital Yaan Hospital, Yaan, Sichuan, China, [3]Chengdu Pidu District People's Hospital, the 3rd Affiliated Hospital of Chengdu Medical College, Chengdu, Sichuan, China

Background: Glioblastoma (GBM) is one of the common malignant tumors of the central nervous system (CNS), characterized by rapid proliferation, heterogeneity, aggressiveness, proneness to recurrence after surgery, and poor prognosis. There is increasing evidence that tumorigenesis is inextricably linked to immune escape, and immunotherapy is undoubtedly an important complement to clinical treatment options for GBM, and will be a focus and hot topic in GBM treatment research. The purpose of this study was to visualize and analyze the scientific results and research trends of immunotherapy for GBM.

Methods: Publications concerning immunotherapy for GBM were retrieved from the Web of Science Core Collection (WOScc) database. Bibliometric and visual analysis was performed mainly using CiteSpace and R software, and the Online Analysis Platform of Literature Metrology (https://bibliometric.com/app) for countries/regions, authors, journals, references and keywords related to publications in the field.

Results: Among totally 3491 publications retrieved in this field, 1613 publications were finally obtained according to the screening criteria, including 1007 articles (62.43%) and 606 reviews (37.57%). The number of publications increased year by year, with an average growth rate (AGR) of 17.41%. Such a number was the largest in the USA (717, 44.45%), followed by China (283, 17.55%), and the USA showed the strongest international collaboration. Among the research institutions, Duke Univ (94, 5.83%) was the largest publisher in the field, followed by Harvard Med Sch (70, 4.34%). In addition, the most prolific authors in this field were OHN H SAMPSON (51) and MICHAEL LIM (43), and the degree of collaboration (DC) between authors was 98.26%. Among the co-cited authors, STUPP R (805) was the most cited author, followed by REARDON DA (448). The journal with the most published publications was FRONTIERS IN IMMUNOLOGY (75), and the most cited journal in terms of co-citation was CLIN CANCER RES (1322), followed by CANCER RES (1230). The high-frequency keyword included glioblastoma (672) and immunotherapy (377). Cluster analysis was performed on the basis of keyword co-occurrence analysis, yielding 17 clusters, based on which the current research status and future trends in the field of immunotherapy for GBM were identified.

Conclusion: Immunotherapy is currently a novel treatment strategy for GBM that has attracted much attention. In the future, it is necessary to strengthen

cooperation and exchanges between countries and institutions towards relevant research to promote the development of this field. Immunotherapy is expected to be an important part of the future treatment strategy for GBM, and it has already become a hot spot of current research and will be the key focus of future research.

KEYWORDS

glioblastoma, immunotherapy, bibliometrics, CiteSpace, research hotspots

1 Introduction

Glioma is the most common primary intracranial malignant tumor arising in adults, and it is difficult to be cured by surgical resection alone. Even treated by surgical resection combined with radiotherapy and chemotherapy, some tumor patients still display a poor prognosis and a high recurrence rate (1). Among all types of gliomas, GBM exhibits the highest degree of malignancy, with a 5-year survival rate of only 5%. In addition, GBM is characterized by high cellular and molecular heterogeneity, and stronger proliferation and invasion abilities (2). The last decade has witnessed dramatic progress in immunotherapy in the treatment of many solid tumors. In particular, immune checkpoint inhibitors (ICIs) have achieved satisfactory results in the treatment of solid tumors such as melanoma (3) and non-small cell lung cancer (NSCLC) (4). ICI molecules such as cytotoxic T-lymphocyte antigen-4 (CTLA-4) and programmed death receptor-1 (PD-1) have been approved for the treatment of various types of cancers and unprecedentedly prolonged the survival of patients (5). In the past, immunosuppressive cells within the glioma tumor microenvironment (TME) were thought to prevent immunotherapy from functioning (6), and the blood-brain barrier (BBB), serving as a physical and biochemical barrier, prevented therapeutic agents from entering the intracranial region (7). In addition, the central nervous system (CNS) has generally been considered an “immunologically privileged” site, which limits the effectiveness of immunotherapy for GBM.

The BBB, an important communication interface between the brain and the rest of the body, has long been thought to play a role in neurological disorders. Girolamo F et al. (8) reported the abnormal functions of forebrain pericytes during angiogenesis and barrier genesis and loss of BBB integrity directly contributes to the development of a variety of diseases. Previous studies have demonstrated that metabolic overload and associated systemic hypo-inflammation directly compromise BBB integrity by increasing paracellular permeability and decreasing trans-endothelial electrical resistance (TEER) to impair BBB function (9), suggesting that the cerebral vascular system is also an important pathological target. McArthur S et al. (10) proposed that treatment with Annexin A1 (ANXA1), a major regulator of BBB integrity and function, could be an effective therapeutic strategy. Therefore, focusing on the role of ANXA1 in the vasculature of the CNS may facilitate an in-depth understanding and the development of new therapeutic options. P-glycoprotein (P-gp) is a 170-kDa transmembrane glycoprotein that acts as an efflux pump and confers multidrug resistance (MDR) in normal tissues and tumors, including neural tissues and brain tumors. Tumor perivascular astrocytes may dedifferentiate and restore progenitor-like P-gp activity to become MDR cells, contributing to the MDR profile of GBM vessels together with perivascular P-gp expressing glioma stem like cells (GSCs) (11). Moreover, multiple cellular sources in the GBM vasculature may be associated with P-gp-mediated chemoresistance and may be accountable for GBM treatment failure and tumor recurrence. In addition, microglia not only appear in and around brain tumors but also contribute significantly to the actual tumor mass (12), with evidence that the behavior of microglia is controlled by tumor cells, supporting their growth and infiltration. Recent data demonstrate that neurons synapse directly onto glioma cells and drive their proliferation and spread through glutamatergic action. Microglia, as CNS-resident myeloid cells, can regulate glioma growth, prune synapses and promote synapse formation (8). Errede M et al. (13) by analyzing the cellular origin of chemokine CCL2, a molecule involved in immune cell recruitment and BBB-microvascular leakage, showedan increase in microglia is the hallmark of encephalomyelitis (EAE) in the mouse neocortex, which is characterized by a high CCL2 expression level. Therefore, targeting molecules in the GBM microenvironment and the oncogenic activity of microglia can help manage and slow down the growth of refractory high-grade gliomas.In recent years, it has been found that the CNS can deliver antigens through various pathways such as lymphatic reflux and crossing the BBB, and recruit immune cells into brain tissues and tumors in the event of gliomas, indicating that gliomas have a physiological structural basis for immunotherapy (14). The meninges, the plasma membrane structures surrounding the CNS, and contain a wide reservoir of immune cells, and the meningeal lymphatics are a key pathway for cerebrospinal fluid (CSF) to enter the peripheral blood, where they provide immune surveillance of brain tissues (15, 16). The brain is connected to the peripheral immune system through the meningeal lymphatics (17), and this important finding makes

immunotherapy the most promising therapeutic strategy for GBM. Recently, the presence of lymph node-like structures, called tertiary lymphoid structures (TLS), has been confirmed in patients with gliomas, but not in healthy individuals (18). TLS contain all the components needed to support on-site lymphocyte activation, which implies that they may positively influence the anti-tumor immune response. In addition, it has been revealed that immunotherapy can regulate the formation of TLS in the brain, providing exciting opportunities to find new ways to regulate the anti-tumor immune response in gliomas. With a comprehensive delineation of the unique immunobiology of gliomas, immunotherapy for gliomas will be fundamentally reshaped.

At present, immunotherapy is the focus of numerous preclinical studies and clinical trials on GBM are focused on. ICIs include PD-1, PD-L1, and CTLA-4 inhibitors, and preclinical studies have shown their promise in the treatment of GBM (19). In a randomized, multi-institutional clinical trial, 35 patients with recurrent, surgically resectable GBM, patients who were randomized to receive neoadjuvant pembrolizumab followed by postoperative adjuvant pembrolizumab therapy had an extended median overall survival (OS) compared those who received postoperative adjuvant pembrolizumab therapy alone (14 months vs. 7.6 months), and OS also showed the same trend (20). This result indicates that neoadjuvant administration of PD-1 blockade enhances local and systemic antitumor immune responses and may represent a more effective treatment for this lethal brain tumor. In June 2020, the Food and Drug Administration (FDA) approved pembrolizumab for the pan-cancer treatment of patients with solid tumors including gliomas of the CNS, showing high tumor mutation burden (TMB-high), defined as ≥ 10 mutations per megabase (mut/mb) (21),. A phase I clinical trial on recurrent GBM (rGBM) confirmed that perioperative intravenous administration of ipilimumab (IPI, a CTLA-4 inhibitor) ± nivolumab (NIVO, a PD-1 inhibitor) in rGBM was safe, and exploratory findings merit further investigation of immunotherapy for GBM (22). Rindopepimut (also known as CDX-110), a vaccine targeting the epidermal growth factor receptor (EGFR) deletion mutation EGFRvIII, has received drug approval from the US FDA for the breakthrough treatment of EGFRvIII-positive gliomas in adult patients (23). In an open-label, first-in-human trial evaluating the safety and therapeutic potential of cytomegalovirus-specific (CMV-specific) adoptive cellular therapy (ACT) in the adjuvant treatment of patients with primary GBM, the data obtained suggest that CMV-specific ACT can be a safe adjuvant therapy for primary GBM and, if performed before recurrence, this therapy may improve OS of GBM patients (24). Intratumoral infusion of nonpathogenic polio-rhinovirus chimera (PVSRIPO) in patients with rGBMdemonstrated no potential neurotoxicity. Patients receiving PVSRIPO immunotherapy had higher survival rates at 24 and 36 months than historical controls (25). Although some small-scale studies have reported that glioma patients can benefit from immunotherapy to varying degrees, there remain challenges requiring more in-depth studies and clinical trials. The rapidly developing immunomics, genomics, sequencing technologies, and ICIs have created new opportunities for immunotherapy, one of the important adjuvant therapies for gliomas. Meanwhile, the evolving nanotechnology (26) enable the targeting of tumor sites across the BBB, which may also bring new possibilities for immunotherapy for gliomas.

Bibliometrics is the discipline that applies mathematical and statistical methods to the study of books and other communication media (27), allowing for the qualitative and quantitative evaluation of trends in literature research. Bibliometric methods and tools can be used to analyze a larger volume of literature data from a more macroscopic perspective in order to accurately grasp the development trend and research hotspots in a field and provide reference for the research of researchers in related fields. This study uses bibliometric tools to measure and visualize the publications in this field in the last decade in order to understand the current status and trends of research in this field and to provide a scientific reference for the researchers working on immunotherapy for GBM.

2 Materials and methods

2.1 Data source

The Web of Science Core Collection (WOScc) online database is an important database for global access to scholarly journals and considered to be the best database for bibliometric analysis (28). In July 2022, literature related to immunotherapy for GBM was searched on WOScc, with the time span from 2012 to July 2022. The search strategy was: TS = (glioblastoma* OR "glioblastoma multiform*" OR " malignant glioma" OR "brain cancer" OR gliosarcoma OR spongioblastoma) AND TS = (Immunotherapy OR Immunotherapies OR immunotherapeutic). Literature inclusion criteria: (1) literature with immunotherapy for GBM as the research topic; (2) articles and reviews; (3) literature published in English. Literature exclusion criteria: (1) Literature irrelevant to immunotherapy for GBM; (2) conference abstracts, news, case studies, bioinformatic analysis without experimental validation, etc.; (3) literature that was not available in full-text format. To ensure the quality of the search, the literature obtained was evaluated by two reviewers, and any disagreements were resolved through discussion until consensus was reached. Flowchart of the literature selection process is shown in Figure 1.

2.2 Analysis method

Bibliometrics analysis and visualization of literature in related fields were performed primarily through CiteSpace (version 5.8.R3) and R (version 4.1.3) software, as well as the online analysis platform of literature metrology (https://bibliometric.com/app), using Microsoft Excel 2019 for data management. CiteSpace software, developed by Prof. Chaomei Chen as a literature visualization tool, was designed to mine literature data and visualize the evolution of a knowledge domain in the form of a map (29). Betweenness centrality is an important parameter in CiteSpace. In general, centrality ≥ 0.1 is considered an important node, and CiteSpace will also mark it with a purple circle. The

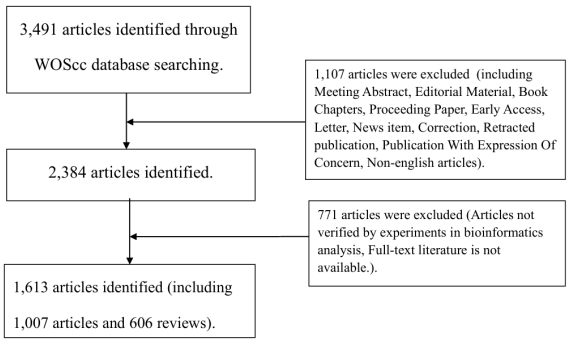

FIGURE 1
Flowchart of the literature selection process.

"bibliometrix" package in R software was used to visualize and analyze journals. Bibliographic data are exported from the WOS database in plain the text format, with full records and cited refercnces, 1,000 records at a time, and saved in a folder. Import the file into CiteSpace or R software through the "File"->"Import" menu to analyse and process the data and output the visualisation maps. The online analysis platform of literature metrology was developed by Chinese scholars for the integral literature analysis, partnership analysis, subject and journal analysis, keyword analysis, and citation network analysis. Moreover, the bibliometric online analysis platform was adopted to analyze country/region collaborations.

2.3 Statistical analysis

Statistical data were processed using SPSS (IBM SPSS Statistics 27). $p<0.05$ indicated a statistically significant difference.

3 Results

3.1 Publishing trend

A total of 3491 publications concerning immunotherapy for GBM published from 2012 to July 2022 were retrieved from WOScc, and 1613 articles (62.43%) and 606 reviews (37.57%) were finally filtered based on the set search criteria. Figure 2 shows the annual publication volume from 2012 to July 2022. The number of publications was almost stable from 2012 to 2015, with a steady increase from 2016 to 2021. The annual publications exceeded 200 in 2019 and 335 in 2020, and the average growth rate (AGR) was 17.41% from 2012 to 2021. Furthermore, the compound annual growth rate (CAGR) of publications (30) gradually increased from 35.01% in 2013 to 40.07% in 2016, before decreasing to 33.58% in 2021 (Supplementary Table S1; Supplementary Figure S1A). This indicates that the CAGR is basically on a downward trend, although the annual production is increasing year by year. As illustrated in Supplementary Table S2; Supplementary Figure S1B, the relative growth rate (RGR) decreased from 2013 (60.04%) to 2021 (26.71%). A direct equivalence relation existed between RGR and doubling time (DT) (30), and the DT increased from 1.15 in 2013 to 2.59 in 2021 (Supplementary Table S2; Supplementary Figure S1C). In addition, the correlation between publications and citations was determined by Pearson correlation analysis, and a p-value < 0.05 was considered as a significant correlation. The results of this analysis showed a high positive correlation between publications and citations ($r=0.973$, $p<0.001$).

3.2 Countries/regions and institutions

A total of 1613 publications from 1868 institutions in 54 different countries/regions were retrieved based on the search

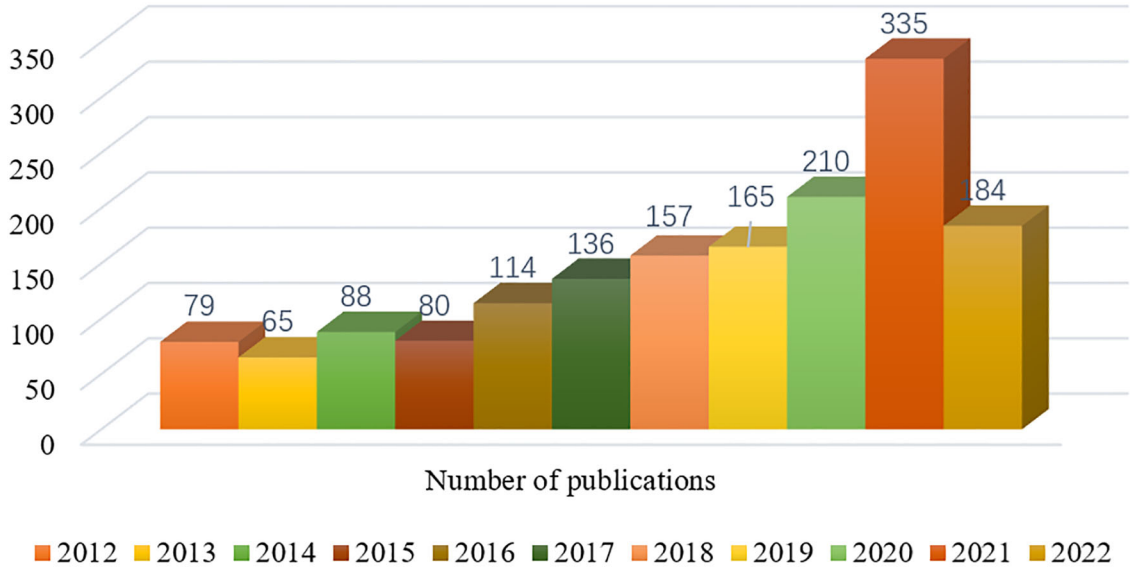

FIGURE 2
Annual number of publications in the relevant literature from 2012 to July 2022.

criteria. The number of publications was the largest in USA (717, 44.45%), followed by China (283, 17.55%), which were much higher than other countries/regions (Supplementary Table S3). The intensity of international cooperation of countries was analyzed using the "bibliometrix" package of the R software. Multiple country publications (MCP) refer to publications with at least one co-author from a different country, while single country publications (SCP) refer to publications with co-authors from a single country. The largest number of MCP was from USA (146), with an MCP-Ratio of 20.36%, followed by China (39) with an MCP-Ratio of 13.49% (Supplementary Table S3; Figure 3A), indicating that USA has the highest intensity of international cooperation, followed by China. Further, online analysis platform of literature metrology was used to visualize the inter-country cooperation. Figure 3B shows the inter-country cooperation network. It was found that the USA cooperated most closely with other countries, and the countries with the most cooperation included China, South Korea and Switzerland, followed by Germany.

The research institution with the most publications was Duke Univ (94 articles, 5.83%), followed by Harvard Med Sch (70 articles, 4.34%). Among these institutions, Duke Univ and Univ Calif Los Angeles showed the highest centrality (0.13), followed by Univ Texas MD Anderson Canc Ctr and German Canc Res Ctr, with the centrality of 0.11 (Table 1). In the CiteSpace visualization atlas, each circle represents an institution, the size of the circle indicates the number of publications of the institution, the connecting lines between the circles indicate the cooperation between institutions, the nodes with high centrality are shown as purple rings, and the thickness of the purple rings depicts the value of centrality in size (Figure 3C).

3.3 Authors and co-cited authors

A total of 8503 researchers participated in the publication of the relevant literature. JOHN H SAMPSON (51) and MICHAEL LIM (43) published the largest number of publications, followed by DAVID A REARDON (29), DUANE A MITCHELL (27) and HIDEHO OKADA (25). The top 10 authors had the highest centrality in MICHAEL LIM (0.21), followed by AMY B HEIMBERGER (0.18) (Supplementary Table S4). The degree of cooperation (DC) between authors was 98.26% (30). Figure 4A shows the visual analysis map of author cooperation network, where each circle node represents an author (the larger the node, the more the publications), the line between the nodes represents

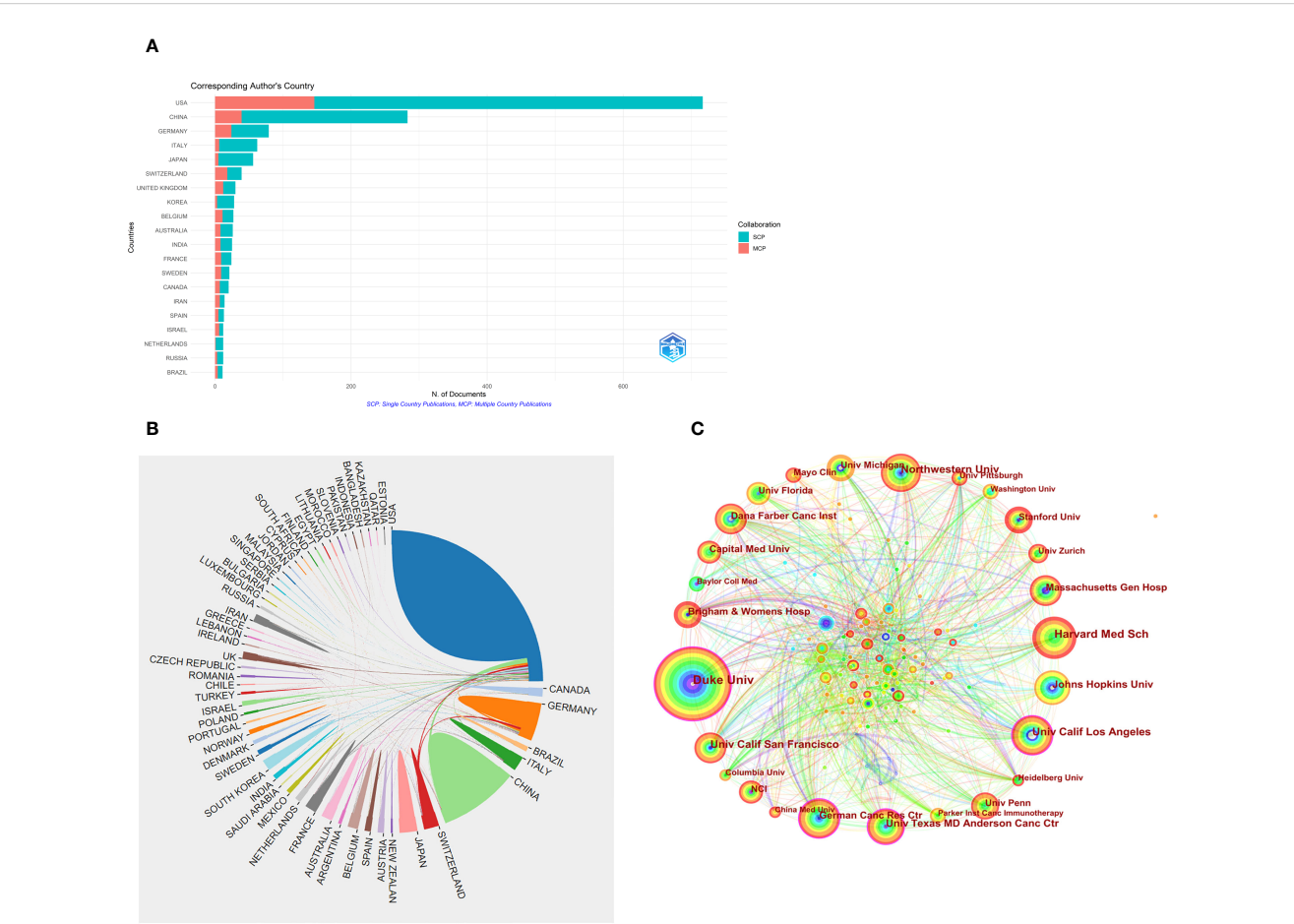

FIGURE 3
(A) International collaboration intensity of a country with relevant publications. **(B)** Inter-country cooperation relations for related publications. **(C)** Cooperation mapping between related publication institutions.

TABLE 1 Top 10 institutions for related publications.

Rank	Count	Centrality	Institutions
1	94	0.13	Duke Univ
2	70	0.08	Harvard Med Sch
3	53	0.04	Northwestern Univ
4	53	0.13	Univ Calif Los Angeles
5	50	0.09	Univ Calif San Francisco
6	45	0.06	Johns Hopkins Univ
7	42	0.11	Univ Texas MD Anderson Canc Ctr
8	40	0.06	Dana Farber Canc Inst
9	39	0.11	German Canc Res Ctr
10	38	0.03	Massachusetts Gen Hosp

the connection between authors (the thicker the line, the closer the cooperation), and the purple circle outside the node marks the higher centrality.

The co-citation of documents was previously used as a measure of the relatedness between documents. Later, co-citation was introduced to the author dimension, and the method of author co-citation analysis (ACA) was developed, by which a co-citation relationship constituted by two or more authors cited by one or more publications at the same time can be analyzed (31). Among the co-cited authors, STUPP R (805) was the most cited author, followed by REARDON DA (448), SAMPSON JH (432). FECCI PE (0.1) had the highest centrality among the top ten co-cited authors (Supplementary Table S4). A clinical study led by Professor Stupp demonstrated that temozolomide (TMZ) combined with radiotherapy prolonged the survival of adult GBM patients, and the Stupp protocol of simultaneous radiotherapy for gliomas, named after the professor, was then widely used in the clinic to date (32). Figure 4B shows a visual network map of the relationship between co-cited authors.

3.4 Journals and co-cited journals

The "bibliometrix" package in R software was used to visualize and analyze the source journals of the publications. FRONTIERS IN IMMUNOLOGY was the journal with the largest number of publications (75), followed by JOURNAL OF NEURO-ONCOLOGY (58). As shown in Supplementary Figure S2A, 7 journals had more than 50 publications. Among the top 10 academic journals, CLINICAL CANCER RESEARCH (13.801) displayed the highest impact factor (IF) (Table 2). Among the 826 co-cited journals, the most cited journal was CLIN CANCER RES (1322), followed by CANCER RES (1230) (Table 3). CANCER RES had the highest centrality (0.2), indicating its high influence in this research field. Journal co-citation reflects the correlation between various journals and disciplines. Figure 5A shows the CiteSpace visualization map of co-cited journals, where the size of the circle represents the frequency of co-citation, and the purple circle indicates the higher centrality.

The dual-map overlay of journals displays information about the distribution, citation trajectory, and shift of gravity of publications across disciplines (33). The left side shows the distribution of citing journals, while the right side displays the distribution of cited journals. In Figure 5B, the colored paths indicate the cited relationships. Among them, the yellow paths indicate that literature published in molecular/biology/immunology journals is frequently cited by molecular/biology/genetics journals, and green paths indicate that literature published in molecular/medical/clinical journals is frequently cited in molecular/biological/genetics journals.

3.5 Co-cited references and citation burst analysis

Table 4 lists the top 10 co-cited references out of 983 co-cited references. Figure 6 shows a visualization of the co-cited references. O'Rourke DM et al. (34) published the article "A single dose of peripherally infused EGFRvIII-directed CAR T cells mediates antigen loss and induces adaptive resistance in patients with

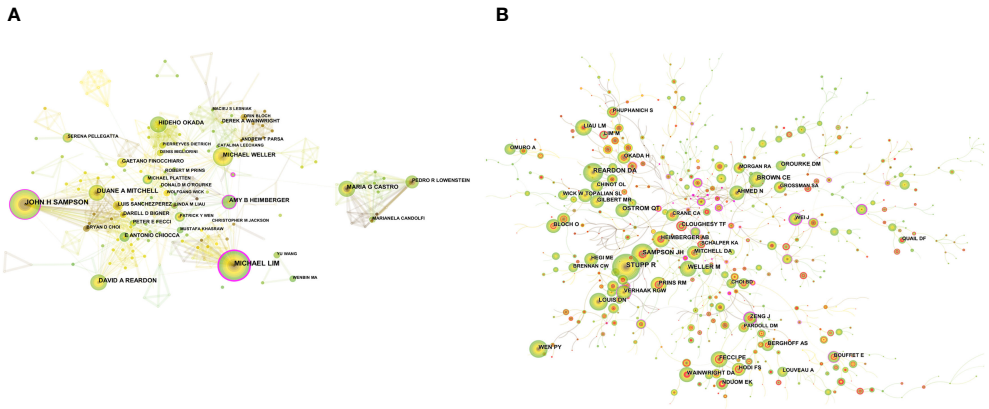

FIGURE 4
(A) CiteSpace visualization maps of the authors of related publications. **(B)** CiteSpace visualization maps of co-cited authors of related publications.

TABLE 2 Top 10 source journals for related publications.

Rank	Count	Sources Journal	IF 2022	JCR
1	75	FRONTIERS IN IMMUNOLOGY	8.786	Q1
2	58	JOURNAL OF NEURO-ONCOLOGY	4.506	Q2
3	56	CLINICAL CANCER RESEARCH	13.801	Q1
4	56	FRONTIERS IN ONCOLOGY	5.738	Q2
5	56	NEURO-ONCOLOGY	13.029	Q1
6	55	CANCERS	6.575	Q1
7	50	ONCOIMMUNOLOGY	7.723	Q1
8	37	CANCER IMMUNOLOGY IMMUNOTHERAPY	6.63	Q1
9	33	INTERNATIONAL JOURNAL OF MOLECULAR SCIENCES	6.208	Q1
10	27	JOURNAL FOR IMMUNOTHERAPY OF CANCER	12.47	Q1

recurrent glioblastoma", which was the most frequently cited article (203), reporting a first-in-human study of intravenous delivery of a single dose of autologous T cells redirected to the EGFRvIII mutation by a chimeric antigen receptor (CAR). The results revealed that the treatment for the first 10 patients with GBM showed feasibility and safety. In addition, ''Regression of Glioblastoma after Chimeric Antigen Receptor T-Cell Therapy", the study of Brown CE et al. (35) evaluated the role of intracranial CAR T-cell therapy targeting interleukin-13 receptor alpha 2 (IL13Rα2) in patients with malignant gliomas. This study provides initial evidence for the safety and antitumor activity of CAR T-cell immunotherapy in patients with malignant brain tumors. Moreover, the titles of the top 10 co-cited references, demonstrated that the corresponding research involved CAR T-Cell Therapy, neoadjuvant immunotherapy, randomized clinical trials, immunotherapy for rGBM, and ICIs.

Citation burst analysis identifies literature that has been of interest to researchers in related fields over time. According to the strongest citation burst (Supplementary Figure S3), the first citation burst started in 2012, with a citation burst strength of 16.99-40.52 for the first 25 references. Among them, the reference with the strongest citation burst was published by Sampson JH et al. (36) in the journal "J Clin Oncol". This phase II, multicenter, prospective trial was conducted to assess the immunogenicity of an EGFRvIII-targeted peptide vaccine and to estimate progression-free survival (PFS) from vaccination and histologic diagnosis in patients newly diagnosed with GBM who expressed EGFRvIII. The findings of this trial warrant investigation in a phase III randomized trial. The two references with the citation burst from 2020 to date are both studies on neoadjuvant immunotherapy for gliomas (20, 37).

3.6 Keyword co-occurrence clustering and time zone analysis

Keywords are the subject of research content, and the co-occurrence analysis of keywords can summarize the research hotspots in a specific field. Supplementary Table S5 shows the top

TABLE 3 Top 10 co-cited journals of related publications.

Rank	Count	Centrality	Co-cited Journals	IF2022	JCR
1	1322	0.05	CLIN CANCER RES	13.801	Q1
2	1230	0.2	CANCER RES	13.312	Q1
3	1216	0	NEURO-ONCOLOGY	13.029	Q1
4	1148	0	NEW ENGL J MED	176.079	Q1
5	995	0.1	NATURE	69.504	Q1
6	960	0.09	J CLIN ONCOL	50.717	Q1
7	949	0.08	J NEURO-ONCOL	4.506	Q2
8	934	0.08	P NATL ACAD SCI USA	12.779	Q1
9	876	0	NAT MED	87.241	Q1
10	838	0	PLOS ONE	3.752	Q2

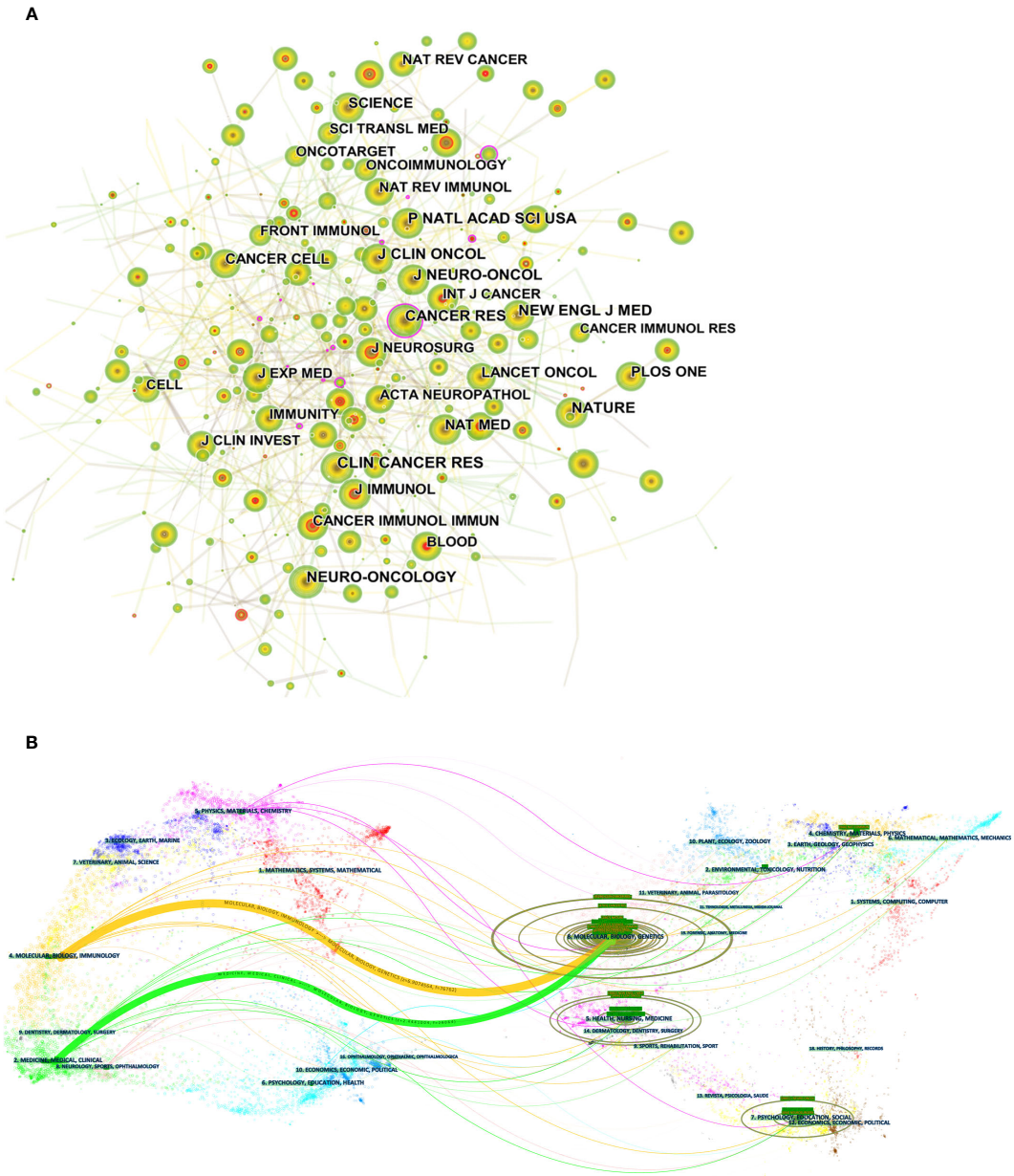

FIGURE 5
(A) CiteSpace visualization maps of co-cited journals of related publications. **(B)** The dual-map overlay of journals of related publications.

10 keywords that emerged frequently in studies related to immunotherapy for GBM, including glioblastoma (672), immunotherapy (377), expression (322), temozolomide (273), cancer (261), T cell (212), survival (178), glioma (173), central nervous system (167), and regulatory T cell (152), indicating that they are the current research hotspots related to immunotherapy for GBM. In the visualization map of keyword co-occurrence, there are 461 nodes and 775 lines (Figure 7). Each node corresponded to a keyword, and larger nodes indicated higher frequency. Besides, the number of links between nodes and distance between nodes reflected the tightness between keywords. Further clustering analysis of keywords based on keyword co-occurrence analysis reflected the hot research directions in this field. Supplementary Figure S4A shows the visualization map of the clustering of keywords, mainly including regulatory T cell, macrophage, peptide vaccination, PD-1, CD8(+), chimeric antigen receptor, innate immunity, phase II trial, tumor microenvironment, tumor heterogeneity, immunotherapy, IDH mutation, glioma, natural killer cell, survival, and resistance 17 clusters. Furthermore, keyword time zone map analysis was conducted to reveal the keywords as time zones according to the time when the keywords first appeared, further showing the time zone evolution of the keywords (Supplementary Figure S4B).

Keyword burst analysis reveals the phase and duration of research hotspots in a field. Herein, the keyword burst map showed the burst strength of the top 25 keywords

TABLE 4 Top 10 co-cited references of related publications.

Rank	Count	Centrality	Year	Co-Cited References
1	203	0.07	2017	A single dose of peripherally infused EGFRvIII-directed CAR T cells mediates antigen loss and induces adaptive resistance in patients with recurrent glioblastoma
2	200	0	2016	Regression of Glioblastoma after Chimeric Antigen Receptor T-Cell Therapy
3	186	0	2017	Rindopepimut with temozolomide for patients with newly diagnosed, EGFRvIII-expressing glioblastoma (ACT IV): a randomised, double-blind, international phase 3 trial
4	180	0.05	2019	Neoadjuvant anti-PD-1 immunotherapy promotes a survival benefit with intratumoral and systemic immune responses in recurrent glioblastoma
5	153	0	2016	The 2016 World Health Organization Classification of Tumors of the Central Nervous System: a summary
6	152	0.01	2018	Current state of immunotherapy for glioblastoma
7	143	0.06	2020	Effect of Nivolumab vs Bevacizumab in Patients With Recurrent Glioblastoma The CheckMate 143 Phase 3 Randomized Clinical Trial
8	129	0.01	2016	Immune Checkpoint Inhibition for Hypermutant Glioblastoma Multiforme Resulting From Germline Biallelic Mismatch Repair Deficiency
9	124	0.15	2017	HER2-Specific Chimeric Antigen Receptor-Modified Virus-Specific T Cells for Progressive Glioblastoma A Phase 1 Dose-Escalation Trial
10	124	0.05	2019	Neoadjuvant nivolumab modifies the tumor immune microenvironment in resectable glioblastoma

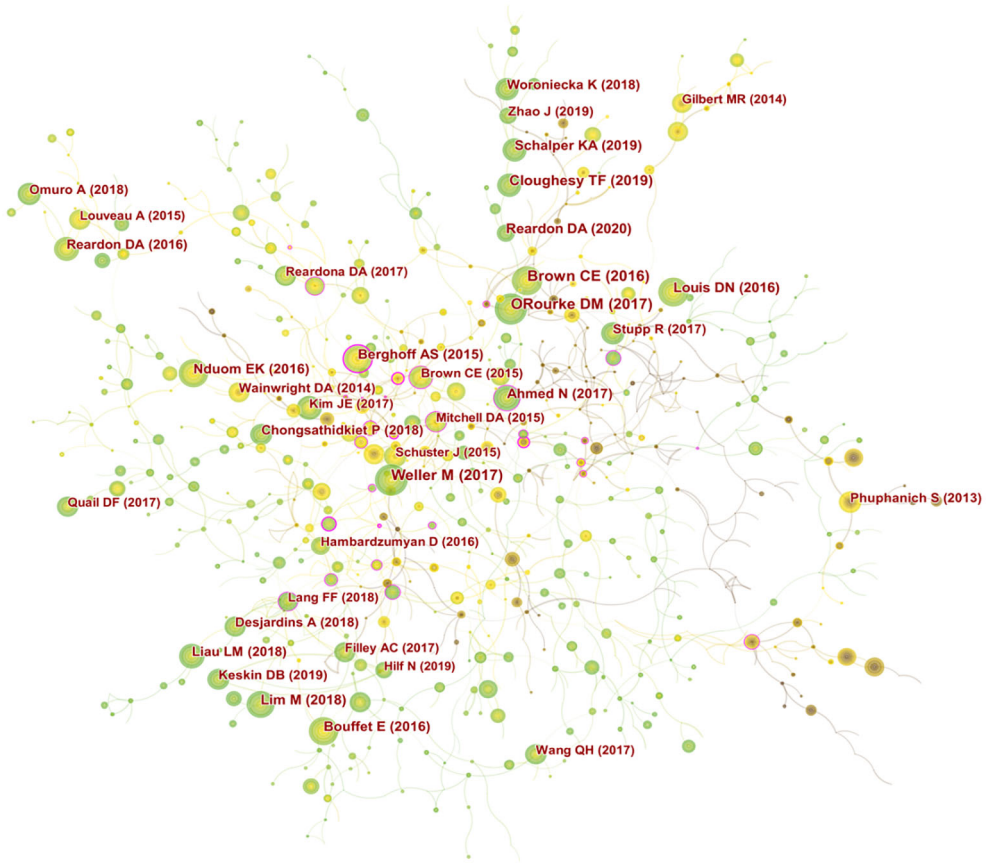

FIGURE 6
Visualization mapping of co-cited references of related publications.

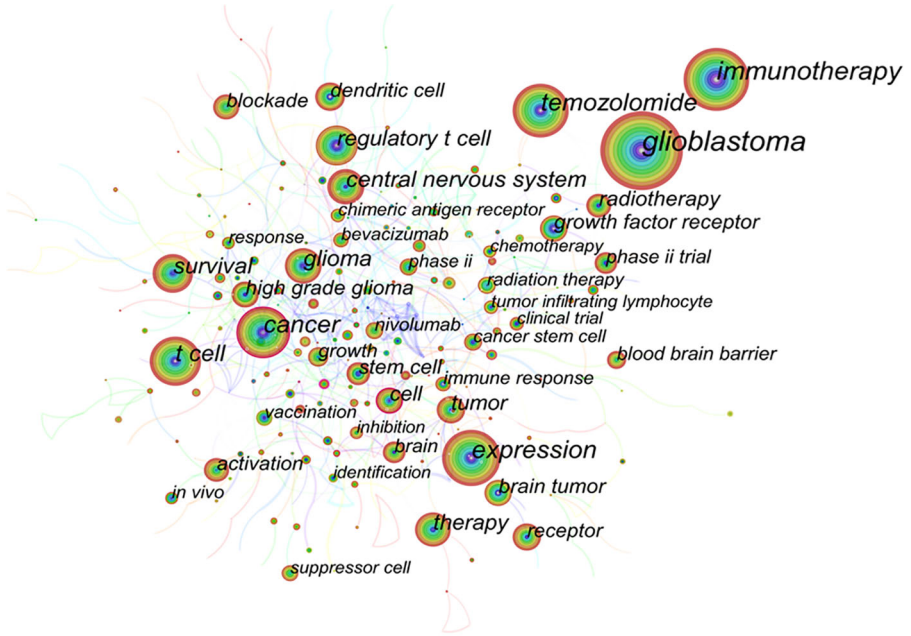

FIGURE 7
Visualization map of keyword co-occurrence for related publications.

(Supplementary Figure S4C), where the blue line indicated the time line, and the red part of the blue time line indicated the burst duration. Among the 25 keywords, nivolumab (6.76) had the highest burst strength, followed by recurrent glioma (6.19); antitumor immunity was the keyword with the longest burst duration; double blind and resistance were the keywords with the burst from 2020 to date.

4 Discussion

4.1 General information

Trends in publications indicate the dynamics of research in a field. Here, Figure 2 shows that the number of GBM immunotherapy-related publications is on the rise, with an AGR of 17.41% from 2012 to 2021. The number of publications by countries/regions and research institutions provided an objective indication of the scientific level and influence of the relevant research field. The largest number of publications was from USA (717, 44.45%), followed by China (283, 17.55%), indicating that USA and China, the main scientific exporters in this research field, have contributed significantly to the development of the field. The analysis of the intensity of international cooperation and partnership networks of countries revealed that USA cooperated most closely with other countries, while there was less cooperation between other research countries. Therefore, it is necessary to strengthen the research cooperation between countries and enhance international exchange in future research to promote the development of the field. Among the 8503 researchers, JOHN H SAMPSON published the most papers (51), followed by MICHAEL LIM (43). Among the top 10 authors, MICHAEL LIM had the highest centrality (0.21), followed by AMY B HEIMBERGER (0.18), which demonstrated their great contribution to the development of the field. Most of Sampson JH's publications were reviews or clinical trial studies on immunotherapy for gliomas. A snapshot of the current GBM clinical trial landscape is provided in a review that offers valuable suggestions for optimizing clinical trial protocols for GBM (38). STUPP R (805) was the most cited author, and the protocol of simultaneous radiotherapy for gliomas named after Stupp is widely used in clinical practice today (32).

The IF of journals is an important indicator to evaluate the academic influence of journals. The largest number of publications appeared in FRONTIERS IN IMMUNOLOGY (75), followed by JOURNAL OF NEURO-ONCOLOGY (58), and among the top 10 academic journals, CLINICAL CANCER RESEARCH had the highest IF (13.801) (Table 2), showing that these journals have a certain influence in immunotherapy for GBM. A dual-map overlay of journals shows that literature published in molecular/biology/immunology journals is frequently cited in molecular/biology/genetics journals. The reference co-citation analysis identifies important publications that form part of the research clustering themes in related fields. According to the top 10 co-cited references, the main research directions in the field included CAR T-Cell Therapy, neoadjuvant immunotherapy, randomized clinical trials, immunotherapy for rGBM, and ICIs. The reference with the highest citation burst strength was reported by Sampson JH et al. (36), which was a phase II, multicenter, prospective trial conducted to assess the immunogenicity of an EGFRvIII-targeted peptide vaccine and to estimate progression-free survival (PFS) from vaccination and histologic diagnosis in patients newly diagnosed with GBM who expressed EGFRvIII. The two references with the citation burst to date are studies on neoadjuvant immunotherapy for gliomas.

4.2 Research hotspots

Keywords represent the content of the literature, and the analysis of the frequency of keywords directly reflects the research hotspots and development trends in a certain subject field. The top 10 high-frequency keywords from publications related to immunotherapy for GBM included glioblastoma (672), immunotherapy (377), expression (322), temozolomide (273), cancer (261), T cell (212), survival (178), glioma (173), central nervous system (167), and regulatory T cell (152). Cluster analysis was performed based on keyword co-occurrence analysis, and 17 clusters were finally established, mainly including regulatory T cell, macrophage, peptide vaccination, PD-1, CD8(+), chimeric antigen receptor, innate immunity, phase II trial, tumor microenvironment, tumor heterogeneity, immunotherapy, IDH mutation, glioma, natural killer cell, survival, and resistance. This analysis identified the current research hotspots and possible future trends in immunotherapy for GBM. The main contents are as follows:

4.2.1 Possibility of immunotherapy for GBM

Immunotherapy is treatment that uses a patient's immune system fight malignant tumors. In 1891, William B. Coley, a bone sarcoma surgeon, carried out the study of immunotherapy for the treatment of malignant tumors for the first time. Coley injected streptococcal organisms into a cancer patient to cause erysipelas and stimulate the immune system. The patient's tumor disappeared, presumably because of an attack by the immune system. Since then, Coley began the lifelong study of immunotherapy, later making him known as the "Father of Immunotherapy" (39). However, the CNS had long been regarded as an immune privileged system for many years, referring to the lack of specialized lymphatic channels in the brain. The concept of immune privilege was based on the original experimental data reported by Peter Medawar 50 years ago, which showed that foreign cells implanted in rodent brains were successfully transplanted, whereas the same cells were eliminated by the host immune system when placed in peripheral tissues (40). Until 2015, Louveau et al. (17) found functional lymphatic vessels within the dural sinus in their search for channels for T cells to enter and exit the meninges. These structures show all the molecular characteristics of lymphatic endothelial cells. They are capable of carrying both fluid and immune cells from the CSF, and connecting deep cervical lymph nodes. This finding suggests that the current dogma on brain tolerance and immune privilege is being revisited, and casts new light to the treatment of gliomas. Although the brain is an immunologically privileged site, the immune microenvironment offers the possibility of implementing immunotherapy for brain tumors. TLS are ectopic lymphoid formations arising in inflamed, infected, or tumoral tissues. They exhibit all the characteristics of structures in the lymph nodes (LN) associated with the generation of an adaptive immune response, including a T cell zone with mature dendritic cells (DC), a germinal center with follicular dendritic cells (FDC) and proliferating B cells (41). In tumors, TLS is thought to provide an alternative to tumor-draining lymph nodes as a site for antigen expression and activation of nascent T cells. Recent studies have demonstrated that the immunostimulatory agonistic CD40 antibody (αCD40) induces the formation of TLS near meningeal tissues in preclinical glioma models. Studies have revealed that the TLS is present in human gliomas and is associated with an increasing number of intratumoral T cells in GBM, suggesting an association between TLS and the regulation of immune responses in glioma patients (18). TLS in the brain can be manipulated therapeutically, probably triggering or suppressing immune responses. As immunotherapy faces many difficulties and challenges, current research continues to explore the immune basis for effective treatment of gliomas, which provides a strong basis for the development of novel therapeutic strategies in the future.

4.2.2 The unique immune environment of GBM

Over the past decade, immunotherapy has dramatically changed the clinical outcome of tumors. However, this promising immunotherapy has encountered serious challenges when applied in the treatment of gliomas, mainly due to the presence of the BBB and the immunosuppressive character of the TME. The BBB serves as an important protective barrier for the brain, controlling the exchange of substances between the blood and the CNS, and maintaining homeostasis within the CNS (42). Meanwhile, the BBB also provides a physical and biochemical barrier for drugs to enter the brain. The tight junctions and adhesions between the endothelial cells of the brain capillaries prevent intercellular diffusion, and molecules from the blood can only enter the brain through the luminal and plasma membranes of the endothelial cells (43). This physical barrier obviously limits the efficiency of intracranial antitumor drug delivery and intra-tumor aggregation. Numerous studies have been conducted to develop novel strategies for delivering therapeutics across the BBB, including focused ultrasound (FUS) (44) and nanotherapeutic drug delivery systems (NDDS) (45). Therefore, priorities in future research should be put on the immune access of the CNS –BBB and new ways to enhance the delivery efficiency and intra-tumor aggregation of immunotherapeutic drugs and to improve the effectiveness of GBM immunotherapy.

With the negative results reported in the CheckMate 143 trial in nivolumab-treated patients with first recurrence of GBM (46), many observers have been convinced that GBM is an immunologically typical "cold tumor", characterized by low T-cell infiltration. To investigate the immunobiology of GBM in the clinical setting, Hao C et al. (47) found that immunohistochemistry in GBM showed sparse T lymphocyte infiltrates and abundant microglia. This phenomenon suggests an "immunosuppressed state" in GBM and may be the reason for the therapeutic failure of immunotherapy in such tumors. The immunosuppressive properties of the GBM TME significantly inhibits T-cell infiltration and activation, and such a unique microenvironment stimulates tumor cell growth and invasion. On the one hand, immunosuppressive factors, such as PD-1 and indoleamine 2,3-dioxygenase (IDO), are highly expressed in glioma cells, which limit antigen presentation. Gliomas express immunosuppressive ligands on the cell surface, including the co-stimulatory molecule B7-homolog 1 (B7-H1), also known as programmed death ligand 1 (PD-L1) (48). Loss of the tumor

suppressor phosphatase and tensin homolog (PTEN) enhances phosphoinositide-3 kinase (PI3K) activity and increases surface expression of B7-H1 in glioma cells (49). This ligand can bind to and stimulate the PD-1 receptor on activated T cells resulting in T cell quiescence and apoptosis (50, 51). Several studies have shown that PD-L1 is highly expressed in GBM cells (52), and combined checkpoint blockade immunotherapy has shown good efficacy in preclinical GBM mouse models (53). However, uncertainty remains regarding the clinical efficacy of PD-1/PD-L1 checkpoint blockade in GBM. Previous studies have shown that the PD-1/PD-L1 pathway plays a role in the malignant biological behavior of GBM, but other molecular signaling networks also play an indispensable role. As demonstrated by a study of Wainwright DA et al. (19), GBM cells express IDO enzymes that can catalyze the rate-limiting step in the catabolism of tryptophan to kynurenine–a pathway that is involved in T cell immune tolerance and immunosuppression. Therefore, there is an urgent need to explore effective sub-targeted combination therapies in TME to improve the clinical response to immunotherapy for GBM.

On the other hand, the glioma microenvironment contains a large population of immunosuppressive cells, mainly including tumor-associated macrophages (TAMs) and regulatory T cells (Tregs). In GBM, TAMs include resident parenchymal microglia, perivascular macrophages and peripheral monocyte-derived cells that are recruited by GBM to release growth factors and cytokines that affect tumors (54), and TAM recruited to tumor sites can be reprogrammed by GBM cells, leading to ineffective antitumor responses (55). Past evidence suggests that context-dependent symbiotic interactions between cancer cells and TAMs are critical for GBM tumor growth through the regulation of different cytokines, chemokines, metabolites, and other factors (56). In addition, TAMs secrete interleukin-10 (IL-10) (57) and transforming growth factor β (TGF-β) (58), which reduce the activity of immune cells in the organism and provide a favorable environment for tumor growth. Tregs have been identified as a pro-tumor subpopulation of CD4+ T cells in GBM tumor tissues and the circulatory system, which can direct cytotoxic T lymphocytes (CTLs) by suppressing tumor cell immune responses (59). Moreover, gliomas exhibit a low tumor mutational burden (TML) (60) and high intra-tumor heterogeneity (61), which are also barriers to immunotherapy for GBM. Such an immune environment leads to the inability of immunotherapy to achieve similar outcomes as other tumors in the treatment of GBM. Decades of efforts to target immunotherapy for GBM have yielded limited outcomes. Further research should focus on the immune microenvironment of GBM, constantly explore new tumor-associated and tumor-specific antigens, and address the immunosuppressive properties of tumors, thus advancing future immunotherapy for GBM.

4.2.3 Current status and trends of immunotherapy for GBM

There are currently more than 80 clinical trials available to evaluate the effects of immunotherapies for GBM (62), and several relevant studies have shown the potential of these immunotherapies for GBM. ICIs represent the most widely studied category of immunotherapies for GBM, including the PD-1, PDL-1 and CTLA-4 signaling pathways, which have shown promising responses in a variety of tumors (63). PD-L1 is highly expressed in GBM, making it an attractive potential target for immunotherapy trials (52). The CheckMate 143 trial was the first extensive evaluation of the efficacy of PD-1/PD-L1 immunotherapy for GBM, which assessed the efficacy of nivolumab (an anti-PD-1 monoclonal antibody) or bevacizumab in 369 patients with rGBM (64). The results showed that there was no significant difference in median OS between the two groups (9.8 months for nivolumab vs. 10.0 months for bevacizumab), but the objective response rate to treatment was higher in the bevacizumab group than that in the nivolumab group. Two recent trials, namely, CheckMate 548 trial and Checkmate 498 trial evaluated the role of nivolumab in newly diagnosed GBM. Patients received standard therapy (RT+TMZ) or standard therapy + nivolumab in Checkmate 548 trial (65), received RT+TMZ or RT + nivolumab in Checkmate 498 trial (66). The results of these two trials manifested that combination immunotherapy did not prolong the survival of GBM patients. In addition, some preclinical and clinical data show that the administration of dexamethasone alongside anti-PD-1 therapy decreases the survival of GBM patients in a dose-dependent manner (67). Dexamethasone reduces T-lymphocyte count by promoting apoptosis, in addition to decreasing lymphocyte functional capacity. Although some GBM patients are receiving long-term dexamethasone therapy for tumor invasion or radiation therapy-related brain edema, the physiological effects of steroids must be addressed in future clinical trials.

CTLA-4, also known as CD152, is a high-affinity receptor for B7 that induces negative costimulatory signaling on activated T cells (68). The CTLA-4 inhibitor, ipilimumab, is currently in clinical trials in GBM including NCT04323046, NCT04396860, NCT04817254 (69). A phase I clinical trial investigated the intracerebral (IC) administration of ipilimumab (IPI) and nivolumab (NIVO) in combination with intravenous administration of NIVO (70). The results showed that IC administration of NIVO and IPI following maximal safe resection of rGBM was feasible, safe, and associated with a prolonged OS. It is evident that ICIs hold great promise in the treatment of primary and recurrent brain tumors and treatment-induced immune-related adverse events (IrAEs) (71). An interim result reported from a phase I/II clinical trial [NCT03174197] of the PD-L1 antagonist atezolizumab with TMZ and RT showed that more than half of the patients enrolled had Grade 3 or higher adverse events that were likely related to treatment (72). In the future, increased awareness of the risks associated with ICIs and combination therapies will be essential to support treatment decisions.

Cancer vaccines work by exposing tumor-associated antigens to antigen-presenting cells (APCs), which activate immune effector cells to achieve an anti-cancer immune response. GBM-specific targets are scarce, but several targets have been identified that are specifically expressed or abundant in tumor cells, including EGFRvIII, which is a mutant version of the EGFR receptor. The cytomegalovirus (CMV) tegument phosphoprotein 65 (pp65) and IDH1 (R132H)-mutant peptides are frequently and specifically expressed in GBM (73–75). Rindopepimut (CDX-110) is a peptide vaccine that targets EGFRvIII, consisting of a unique EGFRvIII peptide sequence conjugated to keyhole limpet

hemocyanin that serves as an adjuvant and activates both the humoral and cellular immunity (76). The phase II trial (36) and phase III trial (77) on EGFRvIII-targeted peptide vaccine showed improved PFS and OS compared to historical cohorts, and patients could be safely treated with Rindopepimut for a longer period. The results of the recently reported double-blind randomized phase II trial of Rindopepimut with Bevacizumab for patients with relapsed EGFRvIII-expressing glioblastoma (ReACT) showed longer OS and better overall response rates in patients receiving the peptide vaccine compared with placebo (78), suggesting a possible synergy between Rindopepimut with Bevacizumab. In future studies, the therapeutic strategy that combines Rindopepimut with other immunotherapies to improve the efficacy of GBM can continue to attract wide attention. In addition, multi-targeted vaccines that initiate immune responses to multiple tumor-associated antigens may better address intra-tumor heterogeneity.

Adoptive cell therapy (ACT) is a highly personalized cancer therapy that involves the administration of immune cells with direct anti-cancer activity to a cancer-bearing host (79). Autologous CAR T-cell therapy was the first ACT therapy to enter clinical translation and commercialization, achieving significant improvements in patients with invasive B-cell malignancies. CAR T-cell therapy is a novel treatment modality that exploits the patient's immune system to fight cancer (80). CAR T cells overcome the limitations of previous T cell-based immunotherapies by redirecting T cell responses to specific tumor antigens (81). First-generation CAR T cells, only containing a single CD3 ζ-signaling module, show poor proliferative responses and low cytotoxicity, resulting in poor antitumor efficacy (82). The currently approved CAR T-cell therapies are second-generation CARs containing CD28 or 4-1BB signaling domains (83). The design of the CAR structure affects the pharmacokinetic profile of CAR T cells, thereby affecting the efficacy and the likelihood of adverse events. Future research will focus on the development of next-generation CAR with the aim of improving the efficacy and safety of CAR T cells. Following the success of the paradigm shift in CAR-engineered adoptive T cell therapies and advances in technologies that can transform cells into powerful antitumor weapons, the interest in NK cells as immunotherapy candidates has grown exponentially (84). T-cell receptors (TCRs) guide NK-92 cells, which have recently been shown to mediate successful antitumor responses (85).

Of all ACT-based immunotherapies currently in development for GBM, genetically engineered CAR T cells are at the forefront, with encouraging results reported in several clinical trials (86). O'Rourke et al. (34) reported 10 rGBM patients treated with a single dose of intravenous second-generation (i.e., 4-1BB, CD3ζ) EGFRvIII CAR T-cell therapy [NCT02209376] and found that the manufacture and infusion of CAR-modified T-cell (CART)-EGFRvIII cells were feasible and safe, without evidence of extratumoral toxicity or cytokine release syndrome. Ahmed N et al. (87) reported an open-label phase I dose-escalation trial, which demonstrated that the infusion of autologous HER2-specific CAR-modified virus-specific T cells (HER2-CAR VSTs) is safe and may be associated with clinical benefit in progressive GBM patients. Moreover, further evaluation of HER2-CAR VSTs as a single agent or in combination with other immunomodulatory methods for the treatment of GBM is warranted in phase 2b study. In addition, the prospect of combining ACT with other treatments for GBM currently under investigation, such as immune checkpoint blockade or oncolytic viruses, has been demonstrated (88, 89). CAR technology has emerged as a particularly attractive area of research related to GBM (90). The clinical trial results of ACT immunotherapy, particularly with CAR T cells, demonstrate a safe and feasible strategy for eliciting an effective immune response in GBM as well as great potential. However, ACT immunotherapy still faces many challenges before the full potential of ACT can be realized, and the need for continued familiarity with ACT in the future may contribute to a deeper understanding of the general mechanisms of cellular immunity and its role in GBM.

Engineered viruses constitute a promising therapeutic approach to addressing the immunosuppression of the GBM microenvironment by killing tumor cells through direct lysis and stimulation of anti-tumor immune responses (91). The most common viruses are herpesviruses, reoviruses, pox virus, or adenoviruses, which are subjected to varying degrees of genetic engineering (91, 92). It has been previously demonstrated that Zika virus (ZIKV) targets GBM stem cells and prevents death of mice with gliomas. In addition, Zika virus can be used to target GBM tissues, generating an immune-sensitized ZIKV strain that is effective alone or in combination with immunotherapy (93, 94). Hence, oncolytic ZIKV treatment can be adopted by immunotherapies, which may facilitate combination therapy for GBM. Desjardins A et al. (95) demonstrated that intratumoral infusion of PVSRIPO in rGBM patients had no neuroviral potential, and that patients treated with PVSRIPO had higher survival rates than historical controls at 24 months and 36 months. DNX-2401 (Delta-24-RGD; tasadenoturev) is a tumor-selective, replication-competent oncolytic adenovirus. Lang FF et al. (25) reported that treatment with DNX-2401 resulted in dramatic responses with long-term survival in recurrent high-grade gliomas, possibly due to the direct tumorolytic effect of the virus, which then stimulates an immune-mediated anti-glioma response. teserpaturev, as one of the genetically engineered oncolytic viruses (OVs) based on herpes simplex virus-1 (G47Δ), is the first oncolytic virus approved for the treatment of malignant gliomas (96). Several other clinical trials on the lysis of viral therapy for GBM are currently underway (97), and attention should be paid to the results of these trial data, as it is crucial to understand the current status of viral therapy for GBM. Several completed trials have demonstrated that OVs therapy is a safe and promising treatment modality for GBM patients, and further optimization of drug delivery and exploration of multimodal combination therapy options are needed to fully realize its therapeutic potential in the future.

Furthermore, gene therapy (98), TAM therapy (99), and recombinant cytokines such as IL-10 (51), interferon transforming growth factor-β (TGF-β) (100), colony- stimulating factor 1 receptor (CSF1R) (62) have been used in GBM clinical trials and have shown some therapeutic potential in specific glioma populations. As research delves deeper and data accumulate, more meaningful advances in immunotherapy regimens for gliomas will be achieved, but many obstacles and difficulties still need to be overcome before these regimens can be used in the clinic, especially difficulties in drug delivery, immune heterogeneity, and tumor heterogeneity. Additionally, the combination strategy of multiple immunotherapies,

or the combination strategy of immunotherapy with targeted therapy and chemotherapy, may be an effective solution to these problems, which is worthy of further exploration in the future.

4.3 Limitations

The limitations of this study are as follows: 1) The data of this study were only obtained from WOScc, in English only, and other database sources and literature in other languages may be missing. 2) WOS literature is constantly updated, but the search time span in this study was from 2012 to July 2022. 3) Manual removal of unrelated documents from the study by the reviewer might lead to selection bias.

5 Conclusions

In the present study, publications were analyzed using multiple bibliometric tools to reveal the metrological characteristics of the literature related to immunotherapy for GBM. Immunotherapy for GBM still faces great challenges, but several relevant preclinical and clinical studies have shown the potential of immunotherapy for GBM. Therefore, immunotherapy is expected to become an essential component of future glioma treatment, providing new promising treatment strategies for GBM.

Data availability statement

The original contributions presented in the study are included in the article/Supplementary Material. Further inquiries can be directed to the corresponding authors.

Author contributions

KL: Investigation, Data curation, Conceptualization, Resources, Writing – original draft, Writing – review & editing. XD: Conceptualization, Writing – original draft. CC: Formal analysis, Methodology, Software, Validation, Visualization, Writing – review & editing. YY: Project administration, Supervision, Funding acquisition, Resources, Writing – review & editing.

Funding

The author(s) declare that no financial support was received for the research, authorship, and/or publication of this article.

Acknowledgments

Thank the reviewers for their review of the manuscript. And the all author would like to thank CiteSpace (version 5.8.R3) and R (version 4.1.3) software.

Conflict of interest

The authors declare that the research was conducted in the absence of any commercial or financial relationships that could be construed as a potential conflict of interest.

Publisher's note

All claims expressed in this article are solely those of the authors and do not necessarily represent those of their affiliated organizations, or those of the publisher, the editors and the reviewers. Any product that may be evaluated in this article, or claim that may be made by its manufacturer, is not guaranteed or endorsed by the publisher.

Supplementary material

The Supplementary Material for this article can be found online at: https://www.frontiersin.org/articles/10.3389/fonc.2024.1361530/full#supplementary-material

References

1. Faustino AC, Viani GA, Hamamura AC. Patterns of recurrence and outcomes of glioblastoma multiforme treated with chemoradiation and adjuvant temozolomide[J]. *Clinics (Sao Paulo)*. (2020) 75:e1553.

2. Śledzińska P, Bebyn MG, Furtak J, Kowalewski J, Lewandowska MA. Prognostic and predictive biomarkers in gliomas[J]. *Int J Mol Sci*. (2021) 22:10373. doi: 10.3390/ijms221910373

3. Carlino MS, Larkin J, Long GV. Immune checkpoint inhibitors in melanoma. *Lancet*. (2021) 398:1002–14. doi: 10.1016/S0140-6736(21)01206-X

4. Reck M, Remon J, Hellmann MD. First-line immunotherapy for non-small-cell lung cancer. *J Clin Oncol*. (2022) 40:586–97. doi: 10.1200/JCO.21.01497

5. Bagchi S, Yuan R, Engleman EG. Immune checkpoint inhibitors for the treatment of cancer: clinical impact and mechanisms of response and resistance. *Annu Rev Pathol*. (2021) 16:223–49. doi: 10.1146/annurev-pathol-042020-042741

6. Platten M, Ochs K, Lemke D, Opitz C, Wick W. Microenvironmental clues for glioma immunotherapy. *Curr Neurol Neurosci Rep*. (2014) 14:440. doi: 10.1007/s11910-014-0440-1

7. Carmeliet P, De Strooper B. Alzheimer's disease: A breach in the blood-brain barrier. *Nature*. (2012) 485:451–2. doi: 10.1038/485451a

8. Girolamo F, de Trizio I, Errede M, Longo G, d'Amati A, Virgintino D. Neural crest cell-derived pericytes act as pro-angiogenic cells in human neocortex development and gliomas. *Fluids Barriers CNS*. (2021) 18:14. doi: 10.1186/s12987-021-00242-7

9. Sheikh MH, Errede M, d'Amati A, Khan NQ, Fanti S, Loiola RA, et al. Impact of metabolic disorders on the structural, functional, and immunological integrity of the blood-brain barrier: Therapeutic avenues. *FASEB J*. (2022) 36:e22107. doi: 10.1096/fj.202101297R

10. McArthur S, Loiola RA, Maggioli E, Errede M, Virgintino D, Solito E. The restorative role of annexin A1 at the blood-brain barrier. *Fluids Barriers CNS*. (2016) 13:17. doi: 10.1186/s12987-016-0043-0

11. de Trizio I, Errede M, d'Amati A, Girolamo F, Virgintino D. Expression of P-gp in Glioblastoma: What we can Learn from Brain Development. *Curr Pharm Des*. (2020) 26:1428–37. doi: 10.2174/1381612826666200318130625

12. Graeber MB, Scheithauer BW, Kreutzberg GW. Microglia in brain tumors. *Glia*. (2002) 40:252–9. doi: 10.1002/glia.10147

13. Errede M, Annese T, Petrosino V, Longo G, Girolamo F, de Trizio I, et al. Microglia-derived CCL2 has a prime role in neocortex neuroinflammation. *Fluids Barriers CNS*. (2022) 19:68. doi: 10.1186/s12987-022-00365-5

14. Yağmurlu K, Sokolowski J, Soldozy S, Norat P, Çırak M, Tvrdik P, et al. A subset of arachnoid granulations in humans drain to the venous circulation via intradural lymphatic vascular channels. *J Neurosurg*. (2021) 136:917–26. doi: 10.3171/2021.2

15. Cugurra A, Mamuladze T, Rustenhoven J, Dykstra T, Beroshvili G, Greenberg ZJ, et al. Skull and vertebral bone marrow are myeloid cell reservoirs for the meninges and CNS parenchyma. *Science*. (2021) 373:eabf7844. doi: 10.1126/science.abf7844

16. Tamura R, Yoshida K, Toda M. Current understanding of lymphatic vessels in the central nervous system. *Neurosurg Rev*. (2020) 43:1055–64. doi: 10.1007/s10143-019-01133-0

17. Louveau A, Smirnov I, Keyes TJ, Eccles JD, Rouhani SJ, Peske JD, et al. Corrigendum: Structural and functional features of central nervous system lymphatic vessels. *Nature*. (2016) 533:278. doi: 10.1038/nature16999

18. van Hooren L, Vaccaro A, Ramachandran M, Vazaios K, Libard S, van de Walle T, et al. Agonistic CD40 therapy induces tertiary lymphoid structures but impairs responses to checkpoint blockade in glioma. *Nat Commun*. (2021) 12:4127. doi: 10.1038/s41467-021-24347-7

19. Wainwright DA, Chang AL, Dey M, Balyasnikova IV, Kim CK, Tobias A, et al. Durable therapeutic efficacy utilizing combinatorial blockade against IDO, CTLA-4, and PD-L1 in mice with brain tumors. *Clin Cancer Res*. (2014) 20:5290–301. doi: 10.1158/1078-0432.CCR-14-0514

20. Cloughesy TF, Mochizuki AY, Orpilla JR, Hugo W, Lee AH, Davidson TB, et al. Neoadjuvant anti-PD-1 immunotherapy promotes a survival benefit with intratumoral and systemic immune responses in recurrent glioblastoma. *Nat Med*. (2019) 25:477–86. doi: 10.1038/s41591-018-0337-7

21. Khasraw M, Walsh KM, Heimberger AB, Ashley DM. What is the burden of proof for tumor mutational burden in gliomas? *Neuro Oncol*. (2020) 23:17–22. doi: 10.1093/neuonc/noaa256

22. Omuro A, Vlahovic G, Lim M, Sahebjam S, Baehring J, Cloughesy T, et al. Nivolumab with or without ipilimumab in patients with recurrent glioblastoma: results from exploratory phase I cohorts of CheckMate 143. *Neuro Oncol*. (2018) 20:674–86. doi: 10.1093/neuonc/nox208

23. Weller M, Butowski N, Tran DD, Recht LD, Lim M, Hirte H, et al. Rindopepimut with temozolomide for patients with newly diagnosed, EGFRvIII-expressing glioblastoma (ACT IV): a randomised, double-blind, international phase 3 trial. *Lancet Oncol*. (2017) 18:1373–85. doi: 10.1016/S1470-2045(17)30517-X

24. Smith C, Lineburg KE, Martins JP, Ambalathingal GR, Neller MA, Morrison B, et al. Autologous CMV-specific T cells are a safe adjuvant immunotherapy for primary glioblastoma multiforme. *J Clin Invest*. (2020) 130:6041–53. doi: 10.1172/JCI138649

25. Desjardins A, Gromeier M, Herndon JE 2nd, Beaubier N, Bolognesi DP, Friedman AH, et al. Recurrent glioblastoma treated with recombinant poliovirus. *N Engl J Med*. (2018) 379:150–61. doi: 10.1056/NEJMoa1716435

26. Tang W, Fan W, Lau J. Deng L , shen Z , chen X. *Emerging blood-brain-barrier-crossing nanotechnology Brain Cancer theranostics. Chem Soc Rev*. (2019) 48:2967–3014. doi: 10.1039/c8cs00805a

27. Smith DR. Bibliometrics, dermatology and contact dermatitis. *Contact Dermatitis*. (2008) 59:133–6. doi: 10.1111/j.1600-0536.2008.01405.x

28. Ma L, Ma J, Teng M, Li Y. Visual analysis of colorectal cancer immunotherapy: A bibliometric analysis from 2012 to 2021. *Front Immunol*. (2022) 13:843106. doi: 10.3389/fimmu.2022.843106

29. Chen C. CiteSpace II: Detecting and visualizing emerging trends and transient patterns in scientific literature. *J. Assoc. Inf. Sci. Technol*. (2006) 57:359–77. doi: 10.1002/asi.20317

30. Santha Kumar R, Kaliyaperumal K. A scientometric analysis of mobile technology publications. *Scientometrics*. (2015) 105:921–39. doi: 10.1007/s11192-015-1710-7

31. White HD, McCain KW. Visualizing a discipline: An author co-citation analysis of information science, 1972–1995. *J Am Soc Inf Sci*. (1998) 49:327–55. doi: 10.1002/(SICI)10974571(19980401)49:4<327::AID-ASI4>3.0.CO;2-W

32. Mirimanoff RO, Gorlia T, Mason W, Van den Bent MJ, Kortmann RD, Fisher B, et al. Radiotherapy and temozolomide for newly diagnosed glioblastoma: recursive partitioning analysis of the EORTC 26981/22981-NCIC CE3 phase III randomized trial. *J Clin Oncol*. (2006) 24:2563–9. doi: 10.1200/JCO.2005.04.5963

33. Chen C, Leydesdorff L. Patterns of connections and movements in dual-map overlays: A new method of publication portfolio analysis[J]. *J Assoc Inf Sci Technol*. (2014) 65:334–51. doi: 10.1002/asi.22968

34. O'Rourke DM, Nasrallah MP, Desai A, Melenhorst JJ, Mansfield K, Morrissette JJD, et al. A single dose of peripherally infused EGFRvIII-directed CAR T cells mediates antigen loss and induces adaptive resistance in patients with recurrent glioblastoma. *Sci Transl Med*. (2017) 9:eaaa0984. doi: 10.1126/scitranslmed.aaa0984

35. Brown CE, Alizadeh D, Starr R, Weng L, Wagner JR, Naranjo A, et al. Regression of glioblastoma after chimeric antigen receptor T-cell therapy. *N Engl J Med*. (2016) 375:2561–9. doi: 10.1056/NEJMoa1610497

36. Sampson JH, Heimberger AB, Archer GE, Aldape KD, Friedman AH, Friedman HS, et al. Immunologic escape after prolonged progression-free survival with epidermal growth factor receptor variant III peptide vaccination in patients with newly diagnosed glioblastoma. *J Clin Oncol*. (2010) 28:4722–9. doi: 10.1200/JCO.2010.28.6963

37. Schalper KA, Rodriguez-Ruiz ME, Diez-Valle R, López-Janeiro A, Porciuncula A, Idoate MA, et al. Neoadjuvant nivolumab modifies the tumor immune microenvironment in resectable glioblastoma. *Nat Med*. (2019) 25:470–6. doi: 10.1038/s41591-018-0339-5

38. Bagley SJ, Kothari S, Rahman R, Lee EQ, Dunn GP, Galanis E, et al. Glioblastoma clinical trials: current landscape and opportunities for improvement. *Clin Cancer Res*. (2022) 28:594–602. doi: 10.1158/1078-0432.CCR-21-2750

39. McCarthy EF. The toxins of William B. Coley and the treatment of bone and soft-tissue sarcomas. *Iowa Orthop J*. (2006) 26:154–8.

40. MEDAWAR PB. Immunity to homologous grafted skin; the fate of skin homografts transplanted to the brain, to subcutaneous tissue, and to the anterior chamber of the eye. *Br J Exp Pathol*. (1948) 29:58–69.

41. Dieu-Nosjean MC, Goc J, Giraldo NA, Sautès-Fridman C, Fridman WH. Tertiary lymphoid structures in cancer and beyond. *Trends Immunol*. (2014) 35:571–80. doi: 10.1016/j.it.2014.09.006

42. van Tellingen O, Yetkin-Arik B, de Gooijer MC, Wesseling P, Wurdinger T, de Vries HE. Overcoming the blood-brain tumor barrier for effective glioblastoma treatment. *Drug Resist Updat*. (2015) 19:1–12. doi: 10.1016/j.drup.2015.02.002

43. Cardoso FL, Brites D, Brito MA. Looking at the blood-brain barrier: molecular anatomy and possible investigation approaches. *Brain Res Rev*. (2010) 64:328–63. doi: 10.1016/j.brainresrev.2010.05.003

44. Timbie KF, Mead BP, Price RJ. Drug and gene delivery across the blood-brain barrier with focused ultrasound. *J Control Release*. (2015) 219:61–75. doi: 10.1016/j.jconrel.2015.08.059

45. Jain V, Jain S, Mahajan SC. Nanomedicines based drug delivery systems for anti-cancer targeting and treatment. *Curr Drug Deliv*. (2015) 12:177–91. doi: 10.2174/1567201811666140822112516

46. Reardon DA, Brandes AA, Omuro A, Mulholland P, Lim M, Wick A, et al. OS10.3 randomized phase 3 study evaluating the efficacy and safety of nivolumab vs bevacizumab in patients with recurrent glioblastoma: checkMate 143. *Neuro-Oncology*. (2017) 19:iii21–1.

47. Hao C, Parney IF, Roa WH, Turner J, Petruk KC, Ramsay DA. Cytokine and cytokine receptor mRNA expression in human glioblastomas: evidence of Th1, Th2 and Th3 cytokine dysregulation. *Acta Neuropathol*. (2002) 103:171–8. doi: 10.1007/s004010100448

48. Wintterle S, Schreiner B, Mitsdoerffer M, Schneider D, Chen L, Meyermann R, et al. Expression of the B7-related molecule B7-H1 by glioma cells: a potential mechanism of immune paralysis. *Cancer Res*. (2003) 63:7462–7.

49. Parsa AT, Waldron JS, Panner A, Crane CA, Parney IF, Barry JJ, et al. Loss of tumor suppressor PTEN function increases B7-H1 expression and immunoresistance in glioma. *Nat Med*. (2007) 13:84–8. doi: 10.1038/nm1517

50. Tsushima F, Yao S, Shin T, Flies A, Flies S, Xu H, et al. Interaction between B7-H1 and PD-1 determines initiation and reversal of T-cell anergy. *Blood*. (2007) 110:180–5. doi: 10.1182/blood-2006-11-060087

51. Dong H, Strome SE, Salomao DR, Tamura H, Hirano F, Flies DB, et al. Tumor-associated B7-H1 promotes T-cell apoptosis: a potential mechanism of immune evasion. *Nat Med*. (2002) 8:793–800. doi: 10.1038/nm730

52. Nduom EK, Wei J, Yaghi NK, Huang N, Kong LY, Gabrusiewicz K, et al. PD-L1 expression and prognostic impact in glioblastoma. *Neuro Oncol*. (2016) 18:195–205. doi: 10.1093/neuonc/nov172

53. Reardon DA, Gokhale PC, Klein SR, Ligon KL, Rodig SJ, Ramkissoon SH, et al. Glioblastoma eradication following immune checkpoint blockade in an orthotopic, immunocompetent model. *Cancer Immunol Res*. (2016) 4:124–35. doi: 10.1158/2326-6066.CIR-15-0151

54. Pires-Afonso Y, Niclou SP, Michelucci A. Revealing and harnessing tumour-associated microglia/macrophage heterogeneity in glioblastoma. *Int J Mol Sci*. (2020) 21:689. doi: 10.3390/ijms21030689

55. Morisse MC, Jouannet S, Dominguez-Villar M, Sanson M, Idbaih A. Interactions between tumor-associated macrophages and tumor cells in glioblastoma: unraveling promising targeted therapies. *Expert Rev Neurother*. (2018) 18:729–37. doi: 10.1080/14737175.2018.1510321

56. Xuan W, Lesniak MS, James CD, Heimberger AB, Chen P. Context-dependent glioblastoma-macrophage/microglia symbiosis and associated mechanisms. *Trends Immunol*. (2021) 42:280–92. doi: 10.1016/j.it.2021.02.004

57. Widodo SS, Dinevska M, Furst LM, Stylli SS, Mantamadiotis T. IL-10 in glioma. *Br J Cancer*. (2021) 125:1466–76. doi: 10.1038/s41416-021-01515-6

58. Bodmer S, Strommer K, Frei K, Siepl C, de Tribolet N, Heid I, et al. Immunosuppression and transforming growth factor-beta in glioblastoma. Preferential production of transforming growth factor-beta 2. *J Immunol*. (1989) 143:3222–9.

59. DiDomenico J, Lamano JB, Oyon D, Li Y, Veliceasa D, Kaur G, et al. The immune checkpoint protein PD-L1 induces and maintains regulatory T cells in glioblastoma. *Oncoimmunology*. (2018) 7:e1448329. doi: 10.1080/2162402X.2018.1448329

60. Hodges TR, Ott M, Xiu J, Gatalica Z, Swensen J, Zhou S, et al. Mutational burden, immune checkpoint expression, and mismatch repair in glioma: implications for immune checkpoint immunotherapy. *Neuro Oncol*. (2017) 19:1047–57. doi: 10.1093/neuonc/nox026

61. Patel AP, Tirosh I, Trombetta JJ, Shalek AK, Gillespie SM, Wakimoto H, et al. Single-cell RNA-seq highlights intratumoral heterogeneity in primary glioblastoma. *Science*. (2014) 344:1396–401. doi: 10.1126/science.1254257

62. Kreatsoulas D, Bolyard C, Wu BX, Cam H, Giglio P, Li Z. Translational landscape of glioblastoma immunotherapy for physicians: guiding clinical practice with basic scientific evidence. *J Hematol Oncol*. (2022) 15:80. doi: 10.1186/s13045-022-01298-0

63. Amaria RN, Reddy SM, Tawbi HA, Davies MA, Ross MI, Glitza IC, et al. Neoadjuvant immune checkpoint blockade in high-risk resectable melanoma. *Nat Med*. (2018) 24:1649–54. doi: 10.1038/s41591-018-0197-1

64. Reardon DA, Brandes AA, Omuro A, Mulholland P, Lim M, Wick A, et al. Effect of nivolumab vs bevacizumab in patients with recurrent glioblastoma: the checkMate 143 phase 3 randomized clinical trial. *JAMA Oncol*. (2020) 6:1003–10. doi: 10.1001/jamaoncol.2020.1024

65. Lim M, Weller M, Idbaih A, Steinbach J, Finocchiaro G, Raval RR, et al. Phase 3 trial of chemoradiotherapy with temozolomide plus nivolumab or placebo for newly diagnosed glioblastoma with methylated MGMT promoter. *Neuro Oncol*. (2022) 24:1935–49. doi: 10.1093/neuonc/noac116

66. Omuro A, Brandes AA, Carpentier AF, Idbaih A, Reardon DA, Cloughesy T, et al. Radiotherapy combined with nivolumab or temozolomide for newly diagnosed glioblastoma with unmethylated MGMT promoter: an international randomized phase 3 trial. *Neuro Oncol*. (2022) 25:123–34. doi: 10.1093/neuonc/noac099

67. Iorgulescu JB, Gokhale PC, Speranza MC, Eschle BK, Poitras MJ, Wilkens MK, et al. Concurrent dexamethasone limits the clinical benefit of immune checkpoint blockade in glioblastoma. *Clin Cancer Res*. (2021) 27:276–87. doi: 10.1158/1078-0432.CCR-20-2291

68. Wolchok JD, Saenger Y. The mechanism of anti-CTLA-4 activity and the negative regulation of T-cell activation. *Oncologist*. (2008) 13 Suppl 4:2–9. doi: 10.1634/theoncologist.13-S4-2

69. Woroniecka K, Fecci PE. Immuno-synergy? Neoantigen vaccines and checkpoint blockade in glioblastoma. *Neuro Oncol*. (2020) 22:1233–4. doi: 10.1093/neuonc/noaa170

70. Duerinck J, Schwarze JK, Awada G, Tijtgat J, Vaeyens F, Bertels C, et al. Intracerebral administration of CTLA-4 and PD-1 immune checkpoint blocking monoclonal antibodies in patients with recurrent glioblastoma: a phase I clinical trial. *J Immunother Cancer*. (2021) 9:e002296. doi: 10.1136/jitc-2020-002296

71. Postow MA, Sidlow R, Hellmann MD. Immune-related adverse events associated with immune checkpoint blockade. *N Engl J Med*. (2018) 378:158–68. doi: 10.1056/NEJMra1703481

72. Weathers PS-S, Kamiya-Matsuoka C, Harrison RA, Liu DD, Dervin S, Yun C, et al. Phase I/II study to evaluate the safety and clinical efficacy of atezolizumab (atezo; aPDL1) in combination with temozolomide (TMZ) and radiation in patients with newly diagnosed glioblastoma (GBM). *J Clin Oncol*. (2020) ;38:2511.

73. An Z, Aksoy O, Zheng T, Fan QW, Weiss WA. Epidermal growth factor receptor and EGFRvIII in glioblastoma: signaling pathways and targeted therapies. *Oncogene*. (2018) 37:1561–75. doi: 10.1038/s41388-017-0045-7

74. Mitchell DA, Xie W, Schmittling R, Learn C, Friedman A, McLendon RE, et al. Sensitive detection of human cytomegalovirus in tumors and peripheral blood of patients diagnosed with glioblastoma. *Neuro Oncol*. (2008) 10:10–8. doi: 10.1215/15228517-2007-035

75. Bleeker FE, Lamba S, Leenstra S, Troost D, Hulsebos T, Vandertop WP, et al. IDH1 mutations at residue p.R132 (IDH1(R132)) occur frequently in high-grade gliomas but not in other solid tumors. *Hum Mutat*. (2009) 30:7–11. doi: 10.1002/humu.20937

76. Elsamadicy AA, Chongsathidkiet P, Desai R, Woroniecka K, Farber SH, Fecci PE, et al. Prospect of rindopepimut in the treatment of glioblastoma. *Expert Opin Biol Ther*. (2017) 17:507–13. doi: 10.1080/14712598.2017.1299705

77. Schuster J, Lai RK, Recht LD, Reardon DA, Paleologos NA, Groves MD, et al. multicenter trial of rindopepimut (CDX-110) in newly diagnosed glioblastoma: the ACT III study. *Neuro Oncol*. (2015) 17:854–61. doi: 10.1093/neuonc/nou348

78. Reardon DA, Desjardins A, Vredenburgh JJ, O'Rourke DM, Tran DD, Fink KL, et al. Rindopepimut with bevacizumab for patients with relapsed EGFRvIII-expressing glioblastoma (ReACT): results of a double-blind randomized phase II trial. *Clin Cancer Res*. (2020) 26:1586–94. doi: 10.1158/1078-0432.CCR-18-1140

79. Rosenberg SA, Restifo NP. Adoptive cell transfer as personalized immunotherapy for human cancer. *Science*. (2015) 348:62–8. doi: 10.1126/science.aaa4967

80. Lim WA, June CH. The principles of engineering immune cells to treat cancer. *Cell*. (2017) 168:724–40. doi: 10.1016/j.cell.2017.01.016

81. Gross G, Waks T, Eshhar Z. Expression of immunoglobulin-T-cell receptor chimeric molecules as functional receptors with antibody-type specificity. *Proc Natl Acad Sci U S A*. (1989) 86:10024–8. doi: 10.1073/pnas.86.24.10024

82. Guedan S, Ruella M, June CH. Emerging cellular therapies for cancer. *Annu Rev Immunol*. (2019) 37:145–71. doi: 10.1146/annurev-immunol-042718-041407

83. Shimabukuro-Vornhagen A, Böll B, Schellongowski P, Valade S, Metaxa V, Azoulay E, et al. Critical care management of chimeric antigen receptor T-cell therapy recipients. *CA Cancer J Clin*. (2022) 72:78–93. doi: 10.3322/caac.21702

84. Laskowski TJ, Biederstädt A, Rezvani K. Natural killer cells in antitumour adoptive cell immunotherapy. *Nat Rev Cancer*. (2022) 22:557–75. doi: 10.1038/s41568-022-00491-0

85. Mensali N, Dillard P, Hebeisen M, Lorenz S, Theodossiou T, Myhre MR, et al. NK cells specifically TCR-dressed to kill cancer cells. *EBioMedicine*. (2019) 40:106–17. doi: 10.1016/j.ebiom.2019.01.031

86. Choi BD, Curry WT, Carter BS, Maus MV. Chimeric antigen receptor T-cell immunotherapy for glioblastoma: practical insights for neurosurgeons. *Neurosurg Focus*. (2018) 44:E13. doi: 10.3171/2018.2.FOCUS17788

87. Ahmed N, Brawley V, Hegde M, Bielamowicz K, Kalra M, Landi D, et al. HER2-specific chimeric antigen receptor-modified virus-specific T cells for progressive glioblastoma: A phase 1 dose-escalation trial. *JAMA Oncol*. (2017) 3:1094–101. doi: 10.1001/jamaoncol.2017.0184

88. Wing A, Fajardo CA, Posey AD Jr, Shaw C, Da T, Young RM, et al. Improving CART-cell therapy of solid tumors with oncolytic virus-driven production of a bispecific T-cell engager. *Cancer Immunol Res*. (2018) 6:605–16. doi: 10.1158/2326-6066.CIR-17-0314

89. Rafiq S, Yeku OO, Jackson HJ, Purdon TJ, van Leeuwen DG, Drakes DJ, et al. Targeted delivery of a PD-1-blocking scFv by CAR-T cells enhances anti-tumor efficacy in vivo. *Nat Biotechnol*. (2018) 36:847–56. doi: 10.1038/nbt.4195

90. Choi BD, Maus MV, June CH, Sampson JH. Immunotherapy for glioblastoma: adoptive T-cell strategies. *Clin Cancer Res*. (2019) 25:2042–8. doi: 10.1158/1078-0432.CCR-18-1625

91. Martikainen M, Essand M. Virus-based immunotherapy of glioblastoma. *Cancers (Basel)*. (2019) 11:186. doi: 10.3390/cancers11020186

92. Farrera-Sal M, Moya-Borrego L, Bazan-Peregrino M, Alemany R. Evolving status of clinical immunotherapy with oncolytic adenovirus. *Clin Cancer Res*. (2021) 27:2979–88. doi: 10.1158/1078-0432.CCR-20-1565

93. Zhu Z, Mesci P, Bernatchez JA, Gimple RC, Wang X, Schafer ST, et al. Zika virus targets glioblastoma stem cells through a SOX2-integrin $\alpha_v\beta_5$ axis. *Cell Stem Cell*. (2020) 26:187–204. doi: 10.1016/j.stem.2019.11.016

94. Nair S, Mazzoccoli L, Jash A, Govero J, Bais SS, Hu T, et al. Zika virus oncolytic activity requires CD8+ T cells and is boosted by immune checkpoint blockade. *JCI Insight*. (2021) 6:e144619. doi: 10.1172/jci.insight.144619

95. Lang FF, Conrad C, Gomez-Manzano C, Yung WKA, Sawaya R, Weinberg JS, et al. Phase I study of DNX-2401 (Delta-24-RGD) oncolytic adenovirus: replication and immunotherapeutic effects in recurrent Malignant glioma. *J Clin Oncol*. (2018) 36:1419–27. doi: 10.1200/JCO.2017.75.8219

96. Zeng J, Li X, Sander M, Zhang H, Yan G, Lin Y. Oncolytic viro-immunotherapy: an emerging option in the treatment of gliomas. *Front Immunol*. (2021) 12:721830. doi: 10.3389/fimmu.2021.721830

97. Shoaf ML, Desjardins A. Oncolytic viral therapy for Malignant glioma and their application in clinical practice. *Neurotherapeutics*. (2022) 19:1818–31. doi: 10.1007/s13311-022-01256-1

98. Kane JR, Miska J, Young JS, Kanojia D, Kim JW, Lesniak MS. Sui generis: gene therapy and delivery systems for the treatment of glioblastoma. *Neuro Oncol*. (2015) 17 Suppl 2:ii24–36. doi: 10.1093/neuonc/nou355

99. Andersen JK, Miletic H, Hossain JA. Tumor-associated macrophages in gliomas-basic insights and treatment opportunities. *Cancers (Basel)*. (2022) 14:1319. doi: 10.3390/cancers14051319

100. Gong L, Ji L, Xu D, Wang J, Zou J. TGF-β links glycolysis and immunosuppression in glioblastoma. *Histol Histopathol*. (2021) 36:1111–24. doi: 10.14670/HH-18-366

frontiers | Frontiers in Oncology

TYPE Original Research
PUBLISHED 19 August 2024
DOI 10.3389/fonc.2024.1442911

OPEN ACCESS

EDITED BY
Jixin Dong,
University of Nebraska Medical Center,
United States

REVIEWED BY
Grinu Mathew,
University of Nebraska Medical Center,
United States
Jianmin Zhang,
University of Toledo, United States

*CORRESPONDENCE
Zhengqin Gu
sjtugzq@163.com

RECEIVED 03 June 2024
ACCEPTED 01 August 2024
PUBLISHED 19 August 2024

CITATION
Liu S, He Y and Gu Z (2024) FATP5 modulates biological activity and lipid metabolism in prostate cancer through the TEAD4-mediated Hippo signaling.
Front. Oncol. 14:1442911.
doi: 10.3389/fonc.2024.1442911

FATP5 modulates biological activity and lipid metabolism in prostate cancer through the TEAD4-mediated Hippo signaling

Shenyang Liu, Yi He and Zhengqin Gu*

Department of urology, Xinhua Hospital, Shanghaijiaotong University, Shanghai, China

Introduction: Prostate cancer (PCa), one of the most prevalent malignant tumors in the genitourinary system, is characterized by distant metastasis and the development of castration-resistant prostate cancer (CRPC), which are major determinants of poor prognosis. Current treatment approaches for PCa primarily involve surgery and endocrine therapy, but effective strategies for managing distant metastasis and CRPC remain limited.

Methods: We utilized qPCR, WB, and other methods to measure the expression levels of respective proteins, concurrently assessing lipid metabolism to validate the role of FATP5 in lipid metabolism. Additionally, we employed bioinformatics analysis and WB techniques to explore the corresponding mechanisms.

Results: In this study, we conducted an analysis of clinical samples and public databases to identify differential expression of FATP5 and further investigated its association with clinical outcomes. Through biochemical and functional experiments, we elucidated the potential underlying mechanisms by which FATP5 facilitates the progression of PCa. Our findings demonstrate that specific upregulation of FATP5 significantly enhances proliferation, migration, and invasion of PCa cell lines, while also modulating lipid metabolism in PCa. Mechanistically, the expression of FATP5 is closely associated with the Hippo signaling pathway, as it promotes the nuclear accumulation of YAP1 by inhibiting AMPK and facilitating the activation of β-catenin and RHOA. Furthermore, the transcription of FATP5 is mediated by TEAD4, and this transcriptional activation requires the involvement of YAP1.

Discussion: FATP5 is highly expressed in prostate cancer and can enhance the biological activity and lipid metabolism of prostate cancer. We have also elucidated that FATP5 is regulated by the Hippo signaling pathway. This provides a new potential target for the treatment of prostate cancer.

KEYWORDS

FATP5, TEAD4, metabolism, Hippo, YAP1, cancer

1 Introduction

PCa is predominantly an adenocarcinoma of epithelial origin, ranking as the second most prevalent malignancy among males worldwide. It accounts for 27% of all incident cases of male cancer (1).There are various treatment options available for localized PCa, with surgical prostatectomy and radiotherapy being the predominant treatment modalities. Despite advancements in clinical interventions for PCa, managing advanced-stage PCa remains a therapeutic challenge. A subset of patients with primary PCa, following initial treatments, will eventually progress to metastatic PCa, which is currently an incurable disease (2). Consequently, there is a crucial need to explore novel biomarkers for the diagnosis and treatment of PCa.

The Hippo pathway is a signaling pathway that plays a critical role in regulating cell growth, proliferation, and organ size. It was initially discovered in fruit flies and has since been found to be highly conserved in mammals, including humans (3). The Hippo pathway consists of a series of protein interactions and phosphorylation events that ultimately control the activity of transcriptional co-activators called Yes-associated protein (YAP) and transcriptional co-activator with PDZ-binding motif (TAZ). When the Hippo pathway is activated, it leads to the phosphorylation and inhibition of YAP/TAZ, preventing their translocation into the nucleus and subsequent activation of target genes involved in cell proliferation and survival. Mutations or dysregulation of the Hippo pathway components have been associated with various diseases, including PCa. Inactivation of the pathway can lead to aberrant YAP/TAZ activity and uncontrolled cell growth, contributing to tumorigenesis and tumor progression (4).

Metabolic reprogramming in the growth of PCa is considered unique in solid tumors because primary prostate tumors tend to enhance oxidative phosphorylation and lipid synthesis, while the elevation of glycolysis is limited (5), this suggests that lipid metabolism may play a more significant role in PCa. Cancer cells acquire fatty acids (FAs) from *de novo* lipid synthesis and exogenous uptake (6). Previous studies on lipid metabolism in PCa have primarily focused on biosynthetic pathways, while research on uptake metabolism has been limited, particularly regarding the FATP (1–6) family. FATP is a member of the solute carrier family 27 (SLC27) and comprises a group of integral membrane proteins with extracellular fatty acid (FA) binding sites, intracellular acyl-CoA synthetase (ACS) active sites, and ATP binding domains (7). *In vitro* and *in vivo* studies have demonstrated that FATP is essential for cancer cell uptake of fatty acids, as well as for growth and invasion (8). And interestingly, in an experiment involving co-culture of PCa cells with adipocytes, it was found that the expression of FATP5 was significantly increased (9). However, the involvement of the six FATP family members in cancer biology remains unclear.

In the present study, we discovered that FATP5 regulates the growth, migration, and invasion of the prostate through the Hippo pathway, while also being deeply involved in lipid metabolism in PCa. Mechanistically, FATP5 promotes the nuclear translocation of YAP1 protein and the transcription of FATP5 is mediated in a YAP1-dependent manner by TEAD4. Additionally, FATP5 is overexpressed in PCa samples, suggesting its potential role in the pathogenesis of PCa.

2 Materials and methods

2.1 Cell Culture

PCa cell lines, including LNCaP(ATCC CRL-1740, USA),PC-3 (ATCC CRL-1435,USA),C4-2B(ATCC CRL-3315,USA),were grown in RPMI-1640 supplemented with 10% fetal bovine serum and 1% penicillin/streptomycin. DU-145(ATCC HTB-81.USA) cells were cultured in DMEM medium supplemented with 10% fetal bovine serum and 1% penicillin/streptomycin. The cells were cultured under the conditions of 37°C, 5% CO2, and passaged at a ratio of 1:2.

2.2 Tissue sample

PCa and adjacent tissue samples were collected from patients undergoing urological surgery at Xinhua Hospital affiliated with Shanghai Jiao Tong University School of Medicine. All procedures in this study were approved by the Ethics Committee of Xinhua Hospital affiliated with Shanghai Jiao Tong University School of Medicine, and written informed consent was obtained from each participant.

2.3 Tissue microarray

Tissue microarrays (TMAs) were procured from Servicebio Co. Ltd. and immunohistochemical staining was conducted using the FATP5 antibody. Following completion of the staining process, the slides were scanned using a microscope, and the obtained images were analyzed using QuPath software for subsequent assessment of the H score for each tissue core. Integration of the H scores with clinical information was performed to enable comprehensive analysis.

2.4 Plasmid construction

The TEAD4 overexpression plasmid, FATP5 overexpression plasmid, pGL3-FATP5(wt), and pGL3-FATP5(mut) plasmids were constructed in-house. Briefly, primers targeting the desired sequences were designed and used for PCR amplification of the target fragments. The amplified fragments were then ligated to the respective plasmids using the In-Fusion® HD Cloning Kit (Takara,Japan) to establish the desired plasmid constructs. The obtained plasmids were subsequently transformed into competent cells for amplification and purification. The pGL3-FATP5(mut) plasmid was generated using the QuickMutation™ Site-directed Gene Mutagenesis Kit (Beyotime, China) through site-directed mutagenesis.

2.5 Transfection

pcDNA3.1 Plasmids were transfected using Lipofectamine 3000 (Thermo Fisher,USA) according to the manufacturer's protocol. Briefly, cells in the logarithmic growth phase were inoculated and cultured overnight in an incubator at 37°C and 5% CO2. The medium was changed to serum-free medium 2 hours before transfection. Then, 5 μg of pcDNA3.1 Plasmids were diluted with 250 μL of serumfree opti-MEM, mixed gently, and kept for 5 minutes. Further, 7.5 μL of Lipofectamine 3000 was diluted using 250 μL of opti-MEM and kept for 5 minutes. Lipofectamine 3000 and plasmids were mixed and kept for 15 minutes. The mixture was added to each Petri dish, and after mixing, cells were cultured in an incubator at 37°C and 5% CO2. 48 hours after culturing, the cells were harvested for transfection efficiency assessment or subsequent experiments.

2.6 Establishment of stable expression cell lines

To generate lentivirus, lentivirus vectors (PLVX-shFATP5-Puro, PLVX-shTEAD4-Puro PLVX-shYAP-Puro, 10μg) and lentiviral components (10μg psPAX2 and 2.5μg pMD2.G) were co-transfected into 293T cells in a 10 cm^2 dish using Polyethylenimine Linear (Yeasen,China). Lentivirus-containing supernatants from 48 and 72 hours post-transfection were collected to infect PCa cells. The stable cell lines were selected using 2μg/ml puromycin for at least 7 days for three passages. Puromycin (1μg/ml) was used to maintain the cells.

2.7 Quantitative real-time PCR

Total RNA was extracted using the EZ-press RNA Purification Kit (EZBioscience,China) and concentration was measured by a Nanodrop 2000 instrument. 500 nanogram of total RNA was for reverse transcription using PrimeScript™ RT Master Mix (Takara, Japan). Gene expression measured by qPCR data was collected by QuantStudio 3 Real-Time PCR System with Hieff® qPCR SYBR Green Master Mix (Yeasen,China) and ensure that each experiment is independently replicated three times. Primer sequences are listed in Supplementary Table S1.

2.8 Western blotting and antibodies

Total proteins were extracted by RIPA lysis buffer (Beyotime, China) together with PMSF (Beyotime,China). The concentration of total protein was determined by BCA protein assay kit (Beyotime, China). After being separated by 10% sodium dodecyl sulfate-polyacrylamide (SDS-PAGE) gels, proteins lysates were transferred to PVDF Membrane (Millipore, USA). The membranes were blocked with 5% BSA for 1hour at room temperature and then immunoblotted at 4°C overnight with primary antibodies: anti-FATP5(1:1000,Proteintech,China), anti-YAP1(1:1000,Proteintech,China), anti-TEAD4(1:1000,Proteintech, China), anti-TAZ(1:1000,Proteintech,China), anti-p-YAP1(1:1000, Proteintech,China),anti-Gapdh(1:1000,Proteintech,China),anti-Tublin(1:1000,Proteintech,China),anti-AMPK(1:1000,Proteintech, China),anti-p-AMPK(1:1000,Proteintech,China),anti-β-catenin (1:1000,Proteintech,China),anti-p-β-catenin(1:1000,Proteintech, China),anti-RHOA(1:1000,Proteintech,China),anti-SMAD2/3 (1:1000,Proteintech,China),anti-p-SMAD2/3(1:1000,Proteintech, China),anti-LATS1(1:1000,ABclonal,China),anti-p-LATS1(1:1000, ABclonal,China),anti-N-Cadherin(1:1000,ABclonal,China),anti-E-Cadherin(1:1000,ABclonal,China),anti-Vimentin(1:1000,ABclonal, China),anti-Snail(1:1000,ABclonal,China),anti-YAP1(1:1000, Proteintech,China),anti-Histone H3(Beyotime,China). After incubated with diluted secondary antibodies for 1hour at room temperature, the bands were scanned and analyzed by Tanon 5200 (Tanon, China).

2.9 Immunofluorescence

PCa cells were seeded on coverslips. Cells were then washed and treated with 0.3% Triton X-100 for 15 minutes. After blocking with 5% BSA for 1 hour, the YAP1 antibody was added and incubated overnight. The following day, the samples were washed three times with TBST and subsequently incubated with Alexa Fluor 488-labeled Goat Anti-Rabbit IgG (Beyotime,China) at room temperature for 1 hour. After another three washes with TBST, the samples were stained with DAPI(0.1μg/ml). Following a final wash with TBST, the samples were ready for observation under a fluorescence microscope.

2.10 EdU incorporation assay

PCa cells were seeded in a 24-well plate and incubated at 37°C for 24 hours. Subsequently, they were treated with 5-ethynyl-20-deoxyuridine (EdU) at a working concentration of 50 μM from the BeyoClick™ EdU Cell Proliferation Kit with Alexa Fluor 488 (Beyotime,China) in 400 μL of culture medium for 2 hours. Following treatment, the cells were washed three times with PBS for 5 minutes each at room temperature. They were then fixed with 4% paraformaldehyde for 30 minutes and incubated with 0.5% Triton X-100 for 15 minutes. Next, nuclear staining was performed using DAPI(0.1μg/ml), followed by thorough rinsing. The samples were observed under a fluorescence microscope, and three random fields were selected for the quantification of positive cells.

2.11 CCK8 assay

PCa cells were seeded into 96-well plates at a density of 2000 cells per well with 100 μl medium. 10μl Cell Counting Kit-8 (Beyotime,China) was added to each well at 0 hour, 24 hours, 48 hours, 72 hours and 96 hours after seeding, respectively. For CCK-8 experiments requiring drug treatment, after seeding the cells, allow them to fully adhere to the culture plate. In the experimental group,

add different concentrations of the drug, while in the control group, add an equivalent amount of DMSO. Subsequently, follow the same procedure as described earlier. Optical density (OD) at 450 nm was detected by a Multiskan SkyHigh Microplate Spectrophotometer (Thermo Fisher,USA).

2.12 Colony formation assay

PCa cells were seeded into 6-well plates at a density of 2000 cells per well. After approximately fifteen days of incubation, the formation of colonies can be observed. Cell colonies were subsequently washed with phosphate buffered saline (PBS), Subsequently, fix the colonies with 10% para-formaldehyde for 30 minutes. Wash the colonies three times with PBS, and then stain them with 0.1% crystal violet for 15 minutes. The representative photographs were taken and the number of colonies were counted.

2.13 Transwell assay

PCa cells were resuspended in serum-free media. $5x10^3$ cells in serum-free media were planted into 6.5 mm Transwell® with 8.0 μm Pore Polycarbonate Membrane Insert (Corning, USA) for migration, whereas $5x10^3$cells in serum-free medium were planted into the mentioned chambers, which were precoated with Basement Membrane Matrix High Concentration (Corning, USA) for invasion. After 16 hours of cultivation, fix the chamber in 10% para-formaldehyde and then stain with crystal violet. Subsequently, observe the cells under a microscope and document by capturing images.

2.14 BODIPY and Nile red assay for lipid droplet

Regarding lipid droplet staining, we utilized a protocol developed by others as a reference (10). In brief, cells were cultured to a stable state, followed by washing with PBS. Then, a serum-free culture medium was used to dilute BODIPY 493/503 (MCE,USA) to a concentration of 2 μM/L for lipid droplet staining for 30 minutes. Subsequently, the cells were fixed with 4% paraformaldehyde for 30 minutes, followed by DAPI staining for five minutes. After washing with PBS, the stained cells were observed using a fluorescence microscope. Similar to the procedure, Nile Red (MCE,USA) staining was performed by diluting Nile Red to a concentration of 1 μM/L for 30 minutes. Fluorescence intensity was observed and recorded under a fluorescence microscope. All samples from the same experiment were imaged by using the same settings (gain, laser power). For lipid uptake, a serum-free culture medium was used to dilute BODIPY 500/510 C1, C12 (MCE,USA) to a concentration of 6 μM/L. The cells were then incubated at 37°C for 30 minutes. Subsequently, fluorescence intensity was measured using a fluorescence microscope. Additionally, stained cells were analyzed using a flow cytometer (BD,USA), and the data were analyzed using FlowJo software.

2.15 Dual-Luciferase reporter gene assay

The experiment was performed as per the standard protocol. Briefly, the cells were transfected with Lipofectamine 3000 (Thermo Fisher,USA), and then Dual Luciferase Reporter Gene Assay Kit (Yeasen,China) was used. After cell lysis and thorough mixing, transfer the lysate into a 96-well plate for further testing. The fluorescence analyzer was used to detect firefly and renilla luciferin enzyme activity. Then the ratio of firefly to renilla luciferase was calculated.

2.16 *In vivo* animal studies

A subcutaneous xenograft model was employed to investigate the effects of oeFATP5, shTEAD4, and TED-347 on tumor growth. A total of six 4-5-week-old male nude mice (SLAC, China) were randomly divided into the experimental and control groups. One million PC-3 cells that overexpressing FATP5 or shTEAD4 were mixed with a 1:1 ratio of serum-free medium and matrix gel and injected into the axillary region of the nude mice. In the case of the TED-347 experimental group, mice were injected with TED-347 at a dose of 20 mg/kg for three times on days 1, 7, and 14, while the control group received an equivalent volume of DMSO. Tumor size was measured every three days, and on day 21, the mice were euthanized to measure tumor size and weight. All animal experiments were conducted in accordance with the guidelines of the Ethics Committee of Xinhua Hospital affiliated with Shanghai Jiao Tong University School of Medicine.

2.17 Drug treatments

All drugs, including TED-347 (MCE), Enzalutamide (MCE, USA) and Leptomycin B (Beyotime,China) were dissolved in DMSO to prepare a 10 mM stock solution. For *in vitro* assays, the stock solutions were diluted with serum-free culture medium to the desired concentrations and added to the cell culture medium. The cells were treated for different durations according to experimental requirements. The control group received the corresponding amount of DMSO without any drug treatment.

2.18 IC50 assay

PCa cells were seeded into 96-well plates at a density of 5000 cells per well with 100 μl medium. After the cells have fully adhered, different concentrations of Enzalutamide are sequentially added to the experimental groups, while the control group receives an equal volume of DMSO. The cells are then incubated undisturbed for 48 hours. Following the incubation period, 10 μL of CCK-8 reagent is

added to each well, and the cells are further incubated for 90 minutes. Subsequently, the absorbance at 450 nm is measured using Spectrophotometer. The data is analyzed using GraphPad Prism 9.0 software to calculate the IC50 value for each group of cells.

2.19 Malondialdehyde levels

The content of malondialdehyde (MDA) can be determined by measuring thiobarbituric acid (TBA) using Lipid Peroxidation MDA Assay Kit (beyotime, China). The experiments were performed as per the kit's manual. In simple terms, the procedure involves collecting cells and determining their protein concentration using the BCA assay. The working solution is then added to the cell lysates or standard samples. The mixture is heated at a minimum of 100°C in a metal bath for at least 15 minutes. After centrifugation, the supernatant is collected, and the optical density (OD) is measured at 532 nm. The MDA concentration is calculated by comparing the obtained OD values with a standard concentration curve.

2.20 ROS levels

The experiment is conducted following the instructions provided in the Reactive Oxygen Species Assay Kit (Beyotime, China). In brief, after cell adherence, 1 ml of diluted DCFH is added to the culture dish. The dish is then incubated at 37°C for 20 minutes. Subsequently, the cells are washed three times with serum-free culture medium. The fluorescence microscope is set to an excitation wavelength of 488 nm and an emission wavelength of 525 nm. Under consistent imaging parameters, photographs are taken for both the experimental and control groups. Subsequently, the average fluorescence intensity is calculated for each group, allowing for the determination of the reactive oxygen species (ROS) levels.

2.21 NADPH levels

The experiment is conducted following the instructions provided in the $NADP^+$/NADPH Assay Kit with WST-8.After cell collection, the cells are lysed using NADP+/NADPH extraction buffer. The lysate is divided into two portions. One portion is centrifuged at 12,000 g for 10 minutes at 4°C, and the supernatant is collected. A 200 µl sample is taken for further analysis. The other portion of the sample is subjected to a 60°C water bath treatment for 30 minutes, followed by centrifugation at 10,000 g for 5 minutes at 4°C. The supernatant is collected and mixed with G6PDH working solution and a color reagent. The mixture is then incubated at 37°C in the dark for 20 minutes. The absorbance of the sample at 450 nm is measured using the Multiskan SkyHigh Microplate Spectrophotometer. The NADPH oxidase activity is calculated based on the standard curve.

2.22 Bioinformatics analysis

We utilized the GEPIA2 web server to analyze the expression profile of the FATP protein family in the TCGA dataset. The QuPath software was employed for the analysis of tissue microarray staining. The H-score was calculated using the formula H-score=Σ(Pi*i), where Pi represents the proportion of positive cells and i represents the staining intensity. Based on the expression status of FATP5 in prostate cancer patients from the TCGA database, they were divided into the FATP5 high-expression group and the FATP5 low-expression group. Gene Set Enrichment Analysis (GSEA) V4.3.3 and MSigDB were used for gene enrichment analysis.

2.23 Statistical analysis

The data are presented as mean ± standard deviation (SD). GraphPad Prism 9.0 software is used for data analysis. Statistical analysis includes unpaired two-tailed t test, paired t test, two-way analysis of variance (ANOVA) followed by Tukey's multiple comparisons test. A p-value less than 0.05 ($P < 0.05$) is considered statistically significant.

3 Results

3.1 FATP5 shows upregulated expression in PCa tissues and cell lines

To investigate the role of the FATP protein family in the occurrence and progression of PCa, we initially analyzed the expression profiles of the FATP family in PCa using publicly available TCGA data. We found that FATP (2, 4, 5) expression was upregulated, while FATP (1, 3, 6) expression was downregulated in PCa (Figure 1A). Furthermore, we examined the mRNA expression of the FATP family in several common PCa cell lines (LNCaP, PC-3, DU-145) compared to benign prostatic hyperplasia (BPH) cell lines. In contrast to the TCGA database, only FATP (5, 6) showed increased expression in all three cell lines (Figure 1B). Similar results were observed in two additional PCa cell lines, DU-145 and C4-2B (Supplementary Figure S1A). Consequently, we hypothesized that FATP5 may play a crucial role in the development of PCa. Subsequently, we obtained paired tissue samples from Xinhua Hospital affiliated with Shanghai Jiao Tong University School of Medicine, to confirm the expression levels of FATP5 in PCa tissues. Ten pairs of samples were used for qRT-PCR analysis, and twenty pairs were used for Western blotting. The results showed that FATP5 expression was higher in PCa tissues compared to adjacent normal tissues (Figures 1C, D). Tissue microarray (TMA), a technique used for high-throughput analysis of tissue samples, was employed. The TMA used in our study included tissue samples from one hundred PCa patients. Quantitative analysis of the staining results for each tissue spot was performed using QuPath software, and the corresponding H score was obtained. The results demonstrated significantly higher expression levels of FATP5 in tumor tissues compared to normal adjacent tissues (Figure 1E). Additionally, immunohistochemistry staining confirmed significantly stronger staining for FATP5 in cancer tissues compared to adjacent non-cancerous tissues

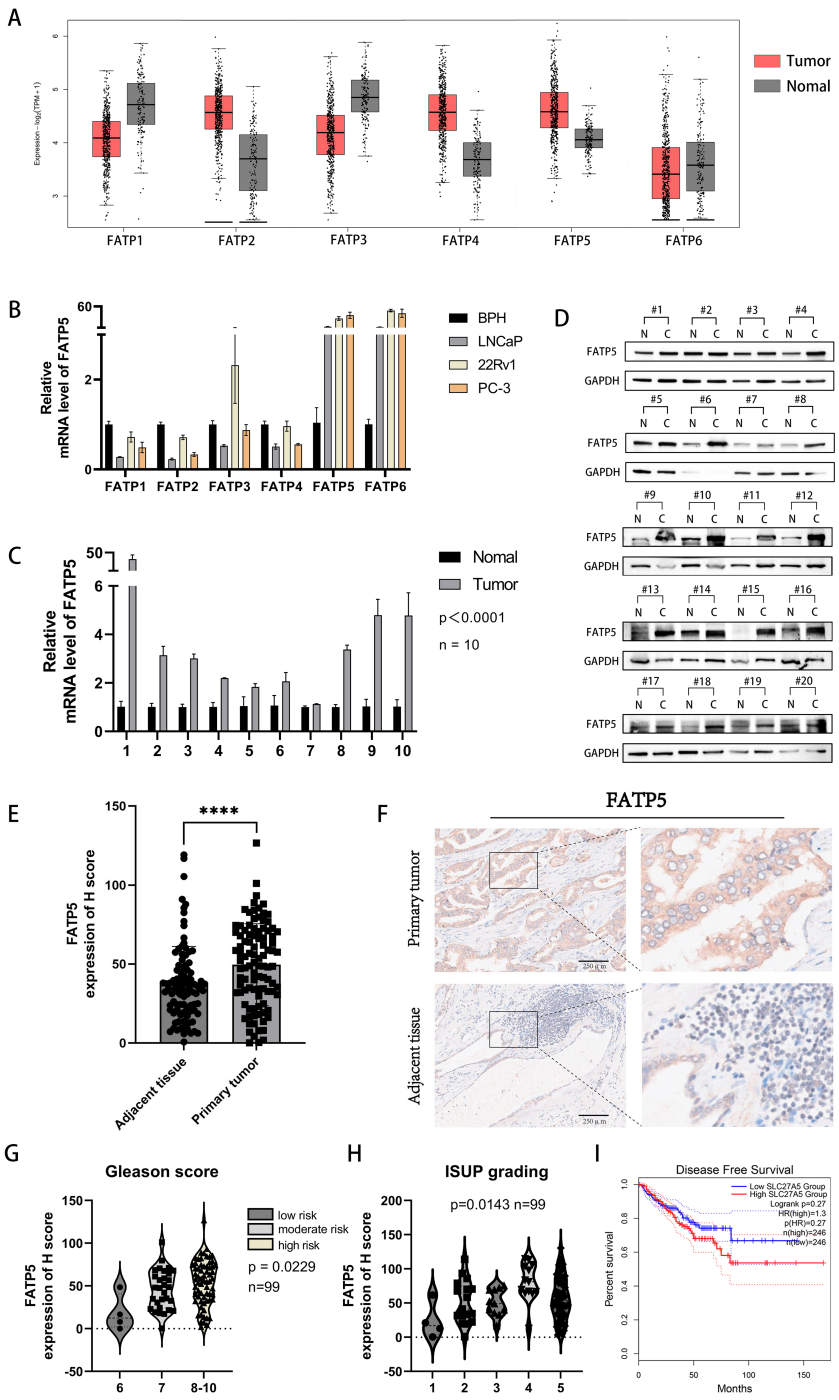

FIGURE 1
FATP5 shows upregulated expression in PCa tissues and cell lines. **(A)** Download the expression transcriptome profile of FATPs mRNA in PCa tissues (n = 492) and adjacent normal tissues (n = 192) from the TCGA-PRAD database. **(B)** Assess the mRNA expression levels of FATPs in PCa cell lines. **(C)** Determine the expression levels of FATP5 mRNA in cancer and adjacent tissues in 10 PCa patients. **(D)** Measure the protein expression levels of FATP5 in cancer and adjacent tissues in 20 PCa patients. **(E)** Generate H score scoring charts based on FATP5 immunostaining in 100 patient tissue chips. **(F)** Present immunohistochemistry staining results for FATP5. **(G, H)** Investigate the correlation between FATP5 and Gleason score and ISUP grading based on clinical data from patient tissue chips. **(I)** FATP5 and disease-free survival of prostate cancer. Mean ± SD, n = 3. ****p < 0.0001.

(Figure 1F). Subsequently, based on the Gleason score, the samples were divided into three groups: low-risk group with a Gleason score of 6, intermediate-risk group with a Gleason score of 7, and high-risk group with a Gleason score of 8-10. It was observed that as the risk level increased, the expression of FATP5 also significantly increased (Figure 1G). According to the ISUP grading results, there is a gradual increase in the expression of FATP5 with higher grades. This indicates that in PCa, as the malignancy level increases, there is a corresponding elevation in the expression level of FATP5. (Figure 1H). Furthermore, FATP5 also showed a trend

associated with DFS (Figure 1I). Furthermore, FATP5 also showed a trend associated with DFS (Figure 1I).Overall, these findings confirm the high expression of FATP5 in patient tissues and cell lines, as well as its association with Gleason score risk stratification and ISUP grading.

3.2 FATP5 is involved in regulating the proliferation and migration of PCa cells

To investigate the impact of FATP5 on the proliferation and metastasis of PCa, extensive functional studies were conducted using PCa cell lines. Lentiviral vectors were used to overexpress FATP5 and introduce short hairpin RNA (shRNA) targeting FATP5 into the relevant cell lines, resulting in stable cell lines with low (LNCaP-shFATP5, C4-2B-shFATP5) and high (PC3-oeFATP5) expression of FATP5 (Figures 2A, B). Metastasis is a major cause of mortality in PCa (11). After overexpressing FATP5, we observed significant changes in the morphology of PC-3 cells (Figure 2C). Subsequently, gene set enrichment analysis (GSEA) based on TCGA database was employed to investigate the biological processes regulated by FATP5 and its impact on PCa carcinogenesis and progression (Figure 2D). The findings indicated a significant association between FATP5 and EMT signaling characteristics, suggesting a potential influence of FATP5 on EMT processes. Transwell assays were performed in the aforementioned cell lines to determine the role of FATP5 in cell migration. As expected, LNCaP-shFATP5 and C4-2B-shFATP5 cells exhibited decreased migration capability, while PC-3-oeFATP5 cells showed increased migration ability (Figure 2E). Similarly, transwell assays were employed to assess cell invasion, and consistent with previous observations, LNCaP-shFATP5 and C4-2B-shFATP5 cells demonstrated reduced invasive potential, whereas PC3-oeFATP5 cells exhibited enhanced invasion (Figure 2E). Scratch assays were also conducted, revealing increased migration ability upon FATP5 overexpression (Figure 2F). Furthermore, multiple EMT markers were examined in the aforementioned cell lines to validate the results. Western blot analysis demonstrated decreased expression levels of Vimentin and Snail, while E-cadherin expression increased in LNCaP-shFATP5 and C4-2B-shFATP5 cells, with opposite results observed in FATP5 overexpressing cell lines (Figure 2G). In summary, FATP5 overexpression promoted PCa EMT *in vitro*, while knockdown of FATP5 inhibited PCa EMT.

We also assessed the influence of FATP5 on the proliferation of PCa cells. The CCK-8 assay was employed to evaluate the cellular proliferation capacity of PCa cells. The results revealed a significant reduction in the proliferation rate of cells lacking FATP5 (LNCaP-shFATP5, C4-2B-shFATP5) (Figure 2H). Conversely, overexpression of FATP5 resulted in an elevated proliferation rate of PCa cells (Figure 2H). Clonogenic assays demonstrated that FATP5 knockdown led to smaller and fewer colony formations in PCa cells, while FATP5 overexpression yielded the opposite results (Figure 2I, Supplementary Figure S1B). In addition, we conducted EdU assays, where both fast-proliferating and slow-proliferating cells incorporate EdU during active DNA synthesis, and the signal intensity of EdU in cells indicates the proliferation rate. Our results showed that the proportion of EdU-positive cells was lower in FATP5 knockdown cells, while it was higher in FATP5 overexpressing cells. (Figure 2J). Given that our functional studies on FATP5 were conducted *in vitro*, further *in vivo* functional validation was performed. PC-3 cells overexpressing FATP5 were implanted subcutaneously in nude mice, and tumor size was measured every 3 days. On the 21st day, the subcutaneous tumors were excised. The results demonstrated that overexpression of FATP5 significantly increased tumor weight and volume (Figures 2K–M). In summary, these *in vitro* and *in vivo* functional investigations clearly indicate that FATP5 plays a promoting role in the migration, invasion, and proliferation of tumors.

3.3 FATP5 significantly promotes lipid accumulation in PCa cells

In PCa cells, enhanced lipid accumulation is often observed (12). Next, we performed gene set enrichment analysis (GSEA) to analyze the enrichment of lipid metabolism-related genes in the TCGA database after FATP5 alteration. The results showed a strong correlation between pathways related to lipid metabolism and high expression of FATP5 (Figure 3A), suggesting that FATP5 is involved in the regulation of lipid metabolism in PCa. To validate this hypothesis, we stained cells with Nile red and BODIPY 493/503 in three cell lines overexpressing or knockdown of FATP5. The results revealed that cells with high FATP5 expression exhibited increased lipid accumulation, while cells with low FATP5 expression showed decreased lipid content (Figure 3B). Subsequently, we measured the levels of triglycerides (TG), total cholesterol (T-CHO), and non-esterified fatty acids (NEFA) as quantitative indicators of lipid accumulation in the three FATP5-treated cell lines. As shown in Figure 3C, cells with high FATP5 expression had elevated levels of TG, T-CHO, and NEFA, while the opposite was observed in cells with low FATP5 expression (Figure 3C).

Subsequently, we conducted liquid chromatography/mass spectrometry (LC/MS) lipidomic analysis on PC-3 cells with either overexpression of FATP5. The results, depicted in Figure 3D, demonstrated a significant increase in the levels of triglycerides (TG), fatty acids, phosphatidylcholine (PC), and phosphatidylinositol (PI) in PC-3 cells with stable FATP5 overexpression compared to the control cells. Furthermore, KEGG metabolic pathway analysis revealed the correlation of differential metabolites with multiple lipid metabolism pathways (Figure 3E).

Considering the anticipated association between lipid accumulation and increased reactive oxygen species (ROS) generation, we quantified the $NADP^+$/NADPH ratio, intracellular ROS levels, and lipid peroxidation levels in PCa cell lines. As expected, FATP5 overexpression resulted in an elevation of the $NADP^+$/NADPH ratio within the cells (Figure 3F), an induction of lipid peroxidation, including elevated malondialdehyde (MDA) levels (Figure 3G) and an augmentation of intracellular ROS

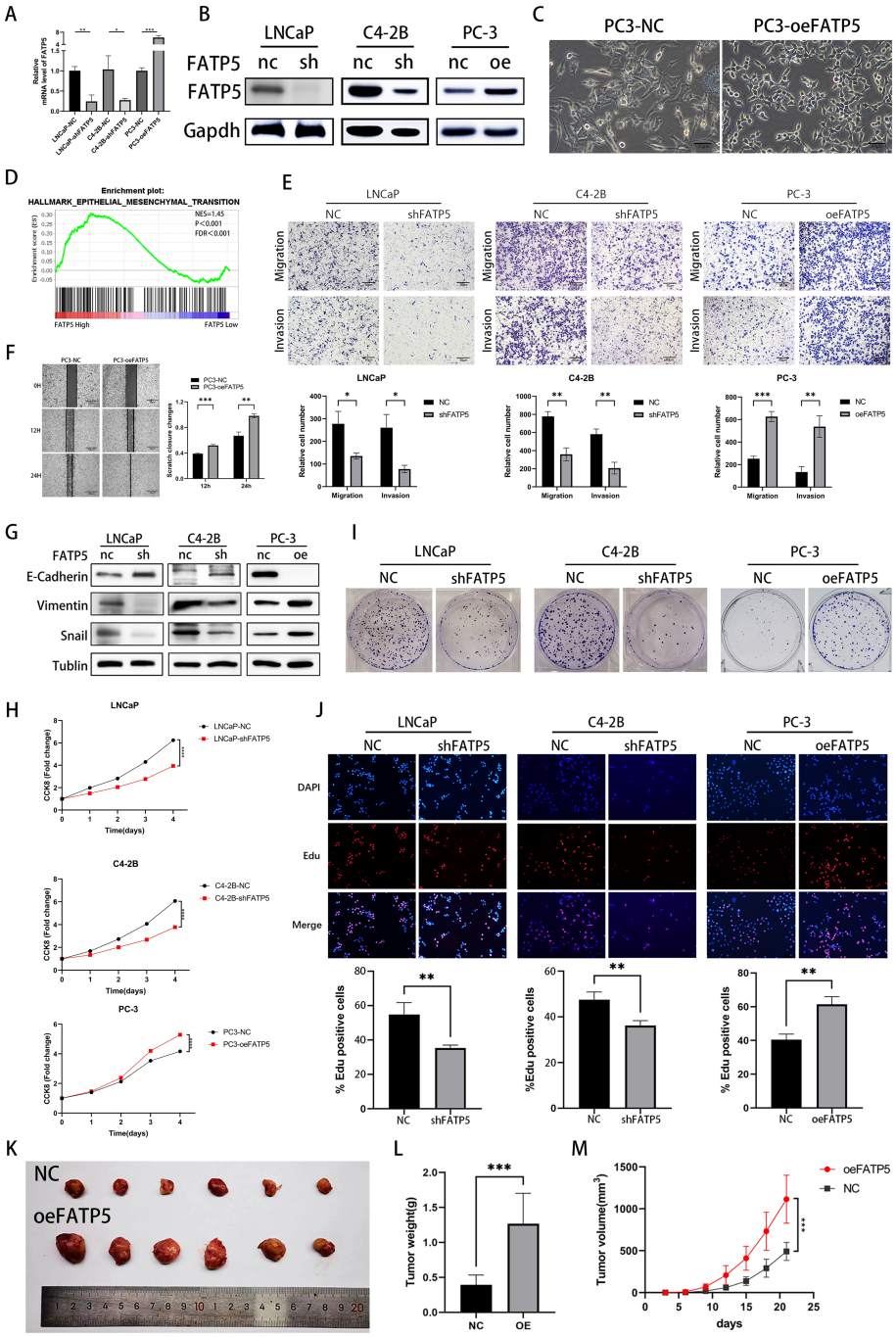

FIGURE 2
FATP5 is involved in regulating the proliferation and migration of PCa cells **(A, B)** Evaluate the protein and mRNA levels of FATP5 after overexpression or knockdown. **(C)** Morphologically observe PC-3 cells after overexpressing FATP5 under light microscopy. **(D)** Perform Gene Set Enrichment Analysis (GSEA) to assess the correlation between EMT signaling pathways and FATP5 mRNA levels based on TCGA database. **(E)** Investigate the migration and proliferation abilities of PCa cells using the Transwell assay (Magnification: 100x). **(F)** Validate the planar migration capability of PCa cells using the scratch assay. **(G)** Assess the expression levels of EMT-related markers after FATP5 knockdown or overexpression. **(H)** Determine cell growth curves using the CCK8 assay. **(I)** Conduct colony formation assays to observe the size and quantity of PCa cell colonies. **(J)** Assess proliferation ability of PCa cells using the EdU assay. **(K–M)** Measure tumor size, weight, and volume in *in vivo* experiments. Mean ± SD, n = 3. *p < 0.5, **p < 0.01, ***p < 0.001, and ****p < 0.0001.

levels (Figure 3H). Conversely, downregulation of FATP5 exerted opposing effects on the $NADP^+$/NADPH ratio, intracellular ROS levels, and MDA levels in PCa cells (Figures 3F–H).

In order to elucidate the reasons for lipid accumulation, we supplemented the culture medium with BODIPY 500/510 C1, C12 fluorescent probe and performed flow cytometry analysis to measure the fluorescence intensity of PCa cells with different FATP5 treatments after thirty minutes of incubation. It was observed that following FATP5 overexpression, the fluorescence intensity was significantly enhanced compared to the control group,

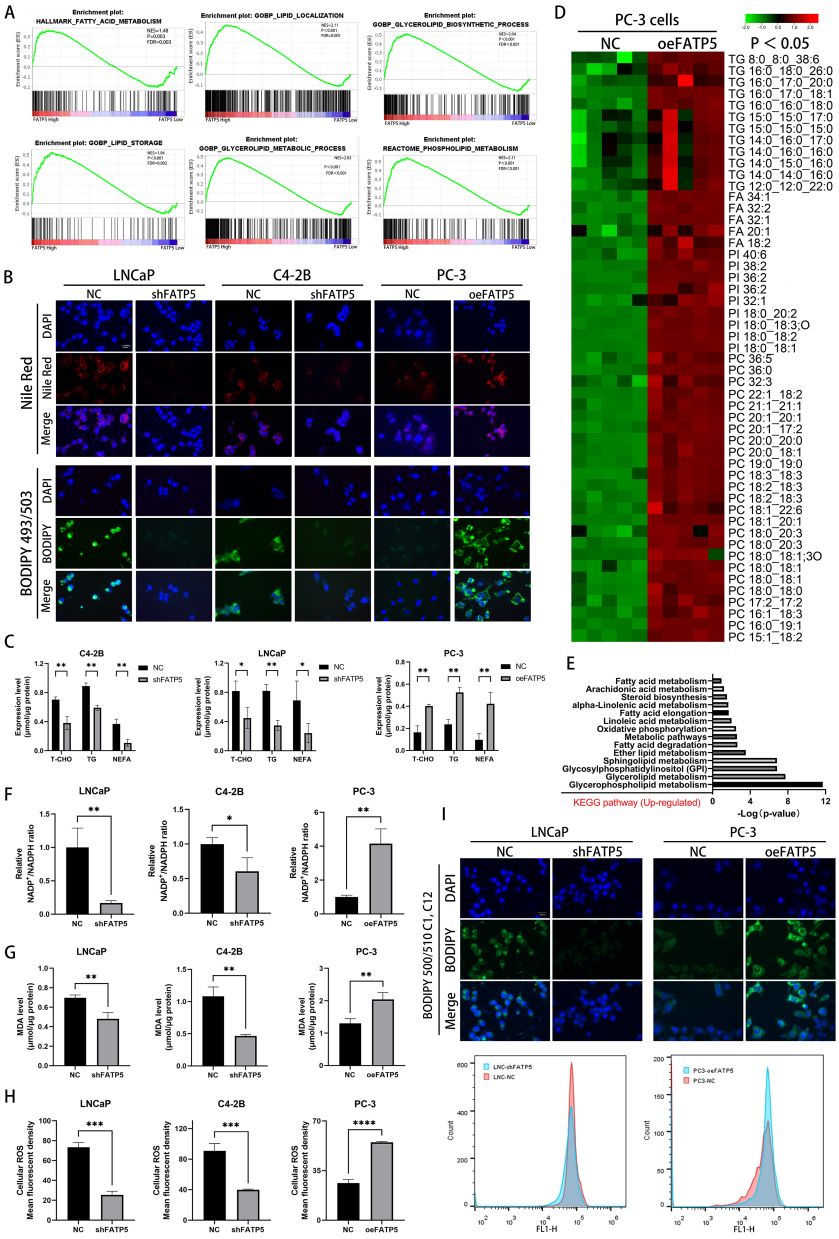

FIGURE 3
FATP5 significantly promotes lipid accumulation in PCa cells. **(A)** Perform GSEA to explore the correlation between lipid metabolism-related pathways and FATP5 mRNA levels based on TCGA database. **(B)** Stain FATP5-overexpressing or knockdown cell lines with Nile red and BODIPY 493/503 (Magnification: 400×). **(C)** Quantify the content of corresponding lipids in FATP5-overexpressing or knockdown cell lines. **(D)** Employ LC/MS lipidomics to detect intracellular lipids in stable or unstable FATP5-overexpressing PC-3 cells (n = 5), highlighting statistically significant metabolites ($p < 0.05$) in the heatmap using red and green colors. **(E)** Present KEGG pathway enrichment analysis of metabolite enrichment based on LC/MS lipidomics analysis. **(F–H)** Analyze the NADP+/NADPH ratio, MDA levels, and ROS levels in cells after FATP5 overexpression or knockdown, normalized to total protein content. **(I)** Analyze fluorescence intensity of BODIPY 500/510 C1,C12 staining using flow cytometry. Mean ± SD, n = 3. *p < 0.5, **p < 0.01, ***p < 0.001, and ****p < 0.0001.

while cells with FATP5 knockdown exhibited lower fluorescence intensity (Figure 3I). These experimental results suggest that the lipid accumulation induced by FATP5 is at least partially attributed to enhanced uptake of exogenous fatty acids. Based on these findings, we propose that FATP5 enhances lipid accumulation in PCa and that part of this accumulation is due to increased uptake of exogenous fatty acids. Additionally, FATP5 also promotes ROS generation and lipid peroxidation levels.

3.4 FATP5 is regulated by the Hippo signaling pathway and promotes the nuclear translocation of YAP1 protein

C4-2B cells with FATP5 knockdown were selected for whole transcriptome sequencing to gain deeper insights into the mechanistic role of FATP5. The transcriptomic analysis demonstrated significant alterations in gene expression, with

1,727 genes being downregulated and 1,064 genes being upregulated (Figure 4A). Subsequent KEGG pathway analysis of the differentially expressed genes revealed enrichment in multiple lipid metabolism pathways and tumor metastasis pathways upon FATP5 knockdown (Figures 4B, C), the reliability of the previous experimental results is verified again. Furthermore, a notable enrichment of differentially expressed genes was observed in the Hippo pathway (Figure 4D), which was further validated by Gene Set Enrichment Analysis (GSEA) (Figure 4E). Therefore, we reasonably suspect that FATP5 is regulated by the Hippo signaling pathway.

We subsequently validated this in cells by examining the levels of total YAP1, TAZ, and phosphorylated YAP1 (p-YAP1) in FATP5 knockdown or overexpression cell lines. The results showed that upon FATP5 knockdown, the levels of total YAP1 and TAZ decreased, while the level of phosphorylated YAP1 increased. Conversely, cells overexpressing FATP5 exhibited the opposite results (Figure 4F). As YAP1 protein requires nuclear localization to exert its function (13), we further investigated the impact of FATP5 on YAP1 nuclear translocation. We isolated nuclear and cytoplasmic proteins from PCa cells and measured the expression levels of YAP1 in each fraction (Figure 4G). Following FATP5 knockdown, the level of YAP1 in the nucleus significantly decreased, while overexpression of FATP5 led to a notable increase in nuclear YAP1 protein. We also employed Leptomycin B (LMB), a nuclear export inhibitor that prevents protein transport from the nucleus to the cytoplasm (14). Concurrently with FATP5 knockdown, we added LMB to the culture medium and subsequently assessed the nuclear YAP1 content. The results showed that the addition of LMB partially attenuated the reduction in nuclear YAP1 (Figure 4H). Furthermore, we performed immunofluorescence staining on treated cells and calculated the average fluorescence intensity in the nuclear region. The results revealed a significant reduction in nuclear fluorescence intensity following FATP5 knockdown (Figure 4I).

To investigate the mechanism by which FATP5 promotes YAP1 nuclear translocation, we examined the expression levels of intracellular ACSL4 (Supplementary Figure S2A). Overexpression of FATP5 enhanced the levels of intracellular fatty acids, while ACSL4, as a member of the ACSL protein family, facilitates the binding of long-chain fatty acids to coenzyme A, forming acyl-CoA. Acyl-CoA is a key intermediate in fatty acid β-oxidation. Consequently, we subsequently assessed the expression of key genes involved in fatty acid β-oxidation and found that FATP5 was able to promote the expression of these key genes (Supplementary Figure S2B). The enhanced fatty acid β-oxidation inevitably leads to an increase in intracellular ATP levels, consistent with our expectations, as FATP5 elevated the intracellular ATP content (Supplementary Figure S2C). The elevated ATP inhibited the activation of the AMPK signaling pathway, which has been demonstrated to promote the degradation of YAP1 (15). In summary, we propose that FATP5 enhances intracellular ATP levels by augmenting fatty acid β-oxidation, thereby inhibiting the activation of the AMPK signaling pathway and facilitating YAP1 nuclear translocation. We also examined the expression of key proteins involved in multiple signaling pathways regulating YAP1 nuclear translocation, including the HGF-induced β-catenin pathway, TGF-β-induced SMAD pathway, and Ephrin A2-induced RHO-dependent pathway. The results showed (Figure 4J) that after FATP5 overexpression, the protein expression of β-catenin and phosphorylated β-catenin at S552 (p-β-catenin) significantly increased, as did the protein level of RHOA. However, the expression levels of SMAD2/3 and phosphorylated SMAD2/3 did not show significant changes. In cells with FATP5 knockdown, the opposite protein expression patterns were observed. Additionally, we examined the levels of Large Tumor Suppressor Kinase 1 (LATS1) and phosphorylated LATS1 (p-LATS1). Phosphorylation of LATS1 in the Hippo pathway leads to increased degradation of YAP1 and inhibition of downstream gene transcription (16). The results revealed that in PCa cells with FATP5 overexpression, the level of phosphorylated LATS1 significantly decreased, whereas in cells with FATP5 knockdown, the phosphorylation level of LATS1 significantly increased (Figure 4K). Previous studies have demonstrated that the AMPK signaling pathway can directly regulate the activity of β-catenin and RHOA, and activation of AMPK inhibits the activity of β-catenin and RHOA (17, 18). Therefore, our findings suggest that knockdown of FATP5 reduces lipid metabolism in PCa and activates the AMPK signaling pathway, thereby inhibiting the activity of β-catenin and RHOA, suppressing YAP1 nuclear translocation, leading to YAP1 accumulation in the cytoplasm, phosphorylation, and subsequent degradation, and ultimately inhibiting downstream gene transcription.

3.5 TEAD4 positively regulates the transcription of FATP5 and influences the activity of PCa

Upon translocation into the nucleus, YAP1 protein usually forms a complex with the TEAD family to exert its functional role (19). TEAD carries a TEA DNA-binding domain near its N-terminus and a YBD (YAP binding domain) near its C-terminus (20). Based on our transcriptomic data, we observed a significant downregulation of TEAD4 expression following FATP5 knockdown (Figure 5A). Therefore, we had a rationale to suspect that FATP5 transcription might be regulated by TEAD4. To validate our hypothesis, we overexpressed TEAD4 in PCa cells and measured the mRNA expression of FATP5. As shown in Figure 5B, FATP5 expression was significantly increased upon TEAD4 overexpression, which was further confirmed by Western blot analysis (Figure 5C). Similarly, the reduction of TEAD4 also affected the nuclear accumulation of YAP1 (Figure 5D). Correspondingly, there were alterations in EMT markers (Figure 5E). Luciferase reporter gene analysis demonstrated that upregulation of TEAD4 enhanced the luciferase activity of the FATP5 promoter (Figure 5F). Subsequently, using JASPAR, we predicted the TEAD4 binding sites in the FATP5 promoter region and performed site-directed mutagenesis using a mutation kit to disrupt these binding sites. The luciferase activity was then measured, revealing a decrease in luciferase activity upon mutation (Figure 5F). Furthermore, we conducted experiments in

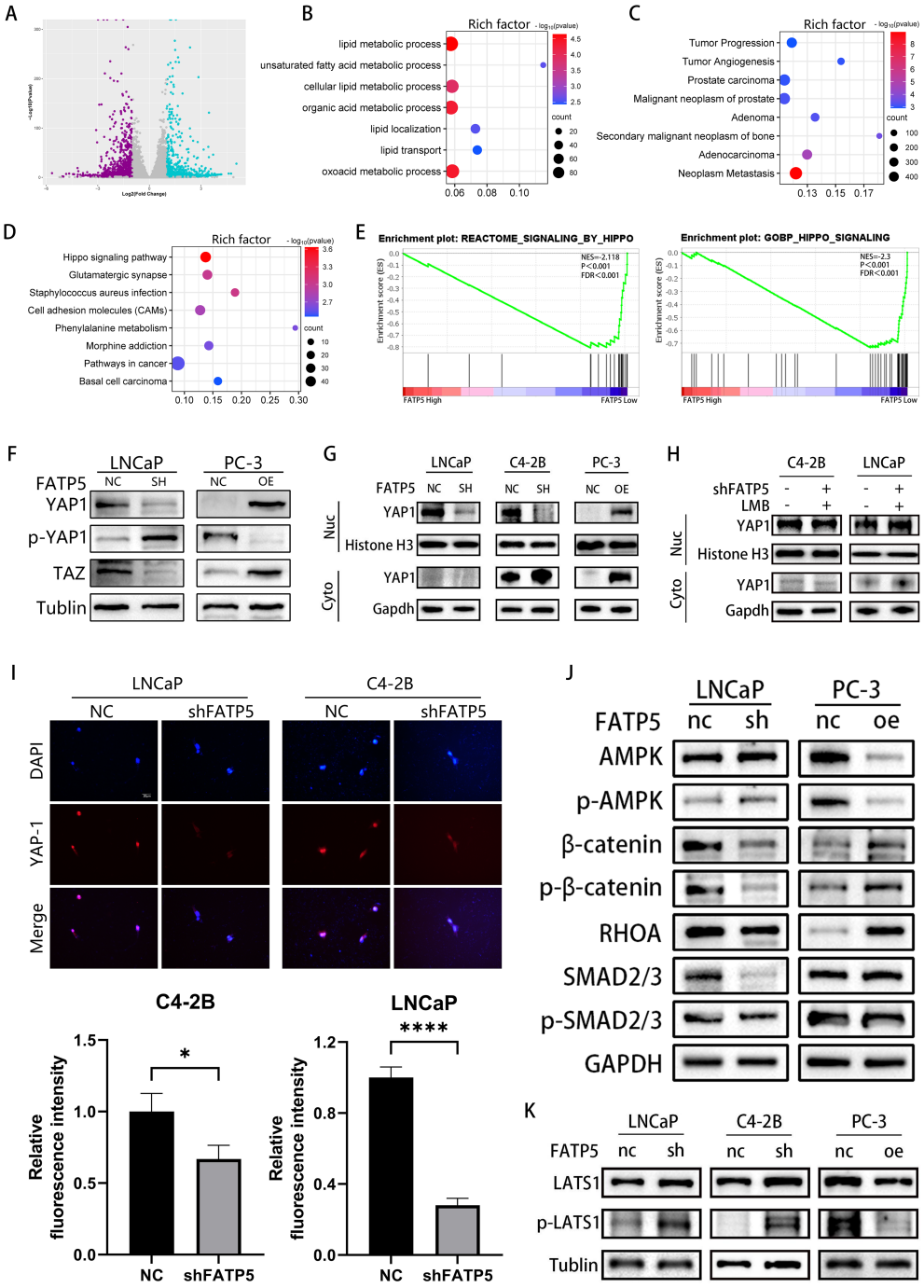

FIGURE 4
FATP5 is regulated by the Hippo signaling pathway and promotes the nuclear translocation of YAP1 protein. **(A)** Generate volcano plots to display the differential gene expression profile following FATP5 knockdown. **(B–D)** Conduct KEGG pathway analysis on the differentially expressed genes identified from RNA-seq data. Criteria for selection: |Log2(fold change)| ≥ 2 and p-value ≤ 0.05. **(E)** Investigate the correlation between the Hippo signaling pathway and FATP5 mRNA levels using Gene Set Enrichment Analysis (GSEA) based on data from the TCGA database. **(F)** The expression status of key proteins in the Hippo signaling pathway following knockdown or overexpression of FATP5. **(G)** Measure the expression levels of YAP1 in the nuclear and cytoplasmic fractions following FATP5 overexpression or knockdown. Cyto, cytoplasm; nuc, nucleus. **(H)** Determine the expression levels of YAP1 in the nuclear and cytoplasmic fractions after the addition of Leptomycin B (LMB) to the cells. **(I)** Perform immunofluorescence staining to examine the fluorescence intensity of nuclear YAP1 (Magnification: 400×). **(J, K)** The expression profile of key proteins in the signaling pathway following knockdown or overexpression of FATP5. Mean ± SD, n = 3. *p < 0.5, ****p < 0.0001.

two additional FATP5 knockdown cell lines and observed a significant decrease in luciferase activity (Figure 5G). In conclusion, we can infer that TEAD4 mediates the transcription of FATP5.

Subsequently, we performed *in vivo* validation of the impact of TEAD4 on proliferation. Upon TEAD4 knockdown, there was a significant decrease in tumor size, weight, and volume in mice (Figures 5H–J). To further establish the correlation between FATP5

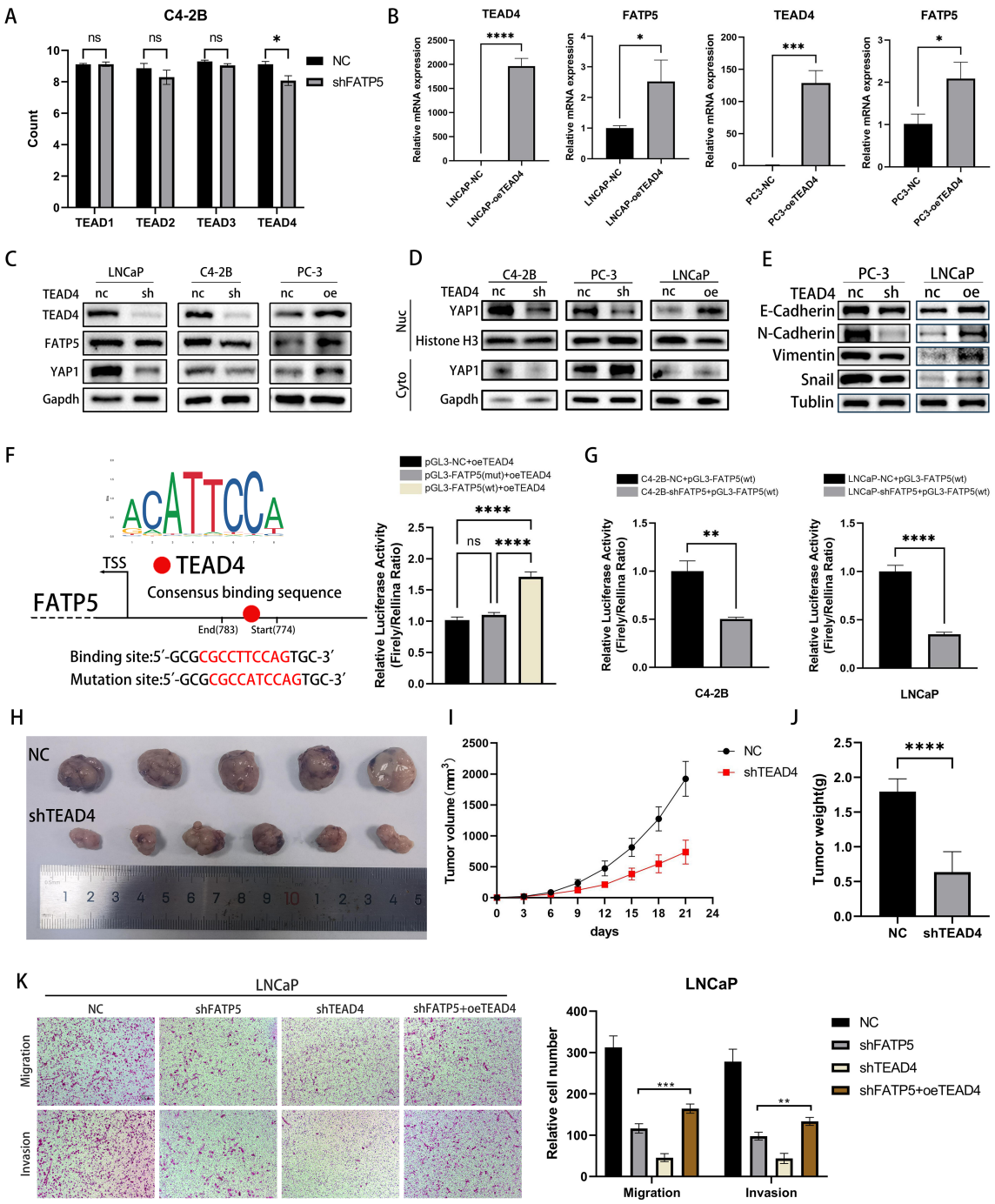

FIGURE 5
TEAD4 positively regulates the transcription of FATP5 and influences the activity of PCa. **(A)** Quantify the read counts of TEAD family members in the RNA-seq data. **(B, C)** Determine the mRNA and protein levels of TEAD4 and FATP5 in PCa cells following transfection with TEAD4 overexpression. **(D, E)** Assess the protein levels of YAP1 in the nuclear and cytoplasmic fractions, as well as the protein levels of corresponding EMT markers, after TEAD4 knockdown or overexpression. **(F, G)** Present the results of the dual-luciferase reporter gene assay. TSS, Transcription Start Site; wt, wild type; mut, mutant. **(H–J)** Evaluate the tumor size, weight, and volume in mice following TEAD4 knockdown. **(K)** Conduct migration and invasion experiments on specific PCa cells (Magnification: 100×). Mean ± SD, n = 3. *p < 0.5, **p < 0.01, ***p < 0.001, and ****p < 0.0001. ns, no significance.

and TEAD4 in PCa, we conducted functional rescue experiments. Utilizing the aforementioned methodology, we generated four cell line groups for experimentation: control cell line (NC), FATP5 knockdown cell line (shFATP5), TEAD4 knockdown cell line (shTEAD4), and FATP5 knockdown cell line with TEAD4 overexpression (shFATP5 +oeTEAD4). As previously mentioned, knockdown of FATP5 significantly attenuated the migration and invasion capabilities of PCa cells. However, TEAD4 overexpression partially restored these abilities (Figure 5K). Proliferation capacity was assessed using the CCK8 assay, and consistent with the previous findings, TEAD4

overexpression partially reversed the growth inhibition caused by FATP5 knockdown (Figure 6A). Lipid staining results also demonstrated a partial recovery of lipid accumulation in PCa cells upon TEAD4 overexpression (Figure 6B). Hence, we can draw a consistent conclusion regarding the relationship between FATP5 and TEAD4, indicating that FATP5 primarily modulates the biological activity and lipid metabolism of PCa through the TEAD4-mediated Hippo signaling pathway.

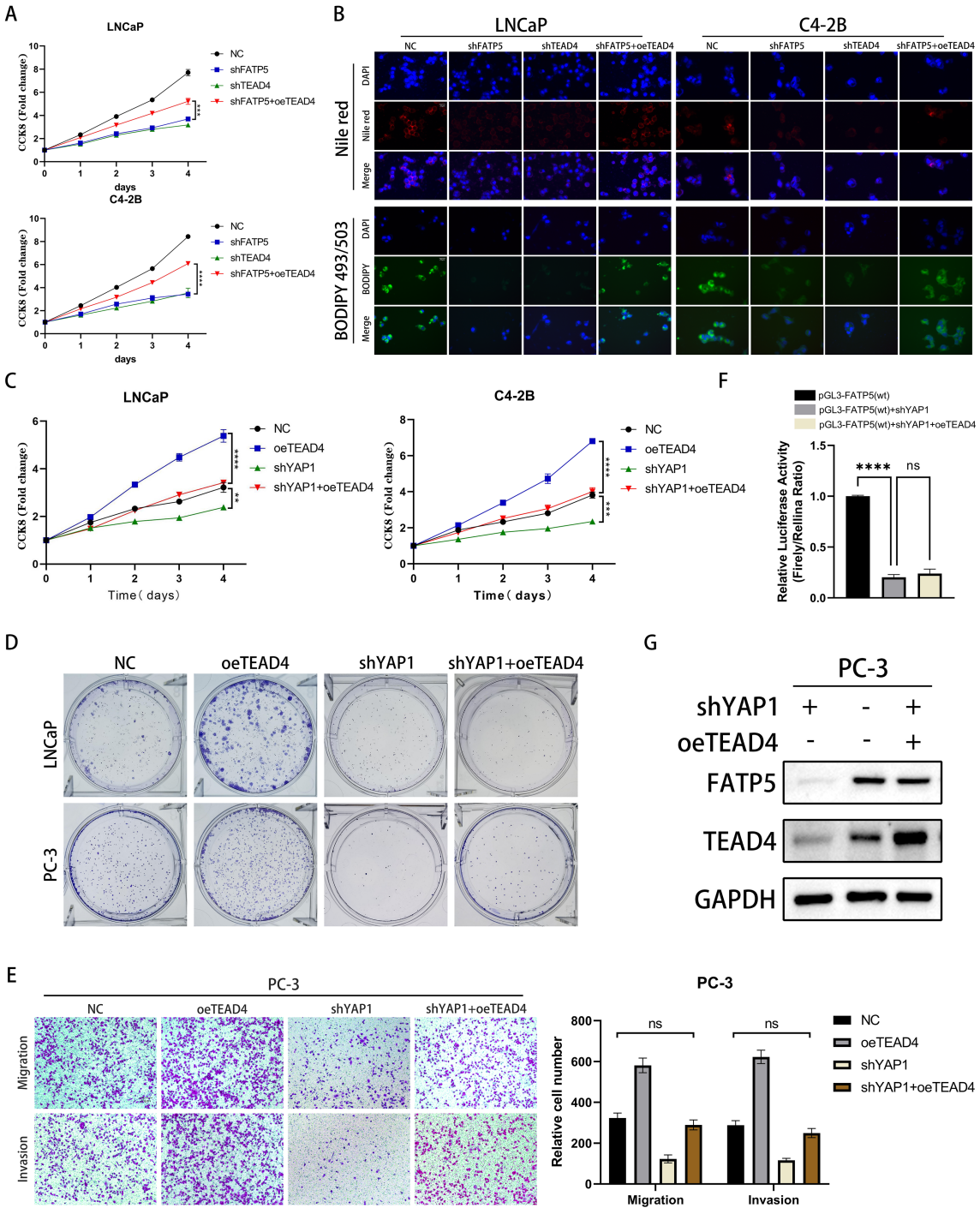

FIGURE 6
TEAD4 regulates the expression of FATP5 and the activity of PCa in a YAP1-dependent manner. **(A)** Conduct a CCK8 assay on the designated cells to assess the cell growth curve. **(B)** Present Nile red and BODIPY 493/503 staining images of the designated cells (Magnification: 400×). **(C)** Perform a CCK8 assay on the designated cells to determine the cell growth curve. **(D)** Perform colony formation assays on the designated cells and document the size and quantity of the resulting colonies. **(E)** Perform Transwell assays on the designated cells to assess their migration and invasion abilities (Magnification: 100×). Mean ± SD, n = 3. **(F)** Present the results of the dual-luciferase reporter gene assay conducted on the designated cells. **(G)** Evaluate the protein expression levels of FATP5 following the corresponding gene manipulation. **p < 0.01,***p < 0.001, and ****p < 0.0001. ns, no significance.

3.6 TEAD4 regulates the expression of FATP5 and the activity of PCa in a YAP1-dependent manner

As a DNA anchor protein, TEAD4's transcriptional reprogramming ability is largely dependent on its interaction with co-activators, such as YAP, which can be classified into two major classes: YAP-dependent and YAP-independent (21). To determine which type of regulation is involved in TEAD4-mediated regulation of FATP5, we established four cell line models: control cell line (NC), TEAD4 overexpression cell line (oeTEAD4), YAP1 knockdown cell line (shYAP1), and YAP1 knockdown cell line with TEAD4 overexpression (shYAP1+oeTEAD4). The results of CCK8 and clonogenic assays demonstrated that knockdown of YAP1 significantly attenuated the proliferative enhancement caused by TEAD4 overexpression (Figures 6C, D, Supplementary Figure S3A). Similarly, Transwell assays confirmed that the enhanced migration and proliferation induced by TEAD4 overexpression were reversed upon YAP1 knockdown (Figure 6E). Furthermore, we performed dual-luciferase reporter gene experiments to analyze the transcriptional regulation of FATP5 after YAP1 knockdown. The results showed that the transcriptional promotion of FATP5 by TEAD4 was greatly inhibited upon YAP1 knockout (Figure 6F). These findings were further supported by Western blot experiments (Figure 6G). Based on our previous experiments, the overexpression of FATP5 promotes YAP1 nuclear translocation, and nuclear YAP1, in turn, binds to TEAD4 to enhance the transcription of FATP5, forming a malignant cycle that promotes the progression of PCa. In summary, we can conclude that TEAD4 regulates the transcription of FATP5 in a YAP1-dependent manner, and the transcriptional activation of FATP5 promotes YAP1 nuclear localization, establishing a malignant cycle that enhances the biological functions of PCa.

3.7 FATP5 affects enzalutamide resistance and targeting the interaction of TEAD4 and YAP1 can reduce the activity of PCa

Previous research has reported that the Hippo signaling pathway often plays a role in drug resistance, and in PCa, androgen deprivation therapy (ADT) frequently leads to drug resistance (22). Therefore, we hypothesized that the knockout of FATP5 may reverse PCa's resistance to enzalutamide and enhance drug sensitivity. We conducted CCK8 experiments first and observed that knocking down FATP5 significantly increased the sensitivity to enzalutamide in both hormone-sensitive LNCaP cells and hormone-resistant C4-2B cells (Figure 7A). Clonogenic assays yielded consistent results, as the formation of colonies was more difficult in FATP5-knockdown cells compared to control cells when treated with varying concentrations of enzalutamide. Subsequently, we determined the IC50 values of the cell groups for enzalutamide and found a noticeable decrease in IC50 values after FATP5 knockdown, supporting our hypothesis. These findings collectively demonstrate that FATP5 can sensitize PCa cells to enzalutamide and partially reverse hormone resistance (Figures 7B, C, Supplementary Figure S3B).

TED-347 is a YAP1-selective inhibitor at the protein level, which dose- and time-dependently inhibits the binding of TEAD4 and YAP1 (23), subsequently affecting biological processes. We treated cells with different concentrations of TED-347 and assessed its impact on FATP5 transcription using dual-luciferase reporter gene experiments. The results indicated that higher TED-347 concentrations resulted in stronger inhibition of FATP5 transcription (Figure 7D). mRNA and protein level analyses also confirmed the inhibitory effect of TED-347 on FATP5 transcription (Figures 7E, F). Transwell assays revealed that TED-347 could influence the migration and invasion abilities of PCa cells (Figure 7G). Furthermore, we investigated the effect of TED-347 on PCa proliferation and demonstrated its ability to inhibit PCa cell growth. Interestingly, when conducting experiments in FATP5-overexpressing cell lines, we observed a decreased sensitivity to TED-347 (Figures 7H, I, Supplementary Figure S3C), suggesting a certain degree of resistance to TED-347 after FATP5 overexpression. Finally, we validated the inhibitory effect of TED-347 *in vivo*, and the results showed that administering TED-347 to mice significantly reduced tumor size, weight, and volume (Figures 7J–L). Furthermore, we repeated the experiment in PC3-oeFATP5 cell line, and the results demonstrated that TED-347 also inhibits the enhanced proliferation induced by FATP5 (Supplementary Figure S4).

4 Discussion

There is mounting evidence suggesting that the FATP family plays a significant role in various types of tumors. For instance, FATP1 has been shown to promote tumor progression in melanoma (8), while FATP3 contributes to immune suppression and tumor activity in lung cancer (24). FATP5 is overexpressed in colorectal cancer and can serve as a prognostic marker (25). These findings underscore the importance of the FATP family in tumorigenesis. However, the role of the FATP family in PCa remains unclear. FATP5 has been found to be upregulated in PCa tissues and cells, consistent with previous findings in colorectal cancer but contradictory to results observed in liver cancer (25, 26). These discoveries imply that FATP5 may exert its effects in multiple cancer types, and the tumor microenvironment and genetic background may influence the physiological function of FATP5 in different tumors. Through a series of *in vitro* and *in vivo* functional experiments, we have demonstrated that FATP5 may promote proliferation, migration, and invasion capabilities in PCa.

Our research has revealed that FATP5 is deeply involved in the lipid metabolism process of PCa. FATP5 is a human protein encoded by the SLC27A5 gene, with a molecular weight of approximately 70-80 kDa and consisting of 690 amino acids (27). It is typically expressed in tissues and cells, and plays a significant role in regulating the transport of exogenous fatty acids and maintaining intracellular lipid homeostasis. FATP5 likely mediates the entry of long-chain fatty acids (LCFAs) into cells by facilitating their translocation across the cell membrane. Furthermore, it catalyzes the ATP-dependent conversion of LCFA and VLCFA into acyl-CoA (28). Through a series of lipid staining experiments and lipidomics analysis, we have discovered that FATP5 enhances lipid accumulation in PCa and significantly

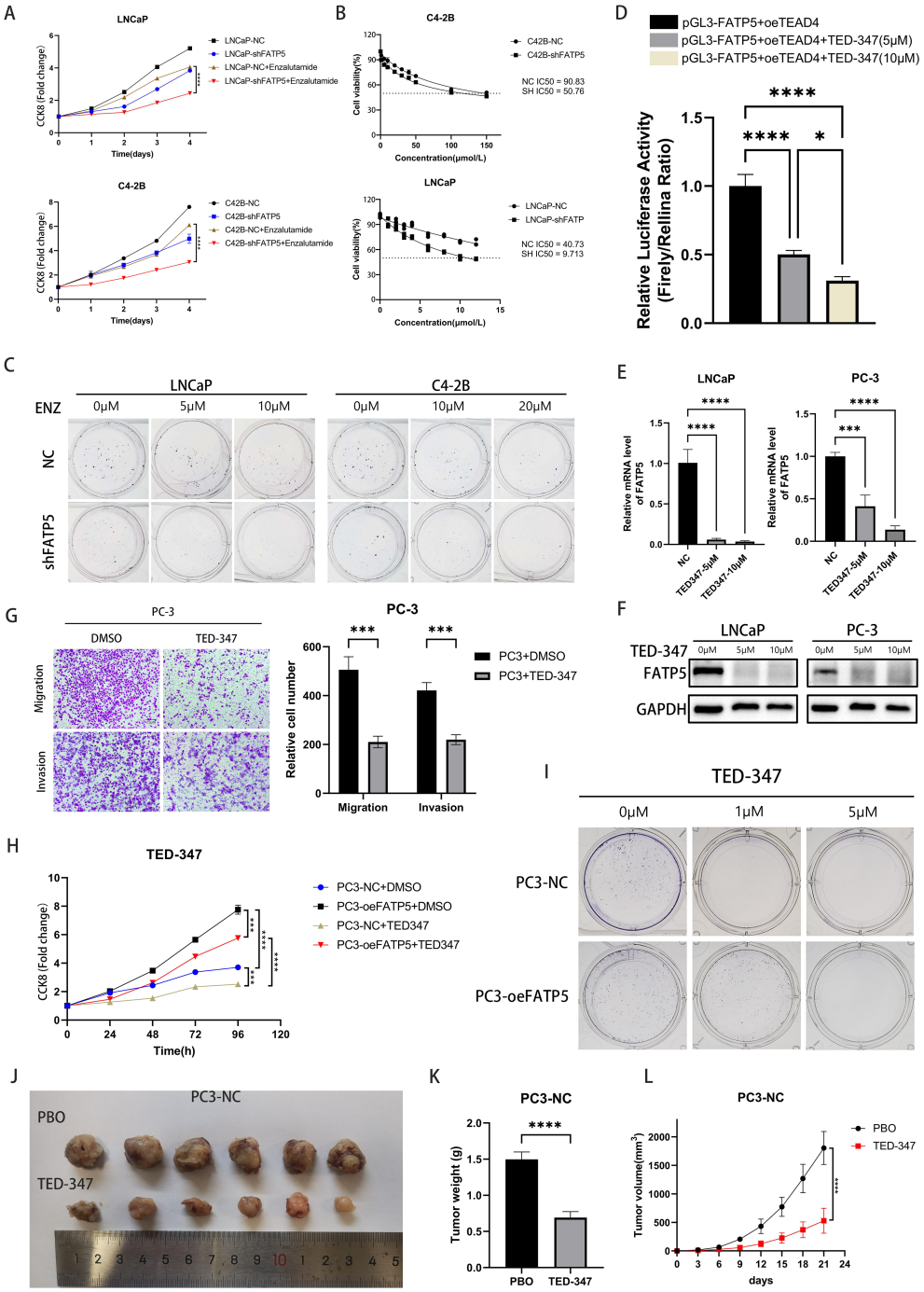

FIGURE 7
FATP5 affects enzalutamide resistance and targeting the interaction of TEAD4 and YAP1 can reduce the activity of PCa. **(A)** Conduct a CCK8 assay on the specified cells to determine the cell growth curve. **(B)** Determine the IC50 values for LNCaP and C4-2B cells. IC50:half maximal inhibitory concentration. **(C)** Perform colony formation assays after knocking down FATP5 and adding varying concentrations of Enzalutamide. **(D)** Measure the dual-luciferase activity in PC3 cells after treating them with different concentrations of TED-347. **(E, F)** Assess the mRNA and protein levels of FATP5 in PC-3 and LNCaP cells following treatment with different concentrations of TED-347. **(G)** Evaluate the migration and invasion capacities of cells after treatment with TED-347. **(H)** Conduct a CCK8 assay on the designated cells following the addition of TED-347 to determine the cell growth curve. **(I)** Conduct colony formation assays on the designated cells after treating them with varying concentrations of TED-347. **(J–L)** Implant tumors in mice and administer either a placebo or TED-347. After 21 days, record the tumor size, weight, and volume in the mice. Mean ± SD, n = 3. *p < 0.5, ***p < 0.001, and ****p < 0.0001.

increases the levels of various lipid metabolites. Additionally, we have validated the ability of FATP5 to enhance fatty acid uptake to some extent using fluorescence probes. These findings are consistent with previous studies on the function of FATP5 and demonstrate its important role in lipid metabolism in PCa. Moreover, the elevated lipid levels within PCa cells have been found to elevate cellular metabolism. We observed that overexpression of FATP5 leads to increased levels of ROS, NADP

+/NADPH, and MDA within the cells, suggesting that the enhanced tumor biological functions resulting from FATP5 overexpression may be Partially attributed to its augmented lipid metabolism levels.

The results of whole transcriptome sequencing reveal a strong correlation between the transcription of FATP5 and the Hippo pathway. In recent years, the Hippo signaling pathway has been found to play a role in various biological processes of tumors, including proliferation, migration, and drug resistance (21). The key protein molecule in the Hippo pathway is YAP1. When the Hippo signaling pathway is inhibited, YAP1 undergoes decreased phosphorylation and degradation, leading to its translocation into the nucleus and subsequent promotion of downstream gene transcription (16). Our study demonstrates that knocking down FATP5 in PCa cells significantly reduces the nuclear levels of YAP1, indicating that FATP5 is capable of driving the nuclear translocation of YAP1. Further investigations revealed that the YAP1 nuclear translocation induced by FATP5 and activation of the Hippo signaling pathway are attributed to its inhibition of AMPK activation, which in turn promotes the activation of β-catenin and RHOA. Consequently, YAP1 nuclear translocation is facilitated. Additionally, the activation of AMPK itself promotes the cytoplasmic retention of YAP1, leading to its phosphorylation and subsequent degradation. Additionally, our research identifies TEAD4, a member of the TEAD transcription factor family, as being involved in the transcriptional process of FATP5, and this transcription is highly dependent on the interaction between TEAD4 and YAP1. Activation of FATP5 transcription occurs only when TEAD4 forms a transcriptional complex with YAP1. Therefore, nuclear YAP1 promotes the transcription of FATP5, and FATP5, in turn, enhances YAP1 nuclear localization, forming a malignant cycle that greatly facilitates the progression of PCa (Figure 8).

The Hippo signaling pathway has been reported to be implicated in drug resistance in tumors. Long-term androgen deprivation therapy (ADT) in PCa patients often leads to the development of irreversible castration-resistant PCa (CRPC) (29), highlighting the crucial need for novel therapeutic approaches. Our study reveals that knockdown of FATP5 enhances the sensitivity of PCa cells to enzalutamide, suggesting that FATP5 may serve as a potential therapeutic target for CRPC. Additionally, small molecule inhibitors targeting the interaction between TEAD4 and YAP1, such as TED-347, have already demonstrated excellent therapeutic efficacy in PCa cells.

However, our study also has certain limitations. For example, we did not investigate the specific mechanism by which FATP5 enhances sensitivity to enzalutamide. Additionally, it has been reported that the FATP family plays a crucial role in promoting the formation of an immunosuppressive tumor microenvironment. Therefore, our future research will focus on elucidating the precise mechanisms by which FATP5 mitigates enzalutamide resistance and its impact on the immune microenvironment. In summary, FATP5 exhibits

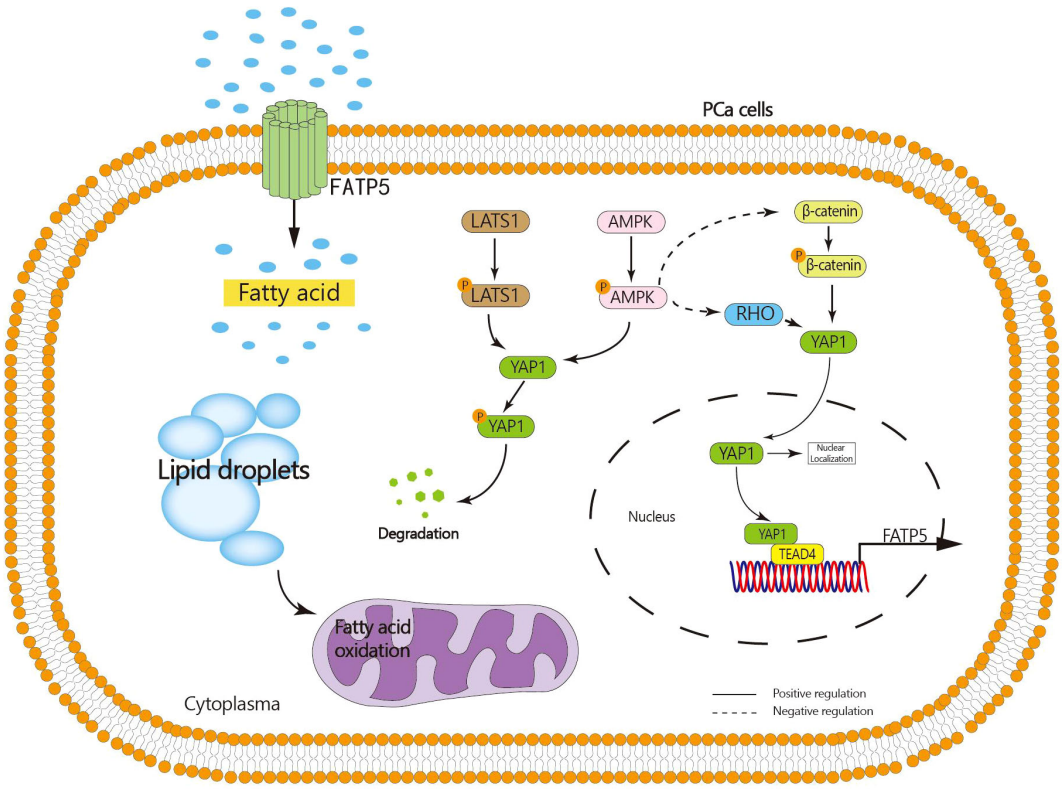

FIGURE 8
Graphical abstract: FATP5 promotes lipid metabolism in PCa cells, inhibits AMPK activation, facilitates nuclear translocation of YAP1, and nuclear YAP1 interacts with TEAD4 to enhance FATP5 transcription.

upregulation in PCa, and TEAD4 mediates the transcription of FATP5 in a YAP1-dependent manner. Furthermore, FATP5 holds potential as a novel diagnostic biomarker and prognostic factor in PCa, offering new therapeutic options for the management of PCa.

In conclusion, the results of this study indicate that FATP5 plays a crucial regulatory role in the progression of PCa. Specifically, overexpression of FATP5 promotes both *in vivo* and *in vitro* progression of PCa and is deeply involved in PCa lipid metabolism, which is dependent on the interaction between TEAD4 and YAP1 in the Hippo signaling pathway. Therefore, targeting the expression of FATP5 or the interaction between TEAD4 and YAP1 may represent a promising therapeutic strategy to reduce PCa proliferation and inhibit disease progression.

Data availability statement

The raw data supporting the conclusions of this article will be made available by the authors, without undue reservation.The data presented in the study are deposited in the NCBI repository, accession number PRJNA1146434

Ethics statement

The studies involving humans were approved by Xinhua Hospital, affiliated with Shanghai Jiao Tong University School of Medicine Ethics Committee. The studies were conducted in accordance with the local legislation and institutional requirements. The human samples used in this study were acquired from primarily isolated as part of your previous study for which ethical approval was obtained. Written informed consent for participation was not required from the participants or the participants' legal guardians/ next of kin in accordance with the national legislation and institutional requirements. The animal study was approved by Xinhua Hospital, affiliated with Shanghai Jiao Tong University School of Medicine Ethics Committee. The study was conducted in accordance with the local legislation and institutional requirements.

Author contributions

SL: Data curation, Investigation, Methodology, Software, Writing – original draft, Writing – review & editing. YH: Data curation, Formal analysis, Investigation, Methodology, Resources, Writing – review & editing. ZG: Conceptualization, Formal analysis, Methodology, Project administration, Supervision, Validation, Writing – review & editing.

Funding

The author(s) declare that no financial support was received for the research, authorship, and/or publication of this article.

Conflict of interest

The authors declare that the research was conducted in the absence of any commercial or financial relationships that could be construed as a potential conflict of interest.

Publisher's note

Supplementary material

The Supplementary Material for this article can be found online at: https://www.frontiersin.org/articles/10.3389/fonc.2024.1442911/full#supplementary-material

References

1. Siegel RL, Miller KD, Fuchs HE, Jemal A. Cancer statistics, 2022. *Ca-a Cancer J Clin*. (2022) 72:7–33. doi: 10.3322/caac.21708

2. Smits M, Ekici K, Naga SP, van Oort IM, Sedelaar MJP, Schalken JA, et al. Prior PSMA PET-CT imaging and hounsfield unit impact on tumor yield and success of molecular analyses from bone biopsies in metastatic prostate cancer. *Cancers*. (2020) 12. doi: 10.3390/cancers12123756

3. Yu F-X, Zhao B, Guan K-L. Hippo pathway in organ size control, tissue homeostasis, and cancer. *Cell*. (2015) 163:811–28. doi: 10.1016/j.cell.2015.10.044

4. Xu X, Wang B, Liu Y, Jing T, Xu G, Zhang L, et al. ETV4 potentiates nuclear YAP retention and activities to enhance the progression of hepatocellular carcinoma. *Cancer Lett*. (2022) 537. doi: 10.1016/j.canlet.2022.215640

5. Costello LC, Franklin RB. The clinical relevance of the metabolism of prostate cancer; zinc and tumor suppression: connecting the dots. *Mol Cancer*. (2006) 5. doi: 10.1186/1476-4598-5-17

6. Koundouros N, Poulogiannis G. Reprogramming of fatty acid metabolism in cancer. *Br J Cancer*. (2020) 122:4–22. doi: 10.1038/s41416-019-0650-z

7. Hirsch D, Stahl A, Lodish HF. A family of fatty acid transporters conserved from Mycobacterium to man. *Proc Natl Acad Sci United States America*. (1998) 95:8625–9. doi: 10.1073/pnas.95.15.8625

8. Zhang M, Di Martino JS, Bowman RL, Campbell NR, Baksh SC, Simon-Vermot T, et al. Adipocyte-derived lipids mediate melanoma progression via FATP proteins. *Cancer Discovery*. (2018) 8:1006–25. doi: 10.1158/2159-8290.CD-17-1371

9. Altuna-Coy A, Ruiz-Plazas X, Sanchez-Martin S, Ascaso-Til H, Prados-Saavedra M, Alves-Santiago M, et al. The lipidomic profile of the tumoral periprostatic adipose tissue reveals alterations in tumor cell's metabolic crosstalk. *BMC Med*. (2022) 20. doi: 10.1186/s12916-022-02457-3

10. Nguyen TTM, Nguyen TH, Kim HS, Dao TTP, Moon Y, Seo M, et al. GPX8 regulates clear cell renal cell carcinoma tumorigenesis through promoting lipogenesis by NNMT. *J Exp Clin Cancer Res*. (2023) 42. doi: 10.1186/s13046-023-02607-2

11. Zhang X. Interactions between cancer cells and bone microenvironment promote bone metastasis in prostate cancer. *Cancer Commun*. (2019) 39. doi: 10.1186/s40880-019-0425-1

12. Ioannidou AG, Watts EJ, Perez-Cornago AC, Platz EK, Mills I, Key T, et al. The relationship between lipoprotein A and other lipids with prostate cancer risk: A multivariable Mendelian randomisation study. *PLoS Med*. (2022) 19. doi: 10.1371/journal.pmed.1003859

13. Clark KL, George JW, Przygrodzka E, Plewes MR, Hua GH, Wang C, et al. Hippo signaling in the ovary: Emerging roles in development, fertility, and disease. *Endocrine Rev*. (2022) 43:1074–96. doi: 10.1210/endrev/bnac013

14. Zhu HP, Yang Y, Wang L, Xu XB, Wang TT, Qian HR. Leptomycin B inhibits the proliferation, migration, and invasion of cultured gastric carcinoma cells. *Bioscience Biotechnol Biochem*. (2020) 84:290–6. doi: 10.1080/09168451.2019.1673148

15. DeRan M, Yang J, Shen C-H, Peters EC, Fitamant J, Chan P, et al. Energy stress regulates hippo-YAP signaling involving AMPK-mediated regulation of angiomotin-like 1 protein. *Cell Rep*. (2014) 9:495–503. doi: 10.1016/j.celrep.2014.09.036

16. Hong AW, Meng ZP, Guan KL. The Hippo pathway in intestinal regeneration and disease. *Nat Rev Gastroenterol Hepatology*. (2016) 13:324–37. doi: 10.1038/nrgastro.2016.59

17. Yao Q, Wu X, Tao C, Gong W, Chen M, Qu M, et al. Osteoarthritis: pathogenic signaling pathways and therapeutic targets. *Signal Transduction Targeted Ther*. (2023) 8. doi: 10.1038/s41392-023-01330-w

18. Gayard M, Guilluy C, Rousselle A, Viollet B, Henrion D, Pacaud P, et al. AMPK alpha 1-induced rhoA phosphorylation mediates vasoprotective effect of estradiol. *Arterioscler Thromb Vasc Biol*. (2011) 31:2634–U704. doi: 10.1161/ATVBAHA.111.228304

19. Hsu SC, Lin CY, Lin YY, Collins CC, Chen CL, Kung HJ. TEAD4 as an oncogene and a mitochondrial modulator. *Front Cell Dev Biol*. (2022) 10. doi: 10.3389/fcell.2022.890419

20. Hwang JJ, Chambon P, Davidson I. Characterization of the transcription activation function and the dna-binding domain of transcriptional enhancer factor-I. *EMBO J*. (1993) 12:2337–48. doi: 10.1002/embj.1993.12.issue-6

21. Dey A, Varelas X, Guan KL. Targeting the Hippo pathway in cancer, fibrosis, wound healing and regenerative medicine. *Nat Rev Drug Discovery*. (2020) 19:480–94. doi: 10.1038/s41573-020-0070-z

22. Nguyen CDK, Yi CL. YAP/TAZ signaling and resistance to cancer therapy. *Trends Cancer*. (2019) 5:283–96. doi: 10.1016/j.trecan.2019.02.010

23. Su WJ, Zhu SK, Chen K, Yang HJ, Tian MW, Fu Q, et al. Overexpressed WDR3 induces the activation of Hippo pathway by interacting with GATA4 in pancreatic cancer. *J Exp Clin Cancer Res*. (2021) 40. doi: 10.1186/s13046-021-01879-w

24. Chiou J, Hsiao M. Down-regulation of fatty acid transporter-encoding gene SLC27A3 modulates immuno-response and correlates with poor prognosis in lung adenocarcinoma. *FASEB J*. (2019) 33. doi: 10.1096/fasebj.2019.33.1_supplement.127.5

25. Geng Q-S, Yang M-J, Li L-F, Shen Z-B, Wang L-H, Zheng Y-Y, et al. Over-expression and prognostic significance of FATP5, as a new biomarker, in colorectal carcinoma. *Front Mol Biosci*. (2022) 8. doi: 10.3389/fmolb.2021.770624

26. Gao QZ, Zhang GJ, Zheng YQ, Yang Y, Chen C, Xia J, et al. SLC27A5 deficiency activates NRF2/TXNRD1 pathway by increased lipid peroxidation in HCC. *Cell Death Differentiation*. (2020) 27:1086–104. doi: 10.1038/s41418-019-0399-1

27. Uchiyama A, Aoyama T, Kamijo K, Uchida Y, Kondo N, Orii T, et al. Molecular cloning of cDNA encoding rat very long-chain acyl-CoA synthetase. *J Biol Chem*. (1996) 271:30360–5. doi: 10.1074/jbc.271.48.30360

28. Zhou W, Madrid P, Fluitt A, Stahl A, Xie XM. Development and validation of a high-throughput screening assay for human long-chain fatty acid transport proteins 4 and 5. *J Biomolecular Screening*. (2010) 15:488–97. doi: 10.1177/1087057110369700

29. Cheng Q, Butler W, Zhou YL, Zhang H, Tang L, Perkinson K, et al. Pre-existing castration-resistant prostate cancer-like cells in primary prostate cancer promote resistance to hormonal therapy. *Eur Urology*. (2022) 81:446–55. doi: 10.1016/j.eururo.2021.12.039

frontiers | Frontiers in Immunology

TYPE Review
PUBLISHED 18 October 2024
DOI 10.3389/fimmu.2024.1476030

OPEN ACCESS

EDITED BY
Ezequiel Moisés Fuentes-Pananá,
Federico Gómez Children's Hospital, Mexico

REVIEWED BY
Qian Yang,
Cedars Sinai Medical Center, United States
Xiuting Liu,
Washington University in St. Louis, United States
Minhong Shen,
Wayne State University, United States
Yenkel Grinberg-Bleyer,
INSERM U1052 Centre de Recherche en Cancerologie de Lyon, France

*CORRESPONDENCE
Bingwei Shi
sbw8133211@163.com
Chongxu Han
Hanchongxu@126.com

†These authors share first authorship

RECEIVED 05 August 2024
ACCEPTED 30 September 2024
PUBLISHED 18 October 2024

CITATION
Cao Y, Yi Y, Han C and Shi B (2024) NF-κB signaling pathway in tumor microenvironment.
Front. Immunol. 15:1476030.
doi: 10.3389/fimmu.2024.1476030

NF-κB signaling pathway in tumor microenvironment

Yaning Cao[1†], Yanan Yi[2†], Chongxu Han[2*] and Bingwei Shi[1*]

[1]Department of Blood Transfusion, Changzhou Hospital of Traditional Chinese Medicine, Changzhou, Jiangsu, China, [2]Department of Laboratory Medicine, Northern Jiangsu People's Hospital Affiliated to Yangzhou University, Yangzhou, Jiangsu, China

The genesis and progression of tumors are multifaceted processes influenced by genetic mutations within the tumor cells and the dynamic interplay with their surrounding milieu, which incessantly impacts the course of cancer. The tumor microenvironment (TME) is a complex and dynamic entity that encompasses not only the tumor cells but also an array of non-cancerous cells, signaling molecules, and the extracellular matrix. This intricate network is crucial in tumor progression, metastasis, and response to treatments. The TME is populated by diverse cell types, including immune cells, fibroblasts, endothelial cells, alongside cytokines and growth factors, all of which play roles in either suppressing or fostering tumor growth. Grasping the nuances of the interactions within the TME is vital for the advancement of targeted cancer therapies. Consequently, a thorough understanding of the alterations of TME and the identification of upstream regulatory targets have emerged as a research priority. NF-κB transcription factors, central to inflammation and innate immunity, are increasingly recognized for their significant role in cancer onset and progression. This review emphasizes the crucial influence of the NF-κB signaling pathway within the TME, underscoring its roles in the development and advancement of cancer. By examining the interactions between NF-κB and various components of the TME, targeting the NF-κB pathway appears as a promising cancer treatment approach.

KEYWORDS

NF-κB signaling pathway, inflammation, tumor microenvironment, cancer metabolism, tumor immunity

1 Introduction

The occurrence and development of tumors, from metastasis to treatment resistance, result from the mutual interaction between cancer cells and the tumor microenvironment (TME). The TME, a complex and dynamic system, primarily comprises tumor cells, adjacent immune and inflammatory cells, tumor-related fibroblasts, surrounding stromal tissues, microvessels, and various cytokines and chemokines (1). Tumor formation is a complex and detailed biological process where cancer cells and their surrounding TME continuously interact and regulate tumor progression. The mutations within tumor cells,

abnormalities in biological traits, persistent inflammation around the tumor and the remodeling of the extracellular Matrix (ECM) represent several closely related biological processes (2, 3). Notably, the components of the TME contribute to various cancer hallmarks, thereby being acknowledged as potential targets for cancer therapy. The TME encompasses both stromal and non-cellular components. Stromal cells consist of immune cells (lymphoid cells, tumor-associated macrophages (TAMs), dendritic cells (DCs), cancer-associated fibroblasts (CAFs), endothelial cells, and pericytes). Non-cellular components include the Extracellular Matrix (ECM), extracellular vesicles (EVs) or exosomes, and the microbiome (3). Tumor-associated stromal cells provide physical support to cancer cells and secrete growth factors, cytokines, chemokines, and ECM proteins that promote tumor growth.

The NF-κB signaling pathway plays a critical role in these processes, which is well-known for its role in regulating immune and inflammatory responses, and its activity is intricately linked with various components of the TME. Persistent activation of NF-κB within the TME can promote chronic inflammation, which in turn supports tumor growth, survival, and metastasis. Given its central role in inflammatory signaling, the relationship between the NF-κB signaling pathway and the TME has garnered considerable interest. Understanding this link is essential for developing targeted therapies aimed at disrupting the pro-tumorigenic interactions within the TME.

2 NF-κB signaling pathway in glance

The nuclear transcription factor NF-κB, recognized for its ability to bind to the enhancer element of the Kappa light chain gene in B cells, plays a pivotal role in regulating innate and adaptive immune responses. Its influence extends across a wide array of biological functions, including cell proliferation, apoptosis, angiogenesis, and tumor metastasis (4). The NF-κB signaling pathway is divided into canonical and non-canonical pathways (5). The canonical NF-κB pathway facilitates the activation of transcription factors such as NF-κB1 (p50), Rel- A (p65), and c-Rel, integral members of the classical NF-κB family. This pathway is quickly and transiently triggered by various extracellular stimuli through receptors like cytokine receptors, pattern recognition receptors (PRRs), tumor necrosis factor receptors (TNFRs), G protein-coupled receptors (GPCRs), T cell receptors (TCRs), and B cell receptors (BCRs) (6).

Conversely, the non-canonical pathway is specifically activated by a selective group of TNF-family cytokines, including lymphotoxin (LT), receptor activator of NF-κB ligand (RANKL), CD40 ligand (CD40L), and B cell activating factor of the TNF family (BAFF/TNFSF13B) (7). Unlike the canonical pathway, the non-canonical route gradually induces the activation of IKK1 and NF-κB inducing kinase (NIK), ultimately influencing the interaction between p52 and Rel-B (8).

In an inactive state, NF-κB is sequestered in the cytoplasm by the IκB-α proteins, which inhibit NF-κB signaling. In respond to inflammatory stimulation, IκB kinases (IKKs) are activated, phosphorylating IκB-α and leading to its ubiquitination by the E3 ubiquitin ligase β-TRCP. This process results in the degradation of IκB-α, freeing NF-κB to migrate to the nucleus and modulate the expression of genes such as tumor necrosis factors-α (TNF-α), interleukin-1(IL-1), and IL-2 (9, 10).

Notably, IKKs consists of two catalytic subunits, IKKα (IKK1) and IKKβ (IKK2), and a regulatory subunit, IKKγ (NEMO). IKKβ is essential for classical NF-κB activation, while IKKα primarily facilitates non-classical NF-κB activation (11) (Figure 1).

3 NF-κB-mediated shaping of the tumor immunity

3.1 NK cells

Natural killer (NK) cells, key effector lymphocytes of the innate immune system, play a crucial role in the suppression of various neoplasms through the secretion of cytolytic mediators such as perforin and granzyme B (12). It was also reported that NK cells turn cancer cells to death directly via perforin and granzyme B, which endorses them to be a valuable tool in cancer treatment (13, 14).

The NF-κB pathway is a key regulator of perforin expression, as demonstrated by Jun Zhou et al. in 2002 (15). Subsequent research by Chunjian Huang et al. in 2006 unveiled a novel NF-κB binding site instrumental in modulating human granzyme B gene transcription in a IL-2 signaling-dependent way (16). Recent studies have demonstrated that, in a head and neck squamous cell carcinoma (HNSCC) model, the ablation of the CHMP2A gene precipitates NF-κB activation in neoplastic cells, culminating in augmented chemokine secretion that facilitates NK cells migration towards the tumor microenvironment (17). In the breast cancer model, the protein Morgana—ubiquitously expressed and pivotal for embryonic development as well as tumorigenesis—has been shown to amplify NF-κB activation, thereby enhancing the recruitment of NK cells and other immune cells to the TME (18, 19).

3.2 T cells

It is well established that NF-κB is essential in the differentiation and function of lymphocytes (20). During T cell development, NF-κB is activated by TCR-peptide-MHC complexes via CARMA1-Bcl1-Malt1(CBM) complex(activated by PKCθ), controlling both the positive and negative selction (20). In contrast to its role in normal lymphocyte development, T cells and B cells recruited to the tumor microenvironment (TME) can either promote or inhibit tumor growth, depending on their specific functions. $CD8^+$ T cells, namely cytotoxic T cells, kill immunogen by secreting cytotoxic cytokines, including IFN-γ and Granzyme (21). Research has shown that expressing a constitutively active form of IKKβ in T cells enhances NF-κB activity, promoting an anti-tumor response that depends on IFN-γ-producing tumor-specific $CD8^+$ T cells (22), highlighting the therapeutic potential of acceleration the IKKβ/NF-κB axis to augment antitumor immunity. A20, a ubiquitin-modifying enzyme encoded by the TNFAIP3 gene, is a critical negative regulator

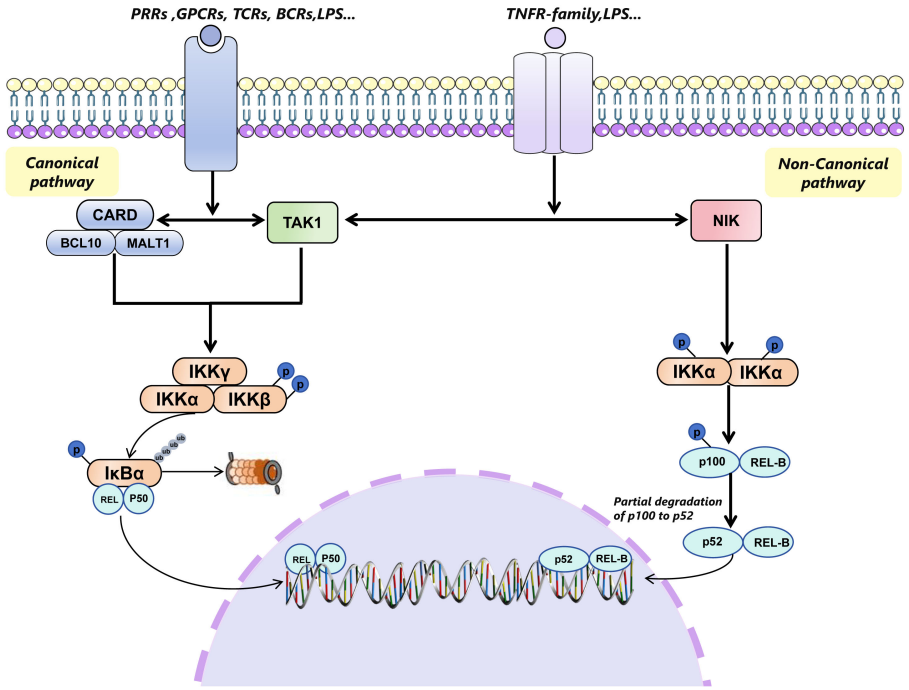

FIGURE 1
Canonical pathway and non-canonical pathway of NF-κB signaling pathway. The canonical NF-κB signaling pathway is initiated by various extracellular stimuli through different receptors, including TLRs, PRRs, TNFRs, GPCRs, TCRs, and BCRs. This activation occurs through the CARD-BCL10-MALT1 (CBM) complex and TAK1, leading to the phosphorylation and activation of the IKK complex (comprising IKKγ(NEMO), IKKα, and IKKβ) specifically through the phosphorylation of IKKβ. The activated IKK complex then phosphorylates members of the inhibitor of κB (IκB) family, such as IκBα, targeting them for ubiquitin (Ub)-dependent degradation in the proteasome. This degradation process releases the Rel-A/p50 or c-Rel/p50 or p50/p50(only Rel-A/50 is shown in Figure 1), which translocates to the nucleus to regulate gene transcription. In contrast, the non-canonical pathway is activated by the members of TNFR superfamily (such as CD40, LTβR and RANK), which specifically engage NIK. NIK then phosphorylates IKKα, leading to the phosphorylation of p100 on its carboxy-terminal serine residues. The phosphorylated p100 undergoes partial degradation to p52, which then associates with REL-B and translocates to the nucleus to participate in transcription events. TLRs, TLR toll-like receptor; PRPs, pattern recognition receptors; TNFRs, tumor necrosis factor receptors; GPCRs, G protein-coupled receptors; TCRs, T cell receptors; BCRs, B cell receptors; TANK1, TGF-β-activated kinase 1; LTβR, LTB lymphotoxin β;RANK, Receptor Activator of NF-κB; NIK, NF-κB-inducing kinase.

of NF-κB. Giordano et al. demonstrated that deleting A20 in $CD8^+$ T cells enhances their cytotoxic function in an NF-κB-dependent manner, illustrating NF-κB's positive role in anti-tumor activity (23). Analysis of patient tumor samples revealed that overall lung tumor NF-κB activity fosters T cell infiltration, attributable to the downregulation of chemokine ligand 20(CCL2)expression linked with tumor growth (24). This inspires us that the maintenance of appropriate NF-κB activity in CD8 T cells is of great importance for antitumor immunity, offering potential clinical applications. Another evidence of a pro-tumoral effect of NF-κB is that overexpression of NIK significantly reduced tumor size and extended survival in MC38 colorectal cancer and B16F10 melanoma models. This was accompanied by an increase in tumor-infiltrating $CD4^+$ and $CD8^+$ T cells, including IFN-γ-producing $CD8^+$ T cells (25).

Compared to $CD8^+$T cells, the indirect impact of $CD4^+$ in TME has aroused increasing attention. Upon stimulated by antigen-peptide-MHC class II complex, $CD4^+$ T cells undergo a multi-step differentiation process to give rise to different $CD4^+$ helper T cell subsets, including Th1, Th2, Th17, Th9 and regulatory T cells (Tregs). In TME, $CD4^+$T cells are recruited to cancer cells by various chemotactic factors and adhesion molecules. Depending on the expression of MHC class II molecules on the tumor cell's surface, CD4 T cells will adopt different strategies to try to kill the cancer cells. When cancer cells highly express MHC II molecules, antigen-presenting cells (APCs) present cancer cells to $CD8^+$ T cells. In such cases, $CD4^+$ T cells mainly play an indirect function in helping effector T cells kill cancer cells. However, when tumor cells lack MHC class II molecules, $CD4^+$ T cells will play a role by secreting various cytokines or assisting other immune cells (26). Conventional $CD4^+Foxp3^-$ T cells (Tconv) is considered as a critical role in the effect of anti-tumor responses. And the function in various diseases is relay on the differentiation of Tconv, which is the result from the stimulation of antigen or drive of cytokine microenvironment. Guilhem Lalle found that different NF-κB subunits has different functions relevant to the context of autoimmunity. In an active murine model experimental autoimmune encephalomyelitis (EAE) model, Rel-A is indispensable for the transition from Tconv to Th17 and thereby protects against inflammation (27). In contrast, in B16-OVA melanoma tumor bearing model, c-Rel rather than Rel-A, was essential for the control of tumor growth and enhancement of anti-PD-1 treatment by impacting $CD4^+$ Tconv (27). Hyunju Oh and Yenkel Grinberg-Bleyer identified c-Rel as crucial for thymic regulatory T cell development, while p65 is vital for maintaining mature Treg identity and immune tolerance (28). Activated Tregs (aTregs), a subset of Tregs, are known to migrate to inflammatory tissues and

the tumor microenvironment, where they act as effective inhibitors of anti-tumor activity. The same research team ulteriorly demonstrated deletion of NF-κB subunit c-Rel in tumor-bearing mice displays a profound decrease of aTregs in TME and ultimately suppresses melanoma growth by boosting the anti-tumor response (29). The different effects of c-Rel on different T cell subsets and the partially redundant effects of different NF-κB isoforms suggest that the integration and construction of the tumor immune microenvironment by NF-κB is complex and requires a nuanced approach to balance complex processes when targeting NF-κB as a tumor therapy.

The CBM (CARMA1-BCL10-MALT1) complex acts as a nexus for the activation of canonical NF-κB signaling following extracellular antigen stimulation through TCR and BCR (30). The loss of *Carma1* in a fraction of Tregs is sufficient to augment antitumor activity and control of tumor size. Importantly, the deletion of CARMA1 or inhibition of MALT1 reverses the insensitivity to the PD-1 blockade therapy via inducing IFN-γ-secretion in TME. The CBM complex/NF-κB pathway activation also triggers the expression of hypoxia-inducible factor-1 (HIF-1α) and IL-6, which initiate the formation of the TME. These molecules further drive Treg proliferation and migration through the MAPK/CDK4/6/Rb and STAT3/SIAH2/P27 pathways, reinforcing the immunosuppressive nature of the TME and accelerating tumor progression (31).

However, in the process of infection and cancer, the cytotoxicity function of $CD8^+$ T undergoes a slow decay which is termed as T cells exhaustion. This exhaustion, driven by factors in the TME, results in a weakened immune response and is marked by the expression of immune checkpoint proteins. One of the primary strategies employed by tumors to evade immune surveillance is through the expression of immunosuppressive receptors such as Programmed Cell Death-1(PD-1) and cytotoxic T lymphocyte-associated antigen-4 (CTLA-4) on effector T cells by their ligands present in the different cell types in TME (32), which leads to the blockade of effector function of normal T cells. Strategies for targeting T and B lymphocytes focus on blocking immune checkpoints, such as CTLA-4 and the PD-1/PD-L1 axis (33). The conditional CD28 knockout model proved that CD28 is needed for $CD8^+$T cells proliferation after PD-1 therapy. The reversion of exhaustion of T cells is CD28-dependent and ultimately enhances the sensitivity of cancer cells to checkpoint blockade.TCR-CD28 co-stimulation is known to activate the CBM complex/NF-κB pathway in T cells, indicating that NF-κB could have a role in immune checkpoint therapy, although this needs further investigation (34). In addition to lymphoid cells, myeloid cells also express checkpoints that used to be targeted in cancer therapy. So some metabolic research has already tried to explain this by the regulation of NF-κB for metabolic reprogramming between oxidative phosphorylation (OXPHOS) and glycolysis in MDSC, which alongside with the change of checkpoints such as PD-1 in MDSC. This process eventually influences anti-immunity such as $CD8^+$T cells responses (35).

3.3 B cells

Compared to T cell, the role of B cells within the TME is multifaceted and presents significant challenges. It has been established that NF-κB signaling pathway is essential in the maturation of B cells. Thomas Pohl et al. found the combined deletion of c-Rel and NF-κB1(p105/p50) displays severe humoral immunity due to profound B cell activation defects (36). In TME, the cancer local environment exhibits an increased presence of switched memory B cells and antibody-secreting B cells, suggesting a potential regulatory role of B cells in tumor progression via the modulation of cytokines, including inflammatory factors (37). Under CXCL13 stimulation, the NF-κB signaling pathway in B cells is activated, leading to the secretion of lymphotoxin (LT), a cytokine that triggers an IKKα–Polycomb complex protein BMI1 pathway. This pathway promotes the metastasis of prostate cancer stem cells by increasing leukocyte infiltration (38).

3.4 TAMs

Macrophages, particularly tumor-associated macrophages (TAMs), are the most abundant and critical cellular components of the TME, orchestrating various aspects of tumor immunity. M1 macrophages, activated through classical pathways, promote antitumor immunity and secrete pro-inflammatory cytokines such as TNF-α, IL-1β, and IL-6. In contrast, alternatively, activated M2 macrophages are linked to pro-tumorigenic activities and anti-inflammatory functions, including tissue repair, angiogenesis, and immunosuppression mediated by IL-10 and transforming growth factor-beta(TGF-β) (39, 40). The classical activation of macrophages, initiated by interferon-gamma (IFN-γ), differs from the alternative activation pathway, which is induced by glucocorticoids, IL-4, IL-13, and IL-10, leading to an immunosuppressive profile (41). Macrophages embody a paradoxical characteristic, capable of both pro-tumorigenic and anti-tumorigenic activities, reflecting their high plasticity and heterogeneity within the TME. In many cancers, including breast, cervical, and prostate cancers, TAMs, displaying generally M2 phenotype and contributing to tumor progression, and their high infiltration is often associated with poor patient prognosis (42). On the other hand, some reports also proved that the high density of TAMs infiltration in the tumor front has a positive relationship with the prognosis of CRC patients (40). Similarly, in colorectal cancer, macrophage in the TME ultimately polarized toward the anti-tumorgenesis phenotype(M1 phenotype) due to the attraction of T cells and the production of pro-inflammatory cytokines and chemokines (43). Taken together, these finding shows the complicated role of TAMs in cancer, which may be credited to the heterogeneity of different local tumor circumstances. As a result, researchers are increasingly focused on identifying and distinguishing TAM subtypes in the TME to better guide treatment strategies and predict patient prognosis by using innovative technologies.

Various signaling have proved to shape the phenotype of TAM, including STAT3, MAPK, IL12-R, Notch signaling pathway and Sema3A/Neuropilin-1 signaling axis et al (39, 40, 43). Among these signaling pathways, NF-κB is a regulating hub to balance between anti-tumorigenic and the pro-tumorigenic functions of TAMs. In 2008, Thorsten Hagemann and colleagues demonstrated that the

depletion of IKK-β activity within TAMs can revert their tumor-promoting phenotype to antitumor M1 phenotype, indicating that reprogramming TAMs by target IKK-β target to eliminate tumor cells (44). Another intriguing study showed targeting NF-κB to induce an M1-like macrophage phenotype significantly reduced peritoneal metastasis of colon tumor *in vivo*. This effect was attributed to increased frequencies of activated $CD4^+$ and $CD8^+$ T cells and reduced angiogenesis (45). The research mentioned above demonstrated that NF-κB is an important driver of the M2-phenotype of TAMs in the tumor islet and eventually promotes the tumor progression via alteration of the inflammation or T cell infiltration in TME. Furthermore, overexpression of the p50 subunit of NF-κB is responsible for the diminished effect of M1-type macrophages *in vivo* and *in vitro*, which eventually changes the inflammation environment of TME (46). In addition to the inflammatory environment, the regulation of angiogenic factors and chemokines by NF-κB in macrophages represents a critical area of focus in cancer research. Vascular Endothelial Growth Factor (VEGF), as a key component of vasculogenesis and angiogenesis during development and physiological homeostasis, has been proven to be upregulated by the inflammatory mediator lipopolysaccharide (LPS) and by engagement of CD40 by CD40 ligand (CD40L), which is dependent the activation of NF-κB signaling (47). These findings describe that a series of cytokines and chemokines regulated by NF-κB in macrophages in the tumor microenvironment affects the inflammatory environment and pro-angiogenic environment in the tumor islet, thereby affecting the effect of the microenvironment on tumor progression in a different aspect.

However, contradictory results emerged in recent seminal projects. Cycling hypoxia(CyH) is a statement of intermittent hypoxia and particularly exists in TAMs. In monocytes, CyH enhances the pro-inflammatory phenotype of M1 macrophages evidenced by increased production of pro-inflammatory cytokines and expression of pro-inflammatory genes by activation of JNK/p65 signaling axis (48). It is an established fact that NF-κB activation in macrophages in the onset of inflammation is related to the expression of proinflammatory genes(e.g.TNF-α, IL-β), whereas NF-κB activation resolution phase is associated with the expression of anti-inflammatory genes(e.g. TGF-β1).In TME, similar to this phenomenon, TAMs driven by NF-κB during the beginning of the tumor tend to produce proinflammatory cytokines such as TNF-α and IL-β to suppress tumor growth. However, with the occurrence and development of tumors, NF-κB-mediated TAMs gradually turn to an anti-inflammatory property, which is manifested as immunosuppression (49, 50). VEGF also plays an indispensable role in the shaping of immunosuppressive microenvironment. On one hand, VEGF-A(a subunit of the VEGF superfamily) directly upregulates the expression of inhibitory receptors involved in T cell exhaustion including CTLA-4, PD-1 and Lag-3.On the other hand, targeting VEGF-A *in vitro* and *in vivo* reverts the inhibitory molecules which is associated with T exhaustion (51). The two coins inspire us that the relationship and crosstalk between T cells and macrophages regulated by NF-κB shape the characteristics of the tumor immune microenvironment. Furthermore, the duality and complexity of NF-κB-mediated TAMs enlighten us that a nuanced understanding of macrophage dynamics within the TME underscores the complexity of the immunological landscape in cancer. It offers insights into potential therapeutic strategies aimed at modulating macrophage function to combat tumor progression.

Of note, TAMs are shown to promote tumor development by maintaining an inflammatory microenvironment. Targeting TAMs' inflammatory signaling pathways, such as the CSF1R pathway, is a current research focus (52). Additionally, TAMs express immune checkpoint ligands, suggesting that lymphocyte-targeting strategies could apply to TAMs as well (53). Targeting the NF-κB signaling pathway, a key chronic inflammatory pathway, has emerged as a significant research direction for cancer treatment.

3.5 DCs

Under physiological conditions, DCs are recognized as the most efficacious professional antigen-presenting cells (APCs), endowed with the capability to engulf, process, and present a diverse array of antigens, inclusive of tumor antigens, to antigen-specific naïve T cells. The growing evidences supports that the relationship between DCs and T cells, based on reciprocal signals exchanged during physical interactions, helps us to have a better understanding of the tension of immunity at the tumor site. The DCs in tumor islets function as shepherds in T cell anti-tumor effect cause DCs not only drive different signals into T cells which is essential in the development and maturation of effector T cell (54). Within the TME, however, DCs constitute a distinct subset of cells characterized by a unique phenotype and functional capacity, manifesting a dichotomous role that spans both pro-tumorigenic and anti-tumorigenic activities. It is well acknowledged that conventional DCs are generally divided into two subsets–cDC1s and cDC2s, which both develop in response to Flt3L from common myeloid progenitors (CMPs) and give rise to pre-cDC1s and pre-cDC2s (54). Recent findings underscored the dynamic nature of tumor-infiltrating dendritic cells (TIDCs), highlighting a pivotal transition from immunostimulatory to immunosuppressive functions as the neoplasm progresses (55). Barbara Maier identified a new cluster of DCs and named it with mature DCs enriched in immunoregulatory molecules (mregDCs), which express various immunoregulatory genes such as *Cd274, Pdcd1lg2and Cd200*. The expression of PD-L1 in mregDCs is induced by the receptor tyrosine kinase AXL with the negative control of IL-4 and positive regulation of IL-12 (56). This delicate regulator of DCs at the tumor site inspires the possibility of reversing the dysfunction and tolerance of DCs in TME to enhance the immunotherapy of cancer. Together these outcome not only delineates the intricate involvement of DCs within the neoplastic landscape but also elucidate a portion of the underlying complexity associated with their role in tumorigenesis.

Pertaining to the mechanistic underpinnings, it has been elucidated that the expression of PD-1 on DCs impedes NF-κB-dependent cytokine secretion through a mechanism contingent upon SHP-2 activation, which ultimately the dysfunction of DCs (57, 58). Yoshimura and colleagues proved that the expression of costimulatory molecules, MHC molecules, and production of

various cytokines by DCs is downregulated by NF-κB activation, such as MHC class II-SIINFEKL complex, TNF-α, IL-6.In contrast, adhesion molecules are up-regulated after inhibiting the activity of NF-κB, indicating the additional effect of NF-κB on the interaction between DCs and T cells (57, 59). Through comparison between the control group and lung cancer patient sera and analysis of transcriptomic, the researcher found that the dysfunction of DCs in TME is controlled by the attenuating canonical NF-κB and STAT3 signaling, especially by reducing the antigen presentation ability of DCs (60). Of note, $CCR7^+$DCs derived from cDC1s almost retain in tumor site and enhance anti-tumor immunity through mediating the expression of various chemokines and cytokines which are essential in the function of T cells and NK cells. The development of $CCR7^+$DCs from cDC1s is dependent on transcription factor IFN regulatory factor 1 (IRF1), which is proved to be regulated by NF-κB in the maturation of tumor infiltrating cDC1s in melanoma model (61). This revelation contributes to a deeper understanding of the molecular pathways influencing DC functionality within the TME, shedding light on the nuanced interplay between immune surveillance and tumor evasion strategies. However, the general positive anti-tumor effect induced by NF-κB in DCs may be a contradiction to the negative effect of inflammation induced by NF-κB in the immune microenvironment such as TAMs and Treg, which shed light on tipping the nuanced balance in the therapy of cancer.

3.6 MDSCs

MDSCs represent a diverse assembly of pathologically activated, immature cellular entities playing a pivotal role in the orchestration of immunosuppressive networks. Characterized by their potent ability to inhibit T-cell mediated responses, MDSCs significantly contribute to the evasion of immune surveillance by malignant neoplasms (62). Emerging evidence underscores the role of MDSCs in tumor infiltration and promotion of angiogenesis, primarily through the secretion of matrix metallopeptidase 9 (MMP9) and their direct integration into the tumor endothelium, facilitating vasculogenesis (63). The deletion of c-Rel in melanoma and lymphoma mice model dramatically reduces the size and weight of the tumor. Compared to the control, the metabolism in $Rel^{-/-}$ MDSCs was significantly reprogrammed with their mitochondrial respiratory parameters decreased and glycolysis enhanced. Notely, inhibiting c-Rel functions as a selective switch of anti-tumoral genes. All these data underscores the important role of c-Rel in the development of MDSCs that promote cancer (64). Furthermore, MDSCs are proved to be activated by the IL-1-induced NF-κB signaling pathway, which is thought to be one of mechanisms that fosters gastric inflammation and the proliferation of carcinoma cell (65). A crosstalk with STAT3 also regulates the functions of MDSCs. A research proved that the myeloid-related protein S100A9 induced by STAT3 enhances the accumulation and production of MDSCs in cancer (66). Another research proved that S100A8/A9-enhanced NADPH oxidase affects downstream NF-κB signaling pathway, which may play role in positive effect on MDSCs recruitment. This underlines the critical function of MDSCs in the modulation of tumor microenvironments via NF-κB, promoting both tumorigenesis and progression. The roles of different NF-κB subunits in the shaping of tumor immune microenvironment is concluded in Table 1.

4 Altering non-immune cells in the surroundings of tumor

4.1 CAFs

CAFs have been identified as pivotal constituents in the dialog between tumor cells and the TME, playing a central role in tumor progression. The fundamental contribution of CAFs to tumorigenesis, including tumor growth, invasion, and metastasis, is attributed to their capacity to modulate tumor-associated inflammation (67). CAFs contribute to breast and pancreatic cancer development by secreting cytokines like CXCL12 and CXCR4 and promoting metastasis through ECM remodeling (68).

TABLE 1 Roles of NF-κB in the shaping of tumor immune microenvironment.

Cell types	Function in Tumor Immunity	NF-κB pathway numbers involved	Effect of NF-κB to immunity	Reference
NK cells	Anti-tumor	NF-κB1/p50,RelA/p65	Enhancement of cytotoxicity	(15, 16, 19)
$CD8^+$T cells	Anti-tumor	RelA/p65,IKKβ,NIK	Enhancement of cytotoxicity	(24, 25)
$CD4^+$T cells	Anti-tumor	RelA/p65,c-Rel	Secretion of inflammatory cytokines	(26)
Tregs	Immunosuppression	RelA/p65,c-Rel	Development and maturation of Treg	(28, 29)
B cells	Anti-tumor	NF-κB1/p50, c-Rel	Development and function of B cells	(36)
M2 macrophages	Pro-tumor	IKK-β, IκB-α, NF-κB1/p50	Induction of tumoricidal activity; Activation of antitumor activity	(44–46)
M1 macrophages	Anti-tumor	RelA/p65	Enhancement of pro-inflammation	(48)
DCs	Anti-tumor	IKKβ	Development and maturation of DCs	(61)
MDSCs	Pro-tumor	c-Rel	Selective regulation of pro-tumoral genes	(64)

NK cells, Natural killer cells; NIK, NF-κB-inducing kinase; Tregs, regulatory T cells; DCs, Dentritic Cells; MDSCs, Myeloid-Derived Suppressor Cells.

Targeting CAFs has potential in preventing tumor growth, with several drugs, including FAP, under clinical trial (69). NF-κB activation within the TME upregulates chemokines, which sustain the TME by recruiting immune and inflammatory cells, as well as progenitors of CAFs (70, 71). Studies have demonstrated that CAFs originating from skin tumors enhance macrophage recruitment, neovascularization, and tumor growth—effects that are abolished by the inhibition of NF-κB signaling (70).

IKKβ, a critical component of the IKK complex, is recognized not only for its essential role within this complex but also for its upstream regulation and pro-tumorigenic influence on NF-κB signaling. Contrary to previous findings, an interesting study revealed that IKKβ deficiency in CAFs promotes intestinal epithelial cell proliferation, inhibits tumor cell apoptosis, increases $CD4^+Foxp3^+$ regulatory T cell accumulation, and stimulates angiogenesis, thereby facilitating colonic tumor growth (72). As precursors to CAFs, mesenchymal cells also play a significant role in the acquisition of cancer characteristics through their interactions with adjacent epithelial and neoplastic cells, as well as other stromal cells. They contribute to the cancerous milieu by providing cytokines and chemokines, growth and survival factors, proangiogenic molecules, and enzymes for extracellular matrix remodeling. Koliaraki have demonstrated that specific deletion of IKKβ in intestinal mesenchymal cells(IMCs) *in vivo* results in reduced tumor incidence following exposure to azoxymethane (AOM) and dextran sodium sulfate(DSS) treatment, which is associated with diminished inflammatory cell infiltration and tissue damage in the initial stages of disease development (73, 74).

4.2 Epithelial cells/Endothelial cells

Epithelial cells, lining the surfaces of organs and body structures, can undergo significant transformations contributing to tumor development and the orchestration of the TME, angiogenesis, and metabolic reprogramming. Recent findings highlight the crucial role of NF-κB in modulating epithelial cell dynamics, primarily through its interactions with other signaling pathways. This interplay between NF-κB and various pathways is essential for regulating the phenotypic transformation of epithelial cells, laying the foundation for tumorigenesis. Notably, Schwitalla et al. demonstrated that NF-κB potentiates Wnt signaling, facilitating the dedifferentiation of epithelial non-stem cells into tumor-initiating cells. This process underscores the significance of NF-κB in the early stages of cancer development (75).

Additionally, IL-6, a downstream effector of NF-κB predominantly secreted by bone marrow-derived myeloid cells, plays a crucial role in this regulatory network. IL-6 activates the STAT3 pathway in both inflammatory and epithelial cells, leading to an increased nuclear presence of β-catenin. This key event in the pathogenesis of colorectal cancer highlights the interconnected roles of these signaling molecules in carcinogenesis (76).

The epithelial-to-mesenchymal transition (EMT) represents a critical shift where epithelial cells adopt mesenchymal characteristics, shedding their inherent epithelial traits (77). NF-κB influences this process by inducing transcription factors such as Twist and Snail, which are pivotal in orchestrating EMT (78, 79). In breast cancer cells, the involvement of NF-κB extends to mediating the expression of key EMT transcription factors, including Slug, Sip1, and Twist1,alongside NF-κB-dependent regulation of ZEB-1/ZFHX1A and ZEB-2/ZFHX1B, also known as Smad-interacting protein (78, 80). In addition, as an classic hallmarker of EMT,MMPs are zinc-dependent endopeptidases that can participate in proteolysis and can cleave several ECM components and non-ECM molecules (81). Identification of MMP-9 to barrier function in intestinal epithelial cell is not dependent on apoptosis and necrosis, but through the NF-κB mediating myosin light chain kinase (MLCK) protein and IL-6 expression, which gives explanation of the invasion of intestinal tumor (82). Conversely, suppression of p65 through siRNA result in the downregulating of MMP-9 in human oesophageal squamous cell cancer (ESCC) and inhibiting the proliferation and invasion ability ESCC (83). This intricate regulatory mechanism by NF-κB underscores its integral role in the modulation of EMT, further implicating its contribution to cancer progression.

In contrast, endothelial cells(ECs) lining the inner vessel wall are in direct face with flowing blood, which is not only relevant for controlling blood fluidity and permeability and orchestrating tumor angiogenesis but also for regulating the antitumor immune response (84). Angiogenesis is thought to mainly include degradation of the endothelial basement membrane and ECM, and directed migration of endothelial cells into surrounding stroma in response to angiogenic stimuli. In ECs, MMPs as an important ECM protease are also crucial in the process of tumor cells' transendothelial migration and acceleration of invasion and metastasis mainly through angiogenesis. Low fluid shear stress in human umbilical vein endothelial cells (HUVECs) greatly induced MMP-9 expression, which is interrupted by the inhibition of the activity of NF-κB (85). It is a fact that platelet-activating factor (PAF) accelerates angiogenesis by promoting various angiogenic factors in a manner dependent on NF-κB. Similarly, Hyun-Mi Ko found that overexpression of p65 induces the activity of MMP-9 luciferase and the mRNA expression of MMP-9, which plays a key role in PAF-induced angiogenesis (86). VEGF interacts with two primary receptor tyrosine kinases: VEGFR1 (fms-like tyrosine kinase, or Flt-1) and VEGFR2 (kinase insert domain receptor/fetal liver kinase-1, or KDR/flk-1) (87). These receptors, along with VEGF, are notably overexpressed in the endothelial cells of blood vessels associated with tumors (88). Research conducted by Fengyun Dong et al. revealed that DHA specifically reduces VEGFR2 expression and this process is connected by the NF-κB motif, suggesting that inhibition of NF-κB could serve as a viable strategy to mitigate tumor angiogenesis (89). Another important chemokine CXCL12, plays a key role in the communication of tumor cells and another component of TME and eventually affects tumor angiogenesis, proliferation and chemoresistance (90). In vascular endothelial cells, Madge et al. demonstrated that the non-canonical NF-κB pathway is crucial for the expression of CXCL12, emphasizing the pathway's significance in mediating angiogenic signals (91). The NF-κB-inducing kinase (NIK) activates this non-canonical signaling route and is often found highly expressed in tumor tissues. Consistently, Noort et al. observed a notable reduction in the number of CXCL12-positive blood vessels which is dependent on non-canonical NF-κB in the

tumor tissue of Nik-/-mice (92), highlighting non-canonical NF-κB components may serve as a focal point modulating vasculogenesis, angiogenesis and the attraction of immune cells (93). In response to various stimuli, endothelial cells secret and synthesize monocyte chemoattractant protein-1 (MCP-1), which is a major chemoattractant for monocytes, T lymphocytes, and basophils and changes the component and function of TME. NF-κB -like binding site and the AP-1 binding site are required for maximal induction of the human MCP-1 promoter by IL-1β, which suggests cytokines inducing MCP-1 in human endothelial cells is dependent on the coordination of NF-κB and AP-1 siganlings (94). A glance of tumor microenvironment regulated by NF-κB via different cell is reviewed in Figure 2.

4.3 Cancer cells

Many reviewers have concluded the tumorigenic process and draw a consensus that generally three phases of tumor: tumor initiation, tumor promotion and tumor progression. In the first stage of tumor, the DNA of tumor cell undergoes mutation and switches between oncogenes and/or the tumor-suppressor genes (e.g.KRAS and p53). The next step of tumorigenesis is the proliferation and growth of tumor cells which is mainly induced by various cytokines(e.g.IL-1, IL-6, TNF-α), which is concluded in the process of promotion. The final step is the invasion and metastasis of cancer cells, which is characterized by additional mutations and entitles the tumor cell with many malignant phenotypes (5).

It is well acknowledged that the activity of NF-κB within tumor cells is also associated with the dynamics of TME and changes the pace of progression of tumor. NF-κB is proven to be an activator of anti-apoptotic genes. In the process of tumor initiation, the activation of NF-κB in tumor cells mediates the epigenetic changes and instability of telomerase activity. For example, in diffuse large B cell lymphomas (DLBCL),p65 binds to the transcription start site (TSS) and regulates miRNA expression such as histone H3K27me3 and histone H3K4me3, which is associated with the progress of carcinoma (95). In human cancer cells, the reactivation of telomerase reactivation is one of the characteristics of cancer progression, which is attributed to the exhibit of a multitude of properties including increased proliferation, increased

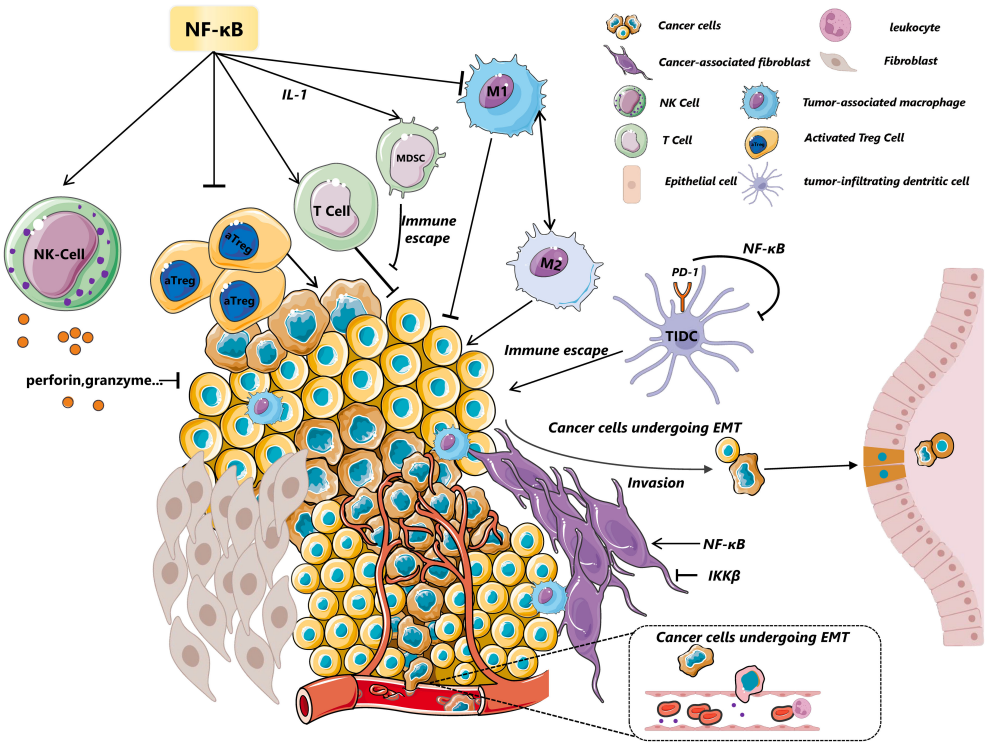

FIGURE 2
A glance of tumor microenvironment regulated by NF-κB. NF-κB modulates the dynamic state of the tumor microenvironment through its effects on various cells, including immune cells and myeloid cells, among others. In NK cells, the activation of the NF-κB pathway upregulates the expression of perforin and granzyme, crucial for inhibiting tumor growth and invasion. MDSCs are influenced by c-Rel-mediated IL-1 signaling, which suppresses T-cell-mediated responses and contributes to immune evasion. Furthermore, p50 or IKKβ drives TAMs towards a tumor-promoting M2 phenotype. In constrast, CyH enhance phenotype of M1 macrophages by activation of JNK/p65 signaling axis. The deletion of the NF-κB subunit c-Rel significantly reduces the generation and maintenance of activated regulatory T cells (aTregs), highlighting its essential role in immunosuppression. NF-κB(p65) also stimulates cancer-associated fibroblasts (CAFs) to enhance macrophage recruitment, neovascularization, and tumor growth via chemokines—a process that contrasts with the effects of IKKβ inhibition. IKKβ deficiency in CAFs promotes intestinal epithelial cell proliferation, inhibits tumor cell apoptosis, increases CD4+Foxp3+ regulatory T cell accumulation, and promote colonic tumor growth. Additionally, NF-κB promotes epithelial-mesenchymal transition (EMT) by inducing the transcription of factors like MMP-9,Twist and Snail, further illustrating its pivotal role in tumor progression and metastasis. CTCs, Circulating Tumor Cells; EMT, Epithelial–Mesenchymal Transition; MDSC, Myeloid-Derived Suppressor Cells; CAFs, Cancer-Associated Fibroblasts; TAMs, Tumor-Associated Macrophages; aTreg, Activated Treg cells; DCs, Dendritic Cells.

resistance to apoptosis and increased invasion. NF-κB transcriptionally upregulates telomerase levels, which binds to p65 and forms feedback to the enhancement of NF-κB -IL-6 axis (96). In the promotion of tumor, NF-κB is an essential switch of anti-apoptosis genes, which include cellular inhibitors of apoptosis (c-IAPs), caspase-8–c-FLIP (FLICE inhibitory protein), A1 (also known as Bfl1), TNFR-associated factor 1 (TRAF1) and TRAF2 (97). The anti-apoptotic properties in tumor cells to some extent endow these cells with the ability of unlimited proliferation and thus promote the occurrence and development of tumors. The inflammation induced by NF-κB is another important part of tumor promotor, which is mainly dependent on the immune cell in TME we have mentioned above. Last but not least, the invasion and metastasis of tumor cells can be regulated by the change of NF-κB. One example of this fact is the expression of matrix-degrading enzymes such as MMP-9 induced by NF-κB. In prostate carcinoma cells, inhibiting NF-κB activity resulted in the downregulation of MMP-9 mRNA, leading to decreased invasion of tumor. In addition, NF-κB signaling blockade inhibited *in vitro* and *in vivo* secretion of VEGF, IL-8, and MMP-9, and hence decreased neoplastic angiogenesis (98). MMP-9, upregulated in angiogenic islets and tumors, enhances the bioavailability of VEGF to its receptors, crucial for angiogenic switching and subsequent tumor growth (99). In breast cancer, the increasing of NF-κB activity leads to the higher expression of testes-specific protease 50 (TSP50) via regulating the secretion of MMP-9,which eventually promotes cell invasion and tumor metastasis (100). VEGF, an acknowledged most endothelial cell-specific angiogenic factor, is produced by various cell types, including endothelial cells(described in the former part) and cancer cells (47). In prostate cancer cells, bombesin(BBS) induced IκB degradation and activated NF-κB, resulting in increased IL-8 and VEGF mRNA expression and stronger migration of HUVECs *in vitro* (101). Consistent with this finding, inhibition of NF-κB activity via IKK2 inhibitor attenuates the expression of VEGF-A and HIF-1α expression and some other inflammatory chemokines CCL2 and CXCL5 in TNF-α-stimulated HUVEC, thereby diminishing the infiltration of inflammatory cells into the corneal stroma (102). Urokinase-type plasminogen activator receptor (uPAR) is displayed high level in in malignant tumors and is thought to be an attractive target for the therapy of many cancers. This interaction between uPAR and uPA initiates a proteolytic cascade that culminates in the degradation of the extracellular matrix (ECM), thereby facilitating the invasion and metastasis of malignant tumors (103). In a pioneering study conducted in 1999, Weixin Wang was the first to demonstrate that uPA is a downstream target gene activated by constitutively active Rel-A in human pancreatic tumor cells (104). This finding underscores the potential critical involvement of constitutive Rel-A activity in tumor progression, specifically in aspects of invasion and metastasis. Further extending our understanding of the molecular mechanisms underlying cancer metastasis, Sliva et al. revealed that Protein Kinase C (PKC) modulates cell motility by regulating uPA expression via the activation of transcription factors AP-1 and NF-κB in breast cancer. This body of work collectively highlights the intricate regulatory networks that govern tumor aggressiveness and offers valuable insights into potential therapeutic targets for combating cancer metastasis (105). The different effects of NF-κB on oncogenesis is concluded in Table 2.

TABLE 2 NF-κB regulates oncogenesis via different ways.

Ways		Cancer types	Target genes	Reference
Shaping of tumor immunity	NK cells	Breast carcinomas, Lung carcinomas, Urothelial carcinomas, Uasal-type NK/T-cell lymphoma	*Perforin*↑	(13, 15)
			Granzyme B↑	(14, 16)
	T cells	Lung carcinomas	*CCL20*↓	(24)
		Colon cancer	*HIF-α*↑	(31)
		Breast cancer	*IL-6*↑	(31)
	B cells	Prostate cancer	*LT*↑	(38)
	TAMs	Ovarian cancer	*IL-1*↓	(44)
		Ovarian carcinomas	*NOS*↓	(44)
	DCs	Ovarian carcinomas	*IL-6*↑	(59)
		Ovarian carcinomas	*TNF-α*↑	(59)
		Ovarian carcinomas	*IL-12*↑	(106)
		Melanoma, Ovarian carcinomas	IFN-γ	(61, 106)
Influencing stromal cells in TME	CAFs	Skin carcinomas	*CXCL1*↑	(70)
		Skin carcinomas	*CXCL12*↑	(70)
		Skin carcinomas	*IL-6*↑	(70)
		Skin carcinomas	*COX-2*↑	(70)

(Continued)

TABLE 2 Continued

Ways		Cancer types	Target genes	Reference
	Epithelial cells	Breast cancer	*Twist*↑	(78)
		Breast cancer	*Snail*↑	(78)
		Breast cancer	*Slug*↑	(78)
		Breast cancer	*Sip1*↑	(78)
	Endothelial cells	Breast cancer	*MMP-9*↑	(86)
		Lung carcinoma	*VEGF*↑	(89)
		breast cancer, colorectal cancer, pancreatic cancer	CXCL12↑	(91, 92)
		Anaplastic thyroid carcinoma	*MCP1*↑	(94, 107)
Angiogenesis and Invasion		Pancreatic tumor, Prostate tumor, Breast cancer	*MMP-9*↑	(99, 100, 108)
		Prostate tumor, Ovarian cancer	*VEGF*↑	(58, 79, 80)
		Melanoma	*CXCL12*↑	(91–93)
		Anaplastic thyroid carcinoma	*MCP1/CCL2*↑	(107, 109)
		Anaplastic thyroid carcinoma	*IL-8/CXCL8*↑	(107, 109, 110)
		Pancreatic tumor, Breast cancer	*uPA(pro-uPA)*↑	(103–105)
Cancer related inflammation		Colitis-associated cancer	*IL-6*↑	(111, 112)
		Pancreatic tumor	*IL-1β*↑	(113)
Crosstalk	STAT3	Colon cancer	*S100A9*↑	(66, 114)
		Colitis-associated cancer	*IL-6*↑	(93)
		Colitis-associated cancer	*COX-2*↑	(5, 33, 70, 115)

TAMs, Tumor-Associated Macrophages; DCs, Dendritic cells; CAFs, Cancer-associated fibroblasts; IL-1,6, Interleukin-1,6; LT, lymphotoxin; NOS, Nitric Oxide Synthase; MMP-9, Matrix metalloproteinase-9; COX-2, Cyclooxygenase-2; MCP-1, monocyte chemotactic protein-1; TNF-α, Tumor Necrosis Factor Alpha; HIF-α, Hypoxia-inducible factor-alpha; CXCL8, C-X-C motif chemokine ligand-8; CCL20, Chemokine Ligand 20; uPA, Urokinase-type plasminogen activator.

5 Crosstalks between different cells regulated by NF-κB in TME

Just as we concluded and reviewed above, TME is a highly complicated system mainly composed of infiltrating immune cells, cancer-associated stromal cells(e.g. CAFs, ECs) and tumor cells, along with the extracellular matrix (ECM) and various molecules (116). It is important to note that their reciprocal interactions either amplify or counteract their effects, giving rise to a complex network within the tumor microenvironment which ultimately governs the occurrence and development of tumors.

The significance of effector T cells as crucial anti-tumor agents within the tumor microenvironment is widely acknowledged, despite their frequent manifestation of anergy or exhaustion. Nevertheless, the other cells in TME present in the tumor microenvironment can modulate effector T cells capacity through interaction and crosstalks, thereby offering potential avenues for ameliorating T cell exhaustion. The dendritic cells (DCs) in tumor-draining lymph nodes of cancer patients can disrupt immunological tolerance by presenting antigens to naive T cells. We now understand that interactions between T cells and DCs not only play a critical role in the cancer immunity cycle, including important reactions within the tumor microenvironment that support anti-tumor responses, but also are essential for controlling tumor and successful cancer immunotherapy (54). So due to the critical role of DCs in shaping the activity of $CD8^+$T cells, increasing effort has been made to repair and enhance the insufficient T cells. The $CCR7^+$DCs that metastasize through lymph nodes migrate to lymph node regions abundant in $CD8^+$ and $CD4^+$ T cells by binding to CLL19 and CCL21 on the cortical surface of lymph nodes(LN). Upon binding antigen peptide-MHC via TCR-CD28 and costimulatory receptors, T cells trigger an immune response, leading to sustained and stable interaction with cDCs in the lymph node region. This promotes cytokine communication between them, resulting in positive feedback that further amplifies the effector T cell-mediated immune effect (54). We have mentioned in the section 3.5, in melanoma model, NF-κB regulate the transcription factor IRF1,which is essential in the development of $CCR7^+$DCs from cDC1s (61). This indicates NF-κB functions as anti-tumoral role through accelerating DCs-T cells interaction. Similarly, Christopher S. Garris found that DCs in TME can sense IFN-γ,which is produce by aPD-1 activated T cells. In turn, DCs produce more IL-12 to enhance the anti-tumor effect of T cells, which is proven to be regulated by non-canonical NF-κB transcription factor pathway (106). Through generating transgenic mice with targeted NIK deletion in $CD11c^+$ DCs, Anand K.

Katakam found that non-canonical NF-κB mediated by NIK is indispensable for DCs to cross-present antigen and initiate $CD8^+$T cells responses to CD40 agonism (117).

Other interactions with different cell types happen in TME as well. a study demonstrated that CAFs is involved in the abnormal differentiation and impaired antigen presenting function of DCs via down-regulating of NF-κB (118). In this aspect, NF-κB appears to play a beneficial role in the anti-tumoral activity by facilitating intercellular communication among different cell types within the tumor microenvironment (TME). Therefore, further investigation is needed to determine whether NF-κB also regulates other crucial immune cell interactions such as B cells-T cells.

6 Linking chronic inflammation to the progression of cancer

Chronic inflammation is widely recognized as a hallmark of cancer, driving tumor progression. NF-κB, a critical inflammatory signaling pathway, acts as a tumor promoter in many cancer types. The inflammatory microenvironment supports tumor growth by enhancing cellular proliferation, survival, migration, and angiogenesis (119). Pro-inflammatory cytokines like TNF-α and IL-6 play key roles in promoting tumor progression.

Notably, in the Mdr2-/- knockout mice model, a model of CAC, a seminal study demonstrated that inhibiting NF-κB signaling in inflammatory and endothelial cells—through IkB-superrepressor induction or anti-TNF-α treatment reverses the process of transformed hepatocytes developing to hepatocellular carcinoma (120), which represented the pioneering attempt to investigate the involvement of NF-κB in both inflammatory processes and carcinogenesis.IL-6, another key factor in this process, is released by myeloid cells under the control of NF-κB and influences various aspects of tumor proliferation (121). Studies have shown that NF-κB signaling can enhance tumor growth both directly and indirectly. Inhibiting IKK-β, a crucial component of the NF-κB pathway, reduces the production of inflammatory mediators like IL-6 and TNF-α, thereby limiting inflammation-driven cell proliferation in CAC (111). Further studies have revealed that the tumor pro-proliferative effects of NF-κB are mediated indirectly through IL-6 and related cytokines produced by myeloid cells. These cytokines activate STAT3 in IECs, affecting both their survival and proliferation (112). Additionally, research has highlighted the role of nitric oxide (NO) in fostering chemoresistance in pancreatic cancer by stimulating IL-1β secretion in tumor cells, thereby safeguarding them against anticancer drugs. This mechanism involves a paracrine-positive feedback loop that activates NF-κB, underlining the complex interplay between inflammation and cancer progression (113).

However, we must admit that the inflammation process is constantly evolving and the effect of NF-κB on cancer is not always positive. So it is complicated and tricky to understand the specific impact of NF-κB on the process of cancer. While NF-κB is a central regulator of gene expression in both innate and adaptive immunity, contributing to the elimination of transformed cells, its function varies contextually. In acute inflammation, NF-κB activation within immune cells often exhibits potent cytotoxic effects against tumor cells (122). Earlier research also reported that in human squamous cell carcinomas (SCCs), co-expression of IκBα, an inhibitor of NF-κB, fires the process of Ras-induced cancer (123), which is consistent with the susceptibility of blockade of NF-κB to squamous cell carcinoma (124). Contradictions emerge regarding the role of IKKβ across different cancer types. In a melanoma mouse model, the deletion of IKKβ in myeloid cells leads to enhanced tumor growth due to the change of myeloid cytokine/chemokine expression (125). Conversely, in a CAC model, the loss of IKKβ in enterocytes accompanies with a diminishment of tumor size even in the presence of heightened inflammation (126). The dual effect of IKKβ may partly account for the lack of clinical success of IKKβ inhibitors to date.

In a chemically induced liver cancer model, the deletion of NEMO in hepatocytes led to spontaneous hepatocellular carcinoma development in mice, suggesting NEMO functions as a tumor suppressor in the liver, revealing a function of NEMO as a tumor suppressor in the liver. However, this effect still requires the activation of NF-κB in Kupffer cells, which induces the expression of cytokines and chemokines (127). This may be explained by the anti-apoptosis character of NF-κB. The deficiency of NEMO in hepatocytes undergoes apoptosis in response to the chemical stimulation which triggers the compensatory proliferation of Kupffer cells and creates a tumor microenvironment associated with inflammation to promote tumor development. The tricky phenomenon may reflect that different cancer systems or different progress of cancer correspond to the involvement of different polarized inflammatory reactions induced by NF-κB. Considering the various effects of NF-κB on tumor progression, it must be cautious to target NF-κB numbers and tip the balance in different biological activity in order to treat cancer.

7 Crosstalks with STAT3 and Wnt/β-catenin signaling pathway

STAT3 plays a pivotal role in various tumor-related processes, including cell proliferation, survival, angiogenesis, and invasion. It is also a crucial factor in tumor-induced immunosuppression at multiple levels (128). In many types of tumor,NF-κB and STAT3 are constitutively activated in response to the upstream autocrine and paracrine factors that are produced within the tumor microenvironment.When receiving the stimulis such as cytokines and growth factors, NF-κB and STAT3 influence the progression of tumor through regulating repression of cytokines, growth factors in tumor cells and some other inflammatory/immune mediators (115).

The most important fact of NF-κB and STAT3 is to regulate the expression of cytokines chemokines and chemoattractants which act in the recruitment and renewal of different cells in the tumor

microenvironment. First of all, STAT3-inducible up-regulation of the myeloid-related protein S100A9 enhances MDSC accumulation, which leads to suppression of anti-tumor immune responses (66). Another research proved that S100A8/A9-enhanced NADPH oxidase affects downstream NF-κB signaling pathway, which may play role in positive effect on MDSCs recruitment (114).

NF-κB and STAT3 act as two major transcriptional factors to link inflammation with tumorigenesis, and they functionally interact with each other at many different layers (33). The interaction between NF-κB and STAT3, however, is complex, as they act as cooperative partners in regulating a variety of target genes that influence tumor progression (33). Key downstream factors of NF-κB such as IL-6 and cyclooxygenase-2 (COX2) not only play critical roles in tumor initiation and progression under the influence of NF-κB but are also involved in STAT3 activation (128). Intriguingly, STAT3 has been shown to mediate the acetylation of NF-κB, enhancing its nuclear retention through the recruitment of acetyltransferase p300.STAT3-mediate acetylation activity leads to continuous NF-κB, which is crucial for alter of tumor microenvironment. On the another hand, constitutive activation of NF-κB results in more secretion of IL-6,which also activates STAT3 and formats a positive activation loop. Moreover, phosphorylated STAT3 has been reported to activate the transcription of proliferative genes through NF-κB, suggesting a positive feedback loop within the NF-κB-IL-6-STAT3 signaling pathway (69). This pathway, as discussed, influences the expression of pro-survival and angiogenic factors like VEGF and MMP9, which are also regulated by STAT3 (79, 128, 129). Additionally, both NF-κB and STAT3 act as transcriptional repressors of p53 expression, a critical tumor suppressor factor in the tumor microenvironment (TME) (69, 130).

Although active NF-κB in immune cells and tumor cells have a crucial role in anti-tumor activity, constitutive activation of NF-κB in tumor cell is recognized as a promoter of pro-survival and angiogenic factors, such as BCL-XL,surviving,MCL1,VEGF and MMP9,which are also regulated by STAT3 (5). It is also proved that STAT3 inhibit IL-12, TNF, IFNβ, CXCL10, CCL5 (also known as RANTES), CD40, CD80, CD86 and MHC class II molecules, which are immune-stimulating genes regulated by NF-κB (131, 132). In this aspect, the relationship of NF-κB and STAT3 seem to be confounding. Another interesting research proved that absence of IKKβ causes STAT3 activation, leading to upregulated ROS accumulation in mouse hepatocellular carcinomas (HCC), and inverse relationships between the activation of NF-κB and STAT3 have also been observed in human HCC (133).

Another important crosstalk of NF-κB is Wnt/β-catenin signaling pathway, which regulates stem cell renewal, organogenesis, cell cycle and inflammation environment of tumor (134, 135). It is now accepted that the abnormal of Wnt/β-catenin signaling pathway is a early event of colorectal tumorigenesis (136, 137). Sarah Schwitalla et al.found NF-κB(p65) directly binds to β-catenin, which increase the expression of Wnt-regulated stem cell gene in IEC, leading to the dedifferentiation of epithelial nonstem cells into tumor-initiating cells (75).

8 The connections of NF-κB and metabolism within TME

8.1 Glycolysis

Metabolic reprogramming is a hallmark of tumor cells, allowing them to meet the material and energy demands of rapid tumor cells proliferation. According to the As outlined by the Warburg hypothesis, cancer cells heavily depend on glycolysis as their main energy source. TME favors anaerobic glycolysis, leading researchers to investigate it as a potential therapeutic target (138, 139). A compelling aspect of NF-κB signaling is its ability to reprogram cellular metabolic networks, thereby sustaining tumor proliferation and driving cancer progression.

Evidence suggests that NF-κB regulates glycolysis in the TME. Rel-A, a key NF-κB subunit, also plays a role in glycolysis regulation. The lack of Rel-A in mouse embryonic fibroblasts (MEFs) shows increasement of glucose consumption and lactate production, which indicates that NF-κB is involved in the process of reprogramming to glycolysis. Furthermore, Rel-A deficient impair the ability of adaptation to glucose starvation and lead to the death of cell instead of reprogramming to OXPHOS (139). Kawauchi et al. found that IKK/NF-κB pathway activation caused increased expression of GLUT3, enhancing glucose uptake and promoting glycolysis. Interestingly, a positive feedback loop between glycolysis and the IKK/NF-κB pathway supports oncogenic transformation driven by H-Ras (140). Interestingly, IKKβ functions as a sensor of glutamine levels in the TME, supporting cancer cell survival through various mechanisms. When glutamine levels are low, IKKβ is activated independently of NF-κB. Through combining with key components of glycosis,such as 6-phosphofructo-2-kinase/fructose-2,6biphosphatase isoform 3 (PFKFB3) and glutamate dehydrogenase 1 (GDH1),IKKβ plays a critical role in inhibiting glycolysis under low glutamine (141).

NF-κB is also a mediator hub of shaping T cell response via reprogramming the metabolism of TME.A study identified that NF-κB-inducing kinase (NIK) stabilize hexokinase 2 (HK2), a rate-limiting enzyme of the glycolytic pathway, by regulating the ROS level and eventually balance the NADPH redox system. The specific deletion of HK2/NIK in mice display impaired aerobic glycolysis and a dysregulated response of T cell to acute infection (25).

8.2 Lipid metabolism

Lipid is an important part of biological membranes and constitution of cells and it is also used by an energy storage and metabolism. Furthermore, lipids also regulate various cellular processes such as uptake, synthesis, and hydrolysis. In the TME, lipid metabolism is reprogrammed to meet the demands of tumor cells, supporting their rapid proliferation, survival, migration, invasion, and metastasis (142).

In gastric cancer, it was proved that FA-induced hyper-O-GlcNAcylation promotes the expression of CD36 by increasing the activity of NF-κB and directly modifying CD36 at S468 and

T470,which is convenient for the metastasis of gastric cancer (143). The deficiency of Rel-A in MEFs and human CRC cell lines leads to the alteration of lipidomic profiles via carboxylesterase 1(CES1), connecting obesity-related inflammation with lipid metabolism in aggressive forms of CRC (144). In *Drosophil*, NF-κB/Relish and Foxo competitively regulate the balance lipid metabolism during metabolic adaptation. Although the process is independent of infection, Relish-Foxo signaling still mediates triglyceride catabolism under chronic bacterial infection, which may also contribution to tumor-associated inflammation (145).

As an important member of NF-κB family, c-Rel is considered as a hazard of cancer and inflammation, which is proved by the fact of lacking c-Rel reduces susceptibility to infectious diseases. A genome-wide associated studies shows that, comparing to control, $Rel^{-/-}$ MDSCs show difference expression of various genes involved in glucose, amino acid, and lipid metabolism and cell cycle checkpoint and proinflammatory activity (64).

GADD45β is a member of the "growth arrest and DNA damage-inducible" (GADD45) gene family. It was identified as a regulator of live fatty acid under fasting stress and keep the balance of normal metabolism of chronic nutrient oversupply (146). In one hand,GADD45β is proved to regulate NF-κB to play a role in antiapoptotic activity in cancer cells. On the other hand, the deletion of GADD45β in MDSCs restores the activation of TAMs and $CD8^+$ T cells infiltration and ultimately hinders the process of tumorgenesis (147).

8.3 Oxidative metabolism and mitochondrial metabolism

In normal cells, glucose deprivation triggers the activation of AMP-activated protein kinase (AMPK), an energy sensor that reprograms cellular metabolism toward fatty acid oxidation and OXPHOS to meet the bioenergetic needs of the cell and maximize energy efficiency (148).

In energy-deficient environments, AMPK, an energy sensor, shifts cellular metabolism towards fatty acid oxidation and OXPHOS to optimize energy production. OXPHOS, a key component of mitochondrial metabolism, is often dysregulated and reprogrammed in malignant tumor cells. This metabolic plasticity is exploited by cancer cells, contributing to tumorigenesis (149).

Just as we demonstrated in section 3.2, regulation of NF-κB for metabolic reprogramming OXPHOS and glycolysis in MDSC, which alongside with the change of checkpoint such as PD-1 in MDSC, which involves in anti-immunity such as $CD8^+$T cells responses. Ting Li et al. found that comparing to wild type cells, $Rel^{-/-}$ MDSCs displayed diminishing OXPHOS flux and mitochondrial ATP production, while increasing glycolysis. While C/EBPβ overexpression in Rel knockout MDSCs isolated from LysM-Cre/RelF/F mice effectively rescued their phenotype, reducing glycolysis and increasing OXPHOS and expression of proinflammatory cytokines (28). These results align with the concept that OXPHOS-based metabolism is a hallmark of immunosuppressive cells, such as Tregs and M2 TAMs (150). Consistently, the inhibition of NF-κB/Rel-A in MEFs resulted in decreased oxygen consumption and glycolytic reprogramming, with augmented glucose consumption and lactate production, which is reversed by p53 reconstitution in Rel-$A^{-/-}$ cells, suggesting the indispensable role of NF-κB/p53 axis in metabolic adaptation in normal cells and cancer (149).

9 Role of NF-κB in the resistance to therapy via TME

It is well documented that NF-κB signaling pathway functions in enhancing drug resistance in chemotherapy, immunotherapy, endocrine, and targeted therapy. Increasing numbers of studies proved that chemotherapy for cancer also depends on the interaction between cancer cells and the surrounding TME components (151). We will conclude the mechanism of resistance induced by NF-κB in different cell components of TME.

Just we mentioned above, TAMs as the most abundant population of tumor-infiltrating immune cells within TME, are generally divided into two subsets– pro-inflammatory classical (M1) and suppressive alternatively activated (M2) subtypes. In most cases, just as we mentioned above, the activation of NF-κB induces the M2 macrophage in TME, which is a promoter of tumor progression (152). TNFα secreting from TAMs promotes melanoma resistance to MAPK pathway inhibitors through NF-κB via regulation of expression of the microphthalmia transcription factor (MITF) (153). Another report found that in the duration of antitumor immunity by inducing interferon (IFN) response, the activation of NF-κB by a long noncoding RNA-IFN-responsive nuclear factor-κB activator (IRENA) in M1 macrophages and increased secretion of pro-inflammatory cytokines, which promote breast cancer chemoresistance (154). In human ovarian cancer (OC) cells, NF-κB mediates the enhanced expression and production of CCL2 and stimulates the activation of the PI3K/Akt pathway, which results in the development of paclitaxel resistance. During this process, CCL2 also functions as a chemotactic factor, inducing macrophage chemotaxis, which may lead to chemotherapy resistance (155). Another research proved triptolide(TPL) could inhibit the migration and invasion of OC cells *in vitro* and *in vivo* by inhibiting the polarization of M2 TAMs, which reduced the tumor burden via PI3K/Akt/NF-κB signaling pathway (156). Using 10x Genomics single-cell sequencing technology, CCL5 was increased secreted undergoing aPKCι-induced EMT and consequently modulated macrophage recruitment and polarization dependent on NF-κB signaling, which eventually leads to gemcitabine resistance (157).

As a major component of the tumor stroma, CAFs function in the dialogue between tumor cells and the TME, playing a central role in tumor progression, including tumorigenesis, supporting angiogenesis, fostering resistance to therapy, and suppressing antitumor immune responses. circZFR was highly expressed in cisplatin (DDP)-resistant HCC cell lines and the CAFs-derived exosome, regulating DDP resistance of the HCC cells via STAT3/NF-κB signaling (158). Lnc RNA UPK1A-AS1 induced by IL8/NF-κB signaling in CAFs serves as a chemoresistance promotor and is critical for active IL8-induced oxaliplatin resistance in pancreatic

ductal adenocarcinoma (PDAC) (159). Similarly, CAF-derived IL-8 promotes chemoresistance in human gastric cancer via NF-κB activation (160).

MDSCs activated the PI3K/AKT NF-κB signaling pathway in B cells through the PD-1/PD-L1 axis, which forms the immunosuppressive functions of PD-1^{+}PD-L1^{+} B cells, which suggests the role of NF-κB in PD-1 therapy resistance and the combined targeting of PI3K/AKT and PD-1/PD-L1 tactics (161). In T cells, the deletion of CARMA1 or inhibition of MALT1 enhances the sensitivity to the PD-1 blockade therapy via inducing IFN-γ-secretion in TME, which we just mentioned in section 3.2 (162).

Considering the positive effect of NF-κB in different components of TME to therapy resistance, the research found strategies for reversing drug resistance mainly involved in NF-κB inhibitors, which showed promising outcomes in preclinical experiments although there is a long distance to get the clinical application before finding a better balance between positive and negative effect.

10 Discussion

A wealth of research in recent years has been paid attention to the role of NF-κB in the orchestration and dynamics of TME. In this review, we intend to highlight the pleiotropic role of the NF-κB signaling pathway in more aspects of TME. NF-κB signaling pathway appears to be crucial in shaping tumor immune microenvironment, changing the function of stromal cells of TME, regulating angiogenesis and invasion and linking inflammation with tumorgenesis, leading to directly or indirectly influence the dynamics switch between anti-tumoral activity and pro-tumoral activity. Although several fundamental research findings presented in this review demonstrate the crucial role of NF-κB signaling in orchestrating the tumor microenvironment, it is important to acknowledge that potential biases may exist due to the methodology employed in these studies, thereby causing confusion regarding the precise involvement of NF-κB in the tumor microenvironment. Firstly, part of the NF-κB signaling involved in the shaping of cytokines affecting the tumor microenvironment has only been verified in tumor cell lines (109). Additionally, RNA sequencing has been employed in several studies to investigate disparities in gene expression among cancer patients (57), with a specific focus on enhancing the NF-κB signaling pathway. However, it is imperative to further explore and elaborate upon these findings due to the potential overlap between signaling pathways and the distinct roles played by certain genes.

A comprehensive understanding of the complicated role of NF-κB signaling in TME entitles researchers to better explain the effect of therapies targeting NF-κB signaling. It is well documented that TNF-αinducing NF-κB signaling and regulate the expression of anti-apoptosis and cell cycle progression genes. So inhibition of NF-κB or anti-TNF-α may offer an attractive combined strategy for immunomodulatory cancer therapy. p50 knockout macrophages exhibited more T cell infiltration and higher expression of pro-inflammatory cytokines *in vivo*, which enlightens us that targeting p50 represents an innovative anticancer strategy, complementary to immunostimulatory strategies (46). In melanoma and lymphoma,c-Rel is proven to play a central role in aTreg and MDSC biology and suggests that c-Rel deletion has effects on anti-tumor responses (64). Pentoxifylline (PTXF), an FDA-approved drug, can cause selective degradation of c-Rel, without affecting p65.PTXF has been widely used in the therapy of type 2 diabetes mellitus and chronic kidney disease (CKD). Although the role of c-Rel in shaping of Treg and MDSC in TME is well acknowledged, the inhibitor of c-Rel such as PTXF or R96A has not been used in the clinical trial. What is more, given the importance of CARMA1-BCL10-MALT1 as an NF-κB platform complex in lymphocyte development and function, multiple studies have confirmed that MALT1 suppression in Treg cells will reshape the immune microenvironment convenience to immune checkpoint therapy (162). Of note, IKKβ inhibitors have demonstrated efficacy in various pre-clinical models of cancer and inflammatory disease. For instance, MLN-120B(the ATP-competitive IKKβ inhibitor) is convinced to be a promoter of therapeutic efficiency in mouse models of rheumatoid arthritis(RA). Furthermore, clinical trials of the drugs inhibiting IKKβ are still rare in considering the various reasons, including the important role of IKKβ in some cases, improper dose plan and impertinent patient group selection (163). In contrast to the fact of tumor-promoting functions of NF-κB in both malignant and inflammatory immune cells, the activation of the IKKβ/NF-κB signaling axis in CAFs was surprisingly found to be a tumor suppressor of intestinal tumor growth (72).

The complexity and heterogeneity of the TME also pose substantial challenges to such targeted approaches. For instance, TAMs exhibit varied phenotypes based on their differentiation, significantly impacting tumor evolution and the TME (164, 165). Moreover, the specificity of the TME to each tumor's organ or tissue of origin, coupled with the pre-existing conditions such as chronic inflammation in cancers of the colon, stomach, and liver (as opposed to gliomas and breast cancers), further complicates therapeutic interventions (166). It is also crucial to acknowledge the sophisticated feedback mechanisms regulating NF-κB activation, necessitating a cautious and well-considered approach in leveraging NF-κB targeting as a cancer treatment strategy.

The fundamental principles and findings from prior clinical trials collectively indicate that NF-κB is more likely to have side effects. This consensus is based on the fact that NF-κB plays an indispensable role in many biological processes, including immune cell development, normal cell proliferation, and so on, and its inhibition may produce undesirable side effects. So before we can safely put targeting or inhibiting NF-κB to clinical application, we must realize the putative efficacy mainly depends on the type of cancer and the dynamics immune microenvironment. But during the dynamic changing of NF-κB in TME, the short-term inhibitor of this signaling in the peak range may be efficient in the therapy of cancer. For example, as a characteristic of activated B cell-like Diffuse large B-cell lymphoma (ABC DLBCL), constitutive activation of NF-κB signaling drives cancer cell proliferation/survival (167), which provides a shred of reasonable evidence for therapeutic strategies targeting IKKβ/NF-κB. On the other side, it is still not an advisable therapy to singly inhibit NF-κB signaling number to achieve the clinical expectation. The use of synergistic

combinations between targeting NF-κB and other immune therapy is to expected be employed to achieve a desired therapeutic effect, thus reducing systemic toxicity. Just as we mentioned above, in some cases, NF-κB may serve as a tumor suppressor, which suggests it must be cautious to control the duration and dosage of this treatment plan.

Author contributions

YC: Writing – original draft, Writing – review & editing. YY: Writing – original draft. BS: Writing – review & editing. CH: Writing – review & editing, Funding acquisition, Validation.

Funding

The author(s) declare financial support was received for the research, authorship, and/or publication of this article. This work was supported by National Key Research and Development Program of China (No.2015CB755402) and Northern Jiangsu People's Hospital (No. SBJC21017).

Acknowledgments

The authors thank to from my colleagues from Changzhou Hospital of Traditional Chinese Medicine for their assistance with figure illustration in the manuscript.

Conflict of interest

The authors declare that the research was conducted in the absence of any commercial or financial relationships that could be construed as a potential conflict of interest.

Publisher's note

References

1. Vitale I, Manic G, Coussens LM, Kroemer G, Galluzzi L. Macrophages and metabolism in the tumor microenvironment. *Cell Metab*. (2019) 30:36–50. doi: 10.1016/j.cmet.2019.06.001

2. Marozzi M, Parnigoni A, Negri A, Viola M, Vigetti D, Passi A, et al. Inflammation, extracellular matrix remodeling, and proteostasis in tumor microenvironment. *Int J Mol Sci*. (2021) 22:8102. doi: 10.3390/ijms22158102

3. Naser R, Fakhoury I, El-Fouani A, Abi-Habib R, El-Sibai M. Role of the tumor microenvironment in cancer hallmarks and targeted therapy (Review). *Int J Oncol*. (2023) 62:23. doi: 10.3892/ijo.2022.5471

4. Wan F, Lenardo MJ. The nuclear signaling of NF-kappaB: current knowledge, new insights, and future perspectives. *Cell Res*. (2010) 20:24–33. doi: 10.1038/cr.2009.137

5. Karin M, Greten FR. NF-kappaB: linking inflammation and immunity to cancer development and progression. *Nat Rev Immunol*. (2005) 5:749–59. doi: 10.1038/nri1703

6. Taniguchi K, Karin M. NF-κB, inflammation, immunity and cancer: coming of age. *Nat Rev Immunol*. (2018) 18:309–24. doi: 10.1038/nri.2017.142

7. Sun SC, Ley SC. New insights into NF-kappaB regulation and function. *Trends Immunol*. (2008) 29:469–78. doi: 10.1016/j.it.2008.07.003

8. Steinberg GR, Hardie DG. New insights into activation and function of the AMPK. *Nat Rev Mol Cell Biol*. (2022). doi: 10.1038/s41580-022-00547-x

9. Vallabhapurapu S, Karin M. Regulation and function of NF-kappaB transcription factors in the immune system. *Annu Rev Immunol*. (2009) 27:693–733. doi: 10.1146/annurev.immunol.021908.132641

10. Hayden MS, Ghosh S. Shared principles in NF-kappaB signaling. *Cell*. (2008) 132:344–62. doi: 10.1016/j.cell.2008.01.020

11. Yu H, Lin L, Zhang Z, Zhang H, Hu H. Targeting NF-κB pathway for the therapy of diseases: mechanism and clinical study. *Signal Transduction Targeting Ther*. (2020) 5:209. doi: 10.1038/s41392-020-00312-6

12. Gaptulbarova KA, Tsyganov MM, Pevzner AM, Ibragimova MK, Litviakov NV. NF-kB as a potential prognostic marker and a candidate for targeted therapy of cancer. *Exp Oncol*. (2020) 42:263–9. doi: 10.32471/10.32471/exp-oncology.2312-8852.vol-42-no-4

13. Fantini M, Arlen PM, Tsang KY. Potentiation of natural killer cells to overcome cancer resistance to NK cell-based therapy and to enhance antibody-based immunotherapy. *Front Immunol*. (2023) 14:1275904. doi: 10.3389/fimmu.2023.1275904

14. Rousalova I, Krepela E. Granzyme B-induced apoptosis in cancer cells and its regulation (review). *Int J Oncol*. (2010) 37:1361–78. doi: 10.3892/ijo_00000788

15. Zhou J, Zhang J, Lichtenheld MG, Meadows GG. A role for NF-kappa B activation in perforin expression of NK cells upon IL-2 receptor signaling. *J Immunol Baltim. Md 1950*. (2002) 169:1319–25. doi: 10.4049/jimmunol.169.3.1319

16. Huang C, Bi E, Hu Y, Deng W, Tian Z, Dong C, et al. A novel NF-kappaB binding site controls human granzyme B gene transcription. *J Immunol Baltim. Md 1950*. (2006) 176:4173–81. doi: 10.4049/jimmunol.176.7.4173

17. Bernareggi D, Xie Q, Prager BC, Yun J, Cruz LS, Pham TV, et al. CHMP2A regulates tumor sensitivity to natural killer cell-mediated cytotoxicity. *Nat Commun*. (2022) 13:1899. doi: 10.1038/s41467-022-29469-0

18. Fusella F, Seclì L, Brancaccio M. Escaping NK cells and recruiting neutrophils: How Morgana/NF-κB signaling promotes metastasis. *Mol Cell Oncol*. (2018) 5:e1432258. doi: 10.1080/23723556.2018.1432258

19. Fusella F, Seclì L, Busso E, Krepelova A, Moiso E, Rocca S, et al. The IKK/NF-κB signaling pathway requires Morgana to drive breast cancer metastasis. *Nat Commun*. (2017) 8:1636. doi: 10.1038/s41467-017-01829-1

20. Gerondakis S, Fulford TS, Messina NL, Grumont RJ. NF-κB control of T cell development. *Nat Immunol*. (2014) 15:15–25. doi: 10.1038/ni.2785

21. Paul MS, Ohashi PS. The roles of CD8+ T cell subsets in antitumor immunity. *Trends Cell Biol*. (2020) 30:695–704. doi: 10.1016/j.tcb.2020.06.003

22. Evaristo C, Spranger S, Barnes SE, Miller ML, Molinero LL, Locke FL, et al. Cutting edge: engineering active IKKβ in T cells drives tumor rejection. *J Immunol Baltim. Md 1950*. (2016) 196:2933–8. doi: 10.4049/jimmunol.1501144

23. Giordano M, Roncagalli R, Bourdely P, Chasson L, Buferne M, Yamasaki S, et al. The tumor necrosis factor alpha-induced protein 3 (TNFAIP3, A20) imposes a brake on antitumor activity of CD8 T cells. *Proc Natl Acad Sci U S A*. (2014) 111:11115–20. doi: 10.1073/pnas.1406259111

24. Hopewell EL, Zhao W, Fulp WJ, Bronk CC, Lopez AS, Massengill M, et al. Lung tumor NF-κB signaling promotes T cell-mediated immune surveillance. *J Clin Invest*. (2013) 123:2509–22. doi: 10.1172/JCI67250

25. Gu M, Zhou X, Sohn JH, Zhu L, Jie Z, Yang J-Y, et al. NF-κB-inducing kinase maintains T cell metabolic fitness in antitumor immunity. *Nat Immunol*. (2021) 22:193–204. doi: 10.1038/s41590-020-00829-6

26. Speiser DE, Chijioke O, Schaeuble K, Münz C. CD4+ T cells in cancer. *Nat Cancer*. (2023) 4:317–29. doi: 10.1038/s43018-023-00521-2

27. Lalle G, Lautraite R, Bouherrou K, Plaschka M, Pignata A, Voisin A, et al. NF-κB subunits RelA and c-Rel selectively control $CD4^+$ T cell function in multiple sclerosis and cancer. *J Exp Med*. (2024) 221. doi: 10.1084/jem.20231348

28. Oh H, Grinberg-Bleyer Y, Liao W, Maloney D, Wang P, Wu Z, et al. An NF-κB transcription-factor-dependent lineage-specific transcriptional program promotes

regulatory T cell identity and function. *Immunity*. (2017) 47:450–465.e5. doi: 10.1016/j.immuni.2017.08.010

29. Grinberg-Bleyer Y, Oh H, Desrichard A, Bhatt DM, Caron R, Chan TA, et al. NF-κB c-rel is crucial for the regulatory T cell immune checkpoint in cancer. *Cell*. (2017) 170:1096–1108.e13. doi: 10.1016/j.cell.2017.08.004

30. Ruland J, Hartjes L. CARD-BCL-10-MALT1 signalling in protective and pathological immunity. *Nat Rev Immunol*. (2019) 19:118–34. doi: 10.1038/s41577-018-0087-2

31. Qi T, Luo Y, Cui W, Zhou Y, Ma X, Wang D, et al. Crosstalk between the CBM complex/NF-κB and MAPK/P27 signaling pathways of regulatory T cells contributes to the tumor microenvironment. *Front Cell Dev Biol*. (2022) 10:911811. doi: 10.3389/fcell.2022.911811

32. Hashimoto M, Kamphorst AO, Im SJ, Kissick HT, Pillai RN, Ramalingam SS, et al. CD8 T Cell exhaustion in chronic infection and cancer: opportunities for interventions. *Annu Rev Med*. (2018) 69:301–18. doi: 10.1146/annurev-med-012017-043208

33. Fan Y, Mao R, Yang J. NF-κB and STAT3 signaling pathways collaboratively link inflammation to cancer. *Protein Cell*. (2013) 4:176–85. doi: 10.1007/s13238-013-2084-3

34. Kamphorst AO, Wieland A, Nasti T, Yang S, Zhang R, Barber DL, et al. Rescue of exhausted CD8 T cells by PD-1-targeted therapies is CD28-dependent. *Science*. (2017) 355:1423–7. doi: 10.1126/science.aaf0683

35. Capece D, Verzella D, Flati I, Arboretto P, Cornice J, Franzoso G, et al. NF-κB: blending metabolism, immunity, and inflammation. *Trends Immunol*. (2022) 43:757–75. doi: 10.1016/j.it.2022.07.004

36. Pohl T, Gugasyan R, Grumont RJ, Strasser A, Metcalf D, Tarlinton D, et al. The combined absence of NF-kappa B1 and c-Rel reveals that overlapping roles for these transcription factors in the B cell lineage are restricted to the activation and function of mature cells. *Proc Natl Acad Sci U S A*. (2002) 99:4514–9. doi: 10.1073/pnas.072071599

37. Downs-Canner SM, Meier J, Vincent BG, Serody JS. B cell function in the tumor microenvironment. *Annu Rev Immunol*. (2022) 40:169–93. doi: 10.1146/annurev-immunol-101220-015603

38. Ammirante M, Kuraishy AI, Shalapour S, Strasner A, Ramirez-Sanchez C, Zhang W, et al. An IKKα-E2F1-BMI1 cascade activated by infiltrating B cells controls prostate regeneration and tumor recurrence. *Genes Dev*. (2013) 27:1435–40. doi: 10.1101/gad.220202.113

39. Wu K, Lin K, Li X, Yuan X, Xu P, Ni P, et al. Redefining tumor-associated macrophage subpopulations and functions in the tumor microenvironment. *Front Immunol*. (2020) 11:1731. doi: 10.3389/fimmu.2020.01731

40. Forssell J, Oberg A, Henriksson ML, Stenling R, Jung A, Palmqvist R, et al. High macrophage infiltration along the tumor front correlates with improved survival in colon cancer. *Clin Cancer Res*. (2007) 13:1472–9. doi: 10.1158/1078-0432.CCR-06-2073

41. Gordon S, Martinez FO. Alternative activation of macrophages: mechanism and functions. *Immunity*. (2010) 32:593–604. doi: 10.1016/j.immuni.2010.05.007

42. Condeelis J, Pollard JW. Macrophages: obligate partners for tumor cell migration, invasion, and metastasis. *Cell*. (2006) 124. doi: 10.1016/j.cell.2006.01.007

43. Ong S-M, Tan Y-C, Beretta O, Jiang D, Yeap W-H, Tai JJY, et al. Macrophages in human colorectal cancer are pro-inflammatory and prime T cells towards an anti-tumour type-1 inflammatory response. *Eur J Immunol*. (2012) 42:89–100. doi: 10.1002/eji.201141825

44. Hagemann T, Lawrence T, McNeish I, Charles KA, Kulbe H, Thompson RG, et al. "Re-educating" tumor-associated macrophages by targeting NF-kappaB. *J Exp Med*. (2008) 205:1261–8. doi: 10.1084/jem.20080108

45. Ryan AE, Colleran A, O'Gorman A, O'Flynn L, Pindjacova J, Lohan P, et al. Targeting colon cancer cell NF-κB promotes an anti-tumour M1-like macrophage phenotype and inhibits peritoneal metastasis. *Oncogene*. (2015) 34:1563–74. doi: 10.1038/onc.2014.86

46. Saccani A, Schioppa T, Porta C, Biswas SK, Nebuloni M, Vago L, et al. p50 nuclear factor-kappaB overexpression in tumor-associated macrophages inhibits M1 inflammatory responses and antitumor resistance. *Cancer Res*. (2006) 66:11432–40. doi: 10.1158/0008-5472.CAN-06-1867

47. Kiriakidis S, Andreakos E, Monaco C, Foxwell B, Feldmann M, Paleolog E, et al. VEGF expression in human macrophages is NF-kappaB-dependent: studies using adenoviruses expressing the endogenous NF-kappaB inhibitor IkappaBalpha and a kinase-defective form of the IkappaB kinase 2. *J Cell Sci*. (2003) 116:665–74. doi: 10.1242/jcs.00286

48. Delprat V, Tellier C, Demazy C, Raes M, Feron O, Michiels C, et al. Cycling hypoxia promotes a pro-inflammatory phenotype in macrophages via JNK/p65 signaling pathway. *Sci Rep*. (2020) 10:882. doi: 10.1038/s41598-020-57677-5

49. Biswas SK, Lewis CE. NF-κB as a central regulator of macrophage function in tumors. *J Leukoc Biol*. (2010) 88:877–84. doi: 10.1189/jlb.0310153

50. Balkwill F, Charles KA, Mantovani A. Smoldering and polarized inflammation in the initiation and promotion of Malignant disease. *Cancer Cell*. (2005) 7:211–7. doi: 10.1016/j.ccr.2005.02.013

51. Voron T, Colussi O, Marcheteau E, Pernot S, Nizard M, Pointet A-L, et al. VEGF-A modulates expression of inhibitory checkpoints on CD8+ T cells in tumors. *J Exp Med*. (2015) 212:139–48. doi: 10.1084/jem.20140559

52. Poh AR, Ernst M. Targeting macrophages in cancer: from bench to bedside. *Front Oncol*. (2018) 8:49. doi: 10.3389/fonc.2018.00049

53. Umezu D, Okada N, Sakoda Y, Adachi K, Ojima T, Yamaue H, et al. Inhibitory functions of PD-L1 and PD-L2 in the regulation of anti-tumor immunity in murine tumor microenvironment. *Cancer Immunol Immunother CII*. (2018) 68:201–11. doi: 10.1007/s00262-018-2263-4

54. Pittet MJ, Di Pilato M, Garris C, Mempel TR. Dendritic cells as shepherds of T cell immunity in cancer. *Immunity*. (2023) 56:2218–30. doi: 10.1016/j.immuni.2023.08.014

55. Ma Y, Shurin GV, Peiyuan Z, Shurin MR. Dendritic cells in the cancer microenvironment. *J Cancer*. (2013) 4:36–44. doi: 10.7150/jca.5046

56. Maier B, Leader AM, Chen ST, Tung N, Chang C, LeBerichel J, et al. A conserved dendritic-cell regulatory program limits antitumour immunity. *Nature*. (2020) 580:257–62. doi: 10.1038/s41586-020-2134-y

57. Yoshimura S, Bondeson J, Brennan FM, Foxwell BM, Feldmann M. Role of NFkappaB in antigen presentation and development of regulatory T cells elucidated by treatment of dendritic cells with the proteasome inhibitor PSI. *Eur J Immunol*. (2001) 31:1883–93. doi: 10.1002/1521-4141(200106)31:6<1883::AID-IMMU1883>3.0.CO;2-V

58. Karyampudi L, Lamichhane P, Krempski J, Kalli KR, Behrens MD, Vargas DM, et al. PD-1 Blunts the Function of Ovarian Tumor-Infiltrating Dendritic Cells by Inactivating NF-κB. *Cancer Res*. (2016) 76:239–50. doi: 10.1158/0008- 5472.CAN-15-0748

59. Yoshimura S, Bondeson J, Foxwell BM, Brennan FM, Feldmann M. Effective antigen presentation by dendritic cells is NF-kappaB dependent: coordinate regulation of MHC, co-stimulatory molecules and cytokines. *Int Immunol*. (2001) 13:675–83. doi: 10.1093/intimm/13.5.675

60. Li R, Fang F, Jiang M, Wang C, Ma J, Kang W, et al. STAT3 and NF-κB are simultaneously suppressed in dendritic cells in lung cancer. *Sci Rep*. (2017) 7:45395. doi: 10.1038/srep45395

61. Ghislat G, Cheema AS, Baudoin E, Verthuy C, Ballester PJ, Crozat K, et al. NF-κB-dependent IRF1 activation programs cDC1 dendritic cells to drive antitumor immunity. *Sci Immunol*. (2021) 6:eabg3570. doi: 10.1126/sciimmunol.abg3570

62. Wu Y, Yi M, Niu M, Mei Q, Wu K. Myeloid-derived suppressor cells: an emerging target for anticancer immunotherapy. *Mol Cancer*. (2022) 21:184. doi: 10.1186/s12943-022-01657-y

63. Ahn G-O, Brown JM. Matrix metalloproteinase-9 is required for tumor vasculogenesis but not for angiogenesis: role of bone marrow-derived myelomonocytic cells. *Cancer Cell*. (2008) 13:193–205. doi: 10.1016/j.ccr.2007.11.032

64. Li T, Li X, Zamani A, Wang W, Lee C-N, Li M, et al. c-rel is a myeloid checkpoint for cancer immunotherapy. *Nat Cancer*. (2020) 1:507–17. doi: 10.1038/s43018-020-0061-3

65. Tu S, Bhagat G, Cui G, Takaishi S, Kurt-Jones EA, Rickman B, et al. Overexpression of interleukin-1beta induces gastric inflammation and cancer and mobilizes myeloid-derived suppressor cells in mice. *Cancer Cell*. (2008) 14:408–19. doi: 10.1016/j.ccr.2008.10.011

66. Cheng P, Corzo CA, Luetteke N, Yu B, Nagaraj S, Bui MM, et al. Inhibition of dendritic cell differentiation and accumulation of myeloid-derived suppressor cells in cancer is regulated by S100A9 protein. *J Exp Med*. (2008) 205:2235–49. doi: 10.1084/jem.20080132

67. Kalluri R. The biology and function of fibroblasts in cancer. *Nat Rev Cancer*. (2016) 16:582–98. doi: 10.1038/nrc.2016.73

68. Xiao Y, Yu D. Tumor microenvironment as a therapeutic target in cancer. *Pharmacol Ther*. (2021) 221:107753. doi: 10.1016/j.pharmthera.2020.107753

69. Hoesel B, Schmid JA. The complexity of NF-κB signaling in inflammation and cancer. *Mol Cancer*. (2013) 12:86. doi: 10.1186/1476-4598-12-86

70. Erez N, Truitt M, Olson P, Arron ST, Hanahan D. Cancer-associated fibroblasts are activated in incipient neoplasia to orchestrate tumor-promoting inflammation in an NF-kappaB-dependent manner. *Cancer Cell*. (2010) 17:135–47. doi: 10.1016/j.ccr.2009.12.041

71. Jung D-W, Che ZM, Kim J, Kim K, Kim KY, Williams D, et al. Tumor-stromal crosstalk in invasion of oral squamous cell carcinoma: a pivotal role of CCL7. *Int J Cancer*. (2010) 127:332–44. doi: 10.1002/ijc.v127:2

72. Pallangyo CK, Ziegler PK, Greten FR. IKKβ acts as a tumor suppressor in cancer-associated fibroblasts during intestinal tumorigenesis. *J Exp Med*. (2015) 212:2253–66. doi: 10.1084/jem.20150576

73. Koliaraki V, Pasparakis M, Kollias G. IKKβ in intestinal mesenchymal cells promotes initiation of colitis-associated cancer. *J Exp Med*. (2015) 212:2235–51. doi: 10.1084/jem.20150542

74. Koliaraki V, Pallangyo CK, Greten FR, Kollias G. Mesenchymal cells in colon cancer. *Gastroenterology*. (2017) 152:964–79. doi: 10.1053/j.gastro.2016.11.049

75. Schwitalla S, Fingerle AA, Cammareri P, Nebelsiek T, Göktuna SI, Ziegler PK, et al. Intestinal tumorigenesis initiated by dedifferentiation and acquisition of stem-cell-like properties. *Cell*. (2013) 152:25–38. doi: 10.1016/j.cell.2012.12.012

76. Bollrath J, Phesse TJ, von Burstin VA, Putoczki T, Bennecke M, Bateman T, et al. gp130-mediated Stat3 activation in enterocytes regulates cell survival and cell-cycle progression during colitis-associated tumorigenesis. *Cancer Cell*. (2009) 15:91–102. doi: 10.1016/j.ccr.2009.01.002

77. Oh A, Pardo M, Rodriguez A, Yu C, Nguyen L, Liang O, et al. NF-κB signaling in neoplastic transition from epithelial to mesenchymal phenotype. *Cell Commun Signal CCS*. (2023) 21:291. doi: 10.1186/s12964-023-01207-z

78. Pires BRB, Mencalha AL, Ferreira GM, de Souza WF, Morgado-Díaz JA, Maia AM, et al. NF-kappaB is involved in the regulation of EMT genes in breast cancer cells. *PloS One*. (2017) 12:e0169622. doi: 10.1371/journal.pone.0169622

79. Yu H, Pardoll D, Jove R. STATs in cancer inflammation and immunity: a leading role for STAT3. *Nat Rev Cancer*. (2009) 9:798–809. doi: 10.1038/nrc2734

80. Wang Y, Zhou BP. Epithelial-mesenchymal transition in breast cancer progression and metastasis. *Chin J Cancer*. (2011) 30:603–11. doi: 10.5732/cjc.011.10226

81. Li Y, He J, Wang F, Wang X, Yang F, Zhao C, et al. Role of MMP-9 in epithelial-mesenchymal transition of thyroid cancer. *World J Surg Oncol*. (2020) 18:181. doi: 10.1186/s12957-020-01958-w

82. Al-Sadi R, Engers J, Haque M, King S, Al-Omari D, Ma TY, et al. Matrix Metalloproteinase-9 (MMP-9) induced disruption of intestinal epithelial tight junction barrier is mediated by NF-κB activation. *PloS One*. (2021) 16:e0249544. doi: 10.1371/journal.pone.0249544

83. Wang F, He W, Fanghui P, Wang L, Fan Q. NF-κBP65 promotes invasion and metastasis of oesophageal squamous cell cancer by regulating matrix metalloproteinase-9 and epithelial-to-mesenchymal transition. *Cell Biol Int*. (2013) 37:780–8. doi: 10.1002/cbin.10089

84. Leone P, Malerba E, Susca N, Favoino E, Perosa F, Brunori G, et al. Endothelial cells in tumor microenvironment: insights and perspectives. *Front Immunol*. (2024) 15:1367875. doi: 10.3389/fimmu.2024.1367875

85. Sun H-W, Li C-J, Chen H-Q, Lin H-L, Lv H-X, Zhang Y, et al. Involvement of integrins, MAPK, and NF-kappaB in regulation of the shear stress-induced MMP-9 expression in endothelial cells. *Biochem Biophys Res Commun*. (2007) 353:152–8. doi: 10.1016/j.bbrc.2006.12.002

86. Ko H-M, Park Y-M, Jung B, Kim H-A, Choi J-H, Park SJ, et al. Involvement of matrix metalloproteinase-9 in platelet-activating factor-induced angiogenesis. *FEBS Lett*. (2005) 579:2369–75. doi: 10.1016/j.febslet.2005.03.035

87. Ferrara N, Gerber H-P, LeCouter J. The biology of VEGF and its receptors. *Nat Med*. (2003) 9:669–76. doi: 10.1038/nm0603-669

88. Kolch W, Martiny-Baron G, Kieser A, Marmé D. Regulation of the expression of the VEGF/VPS and its receptors: role in tumor angiogenesis. *Breast Cancer Res Treat*. (1995) 36:139—155. doi: 10.1007/BF00666036

89. Dong F, Zhou X, Li C, Yan S, Deng X, Cao Z, et al. Dihydroartemisinin targets VEGFR2 via the NF-κB pathway in endothelial cells to inhibit angiogenesis. *Cancer Biol Ther*. (2014) 15:1479–88. doi: 10.4161/15384047.2014.955728

90. Meng W, Xue S, Chen Y. The role of CXCL12 in tumor microenvironment. *Gene*. (2018) 641:105–10. doi: 10.1016/j.gene.2017.10.015

91. Madge LA, Kluger MS, Orange JS, May MJ. Lymphotoxin-alpha 1 beta 2 and LIGHT induce classical and noncanonical NF-kappa B-dependent proinflammatory gene expression in vascular endothelial cells. *J Immunol Baltim. Md 1950*. (2008) 180:3467–77. doi: 10.4049/jimmunol.180.5.3467

92. Noort AR, van Zoest KP, Weijers EM, Koolwijk P, Maracle CX, Novack DV, et al. NF-κB-inducing kinase is a key regulator of inflammation-induced and tumour-associated angiogenesis. *J Pathol*. (2014) 234:375–85. doi: 10.1002/path.4403

93. Teicher BA, Fricker SP. CXCL12 (SDF-1)/CXCR4 pathway in cancer. *Clin Cancer Res*. (2010) 16:2927–31. doi: 10.1158/1078-0432.CCR-09-2329

94. Martin T, Cardarelli PM, Parry GC, Felts KA, Cobb RR. Cytokine induction of monocyte chemoattractant protein-1 gene expression in human endothelial cells depends on the cooperative action of NF-kappa B and AP-1. *Eur J Immunol*. (1997) 27:1091–7. doi: 10.1002/eji.1830270508

95. Vento-Tormo R, Rodríguez-Ubreva J, Lisio LD, Islam ABMMK, Urquiza JM, Hernando H, et al. NF-κB directly mediates epigenetic deregulation of common microRNAs in Epstein-Barr virus-mediated transformation of B-cells and in lymphomas. *Nucleic Acids Res*. (2014) 42:11025–39. doi: 10.1093/nar/gku826

96. Ghosh A, Saginc G, Leow SC, Khattar E, Shin EM, Yan TD, et al. Telomerase directly regulates NF-κB-dependent transcription. *Nat Cell Biol*. (2012) 14:1270–81. doi: 10.1038/ncb2621

97. Karin M, Lin A. NF-kappaB at the crossroads of life and death. *Nat Immunol*. (2002) 3:221–7. doi: 10.1038/ni0302-221

98. Huang S, Pettaway CA, Uehara H, Bucana CD, Fidler IJ. Blockade of NF-kappaB activity in human prostate cancer cells is associated with suppression of angiogenesis, invasion, and metastasis. *Oncogene*. (2001) 20:4188–97. doi: 10.1038/sj.onc.1204535

99. Bergers G, Brekken R, McMahon G, Vu TH, Itoh T, Tamaki K, et al. Matrix metalloproteinase-9 triggers the angiogenic switch during carcinogenesis. *Nat Cell Biol*. (2000) 2:737–44. doi: 10.1038/35036374

100. Song ZB, Ni J-S, Wu P, Bao YL, Liu T, Li M, et al. Testes-specific protease 50 promotes cell invasion and metastasis by increasing NF-kappaB-dependent matrix metalloproteinase-9 expression. *Cell Death Dis*. (2015) 6:e1703. doi: 10.1038/cddis.2015.61

101. Levine L, Lucci JA, Pazdrak B, Cheng J-Z, Guo Y-S, Townsend CM, et al. Bombesin stimulates nuclear factor kappa B activation and expression of proangiogenic factors in prostate cancer cells. *Cancer Res*. (2003) 63:3495–502. doi: 10.4049/jimmunol.153.5.2052

102. Lennikov A, Mirabelli P, Mukwaya A, Schaupper M, Thangavelu M, Lachota M, et al. Selective IKK2 inhibitor IMD0354 disrupts NF-κB signaling to suppress corneal inflammation and angiogenesis. *Angiogenesis*. (2018) 21:267–85. doi: 10.1007/s10456-018-9594-9

103. Zhai B-T, Tian H, Sun J, Zou J-B, Zhang X-F, Cheng J-X, et al. Urokinase-type plasminogen activator receptor (uPAR) as a therapeutic target in cancer. *J Transl Med*. (2022) 20:135. doi: 10.1186/s12967-022-03329-3

104. Wang W, Abbruzzese J, Evans D, Chiao P. Overexpression of urokinase-type plasminogen activator in pancreatic adenocarcinoma is regulated by constitutively activated RelA. *Oncogene*. (1999) 18:4554—4563. doi: 10.1038/sj.onc.1202833

105. Sliva D, English D, Lyons D, Lloyd FP. Protein kinase C induces motility of breast cancers by upregulating secretion of urokinase-type plasminogen activator through activation of AP-1 and NF-kappaB. *Biochem Biophys Res Commun*. (2002) 290:552–7. doi: 10.1006/bbrc.2001.6225

106. Garris CS, Arlauckas SP, Kohler RH, Trefny MP, Garren S, Piot C, et al. Successful anti-PD-1 cancer immunotherapy requires T cell-dendritic cell crosstalk involving the cytokines IFN-γ and IL-12. *Immunity*. (2018) 49:1148–1161.e7. doi: 10.1016/j.immuni.2018.09.024

107. Hoffmann E, Dittrich-Breiholz O, Holtmann H, Kracht M. Multiple control of interleukin-8 gene expression. *J Leukoc Biol*. (2002) 72:847–55. doi: 10.1189/jlb.72.5.847

108. Bruni-Cardoso A, Johnson LC, Vessella RL, Peterson TE, Lynch CC. Osteoclast-derived matrix metalloproteinase-9 directly affects angiogenesis in the prostate tumor-bone microenvironment. *Mol Cancer Res MCR*. (2010) 8:459–70. doi: 10.1158/1541-7786.MCR-09-0445

109. Ueda A, Okuda K, Ohno S, Shirai A, Igarashi T, Matsunaga K, et al. NF-kappa B and Sp1 regulate transcription of the human monocyte chemoattractant protein-1 gene. *J Immunol Baltim. Md 1950*. (1994) 153:2052—2063. doi: 10.4049/jimmunol.153.5.2052

110. Passaro C, Borriello F, Vastolo V, Di Somma S, Scamardella E, Gigantino V, et al. The oncolytic virus dl922-947 reduces IL-8/CXCL8 and MCP-1/CCL2 expression and impairs angiogenesis and macrophage infiltration in anaplastic thyroid carcinoma. *Oncotarget*. (2016) 7:1500–15. doi: 10.18632/oncotarget.6430

111. Greten FR, Eckmann L, Greten TF, Park JM, Li Z-W, Egan LJ, et al. IKKbeta links inflammation and tumorigenesis in a mouse model of colitis-associated cancer. *Cell*. (2004) 118:285–96. doi: 10.1016/j.cell.2004.07.013

112. Grivennikov S, Karin E, Terzic J, Mucida D, Yu G-Y, Vallabhapurapu S, et al. IL-6 and Stat3 are required for survival of intestinal epithelial cells and development of colitis-associated cancer. *Cancer Cell*. (2009) 15:103—113. doi: 10.1016/j.ccr.2009.01.001

113. Müerköster S, Wegehenkel K, Arlt A, Witt M, Sipos B, Kruse M-L, et al. Tumor stroma interactions induce chemoresistance in pancreatic ductal carcinoma cells involving increased secretion and paracrine effects of nitric oxide and interleukin-1beta. *Cancer Res*. (2004) 64:1331–7. doi: 10.1158/0008-5472.can-03-1860

114. Benedyk M, Sopalla C, Nacken W, Bode G, Melkonyan H, Banfi B, et al. HaCaT keratinocytes overexpressing the S100 proteins S100A8 and S100A9 show increased NADPH oxidase and NF-kappaB activities. *J Invest Dermatol*. (2007) 127:2001–11. doi: 10.1038/sj.jid.5700820

115. Grivennikov SI, Karin M. Dangerous liaisons: STAT3 and NF-kappaB collaboration and crosstalk in cancer. *Cytokine Growth Factor Rev*. (2010) 21:11–9. doi: 10.1016/j.cytogfr.2009.11.005

116. Mao X, Xu J, Wang W, Liang C, Hua J, Liu J, et al. Crosstalk between cancer-associated fibroblasts and immune cells in the tumor microenvironment: new findings and future perspectives. *Mol Cancer*. (2021) 20:131. doi: 10.1186/s12943-021-01428-1

117. Katakam AK, Brightbill H, Franci C, Kung C, Nunez V, Jones C, et al. Dendritic cells require NIK for CD40-dependent cross-priming of CD8+ T cells. *Proc Natl Acad Sci U S A*. (2015) 112:14664–9. doi: 10.1073/pnas.1520627112

118. Rahma OE, Hodi FS. The intersection between tumor angiogenesis and immune suppression. *Clin Cancer Res Off J Am Assoc Cancer Res*. (2019) 25:5449–57. doi: 10.1158/1078-0432.CCR-18-1543

119. Balkwill F, Mantovani A. Inflammation and cancer: back to Virchow? *Lancet Lond Engl*. (2001) 357:539–45. doi: 10.1016/S0140-6736(00)04046-0

120. Pikarsky E, Porat RM, Stein I, Abramovitch R, Amit S, Kasem S, et al. NF-kappaB functions as a tumour promoter in inflammation-associated cancer. *Nature*. (2004) 431:461–6. doi: 10.1038/nature02924

121. Kishimoto T. Interleukin-6: from basic science to medicine–40 years in immunology. *Annu Rev Immunol*. (2005) 23:1–21. doi: 10.1146/annurev.immunol.23.021704.115806

122. Disis ML. Immune regulation of cancer. *J Clin Oncol Off J Am Soc Clin Oncol*. (2010) 28:4531–8. doi: 10.1200/JCO.2009.27.2146

123. Dajee M, Lazarov M, Zhang JY, Cai T, Green CL, Russell AJ, et al. NF-kappaB blockade and oncogenic Ras trigger invasive human epidermal neoplasia. *Nature*. (2003) 421:639–43. doi: 10.1038/nature01283

124. van Hogerlinden M, Rozell BL, Ahrlund-Richter L, Toftgård R. Squamous cell carcinomas and increased apoptosis in skin with inhibited Rel/nuclear factor-kappaB signaling. *Cancer Res*. (1999) 59:3299–303.

125. Yang J, Hawkins OE, Barham W, Gilchuk P, Boothby M, Ayers GD, et al. Myeloid IKKβ promotes antitumor immunity by modulating CCL11 and the innate immune response. *Cancer Res*. (2014) 74:7274–84. doi: 10.1158/0008-5472.CAN-14-1091

126. Greten FR, Eckmann L, Greten TF, Park JM, Li Z-W, Egan LJ, et al. IKKβ Links inflammation and tumorigenesis in a mouse model of colitis-associated cancer. *Cell*. (2004) 118:285–96. doi: 10.1016/j.cell.2004.07.013

127. Luedde T, Beraza N, Kotsikoris V, van Loo G, Nenci A, De Vos R, et al. Deletion of NEMO/IKKgamma in liver parenchymal cells causes steatohepatitis and hepatocellular carcinoma. *Cancer Cell*. (2007) 11:119–32. doi: 10.1016/j.ccr.2006.12.016

128. Yu H, Kortylewski M, Pardoll D. Crosstalk between cancer and immune cells: role of STAT3 in the tumour microenvironment. *Nat Rev Immunol*. (2007) 7:41–51. doi: 10.1038/nri1995

129. Yu H, Jove R. The STATs of cancer–new molecular targets come of age. *Nat Rev Cancer*. (2004) 4:97–105. doi: 10.1038/nrc1275

130. Yang J, Liao X, Agarwal MK, Barnes L, Auron PE, Stark GR, et al. Unphosphorylated STAT3 accumulates in response to IL-6 and activates transcription by binding to NFkappaB. *Genes Dev*. (2007) 21:1396–408. doi: 10.1101/gad.1553707

131. Kortylewski M, Kujawski M, Wang T, Wei S, Zhang S, Pilon-Thomas S, et al. Inhibiting Stat3 signaling in the hematopoietic system elicits multicomponent antitumor immunity. *Nat Med*. (2005) 11:1314–21. doi: 10.1038/nm1325

132. Wang T, Niu G, Kortylewski M, Burdelya L, Shain K, Zhang S, et al. Regulation of the innate and adaptive immune responses by Stat-3 signaling in tumor cells. *Nat Med*. (2004) 10:48–54. doi: 10.1038/nm976

133. He G, Yu G-Y, Temkin V, Ogata H, Kuntzen C, Sakurai T, et al. Hepatocyte IKKbeta/NF-kappaB inhibits tumor promotion and progression by preventing oxidative stress-driven STAT3 activation. *Cancer Cell*. (2010) 17:286–97. doi: 10.1016/j.ccr.2009.12.048

134. Zhang X, Wang L, Qu Y. Targeting the β-catenin signaling for cancer therapy. *Pharmacol Res*. (2020) 160:104794. doi: 10.1016/j.phrs.2020.104794

135. Zhang Y, Wang X. Targeting the Wnt/β-catenin signaling pathway in cancer. *J Hematol Oncol.J Hematol Oncol*. (2020) 13:165. doi: 10.1186/s13045-020-00990-3

136. Bienz M, Clevers H. Linking colorectal cancer to Wnt signaling. *Cell*. (2000) 103:311–20. doi: 10.1016/S0092-8674(00)00122-7

137. Zhao H, Ming T, Tang S, Ren S, Yang H, Liu M, et al. Wnt signaling in colorectal cancer: pathogenic role and therapeutic target. *Mol Cancer*. (2022) 21:144. doi: 10.1186/s12943-022-01616-7

138. Halma MTJ, Tuszynski JA, Marik PE. Cancer metabolism as a therapeutic target and review of interventions. *Nutrients*. (2023) 15:4245. doi: 10.3390/nu15194245

139. Chelakkot C, Chelakkot VS, Shin Y, Song K. Modulating glycolysis to improve cancer therapy. *Int J Mol Sci*. (2023) 24:2606. doi: 10.3390/ijms24032606

140. Kawauchi K, Araki K, Tobiume K, Tanaka N. p53 regulates glucose metabolism through an IKK-NF-kappaB pathway and inhibits cell transformation. *Nat Cell Biol*. (2008) 10:611–8. doi: 10.1038/ncb1724

141. Reid MA, Lowman XH, Pan M, Tran TQ, Warmoes MO, Ishak Gabra MB, et al. IKKβ promotes metabolic adaptation to glutamine deprivation via phosphorylation and inhibition of PFKFB3. *Genes Dev*. (2016) 30:1837–51. doi: 10.1101/gad.287235.116

142. Bian X, Liu R, Meng Y, Xing D, Xu D, Lu Z, et al. Lipid metabolism and cancer. *J Exp Med*. (2021) 218:e20201606. doi: 10.1084/jem.20201606

143. Jiang M, Wu N, Xu B, Chu Y, Li X, Su S, et al. Fatty acid-induced CD36 expression via O-GlcNAcylation drives gastric cancer metastasis. *Theranostics*. (2019) 9:5359–73. doi: 10.7150/thno.34024

144. Capece D, D'Andrea D, Begalli F, Goracci L, Tornatore L, Alexander JL, et al. Enhanced triacylglycerol catabolism by carboxylesterase 1 promotes aggressive colorectal carcinoma. *J Clin Invest*. (2021) 131:e137845. doi: 10.1172/JCI137845

145. Molaei M, Vandehoef C, Karpac J. NF-κB shapes metabolic adaptation by attenuating foxo-mediated lipolysis in drosophila. *Dev Cell*. (2019) 49:802–810.e6. doi: 10.1016/j.devcel.2019.04.009

146. Fuhrmeister J, Zota A, Sijmonsma TP, Seibert O, Cıngır Ş, Schmidt K, et al. Fasting-induced liver GADD45β restrains hepatic fatty acid uptake and improves metabolic health. *EMBO Mol Med*. (2016) 8:654–69. doi: 10.15252/emmm.201505801

147. Verzella D, Bennett J, Fischietti M, Thotakura AK, Recordati C, Pasqualini F, et al. GADD45β Loss ablates innate immunosuppression in cancer. *Cancer Res*. (2018) 78:1275–92. doi: 10.1158/0008-5472.CAN-17-1833

148. Moretti M, Bennett J, Tornatore L, Thotakura AK, Franzoso G. Cancer: NF-κB regulates energy metabolism. *Int J Biochem Cell Biol*. (2012) 44:2238–43. doi: 10.1016/j.biocel.2012.08.002

149. Mauro C, Leow SC, Anso E, Rocha S, Thotakura AK, Tornatore L, et al. NF-κB controls energy homeostasis and metabolic adaptation by upregulating mitochondrial respiration. *Nat Cell Biol*. (2011) 13:1272–9. doi: 10.1038/ncb2324

150. Loftus RM, Finlay DK. Immunometabolism: cellular metabolism turns immune regulator. *J Biol Chem*. (2016) 291:1–10. doi: 10.1074/jbc.R115.693903

151. Wu D, Tian S, Zhu W. Modulating multidrug resistance to drug-based antitumor therapies through NF-κB signaling pathway: mechanisms and perspectives. *Expert Opin Ther Targets*. (2023) 27:503–15. doi: 10.1080/14728222.2023.2225767

152. Wilson AJ, Barham W, Saskowski J, Tikhomirov O, Chen L, Lee H-J, et al. Tracking NF-κB activity in tumor cells during ovarian cancer progression in a syngeneic mouse model. *J Ovarian Res*. (2013) 6:63. doi: 10.1186/1757-2215-6-63

153. Smith MP, Sanchez-Laorden B, O'Brien K, Brunton H, Ferguson J, Young H, et al. The immune microenvironment confers resistance to MAPK pathway inhibitors through macrophage-derived TNFα. *Cancer Discovery*. (2014) 4:1214–29. doi: 10.1158/2159-8290.CD-13-1007

154. Liu J, Lao L, Chen J, Li J, Zeng W, Zhu X, et al. The IRENA lncRNA converts chemotherapy-polarized tumor-suppressing macrophages to tumor-promoting phenotypes in breast cancer. *Nat Cancer*. (2021) 2:457–73. doi: 10.1038/s43018-021-00196-7

155. Yang Y-I, Wang Y-Y, Ahn J-H, Kim B-H, Choi J-H. CCL2 overexpression is associated with paclitaxel resistance in ovarian cancer cells via autocrine signaling and macrophage recruitment. *Biomed Pharmacother*. (2022) 153:113474. doi: 10.1016/j.biopha.2022.113474

156. Le F, Yang L, Han Y, Zhong Y, Zhan F, Feng Y, et al. TPL inhibits the invasion and migration of drug-resistant ovarian cancer by targeting the PI3K/AKT/NF-κB-signaling pathway to inhibit the polarization of M2 TAMs. *Front Oncol*. (2021) 11:704001. doi: 10.3389/fonc.2021.704001

157. Yang T, Deng Z, Xu L, Li X, Yang T, Qian Y, et al. Macrophages-aPKCι-CCL5 feedback loop modulates the progression and chemoresistance in cholangiocarcinoma. *J Exp Clin Cancer Res CR*. (2022) 41:23. doi: 10.1186/s13046-021-02235-8

158. Zhou Y, Tang W, Zhuo H, Zhu D, Rong D, Sun J, et al. Cancer-associated fibroblast exosomes promote chemoresistance to cisplatin in hepatocellular carcinoma through circZFR targeting signal transducers and activators of transcription (STAT3)/nuclear factor -kappa B (NF-κB) pathway. *Bioengineered*. (2022) 13:4786–97. doi: 10.1080/21655979.2022.2032972

159. Zhang X, Zheng S, Hu C, Li G, Lin H, Xia R, et al. Cancer-associated fibroblast-induced lncRNA UPK1A-AS1 confers platinum resistance in pancreatic cancer via efficient double-strand break repair. *Oncogene*. (2022) 41:2372–89. doi: 10.1038/s41388-022-02253-6

160. Zhai J, Shen J, Xie G, Wu J, He M, Gao L, et al. Cancer-associated fibroblasts-derived IL-8 mediates resistance to cisplatin in human gastric cancer. *Cancer Lett*. (2019) 454:37–43. doi: 10.1016/j.canlet.2019.04.002

161. Liu M, Wei F, Wang J, Yu W, Shen M, Liu T, et al. Myeloid-derived suppressor cells regulate the immunosuppressive functions of PD-1-PD-L1+ Bregs through PD-L1/PI3K/AKT/NF-κB axis in breast cancer. *Cell Death Dis*. (2021) 12:465. doi: 10.1038/s41419-021-03745-1

162. Di Pilato M, Kim EY, Cadilha BL, Prüßmann JN, Nasrallah MN, Seruggia D, et al. Targeting the CBM complex causes Treg cells to prime tumours for immune checkpoint therapy. *Nature*. (2019) 570:112–6. doi: 10.1038/s41586-019-1215-2

163. Prescott JA, Cook SJ. Targeting IKKβ in cancer: challenges and opportunities for the therapeutic utilisation of IKKβ Inhibitors. *Cells*. (2018) 7:115. doi: 10.3390/cells7090115

164. Mantovani A, Sica A. Macrophages, innate immunity and cancer: balance, tolerance, and diversity. *Curr Opin Immunol*. (2010) 22:231–7. doi: 10.1016/j.coi.2010.01.009

165. Mantovani A, Sozzani S, Locati M, Allavena P, Sica A. Macrophage polarization: tumor-associated macrophages as a paradigm for polarized M2 mononuclear phagocytes. *Trends Immunol*. (2002) 23:549–55. doi: 10.1016/S1471-4906(02)02302-5

166. Martin M, Wei H, Lu T. Targeting microenvironment in cancer therapeutics. *Oncotarget*. (2016) 7:52575–83. doi: 10.18632/oncotarget.v7i32

167. Compagno M, Lim WK, Grunn A, Nandula SV, Brahmachary M, Shen Q, et al. Mutations of multiple genes cause deregulation of NF-kappaB in diffuse large B-cell lymphoma. *Nature*. (2009) 459:717–21. doi: 10.1038/nature07968

frontiers | Frontiers in Immunology

TYPE Original Research
PUBLISHED 17 December 2024
DOI 10.3389/fimmu.2024.1495032

OPEN ACCESS

EDITED BY
Yujia Lan,
Harbin Medical University, China

REVIEWED BY
Ismail Meraz,
University of Texas MD Anderson Cancer Center, United States
Raj Kumar,
University of Alabama at Birmingham, United States

*CORRESPONDENCE
Alexander D. Boiko
alexander.boiko@cshs.org

RECEIVED 11 September 2024
ACCEPTED 22 November 2024
PUBLISHED 17 December 2024

CITATION
Makwana K, Velazquez EJ, Marzese DM, Smith B, Bhowmick NA, Faries MB, Hamid O and Boiko AD (2024) NRF-1 transcription factor regulates expression of an innate immunity checkpoint, CD47, during melanomagenesis.
Front. Immunol. 15:1495032.
doi: 10.3389/fimmu.2024.1495032

NRF-1 transcription factor regulates expression of an innate immunity checkpoint, CD47, during melanomagenesis

Kuldeep Makwana[1], Edwin J. Velazquez[1], Diego M. Marzese[2,3], Bethany Smith[1], Neil A. Bhowmick[1], Mark B. Faries[1,4], Omid Hamid[1,4] and Alexander D. Boiko[1,5]*

[1]Department of Medicine, Comprehensive Cancer Institute, Cedars-Sinai Medical Center, Los Angeles, CA, United States, [2]Department of Surgery, Duke University School of Medicine, Durham, NC, United States, [3]Cancer Epigenetics Laboratory, Health Research Institute of the Balearic Islands (IdISBa), Palma, Spain, [4]The Angeles Clinical and Research Institute, a Cedars-Sinai Affiliate, Los Angeles, CA, United States, [5]Department of Biomedical Sciences, Comprehensive Cancer Institute, Cedars-Sinai Medical Center, Los Angeles, CA, United States

Transmembrane integrin-associated protein *CD47* functions as a potent innate immunity checkpoint and is upregulated by many types of malignant cells, including melanoma during tumor progression. Binding of *CD47* to its target receptor, SIRPα, on myeloid cell lineages leads to the initiation of the downstream signaling cascades that inhibit innate immunity anti-tumor responses. Molecular mechanisms underlying upregulation of *CD47* during melanoma progression remain largely unknown. In this report, we performed ATAC-Sequencing on patient-derived melanoma cells, as well as, the analysis of ATAC-Seq datasets covering clinical melanoma samples to demonstrate a significant increase in chromatin accessibility for the *CD47* promoter region in comparison to normal cells and tissues. Additionally, profiling of multiple *CD47* transcript isoforms established that upregulation of *CD47* in malignant cells occurs at the mRNA level. Using chromatin immunoprecipitation (ChIP) approaches along with the analysis of ChIP-Seq cancer datasets, we identified the transcription factor NRF-1 which binds at multiple sites within the proximal *CD47* promoter region. In combination with serial deletions of *CD47* promoter, we defined the minimal DNA region required for its activation, as well as, specific DNA locations within that region, which are preferentially occupied by NRF-1 in tumor cells.

KEYWORDS

cd47, NRF1, melanoma, promoter regulation, immune checkpoint

Introduction

Understanding mechanisms leading to the acquisition of immune-evasive properties by malignant cells represents a critical step in the design of effective anti-cancer regimens. Previous studies by our group and others identified integrin-associated protein *CD47* as the critical myeloid lineage checkpoint that is overexpressed by various types of tumor cells, including melanoma, and inhibits innate immunity-mediated anti-tumor responses (1–4). First discovered on the cell surface of circulating red blood cells (RBCs), *CD47* is able to interact with the SIRPα receptor present on the macrophages to inhibit their phagocytic function, a phenomenon that later became known as the "don't eat me" signal (5). Subsequent research on hematopoietic malignancies including acute myeloid leukemia (AML) and non-Hodgkin lymphoma (NHL) revealed that malignant cells hijack this mechanism to evade surveillance by an innate immunity during cancer progression (4, 6, 7). These results were later extended into the studies of the solid tumors, where it was shown that high levels of *CD47* are associated with disease progression and/or poor patient prognosis, including epithelial (breast, ovarian, colon, and others) (8–10), mesenchymal (sarcomas) (11, 12), and neuronal/neural crest (GBM, Neuroblastoma, Melanoma) derived malignancies (2, 13). Importantly, past research by our group demonstrated that freshly resected metastatic human melanoma tumors are highly positive for *CD47*, while its blockade (by administering inhibitory antibodies) led to the significant suppression of melanoma metastases *in-vivo* using several independently patient-derived xenografts (PDXs) (2). Clinical significance of these findings has been translated into the development of therapeutic compounds blocking *CD47* interaction with SIRPα in order to reinvigorate anti-tumor immune responses, with some of them reaching Phase I and II human trials (14, 15).

While the immune-suppressive role of *CD47* on the cell surface of tumor cells has been characterized to a great extent, mechanisms underlying its regulation during human cancer progression are only beginning to emerge. These studies reveal substantial variability in the transcription factor machinery involved in the regulation of the *CD47* promoter depending on the tumor type. Thus, it has been shown that in leukemias (both human and mouse) MYC oncogene binds to the distal enhancer regions of the *CD47* promoter to regulate its activity (16), while HIF-1α and NFκB transcription factors have been implicated in the regulation of *CD47* promoter in breast, cervical, and non-small lung carcinoma cells (17–19).

In this report, we find that *CD47* upregulation in melanoma occurs at the mRNA level and is associated with changes in chromatin accessibility at the *CD47* promoter region using the assay for transposase-accessible chromatin with sequencing (ATAC-seq). This leads to an increased *CD47* mRNA production, as determined by real-time PCR covering multiple transcript variants of this gene. To reveal molecular factors regulating *CD47* mRNA expression we performed an extensive analysis of the *CD47* promoter region using the MotifMap algorithm. As a result, we identified multiple locations containing the binding consensus sequence for the Nuclear Respiratory Factor-1 (NRF-1) within the proximal promoter region of the *CD47* gene. Furthermore, Chromatin Immunoprecipitation (ChIP) assays revealed NRF-1 to be bound at multiple proximal *CD47* promoter sites with differential affinity among malignant and normal cell types leading to increased *CD47* mRNA and protein levels. Lastly, using bioluminescence reporter systems, we were able to define the minimum *CD47* promoter region and the number of NRF-1 binding sites required for its efficient activation.

Materials and methods

Cell culture

Melanoma cells M1626 and M727 were maintained in RPMI with 10% FBS, M525 cells were maintained in RPMI with 5% FBS, HepG2 cells were maintained in DMEM with 10% FBS, and M354 cells were maintained in 1:1 of RPMI with 10% FBS and dermal cell basal media from ATCC (PCS-200-030). Normal melanocytes were maintained in dermal cell basal media from ATCC (PCS-200-030). All cells were grown in Tissue Culture incubators set at 5% CO2 and 37°C degrees. For NRF1 siRNA mediated knockdown, a total of 1×10^5 M727 cells were seeded in 6 well plates and incubated overnight at 37 ° C and 5% CO_2. Cells were then transfected using 8 µl of siRNA transfection reagent (Santa Cruz, Cat. No. sc-29528) and 120 pmol of NRF-1 siRNA (Cat. No. sc-38105) or control siRNA-A (Santa, Cruz, Cat. No. sc-37007).

Flow cytometry

Detection and quantification of *CD47* cell surface protein levels were performed using FACS and an anti-human *CD47* antibody (BioLegend, Cat. No. 323106). Briefly, cells were cultured in an exponential phase and harvested before reaching confluency. To harvest the cells, the spent medium was carefully aspirated, cells were washed with PBS, and detached using Accutase™ solution (STEMCELL, Cat. No.07922) for 3 min at 37°C in an incubator with 5% CO_2. The cells were then collected and washed twice with PBS and resuspended in 100 µL of ice-cold cell staining buffer (CSB) (PBS, 1%BSA) at a concentration of 0.5-1x10^6cells/ml. Following resuspension, cells were stained with anti-human *CD47*-FITC antibody (1µg/1x10^6cells) and incubated on ice protected from light for 20 min. After incubation, the cells were centrifuged at 200g for 5 min, the supernatant was carefully aspirated, and the cells were washed twice with 200 µL of CSB. The cells were transferred to FACS tubes and analyzed in a BD FACSymphony A5 cell analyzer, at least 1x10^4 cells live cells were recorded per cell type. Dead cells were excluded with a DAPI staining solution (10µg/mL). Once flow cytometry analysis was completed, data was analyzed in FlowJo v10.10 software, live cells were gated, and the geometric mean fluorescence intensity (GMFI) was obtained for each cell type. GMFI values were normalized (same number of live events per cell type) and compared between cell lines as well as their respective histograms.

qRT-PCR

Cells were grown *in-vitro* on p100 cell culture dishes until reaching ~70% confluency after which they were lysed using 1ml of Trizole reagent. mRNA was precipitated using isopropanol and washed twice with 70% ethanol. cDNA was synthesized using a high-capacity cDNA reverse transcription kit (4368814) and power SYBR green PCR MasterMix (4367659 Thermo Fisher Scientific) was used to quantify total levels of *CD47* or NRF-1 transcripts; 18s gene was used for the normalization of qPCR results. Primer pair sequences are listed in Supplementary Table 1.

ATAC-sequencing

For ATAC-Seq 50,000 cells were collected, washed in 50 µl of cold PBS, and resuspended in 50 µl of cold lysis buffer. Nuclei were isolated by centrifugation at 500 x g for 10 min at 4°C and then incubated with a transposition reaction mix for 30 min at 37°C. Following transposition, DNA was then purified using the MinElute PCR Purification kit (Qiagen, Hilden, Germany). The transposed DNA fragments were barcoded initially amplified for 5 cycles, and further amplified by standardized PCR. The resulting ATAC libraries were sequenced on an Illumina HiSeq 2500 platform in Rapid Mode with the 50-bp paired-end reads output mode. Raw reads were aligned to the human genome reference (1000 Genomes) using BWA-MEM (version 0.7.5a) with default settings. ATAC-Seq peaks were identified using the callpeaks function in MACS2 with a threshold set to -q = 0.01. The resulting peak calls were filtered for sequences that mapped to the mitochondria using shell scripts. BigWig files were normalized and integrated with publicly available genomic and epigenomic data for visualization in the UCSC Genome Browser.

ChIP assay

For the ChIP assay cells were prepared using truChIP Chromatin shearing kit (PN520127) from covaries. Briefly, cells were cultured in 2 x p150 dishes and treated with fixing buffer have 1% formaldehyde for 10 mins followed by quenching of crosslinking with a quenching buffer for 5 mins. Cells were lysed per the manufacturer's protocol and isolated nuclei were transferred into AFA tubes (Cat# 520135 covaris) and chromatin shearing was performed for 15 mins in E220 evolution ultrasonicator from covaries with recommended settings. 50µl of sheared chromatin sample was used to isolate DNA (Supplementary Figure S2) using a DNA purification kit from cell signaling technologies (cat# 14209S) thus the total amount of DNA in sheared chromatin was calculated using nanodrop. For immunoprecipitation, the buffers (cat# 14231) and ChIP-grade magnetic beads (cat# 9006S) were purchased from cell signaling and used as per the manufacturer's protocol. Briefly, 5-7µg of DNA was used per reaction and 2% input material was set aside for quantification using qPCR. Each reaction was incubated overnight with 2.5-3µg of NRF-1, or isotype control IgG antibody followed by 2 hours of incubation with magnetic beads the following day. Immunoprecipitation was performed using a magnetic rack. After successful elution of pulled-down chromatin, DNA was isolated, and real-time qPCR was performed using power SYBR green PCR master mix (cat# 4367659) from Thermo Fisher Scientific. Primer pair sequences are listed in Supplementary Table 1.

Generation of stable cell lines expressing *CD47* promoter reporters

CD47 promoter reporters containing various numbers of NRF-1 binding sites were created by synthesizing respective DNA regions and cloning them into pGF1-4eCOL2A1_LUC lentiviral vector using BamHI and Spe1 restriction sites. Viral packaging was done in HEK293 cells and collected virions were used to infect target cells for two consecutive days. The *CD47* promoter activity of endogenous NRF-1 was assayed by measuring Luciferase bioluminescence.

Datasets Used for *In-Silico* Analysis

TCGA TARGET GTEx study was used to analyze *CD47* expression levels in human melanoma tissues. ENCFF323SMV, ENCFF862EDR, ENCFF605IET, ENCFF785WIA, ENCFF000XJF, ENCFF644ITQ from encodeproject.org studies were used to analyze NRF-1 ChIP seq data across different types of cancer. Patient-derived melanoma cell lines were analyzed for chromatin accessibility at the *CD47* promoter region using the data from the study GSE134432. The ATAC-Seq data for the melanoma patient tissues was fetched from https://gdc.cancer.gov/about-data/publications/ATACseq-AWG. For *in-silico* $H3K4^{Me3}$ analysis of patient-derived melanoma tissue from the database GSE33930, bowtie aligner was used to align the sequence reads, followed by the emoval of mitochondrial reads and duplicates using samtools. Macs2 was used to invoke callpeaks function to obtain peakfiles which were used to generate bigwig datafiles to be visualized in IGV.

Results

CD47 upregulation in melanoma occurs at the mRNA level and is mediated by an open chromatin at its DNA promoter region

We previously established that high levels of *CD47* protein on freshly isolated human tumor cells are associated with melanoma progression and immune evasion (2). To understand whether augmented *CD47* expression results from an increase in corresponding mRNA production, we used metastatic melanoma patient-derived cells M727, M354, and M1626 that were determined to express various levels of *CD47* (Figures 1A, B) and compared them to normal melanocytes or hepatocellular carcinoma cells, HEPG2, (known for low levels of *CD47* protein) using qRT-

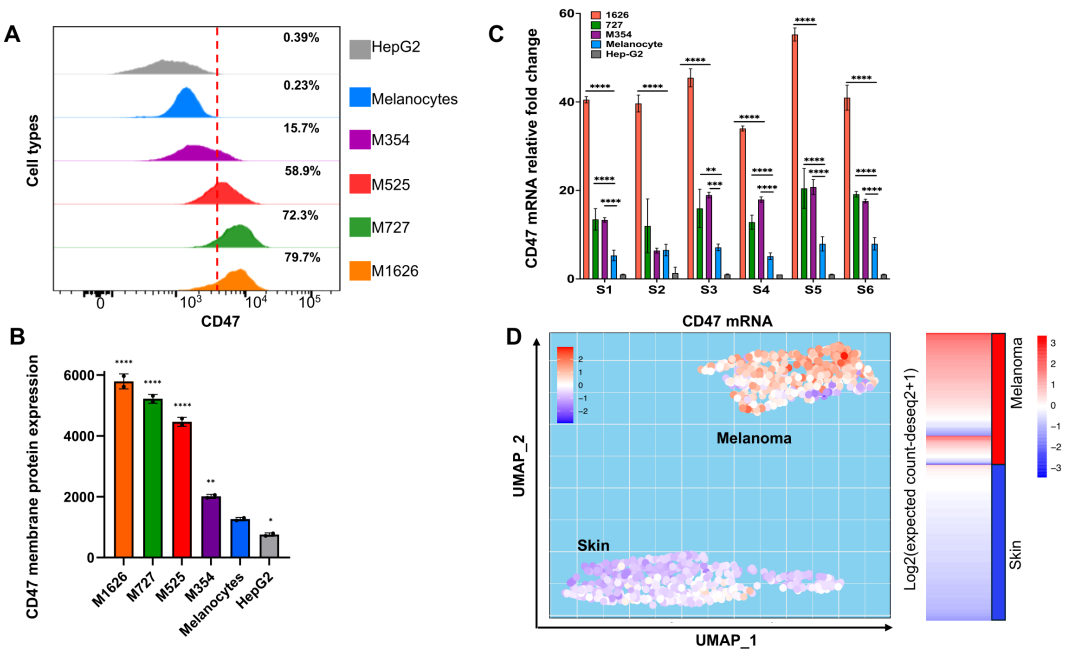

FIGURE 1
Upregulation of *CD47* expression during melanomagenesis. **(A)** Flow cytometry analysis of *CD47* expression in indicated cells. **(B)** Expression of *CD47* protein on the membrane of indicated cells. *CD47* expression is represented as normalized geometric mean fluorescent intensity (GMFI). **(C)** Relative expression of *CD47* mRNA in fold changes comprehensively evaluated by six primer sets to capture all the *CD47* mRNA isoforms abundance levels. **(D)** Unsupervised dimensional reduction analysis of a dataset from TCGA TARGET GTEx study was performed to visualize the distinctive clusters and expression of *CD47* in melanoma and normal skin samples. The transcript matrix was processed in R studio package called "umap" for UMAP generation. Samples with higher *CD47* in melanoma as seen on the heatmap represent the "Melanoma cluster", and samples with lower *CD47* expression represent the "Skin" cluster in UMAP.

PCR. *CD47* gene is comprised of 11 exons and as a result of splicing, most notably between exons 8-10, multiple mRNA isoforms are translated (Supplementary Figure 1A). Therefore, to prospectively quantify levels of all *CD47* transcript isoforms we designed multiple primer sets for a common exon 2, as well as, two primer sets that amplify mRNA regions between exon 2-4 and exon 7-8 (Supplementary Figure 1B, Supplementary Table 1). After performing multiple qRT-PCR assays, our results demonstrate that all metastatic melanomas expressed 10-15 folds (depending on the isoform) elevation in *CD47* mRNA as compared to normal melanocytes or HepG2 cells (Figure 1C). To further explore clinical significance of our findings, we investigated *CD47* mRNA levels among 422 melanoma subjects in comparison to 123 normal skin subjects using TCGA TARGET GTEx dataset. Utilizing an unsupervised dimensional reduction approach, we generated UMAP graphs that visualized patterns of clusters across diagnosed subjects and levels of *CD47* mRNA expression. Significantly, two distinct clusters were formed based on the *CD47* mRNA levels, high and low, which corresponded to the malignant melanoma patients cluster (high) and the normal skin cluster (low) (Figure 1D).

To understand molecular mechanisms of augmented *CD47* mRNA expression in malignant melanoma, we investigated the dynamics of chromatin re-modeling at *CD47* promoter using ATAC-Seq. This approach allows the generation of a cell-specific chromatin accessibility landscape to determine the level of open chromatin and subsequent promoter activation. First, we used *in-silico* ATAC-Seq analysis of the skin cancer melanoma (SKCM) dataset (https://gdc.cancer.gov/about-data/publications/ATACseq-AWG) containing malignant tissues obtained from 13 melanoma subjects (11 samples were analyzed in duplicates) and a melanoma dataset (GSE134432) containing 9 genetically homogenous melanoma patient-derived cell lines to gain insights into the accessibility of the *CD47* promoter region. Our results demonstrate that in both freshly resected melanoma samples, as well as, in melanoma patient-derived cell lines, the DNA region corresponding to the *CD47* promoter has a significantly increased chromatin accessibility which could be conjectured as a sign of active mRNA transcription (Figure 2A). To validate these changes in the chromatin landscape of the *CD47* promoter region during melanomagenesis, we performed ATAC-seq on multiple independent patient-derived melanoma cell lines in comparison to normal adult melanocytes. Importantly, we were able to detect strong peak signals associated with an open chromatin structure around the promoter of *CD47* in malignant melanomas, which were missing in normal adult melanocytes indicating the closed chromatin structure of the *CD47* DNA promoter region in non-transformed cells (Figure 2B).

Open chromatin status is often associated with specific histone modifications such as $H3K4^{Me3}$, which is commonly found at the promoter regions of actively transcribed genes (20). To determine whether this mechanism can account for an increased *CD47* mRNA production during melanomagenesis, we performed *in-silico* analysis of $H3K4^{Me3}$ histone modifications at the *CD47* promoter

in melanoma patients and normal adult melanocytes using the GSE33930 dataset. Our results demonstrate that peak signals for H3K4^{Me3} DNA modification at the *CD47* promoter region are significantly stronger in malignant melanomas in comparison to normal melanocytes (Figure 2C).

Nuclear respiratory factor-1 TF binds to the *CD47* promoter with preferential affinity to the most proximal region in melanoma

To identify transcriptional regulators of the *CD47* promoter we analyzed its DNA region (± 1000bp relative to the transcription start site (TSS)) for the presence of potential TF binding sites using MotifMap and the Eukaryotic Promoter Databases. Results ranking based on FDR (< 0.038) and p-value (< 0.001) scores revealed a number of DNA binding sites within that region (-63bp, -28bp, -22bp, -14bp, and +32bp), all corresponding to the NRF-1 consensus sequence (Figure 3A). To validate predicted interactions of NRF-1 with *CD47* promoter we first performed *in-silico* analysis of ChIP-seq datasets derived from different types of cancer. Importantly, strong peak signals corresponding to NRF-1 binding at the *CD47* promoter were identified in the majority of tumors (results presented as fold changes over control), except for HepG2 hepatocarcinoma (Figure 3B), which was found to express low *CD47* protein and mRNA transcript levels (Figure 1).

Next, to determine NRF-1 regulation of *CD47* promoter, we performed Chromatin Immunoprecipitation (ChIP) assays on malignant patient-derived melanoma cells, as well as, adult normal melanocytes and HepG2 cells. Following incubation of the sheared chromatin (500-1000bp) with NRF-1 Ab the pulled-down DNA fragments were quantified by PCR using primer sets designed to amplify only the *CD47* promoter regions spanning different putative NRF-1 binding sites (Figure 4A). To precisely delineate NRF-1 DNA binding regions within the *CD47* promoter, we designed multiple primer pairs to enrich for the following sites relative to TSS: Set 1 (-38/+28) includes putative binding sites at -28, -22, and -14bp; Set 2, (-38/+56) includes putative binding sites -28, -22, -14, and +32; Set 3 (-63/-36) includes putative binding site at position -63bp only (Figure 4A, Supplementary Table 1). An additional set of primer spanning the promoter region of MEF2A gene (a validated NRF-1 binding target) was used as a positive control for all ChIP experiments (Supplementary Figure 2). ChIP analysis on the above indicated cell types identified NRF-1 loading at the predicted DNA region of the *CD47* promoter with differential affinity for proximal and distal binding sites (Figure 4B). Thus, in malignant melanomas there was a significant increase in binding affinity at the most proximal sites (-28, -22, -14) as compared to normal melanocytes (1.7-fold for M727 and 2.4-fold for M1626). Moreover, when compared to HepG2 cells, which have been characterized by the lowest levels of *CD47* mRNA and protein, differences in NRF-1 binding affinity were found to be even greater (1.85-fold for M727 and 3.8-fold for M1626 Figure 4B middle panel). Inclusion of the proximal downstream binding site (+32bp) resulted in similar differences in the NRF-1 binding affinity between malignant melanoma and low *CD47* expressing cells (adult melanocytes and HepG2 cells) (Figure 4B right panel). However, differences in NRF-1 binding affinity were diminished at the more

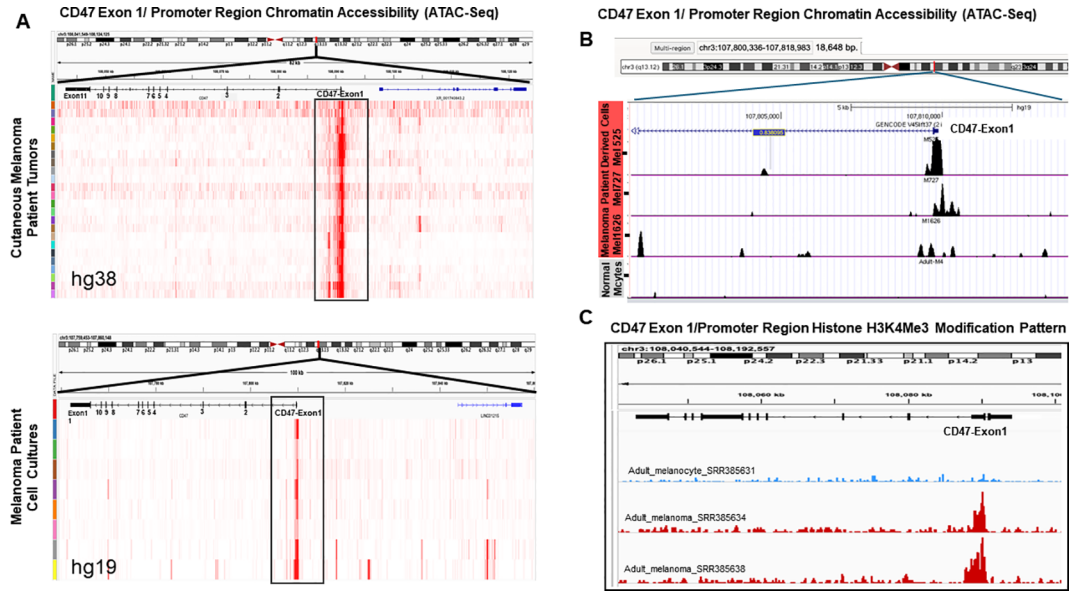

FIGURE 2
Changes in chromatin landscape of *CD47* promoter region in patient melanomas and patient-derived melanoma cell lines. **(A)** Analysis of ATAC-seq peak signals around the *CD47* DNA promoter region in surgically removed melanoma patient tumors and established cell lines using SKCM and GSE134432 databases. **(B)** Analysis of *CD47* promoter region chromatin structure using ATAC-Seq approach on independent patient-derived melanoma cell lines (M727, M1626, M525) and normal melanocytes. **(C)** Analysis of H3K4^{Me3} histone modification mark at the *CD47* promoter DNA region using melanoma patient samples and melanocytes from the database GSE33930. Peaks were called using Macs2 and peak files in the Bigwig format were visualized in the IGV 2.7 version.

10.3389/fimmu.2024.1495032

distal binding site (-63bp) within the *CD47* promoter region (Figure 4B left panel). In summary, these findings indicate that *CD47* transcriptional regulation by NRF-1 is determined by the proximal promoter region in melanoma cells.

Effective activation of *CD47* promoter requires multiple NRF-1 binding sites between -120bp to +50bp promoter region

Initiation of transcription from eukaryotic promoters often requires binding of the TFs at numerous locations within the promoter region. Identification and validation of multiple NRF-1 TF binding sites within the proximal region to the *CD47* TSS (200 bp window) prompted us to investigate the minimum adequate length of DNA required for the *CD47* promoter activation. To achieve this goal, we designed and cloned a series of bioluminescent reporter plasmids expressing Luciferase gene under the control of the proximal *CD47* promoter region containing various numbers of NRF-1 TF binding sites (Figure 5A). Specifically, construct 1 contained all five NRF-1 proximal binding sites and covered the DNA region from -120 to +50bp relative to the TSS, construct 2 contained four out of five NRF-1 binding sites and covered the region from -70 to +30 bp, and lastly construct 3 contained only three out of five NRF-1 binding sites and covered the region from -62 to +30bp of *CD47* promoter relative to the TSS. Lastly, we also used a complete promoter deletion variant of Luciferase expressing plasmid as a negative control (construct 4 Figure 5A). All of the above variants of the *CD47* promoter region were synthesized and cloned into the lentiviral plasmid pGF1-4eCOL2A1_Luc (21) using BamHI and Spe1 restriction sites. In order to evaluate endogenous NRF-1 activity at the *CD47* promoter, we generated melanoma cell lines to stably express all versions of Luc reporters using previously published lentiviral transduction protocols (22, 23). To obtain statistically significant results, raw Luc bioluminescence values were first normalized to the viral copy numbers (VCN) for each reporter plasmid. Briefly, serial dilutions of the known concentration of each Luc reporter plasmid were premixed with 5ng of carrier genomic DNA (isolated from each of the above-indicated cell lines), and the real-time PCR was performed using Luciferase primers. Obtained CT values were used to generate a standard curve which allowed to calculate the VCN values for the known concentration of plasmids according to the given formula:

$$Number\ of\ copies\ (=\ molecules)$$
$$= (X\ ng * 6.02214\ x\ 10^{23}\ molecules/mole)/((MW\ g/mole) * 1\ x\ 100\ ng/g)$$

$$Where: X = amount\ of\ amplicon(ng); N$$
$$= length\ of\ dsDNA\ amplicon; MW$$
$$= molecular\ weight\ of\ plasmid$$

Thus obtained linear regression curves allowed us to calculate viral copy numbers for an equal amount of genomic DNA for each individual cell line (Figure 5B). Moreover, raw bioluminescence values were also normalized to the amount of total protein present in each lysate. Normalized data demonstrated that initiation of *CD47* transcription requires the presence of all five NRF-1 DNA binding sites (Figure 5C). Thus, Luc activity was induced 5-8 fold in melanoma cells containing full-length proximal *CD47* promoter (Construct 1) as compared to low *CD47* expressing HepG2 cells (Figure 5C), while

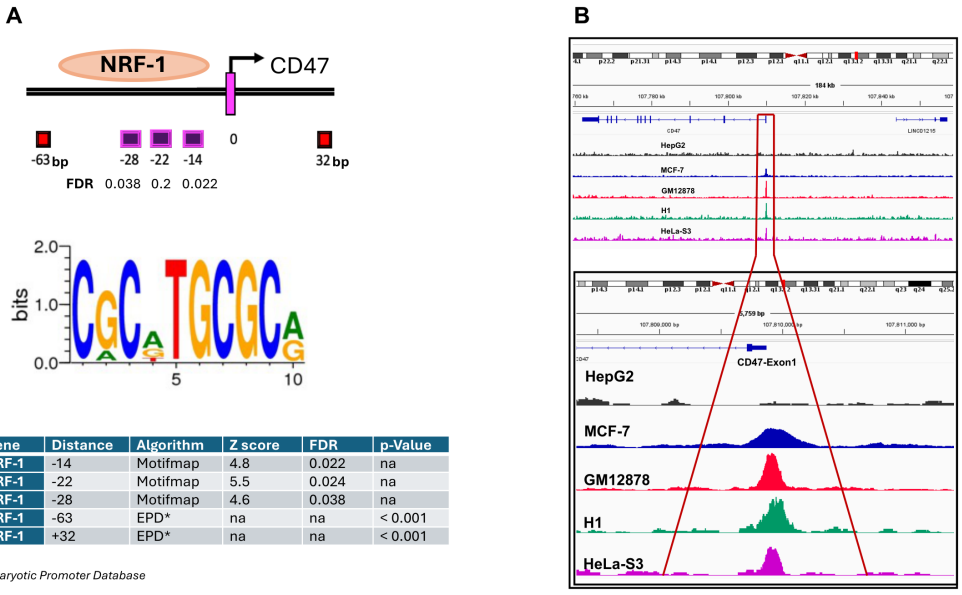

Gene	Distance	Algorithm	Z score	FDR	p-Value
NRF-1	-14	Motifmap	4.8	0.022	na
NRF-1	-22	Motifmap	5.5	0.024	na
NRF-1	-28	Motifmap	4.6	0.038	na
NRF-1	-63	EPD*	na	na	< 0.001
NRF-1	+32	EPD*	na	na	< 0.001

*Eukaryotic Promoter Database

FIGURE 3
Identification of NRF-1 TF as the regulator of *CD47* mRNA expression in melanoma. **(A)** Numerous NRF-1 TF binding sites were predicted and identified in the proximal region of the *CD47* Exon1 DNA Region. The consensus sequence required for the NRF-1 TF binding was extracted using the Motifmap algorithm. **(B)** Analysis of publically available ChIP-seq datasets for indicated cancer types reveals NRF-1 binding at the *CD47* Exon1 promoter region.

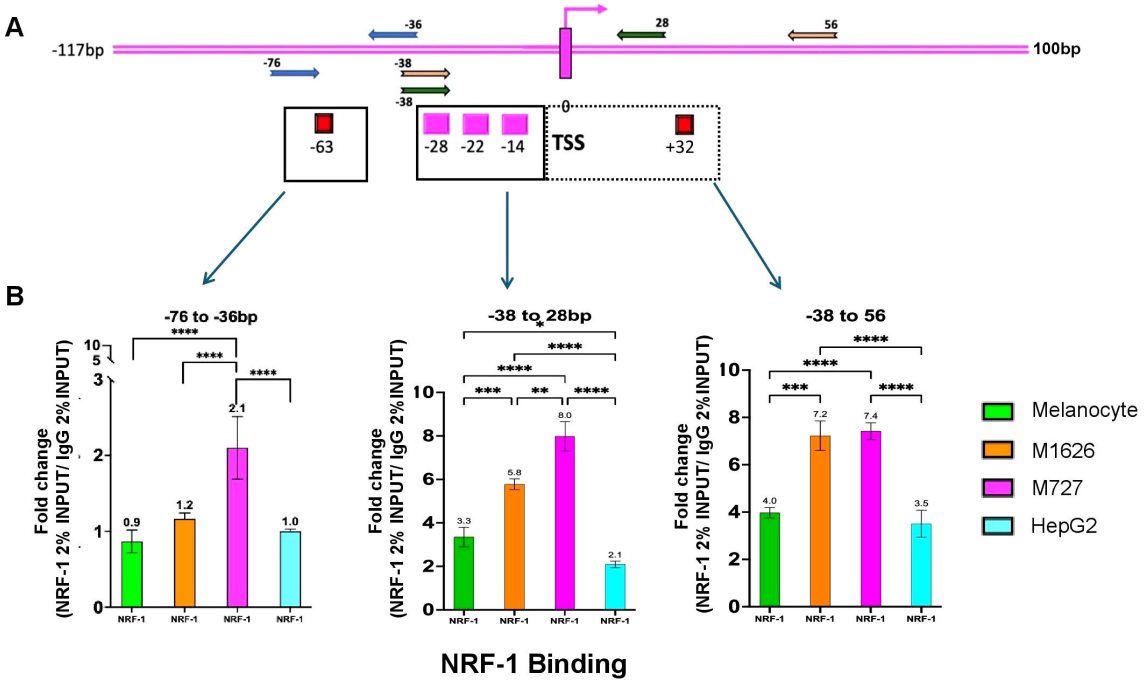

FIGURE 4
NRF-1 TF differentially binds at the proximal *CD47* promoter region spanning between -38 to +56bp relative to TSS. **(A)** Various sets of primers to target and enrich indicated regions of predicted NRF-1 binding at *CD47* promoter. **(B)** ChIP assays demonstrating differential affinity binding of NRF-1 at predicted DNA regions of *CD47* promoter. The strongest affinity for melanoma cells was determined for binding sites located between the -38 to 56bp region of the *CD47* promoter.

CD47 promoter region containing a reduced number of NRF-1 binding elements (Constructs 2 and 3) had marginal or no effect on reporter activity in the same cells (Figures 5C–E). In conclusion, our data demonstrates that the promoter region required for efficient *CD47* transcriptional activation in melanoma lies between -120 to +50bp relative to the TSS.

NRF-1 activity directly contributes to the CD47 expression in melanoma

To demonstrate functional significance of NRF1 TF in the regulation of *CD47* we tranduced melanoma cells expressing *CD47*_Luc promoter reporter (Construct 1 described above) with siRNAs (a pool of 3) targeting NRF1 mRNA to achieve its downregulation (Figure 6A). Subsequent quantification of Luc signal revealed a significant reduction in *CD47* promoter activity (by more than 60% (p=0.0149)) in cells transduced with NRF1 siRNA as compared to matching controls transduced with SC siRNA (Figure 6B). Next, we profiled these cells for an endogenous *CD47* mRNA levels using qRT-PCR and multiple sets of primers corresponding to its various regions. Our data demonstrates that NRF1 downregulation causes at least 50% decrease in *CD47* mRNA expression in target cells (p=0.0245 - 0.00361) (Figure 6C). Lastly, we used FACS and fluorescent conjugated antibodies to quantify *CD47* protein on the cell membrane, critical aspect of its immune modulatory function during tumor progression. Our analysis demonstrates that NRF1 downregulation leads to the significantly reduced proportion of melanoma cells expressing high levels of this innate immunity checkpoint when compared to the original cell population trasduced with control SC-siRNA: 7.04% $CD47^{high}$//91.8% $CD47^{low}$ for NRF1-siRNA and 34.3% $CD47^{hig}$//64.1% $CD47^{low}$ for SC-RNAi transduced cells (Figure 6D). In summary, the above described results provide strong experimental evidence to indicate that NRF1 is directly involved in regulation of *CD47* expression in melanoma.

Discussion

Cluster of Differentiation 47 (*CD47*), also known as Integrin Associated Protein (IAP), is a transmembrane protein belonging to the immunoglobulin superfamily (Ig) which regulates a variety of cell processes including, cell adhesion, motility and apoptosis (24–26). It gained considerable attention in the past decade after its function as a potent innate immunity checkpoint regulator was characterized first for hematopoietic malignancies and later for solid tumors, including melanoma (2, 27–29). Interaction of *CD47* with the signal regulatory protein-alpha (SIRPα) receptor expressed on many myeloid derived cell lineages activates molecular pathways effectively inhibiting an anti-tumor function of innate immunity (30). Upregulation of *CD47* by tumor cells in order to avoid immune recognition and elimination is thus regarded as one of the critical steps during carcinogenesis. Therefore, revealing mechanisms involved in the regulation of *CD47* expression represents a pivotal task in our understanding of tumor progression and immune evasion. Importantly, highly diverse mechanisms of malignant transformation and cancer progression can result in different modes of *CD47* regulation depending on the tissue type of tumor origin. For example, NFκB TF has been shown to

10.3389/fimmu.2024.1495032

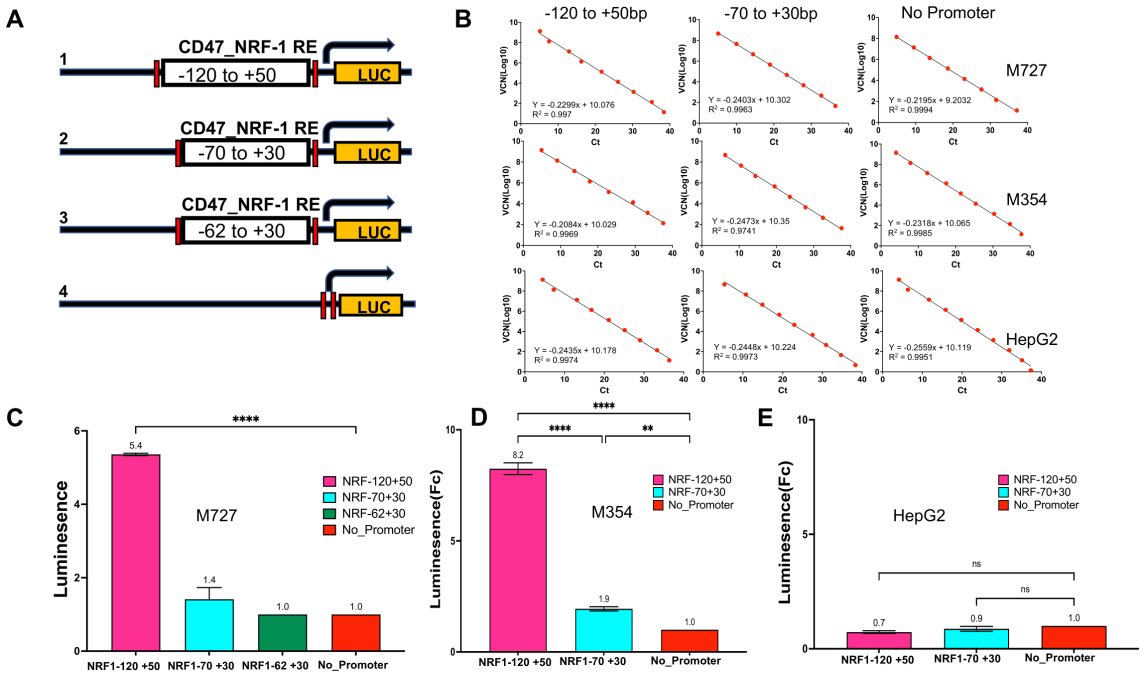

FIGURE 5
Activation of *CD47* promoter requires DNA region containing multiple NRF-1 binding sites located between -120bp to +50bp relative to TSS. **(A)** A series of Luciferase reporter constructs harboring different lengths of *CD47* promoter region were generated to assay the NRF-1 mediated *CD47* promoter activation. **(B)** Luciferase signals were read using a 96-well plate reader and normalized to viral copy number (VCN) and total protein. VCNs were calculated for each plasmid construct for every cell line separately using serial dilutions of plasmids to generate a linear regression curve with a slope equation that was further used to calculate the VCN of samples. **(C–E)** Relative CD47_NRF1 Luc reporter assay signal in fold changes for M727, M354 and HepG2 cells. A construct with no CD47 promoter region was used as a negative control.

activate *CD47* expression by binding to the distal enhancer elements in cells derived from breast, cervical, and non-small lung cell carcinomas (18, 19, 31). Other oncogenic TFs have also been reported to affect *CD47* expression directly as a part of an oncogene-driven process of malignant transformation. Thus, hypoxia inducible TF, HIF-1α, binds to the *CD47* promoter region at -239bp and -200bp relative to the TSS and induces its expression in response to hypoxic conditions *in-vitro* in MCF7 cells (17). Other studies implicated MYC, a well-characterized TF with strong oncogenic potential, in the transcriptional regulation of *CD47* during the progression of leukemia using MYC-induced T cell acute lymphoblastic leukemia mouse model; MYC T-ALL, and human leukemia cells lines; CCRF-CEM and Jurkat (16). Interestingly, binding sites for MYC TF were also identified in our analysis of *CD47* proximal promoter region (Supplementary Figure 3A), however, MYC binding was undetectable in human malignant melanoma within *CD47* DNA promoter region between -120bp to +54 relative to TSS required for its activation (Supplementary Figure 3B).

In our present work, we used numerous clinical human melanoma samples, as well as, previously collected pathological datasets of disease progression to establish that the tumor-specific upregulation of myeloid checkpoint molecule, *CD47*, occurs at the mRNA level during melanomagenesis. We reveal that it is mediated by a significant increase in chromatin accessibility at *CD47* prmoter region, including elevated levels of epigenetic histone modifications at $H3K4^{Me3}$ residues, in melanoma but not in normal melanocytes or HepG2 cells which are known for low *CD47* expression. Using serial DNA deletion analysis in combination with bioluminescence reporter systems, we determine that the minimum promoter region required for *CD47* transcriptional activation in melanoma lies between -120 to +50bp relative to the TSS. Furthermore, we identified NRF-1-TF as a specific transcriptional regulator of *CD47* promoter, which was found to be physically associated with multiple binding sites at the promoter region using ChIP approaches. Our data demonstrate that NRF-1 binding to the most proximal sites at -28, -22, and -14bp sites relative to the TSS appears to be a critical step during *CD47* promoter activation which distinguishes it from the cells of low *CD47* levels. This indicates that the basal level of *CD47* transcription can be initiated by NRF-1 binding to the distal regions of the *CD47* promoter starting at -63bp (which is detected for all cell types); however, upregulation in *CD47* mRNA synthesis occurs only in response to NRF-1 occupying additional proximal sities indicated above. Importantly, downregulation of NRF1 causes notable reduction of *CD47* mRNA (>50%) and as a result, significant decrease in melanoma cell poolations with high *CD47* levels. At the same time *CD47* expression was not completely abolished in response to NRF1 downregulation. pointing to the fact that other TFs mentioned above (such as NFkB and HIF1a) whose biding sites are identified within *CD47* promoter/enchancer regions can contribute to its expression. Further studies focused on combinatorial approaches to simultaneously modulate activity of NRF1 along with other TFs mentioned above at the *CD47* prmoter/enchancer DNA regions will be required to precisely delineate each TF contribution to the activity of *CD47* promoter overall.

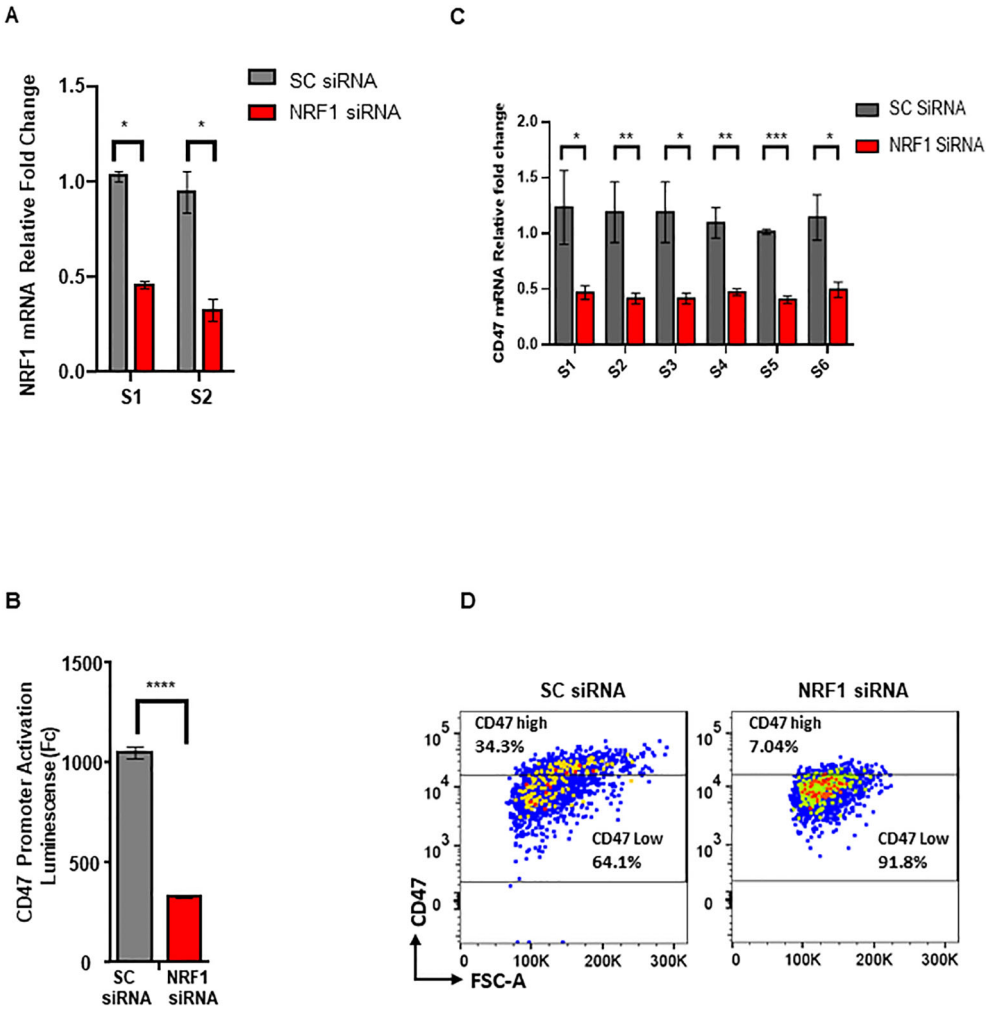

FIGURE 6
NRF-1 downregulation reduces expression of CD47 in melanoma. **(A)** Quantification of NRF1 mRNA following siRNA mediated knockdown in melanoma cells using qRT-PCR and two independent sets of primers, S1 and S2. **(B)** Quantification of CD47 prmoter activation using Luc reporter assay in the cells transduced with NRF1_siRNA or control, SC_siRNA. **(C)** Quantification of CD47 mRNA following siRNA mediated NRF1 knockdown in melanoma cells using qRT-PCR and six independent sets of primers, S1- S6. **(D)** Analysis of cell surface CD47 protein levels using FACS for cell populations transduced with NRF1_siRNA or control, SC_siRNA.

Under normal conditions, NRF-1 TF plays a vital role in maintaining mitochondrial biogenesis, including oxidative phosphorylation, by transcribing multiple proteins involved in processes regulating biogenesis such as TFB1M, TFB2M, TFAM, and *cytochrome c* (32, 33). However, NRF-1 has also been implicated in the process of malignant transformation based on its role in energy metabolism. Specifically, studies using human hepatocellular carcinoma and colorectal tumor tissues show the significance of upregulated NRF-1 protein levels (mediated by neutrophil extracellular trap formation) in inducing mitochondrial biogenesis promoting tumor growth and metastasis (34). In addition, NRF-1 activity has also been associated with estrogen-induced breast carcinogenesis, and renal cell carcinoma where it regulates the expression of the *TFE3* gene required for cellular energy metabolism during proliferation (35, 36).

In our present study, we characterized a novel role of NRF-1 in melanomagenesis as a regulator of the major innate immunity checkpoint, *CD47*, in tumor cells. Importantly, binding of Pal/NRF-1 to the CD47 promoter was also previously reported in human neuroblastoma and hepatoma cell lines (37), as well as, during arising resistance to the oncogenic B-RAF molecular inhibitors (38). These findings open an opportunity for the development of modulatory compunds against NRF1 and functional testing of this TF involvment in an immune evasion by tumor cells during cancer progression. Clinical significance of these approaches can further be tested both *in-vitro* and *in-vivo* in combination with already established immunotherapeutic agents, such as PD1/PDL1/CTLA4 blocking antibodies, commonly used for the treatment of metastatic disease. Malignant transformation is a complex and multifaceted process that combines changes in both metabolism and immune recognition within cancer cells that successfully evolve to give rise to the more aggressive and metastatic tumors. NRF-1 TF therefore represents a key nodal point in this process due to its unique ability to transcriptionally regulate genes underlying both mitochondrial biogenesis and evasion of an innate immunity.

Data availability statement

Publicly available datasets were analyzed in this study. This data can be found here: ENCFF323SMV, ENCFF862EDR, ENCFF605IET, ENCFF785WIA, ENCFF000XJF, ENCFF644ITQ from encodeproject.org. GSE33930, GSE134432 from gene expression omnibus.

Ethics statement

The studies involving humans were approved by Cedars Sinai Office of Research Compliance and Quality Improvement. The studies were conducted in accordance with the local legislation and institutional requirements. The participants provided their written informed consent to participate in this study.

Author contributions

KM: Conceptualization, Data curation, Formal analysis, Methodology, Investigation, software, Visualization, Project administration, Writing – original draft, Writing – review & editing. EV: Formal analysis, Visualization, Methodology, Writing – review & editing. DM: Methodology, Resources, Writing – review & editing. BS: Methodology, Resources, Writing – review & editing. NB: Resources, Writing – review & editing. MF: Methodology, Resources, Writing – review & editing. OH: Methodology, Resources, Writing – review & editing. AB: Conceptualization, Data curation, Formal analysis, Funding acquisition, Investigation, Project administration, Resources, Supervision, Validation, Writing – original draft, Writing – review & editing.

Funding

The author(s) declare financial support was received for the research, authorship, and/or publication of this article. This work was supported by U.S. National Institutes of Health/National Cancer Institute Grant R01CA234892 to AB and funds from the Cedars-Sinai Medical Center to AB.

Conflict of interest

MF is the member of the following advisory board committees : Merck, Bristol Myers Squibb, Replimune, Novartis.

The authors declare that the research was conducted in the absence of any commercial or financial relationships that could be construed as a potential conflict of interest.

Publisher's note

Supplementary material

The Supplementary Material for this article can be found online at: https://www.frontiersin.org/articles/10.3389/fimmu.2024.1495032/full#supplementary-material

SUPPLEMENTARY FIGURE 1
Primer design for *CD47* real-time qPCR assay. **(A)** Schematic representation of different isoforms for the human *CD47* mRNA. **(B)** primer sets (6) that were used to quantify an abundance of indicated *CD47* mRNA isoforms.

SUPPLEMENTARY FIGURE 2
MEF2A gene promoter used as a positive control of anti-NRF-1 ChIP assays.

SUPPLEMENTARY FIGURE 3
Evaluation of MYC binding at the proximal *CD47* promoter region in melanoma. **(A)** MYC binding sites on the *CD47* region as predicted by Eukaryotic Promoter Database. **(B, C)** MYC ChIP on *CD47* promoter in melanoma cells M1626 and hepatocarcinoma cells HepG2. **(D)** MYC ChIP on Nmp-1 promoter (positive control) in M1626 and HepG2 cells.

References

1. Willingham SB, Volkmer JP, Gentles AJ, Sahoo D, Dalerba P, Mitra S, et al. The CD47-signal regulatory protein alpha (SIRPa) interaction is a therapeutic target for human solid tumors. *Proc Natl Acad Sci USA*. (2012) 109:6662–7. doi: 10.1073/pnas.1121623109

2. Ngo M, Han A, Lakatos A, Sahoo D, Hachey SJ, Weiskopf K, et al. Antibody therapy targeting CD47 and CD271 effectively suppresses melanoma metastasis in patient-derived xenografts. *Cell Rep*. (2016) 16:1701–16. doi: 10.1016/j.celrep.2016.07.004

3. Jaiswal S, Jamieson CH, Pang WW, Park CY, Chao MP, Majeti R, et al. CD47 is upregulated on circulating hematopoietic stem cells and leukemia cells to avoid phagocytosis. *Cell*. (2009) 138:271–85. doi: 10.1016/j.cell.2009.05.046

4. Majeti R, Chao MP, Alizadeh AA, Pang WW, Jaiswal S, Gibbs KD, et al. CD47 is an adverse prognostic factor and therapeutic antibody target on human acute myeloid leukemia stem cells. *Cell*. (2009) 138:286–99. doi: 10.1016/j.cell.2009.05.045

5. Oldenborg PA, Zheleznyak A, Fang YF, Lagenaur CF, Gresham HD, Lindberg FP. Role of CD47 as a marker of self on red blood cells. *Science*. (2000) 288:2051–4. doi: 10.1126/science.288.5473.2051

6. Eladl E, Tremblay-LeMay R, Rastgoo N, Musani R, Chen W, Liu A, et al. Role of CD47 in hematological Malignancies. *J Hematol Oncol*. (2020) 13:96. doi: 10.1186/s13045-020-00930-1

7. Chao MP, Tang C, Pachynski RK, Chin R, Majeti R, Weissman IL. Extranodal dissemination of non-Hodgkin lymphoma requires CD47 and is inhibited by anti-CD47 antibody therapy. *Blood*. (2011) 118:4890–901. doi: 10.1182/blood-2011-02-338020

8. Manna PP, Frazier WA. CD47 mediates killing of breast tumor cells via Gi-dependent inhibition of protein kinase A. *Cancer Res*. (2004) 64:1026–36. doi: 10.1158/0008-5472

9. Liu R, Wei H, Gao P, Yu H, Wang K, Fu Z, et al. CD47 promotes ovarian cancer progression by inhibiting macrophage phagocytosis. *Oncotarget*. (2017) 8:39021–32. doi: 10.18632/oncotarget.16547

10. Zhang Y, Sime W Fau - Juhas M, Juhas M Fau - Sjölander A, Sjölander A. Crosstalk between colon cancer cells and macrophages via inflammatory mediators and CD47 promotes tumour cell migration. *Eur J Cancer*. (2013) 49:3320–34. doi: 10.1016/j.ejca.2013.06.005

11. Benesova I, Capkova L, Ozaniak A, Pacas P, Kopeckova K, Galova D, et al. A comprehensive analysis of CD47 expression in various histological subtypes of soft tissue sarcoma: exploring novel opportunities for macrophage-directed treatments. *J Cancer Res Clin Oncol*. (2024) 150:134. doi: 10.1007/s00432-024-05661-1

12. Dancsok AR, Gao D, Lee AF, Steigen SE, Blay JV, Thomas DM, et al. Tumor-associated macrophages and macrophage-related immune checkpoint expression in sarcomas. *Oncoimmunology*. (2020) 9:1747340. doi: 10.1080/2162402X.2020.1747340

13. Theruvath J, Menard M, Smith BAH, Linde MH, Coles GL, Dalton GN, et al. Anti-GD2 synergizes with CD47 blockade to mediate tumor eradication. *Nat Med*. (2022) 28:333–44. doi: 10.1038/s41591-021-01625-x

14. Zhang W, Huang Q, Xiao W, Zhao Y, Pi J, Xu H, et al. Advances in anti-tumor treatments targeting the CD47/SIRPα Axis. *Front Immunol*. (2020) 11:18. doi: 10.3389/fimmu.2020.00018

15. Kaur S, Cicalese KV, Bannerjee R, Roberts DD. Preclinical and clinical development of therapeutic antibodies targeting functions of CD47 in the tumor microenvironment. *Antib Ther*. (2020) 3:179–92. doi: 10.1093/abt/tbaa017

16. Casey SC, Tong L, Li Y, Do R, Walz S, Fitzgerald KN, et al. MYC regulates the antitumor immune response through CD47 and PD-L1. *Science*. (2016) 352:227–31. doi: 10.1126/science.aac9935

17. Zhang H, Lu H, Xiang L, Bullen JW, Zhang C, Samanta D, et al. HIF-1 regulates CD47 expression in breast cancer cells to promote evasion of phagocytosis and maintenance of cancer stem cells. *Proc Natl Acad Sci U.S.A*. (2015) 112:E6215–6223. doi: 10.1073/pnas.1520032112

18. Liu F, Dai M, Xu Q, Zhu X, Zhou Y, Jiang S, et al. SRSF10-mediated IL1RAP alternative splicing regulates cervical cancer oncogenesis via mIL1RAP-NF-κB-CD47 axis. *Oncogene*. (2018) 37:2394–409. doi: 10.1038/s41388-017-0119-6

19. Zhang X, Wang Y, Fan J, Chen W, Luan J, Mei X, et al. Blocking CD47 efficiently potentiated therapeutic effects of anti-angiogenic therapy in non-small cell lung cancer. *J Immunother Cancer*. (2019) 7:346. doi: 10.1186/s40425-019-0812-9

20. Igolkina AA-O, Zinkevich A, Karandasheva KO, Popov AA, Selifanova MV, Nikolaeva D, et al. H3K4me3, H3K9ac, H3K27ac, H3K27me3 and H3K9me3 histone tags suggest distinct regulatory evolution of open and condensed chromatin landmarks. *Cells*. (2019) 8:1034. doi: 10.3390/cells8091034

21. De la Vega RE, Scheu M, Brown LA, Evans CH, Ferreira E, Porter RM. Specific, sensitive, and stable reporting of human mesenchymal stromal cell chondrogenesis. *Tissue Eng Part C Methods*. (2019) 25:176–90. doi: 10.1089/ten.TEC.2018.0295

22. Boiko AD, Porteous Razorenova OV, Krivokrysenko VI, Williams BR, Gudkov AV. A systematic search for downstream mediators of tumor suppressor function of p53 reveals a major role of BTG2 in suppression of Ras-induced transformation. *Genes Dev*. (2006) 20:236–52. doi: 10.1101/gad.1372606

23. Li C, Nguyen V, Clark KN, Zahed T, Sharkas S, Filipp FV, et al. Down-regulation of FZD3 receptor suppresses growth and metastasis of human melanoma independently of canonical WNT signaling. *Proc Natl Acad Sci U.S.A*. (2019) 116:4548–57. doi: 10.1073/pnas.1813802116

24. Polara RA-O, Ganesan RA-O, Pitson SA-O, Robinson NA-O. Cell autonomous functions of CD47 in regulating cellular plasticity and metabolic plasticity. *Cell Death Differ*. (2024) 31:1255–66. doi: 10.1038/s41418-024-01347-w

25. Sick E, Jeanne A, Schneider C, Dedieu S, Takeda K, Martiny L. CD47 update: a multifaceted actor in the tumour microenvironment of potential therapeutic interest. *Br J Pharmacol*. (2012) 167:1415–30. doi: 10.1111/j.1476-5381.2012.02099.x

26. Oldenborg PA. CD47: A cell surface glycoprotein which regulates multiple functions of hematopoietic cells in health and disease. *ISRN Hematol*. (2013) 2013:614619. doi: 10.1155/2013/614619

27. Huang CY, Ye ZH, Huang MY, Lu JJ. Regulation of CD47 expression in cancer cells. *Transl Oncol*. (2020) 13:100862. doi: 10.1016/j.tranon.2020.100862

28. Jiang Z, Sun H, Yu JA-O, Tian W, Song Y. Targeting CD47 for cancer immunotherapy. *J Hematol Oncol*. (2021) 14:180. doi: 10.1186/s13045-021-01197-w

29. Stirling ER, Terabe M, Wilson AS, Kooshki M, Yamaleyeva LM, Alexander-Miller MA, et al. Targeting the CD47/thrombospondin-1 signaling axis regulates immune cell bioenergetics in the tumor microenvironment to potentiate antitumor immune response. *J Immunother Cancer*. (2022) 10:e004712. doi: 10.1136/jitc-2022-004712

30. van Duijn A, van der Burg SH, Scheeren FA. CD47/SIRPα axis: bridging innate and adaptive immunity. *J Immunother Cancer*. (2022) 10. doi: 10.1136/jitc-2022-004589

31. Betancur PA. et al. A CD47-associated super-enhancer links pro-inflammatory signalling to CD47 upregulation in breast cancer. *Nat Commun*. (2017) 8. doi: 10.1038/ncomms14802

32. Scarpulla RC. Nuclear control of respiratory chain expression by nuclear respiratory factors and PGC-1-related coactivator. *Ann N Y Acad Sci*. (2008) 1147:321–34. doi: 10.1196/annals.1427.006

33. Gleyzer N, Vercauteren K, Scarpulla RC. Control of mitochondrial transcription specificity factors (TFB1M and TFB2M) by nuclear respiratory factors (NRF-1 and NRF-2) and PGC-1 family coactivators. *Mol Cell Biol*. (2005) 25:1354–66. doi: 10.1128/MCB.25.4.1354-1366.2005

34. Yazdani HO, Roy E, Comerci AJ, van der Windt DJ, Zhang H, Huang H, et al. Neutrophil extracellular traps drive mitochondrial homeostasis in tumors to augment growth. *Cancer Res*. (2019) 79:5626–39. doi: 10.1158/0008-5472.CAN-19-0800

35. Das JA-O, Felty Q, Poppiti R, Jackson RM, Roy D. Nuclear respiratory factor 1 acting as an oncoprotein drives estrogen-induced breast carcinogenesis. *Cells*. (2018) 7:234. doi: 10.3390/cells7120234

36. Zhuang W, Dong X, Wang B, Liu N, Guo H, Zhang C, et al. NRF-1 directly regulates TFE3 and promotes the proliferation of renal cancer cells. *Oncol Lett*. (2021) 3):679. doi: 10.3892/ol.2021.12940

37. Chang WT, Huang AM. Alpha-Pal/NRF-1 regulates the promoter of the human integrin-associated protein/CD47 gene. *J Biol Chem*. (2004) 279:14542–50. doi: 10.1074/jbc.M309825200

38. Liu F, Jiang CC, Yan XG, Tseng HY, Wang CY, Zhang YY, et al. BRAF/MEK inhibitors promote CD47 expression that is reversible by ERK inhibition in melanoma. *Oncotarget*. (2017) 8:69477–92. doi: 10.18632/oncotarget.17704

Frontiers in Oncology

Advances knowledge of carcinogenesis and tumor progression for better treatment and management

The third most-cited oncology journal, which highlights research in carcinogenesis and tumor progression, bridging the gap between basic research and applications to imrpove diagnosis, therapeutics and management strategies.

Discover the latest Research Topics

See more →

Frontiers

Avenue du Tribunal-Fédéral 34
1005 Lausanne, Switzerland
frontiersin.org

Contact us

+41 (0)21 510 17 00
frontiersin.org/about/contact